Collision Energy Dependence of Hydrodynamic Flow in Relativistic Heavy-Ion Collisions

Chun Shen

The Ohio State University

Collaborators: Ulrich Heinz, Huichao Song, Zhi Qiu

HENPIC Forum, Sept. 27, 2012

Ref: C. Shen and U. Heinz, PRC **85** (2012) 054902

Little Bang

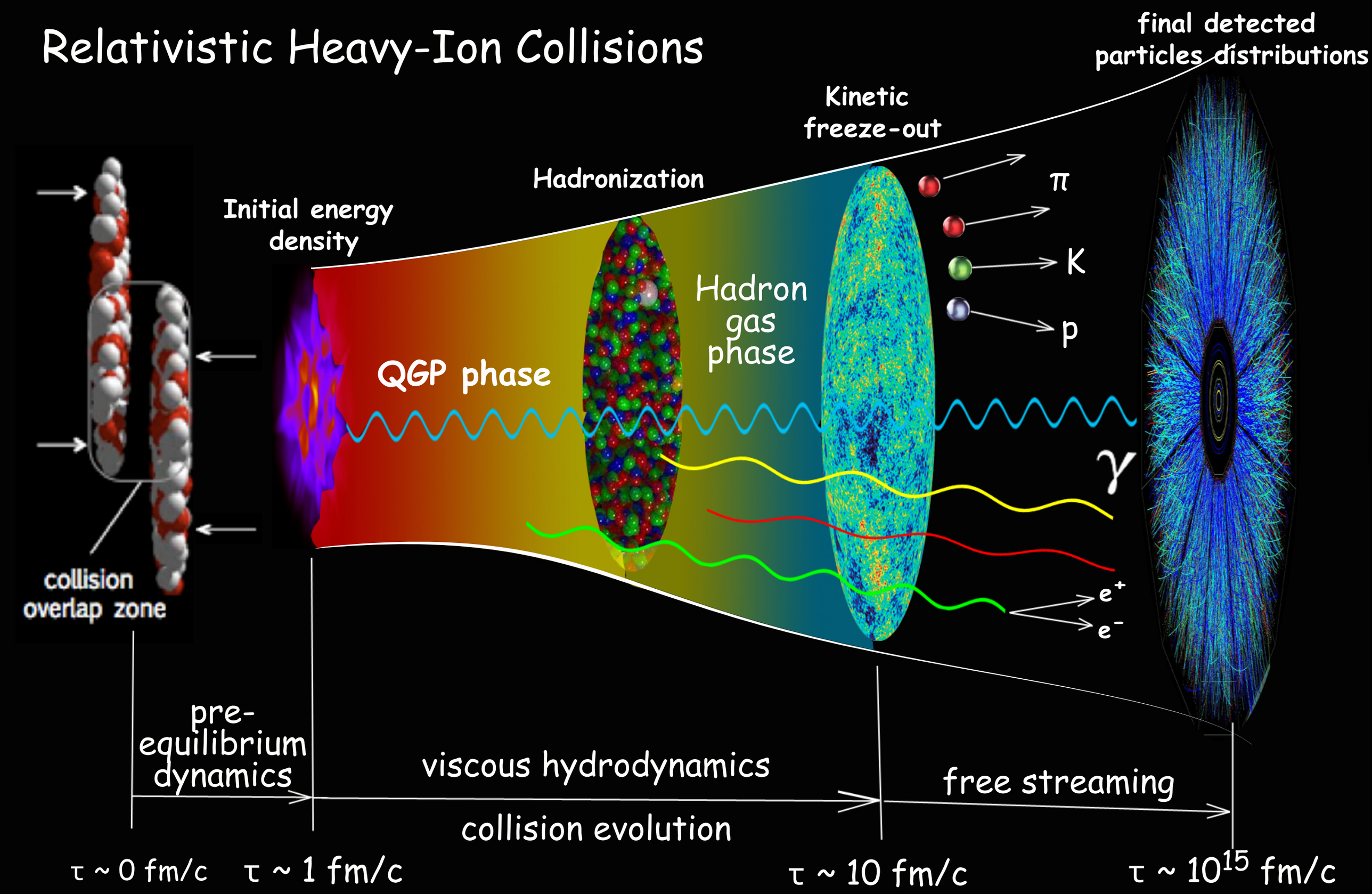
Relativistic Heavy-Ion Collisions
final detected particles distributions
Kinetic freeze-out
Hadronization
Initial energy density
Hadron gas phase
QGP phase
π
K
p
γ
e+
e−
collision overlap zone
pre-equilibrium dynamics
viscous hydrodynamics
free streaming
collision evolution
τ ~ 0 fm/c
τ ~ 1 fm/c
τ ~ 10 fm/c
τ ~ 10^15 fm/c

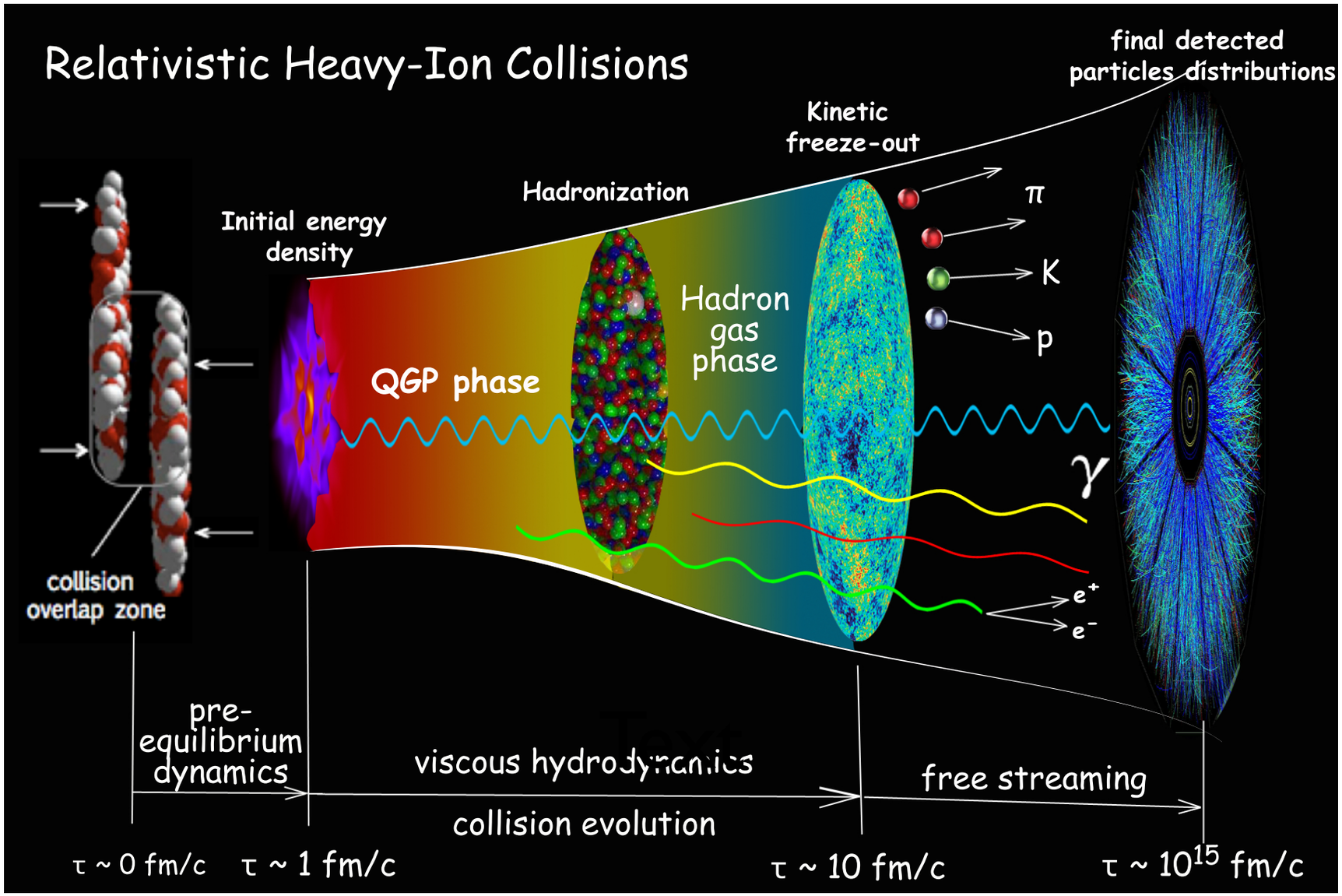
Relativistic Heavy-Ion Collisions
final detected particles distributions
Kinetic freeze-out
Hadronization
Initial energy density
π
K
p
Hadron gas phase
QGP phase
γ
e+
e-
collision overlap zone
pre-equilibrium dynamics
viscous hydrodynamics
free streaming
collision evolution
τ ~ 0 fm/c
τ ~ 1 fm/c
τ ~ 10 fm/c
τ ~ 10^15 fm/c

Initial conditions
T_{dec}
τ_0
η/s
EOS
...
Hydro
...
compare
Exp. data

Motivation

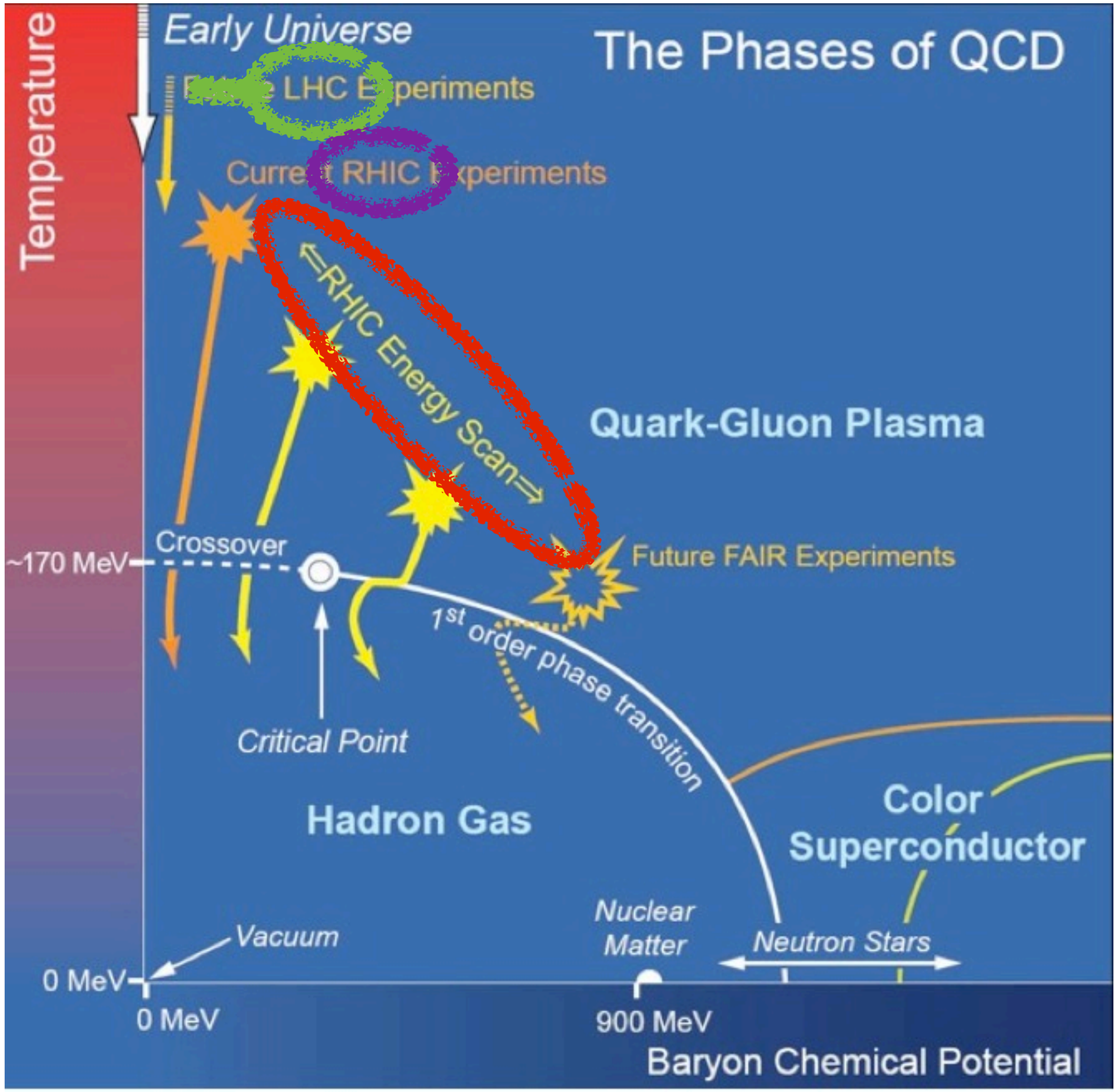
The Phases of QCD
Temperature
Early Universe
LHC Experiments
Current RHIC Experiments
RHIC Energy Scan
Quark-Gluon Plasma
Future FAIR Experiments
Crossover
~170 MeV
1st order phase transition
Critical Point
Hadron Gas
Color Superconductor
Nuclear Matter
Neutron Stars
Vacuum
0 MeV
0 MeV
900 MeV
Baryon Chemical Potential

3d Hydro Movie

Made by Zhi Qiu

3d Hydro Movie

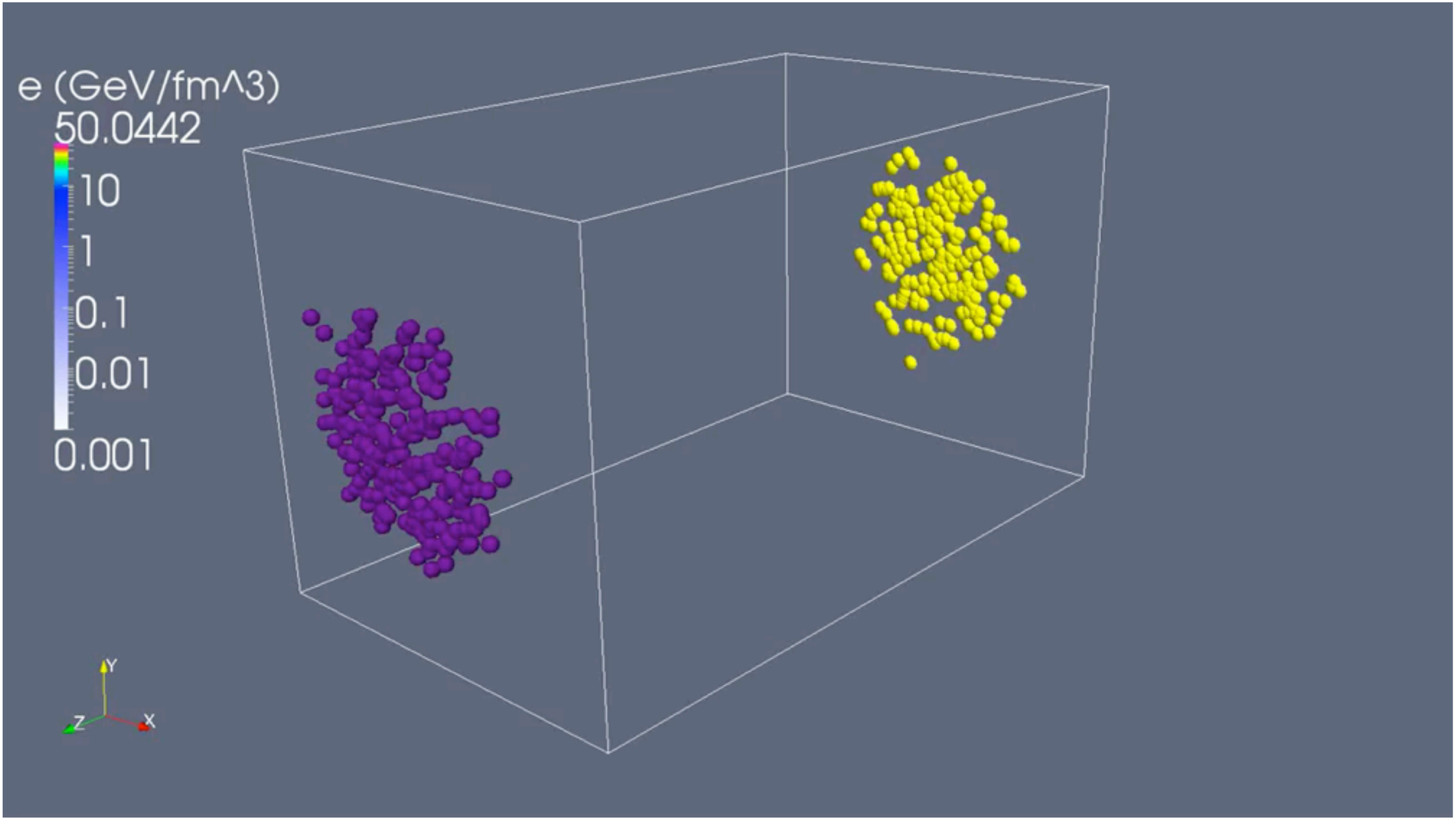

Made by Zhi Qiu

Viscous Hydrodynamics: Israel-Stewart Formalism

Energy momentum tensor (for zero bulk viscosity) :

$$T^{\mu\nu} = eu^\mu u^\nu - p\Delta^{\mu\nu} + \pi^{\mu\nu}$$

Equation of motion :

$$d_\mu T^{\mu\nu} = 0,$$

$$\Delta^{\mu\alpha}\Delta^{\nu\beta} D\pi_{\alpha\beta} = -\frac{1}{\tau_\pi}(\pi^{\mu\nu} - 2\eta\sigma^{\mu\nu}) - \frac{1}{2}\pi^{\mu\nu}\frac{\eta T}{\tau_\pi} d_\lambda\left(\frac{\tau_\pi}{\eta T}u^\lambda\right)$$

where

$$\Delta^{\mu\nu} = g^{\mu\nu} - u^\mu u^\nu \qquad D = u^\mu d_\mu$$

$$\sigma^{\mu\nu} = \frac{1}{2}(\nabla^\mu u^\nu + \nabla^\nu u^\mu) - \frac{1}{3}(\nabla\cdot u)\Delta^{\mu\nu}$$ (velocity shear tensor)

Cooper-Frye freeze-out procedure :

$$E\frac{d^3N_i}{d^3p} = \frac{g_i}{(2\pi)^3}\int_\Sigma p\cdot d^3\sigma(x)[f_{eq,i}(x,p) + \delta f_i(x,p)]$$

where

$$\delta f_i = f_{eq,i}\cdot\frac{1}{2}\frac{p^\mu p^\nu}{T^2}\frac{\pi_{\mu\nu}}{e+p}$$

Explicitly, $\left(\Sigma = \pi^{xx} + \pi^{yy},\ \Delta = \pi^{xx} - \pi^{yy}\right)$

$$\begin{aligned} p^\mu p^\nu \pi_{\mu\nu} &= \pi^{\tau\tau}\left[m_T^2(2\cosh^2(y-\eta) - 1) - 2\frac{p_T}{v_\perp}m_T \times \cosh(y-\eta)\frac{\sin(\phi_p+\phi_v)}{\sin(2\phi_v)} + \frac{p_T^2}{v_\perp^2}\frac{\sin(2\phi_p)}{\sin(2\phi_v)}\right] \\ &+ \Sigma\left[-m_T^2\sinh^2(y-\eta) + p_T m_T\cosh(y-\eta)\times v_\perp\frac{\sin(\phi_p-\phi_v)}{\tan(2\phi_v)} + \frac{p_T^2}{2}\left(1 - \frac{\sin(2\phi_p)}{\sin(2\phi_v)}\right)\right] \\ &+ \Delta\left[p_T m_T\cosh(y-\eta)v_\perp\frac{\sin(\phi_p-\phi_v)}{\sin(2\phi_v)} - \frac{p_T^2}{2}\frac{\sin(2(\phi_p-\phi_v))}{\sin(2\phi_v)}\right] \end{aligned}$$

A State-of-the-art Equation of State: s95p-PCE

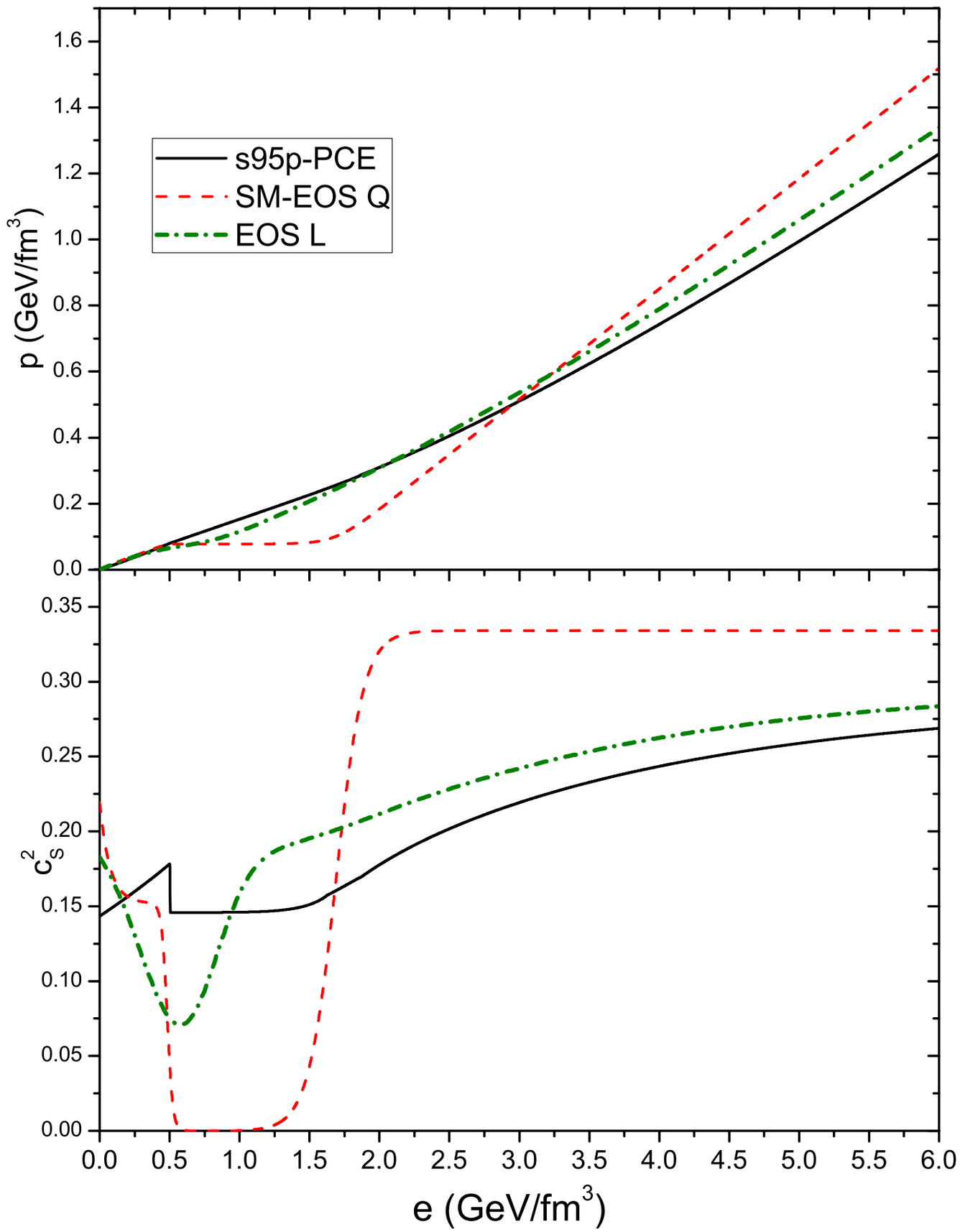

$$\dot{u}^\nu = \frac{\nabla^\nu p}{e+p} = \frac{c_s^2}{1+c_s^2}\frac{\nabla^\nu p}{p}$$

s95p-PCE generated by Peter Petreczky & Pasi Huovinen

Shen, Heinz, Huovinen, Song,Phys.Rev. C82 (2010) 054904

Fit to RHIC data

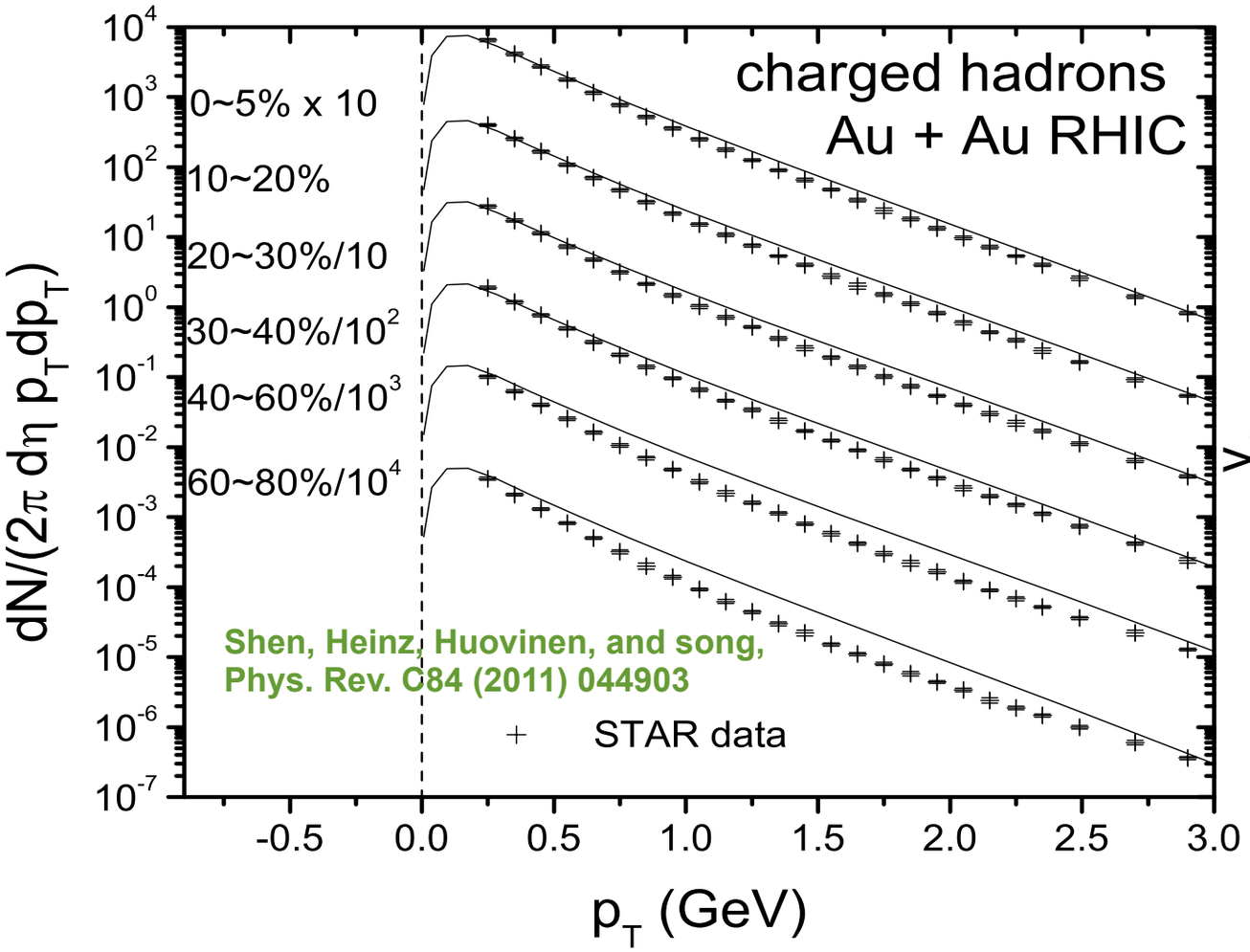

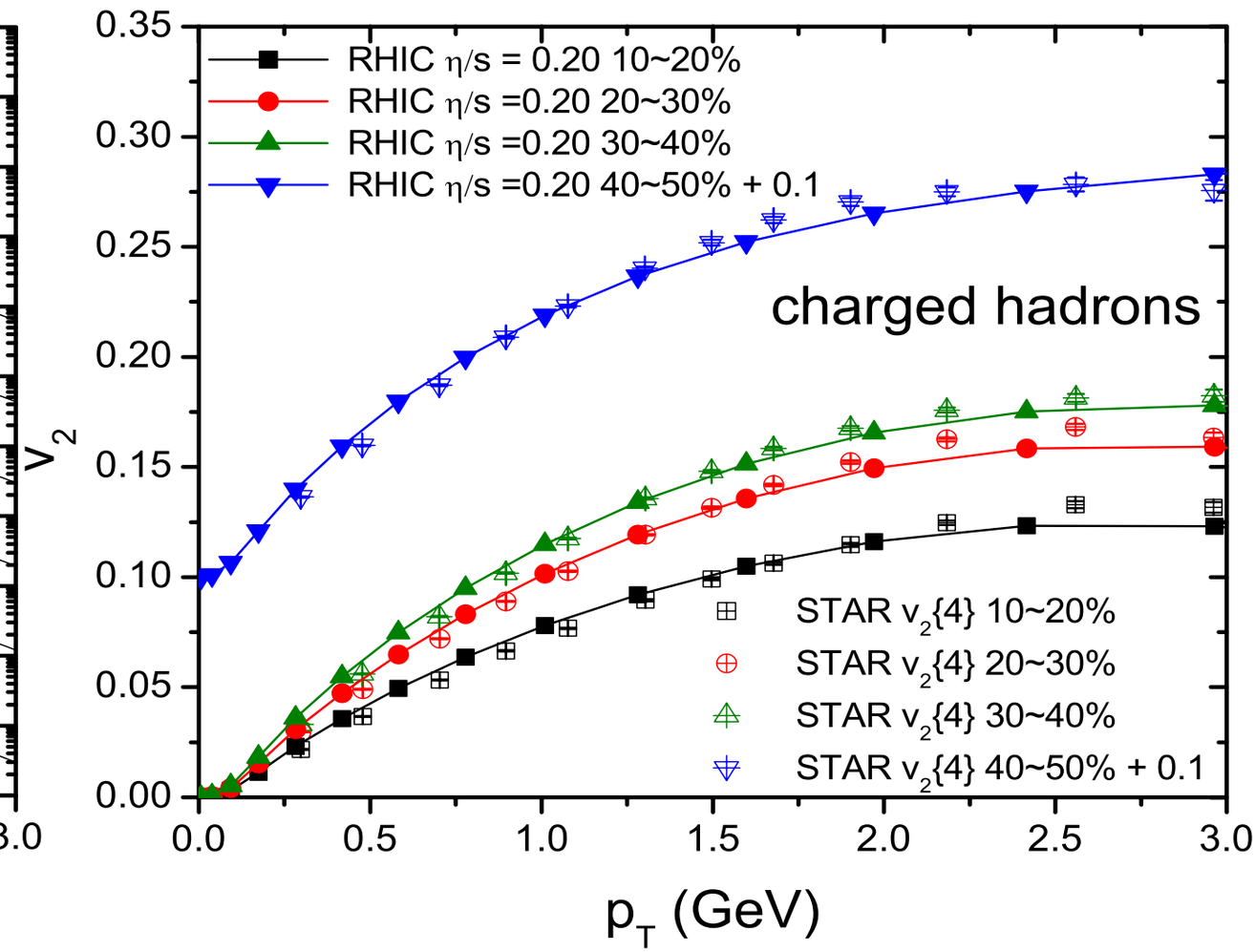

- good fit in the central cases, while too flat in the peripheral cases
- Excellent fit to elliptic flow data up to 60% in centrality

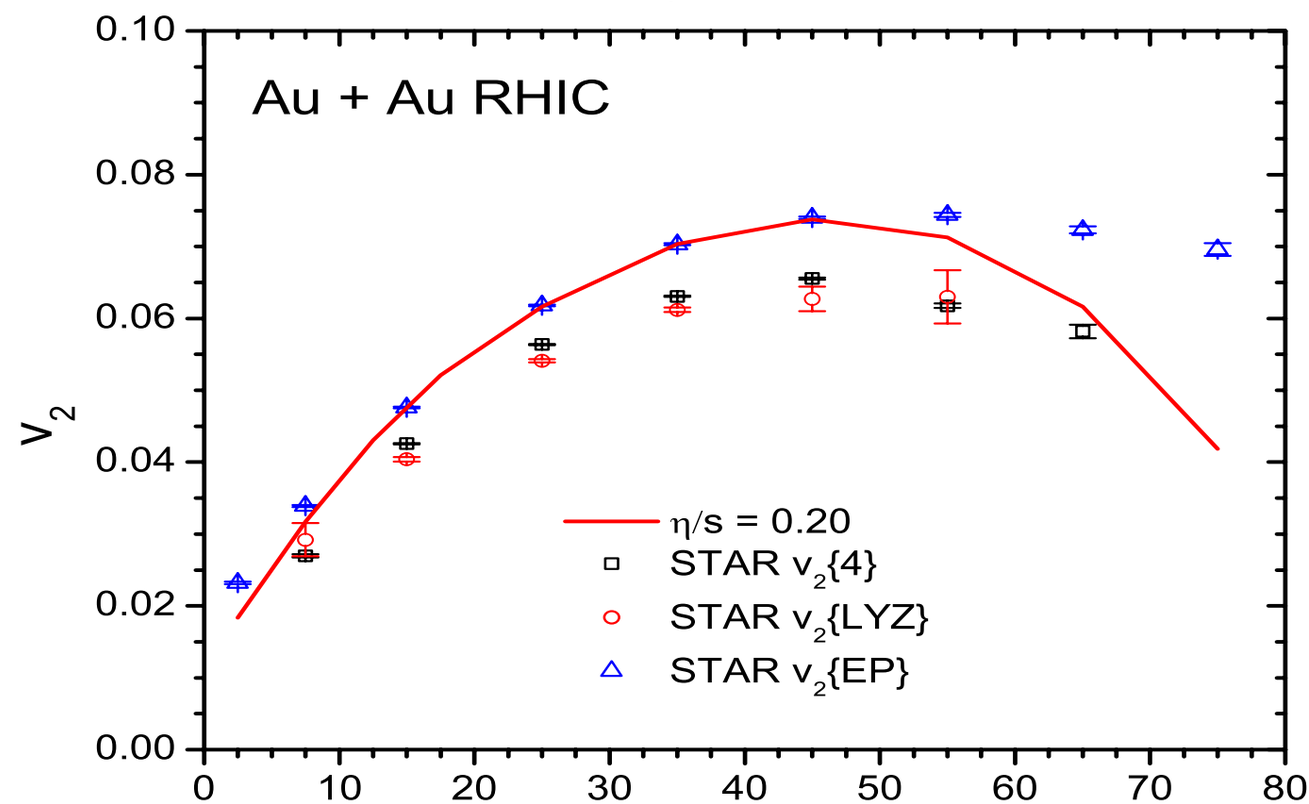

Predictions at LHC

Shen, Heinz, Huovinen, and song, Phys. Rev. C84 (2011) 044903

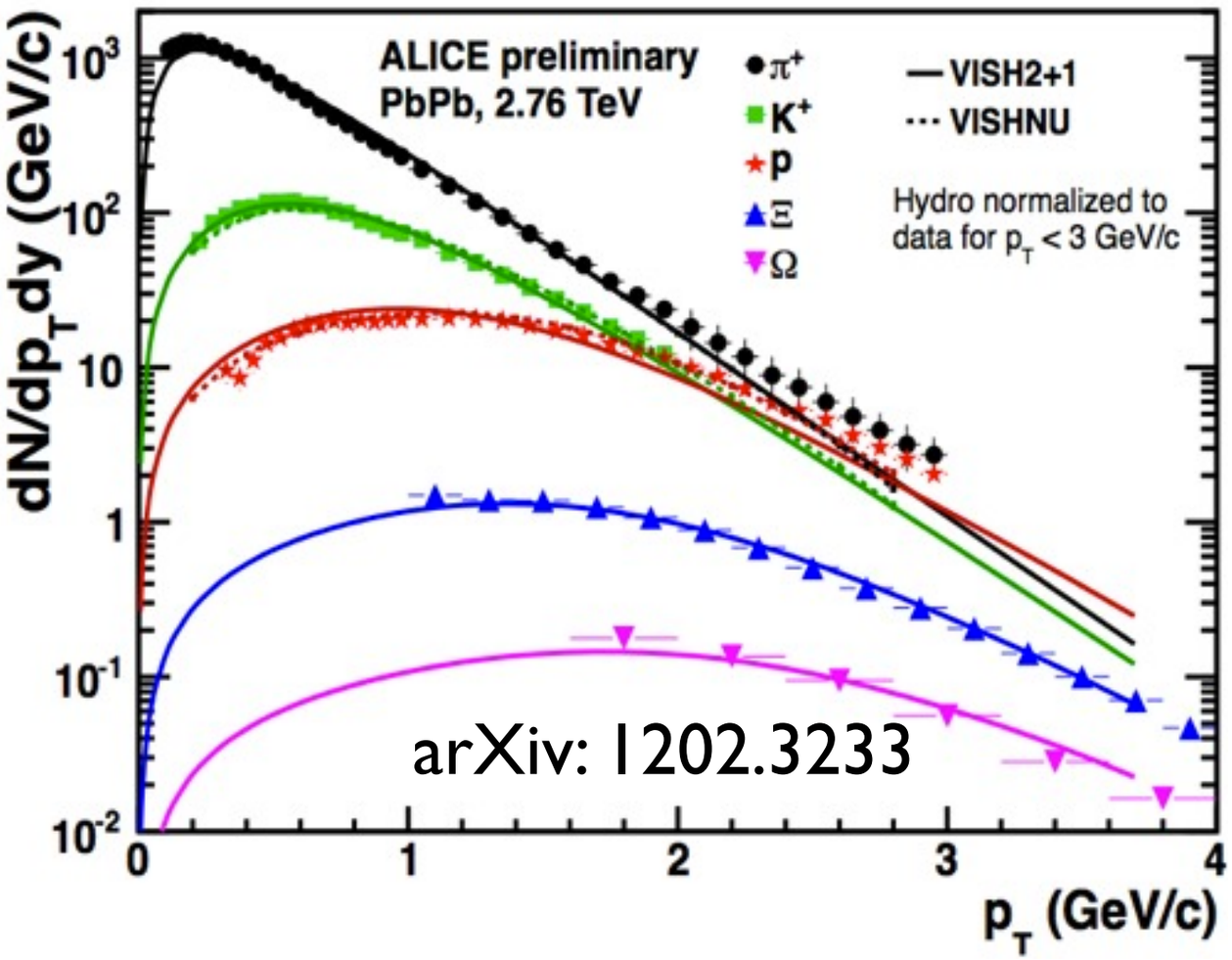

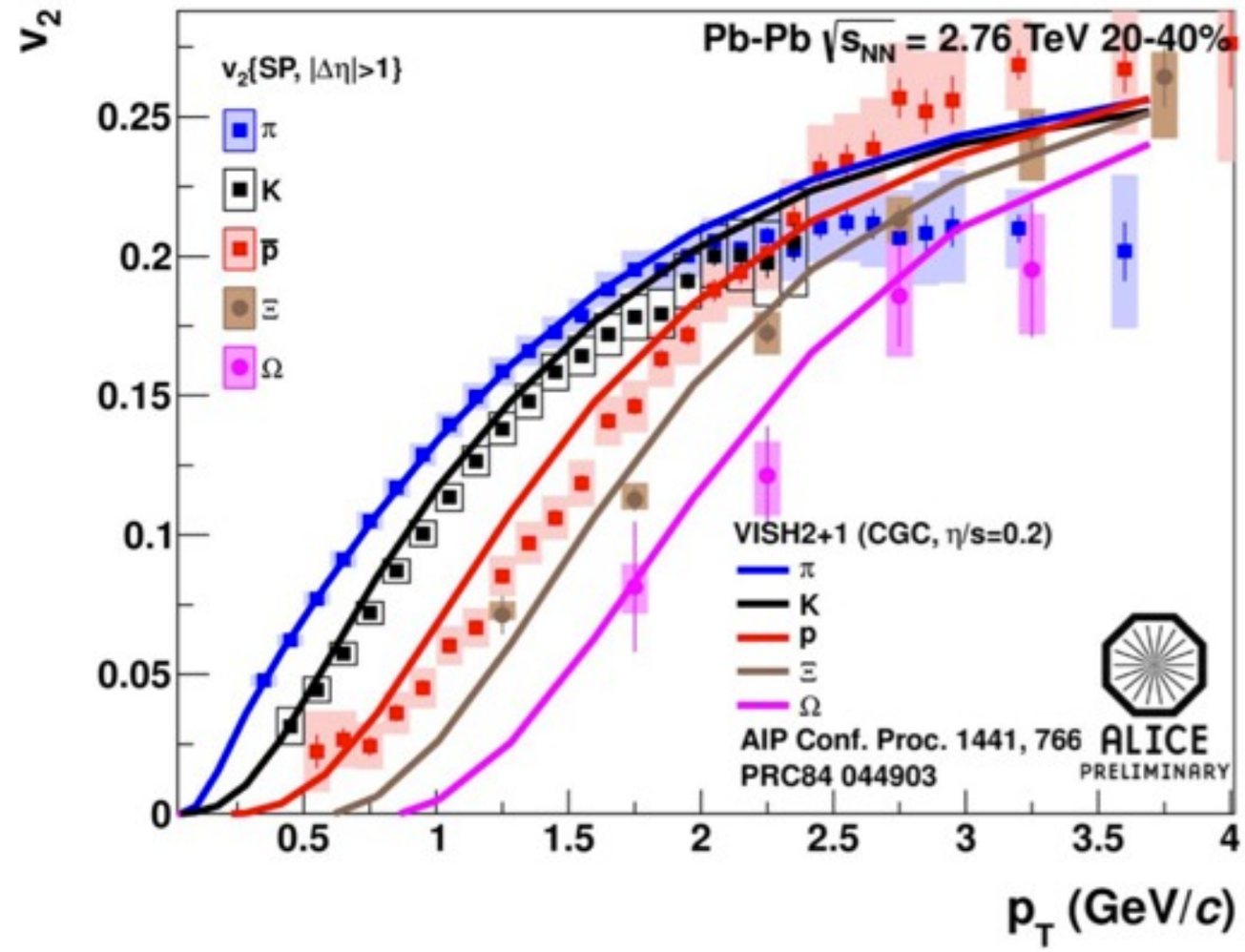

- VISH2+1 predictions agree with ALICE measurements remarkably on identified particle spectra and elliptic flow

More advanced Hybrid Approach

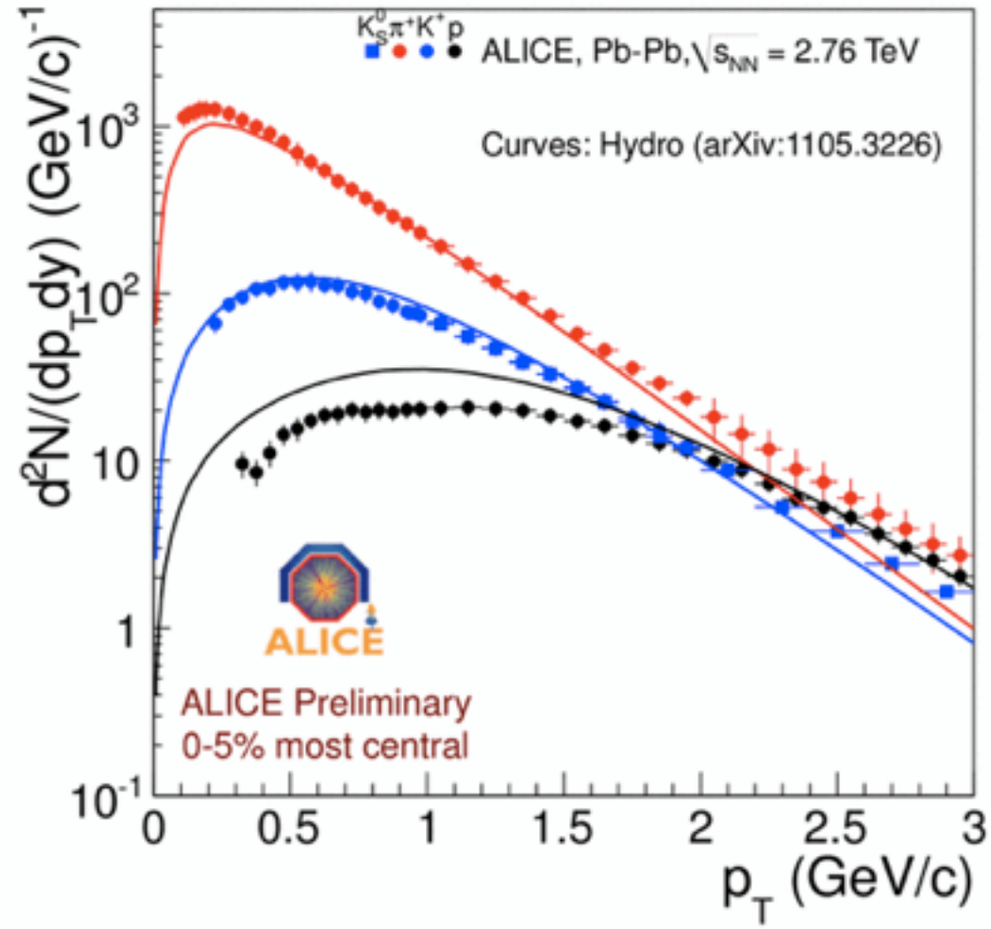

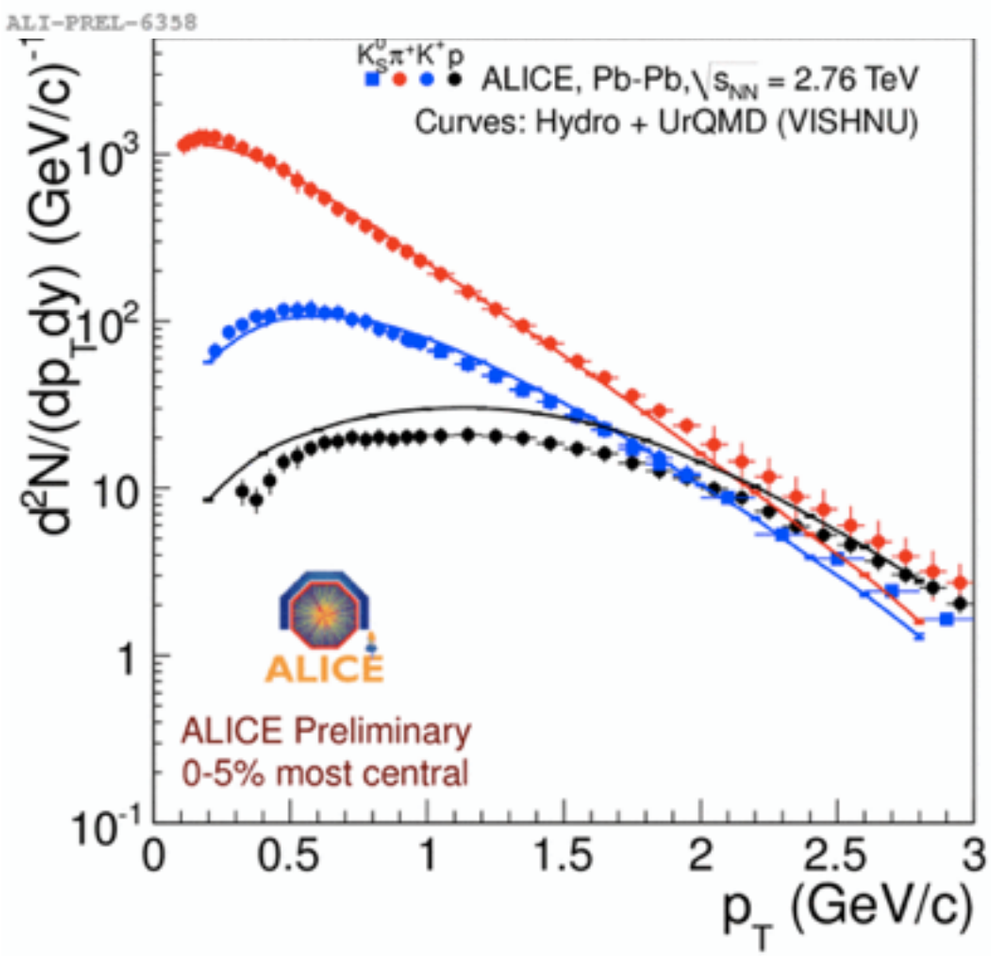

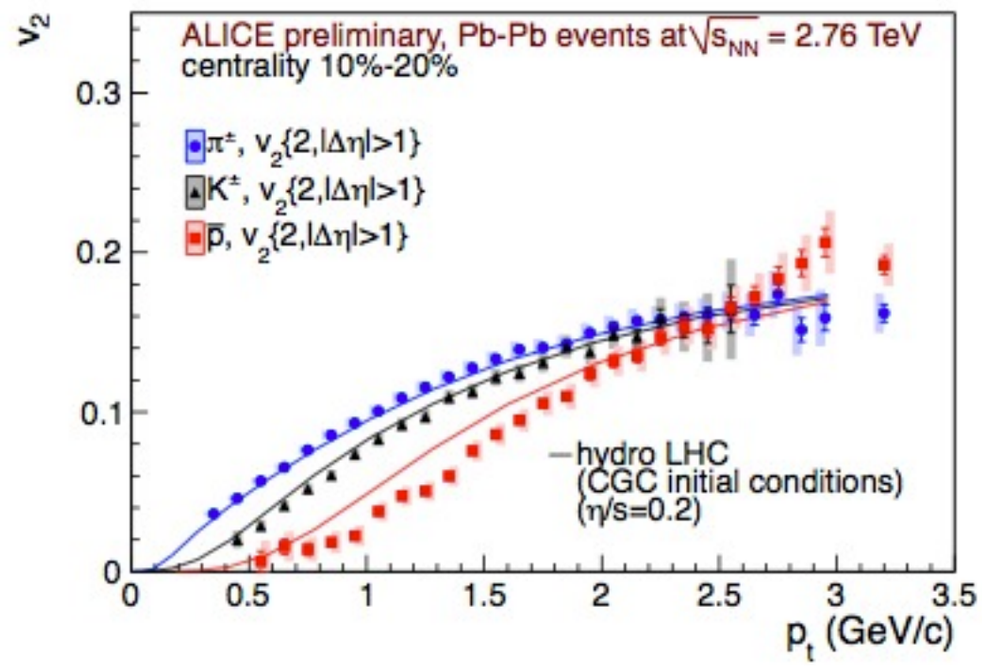

Raimond Snellings
arXiv:1106.6284v2

hydro: Shen et al.,
Phys. Rev. C 84, 044903

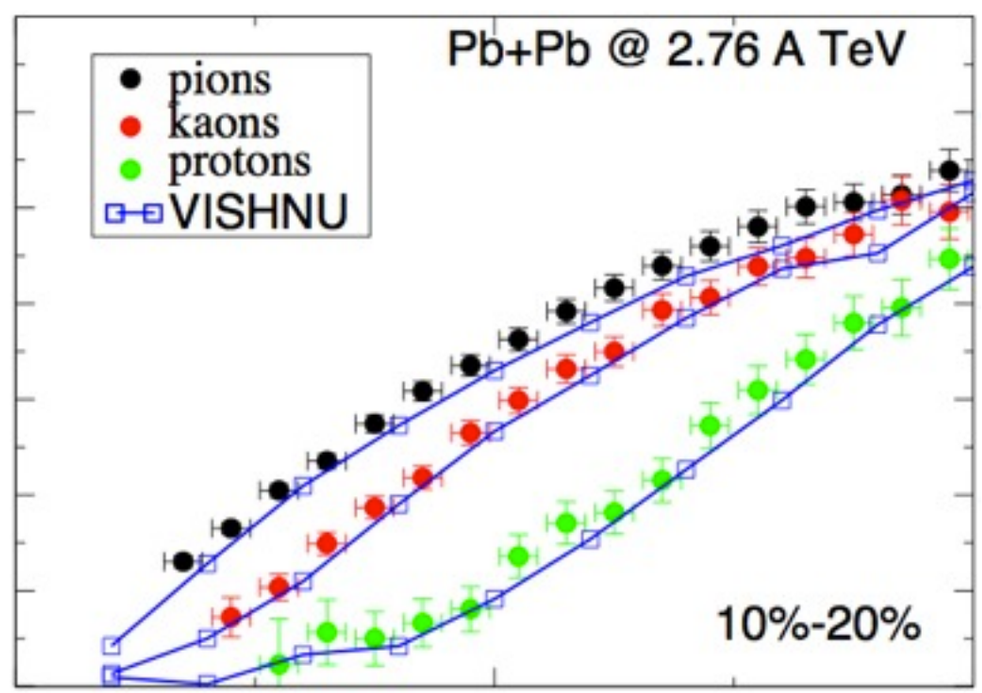

Improved by VISHNU

Heinz, Shen, Song,
AIP Conf.Proc. 1441
(2012) 766-770

More advanced Hybrid Approach

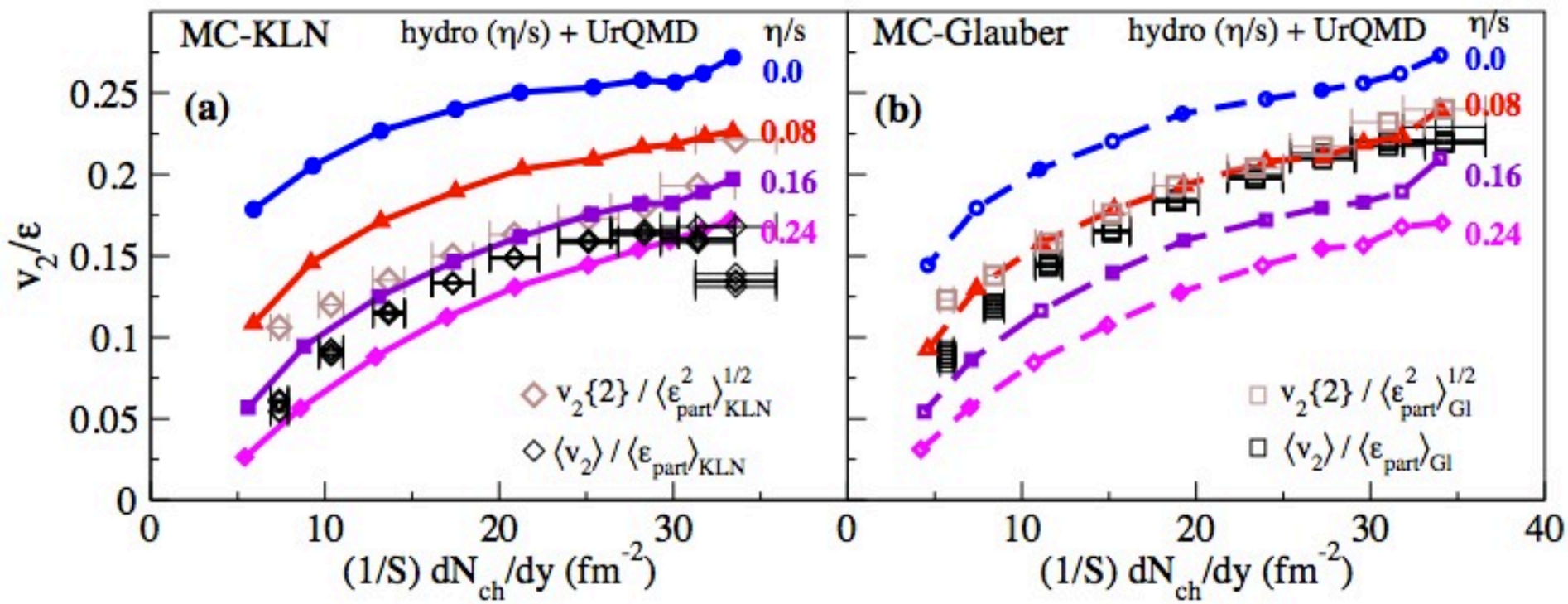

Song et al.
PRL106 (2011)192301

$$\mathbf{1 < 4\pi(\eta/s)_{QGP} < 2.5}$$

- $v_2^{\rm ch}/\varepsilon_x$ vs. $(1/S)(dN_{\rm ch}/dy)$ is "universal", which only depends on η/s .
- Dominant source of uncertainty: $\varepsilon_x^{\rm Gl}$ vs. $\varepsilon_x^{\rm KLN}$

Elliptic and Triangular Flow

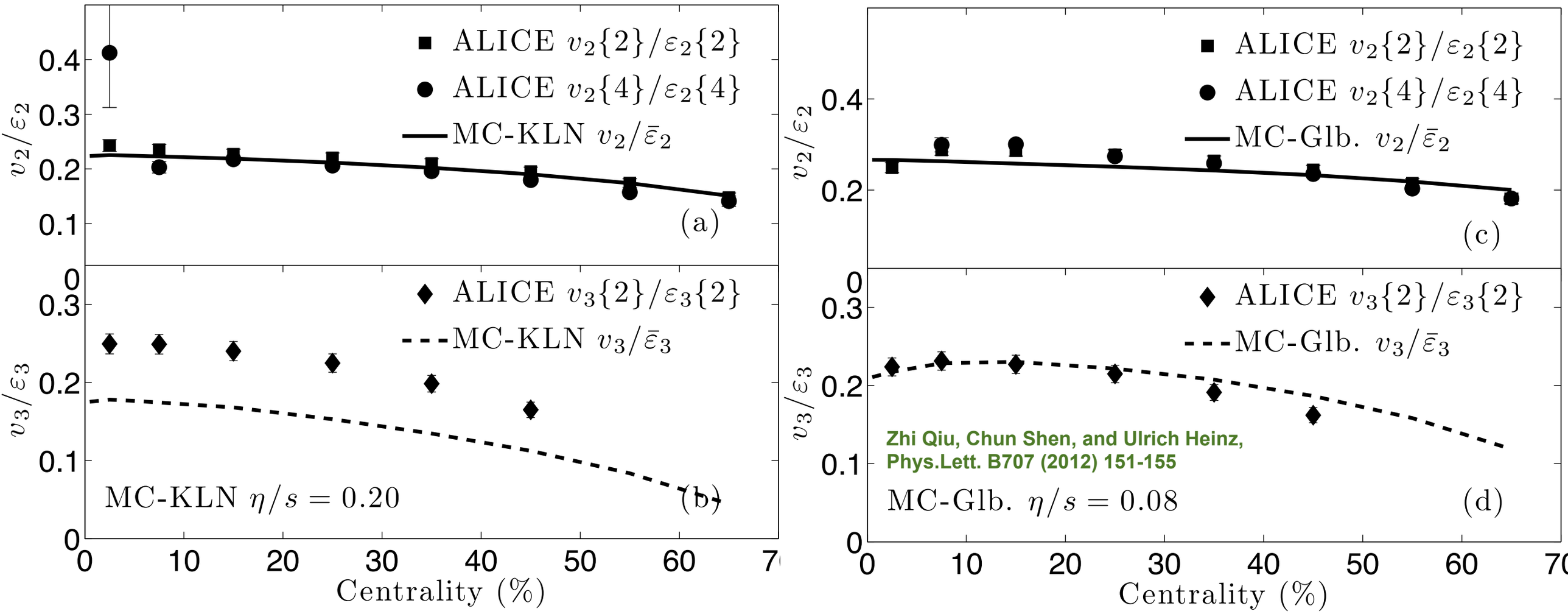

- By tuning η/s, both models can describe elliptic flow of all charged hadrons at LHC energy
- **MCKLN** underestimates v_3/ϵ_3 by 30%, while **MCGlb** gives fairly good agreement with ALICE data

Little Bang

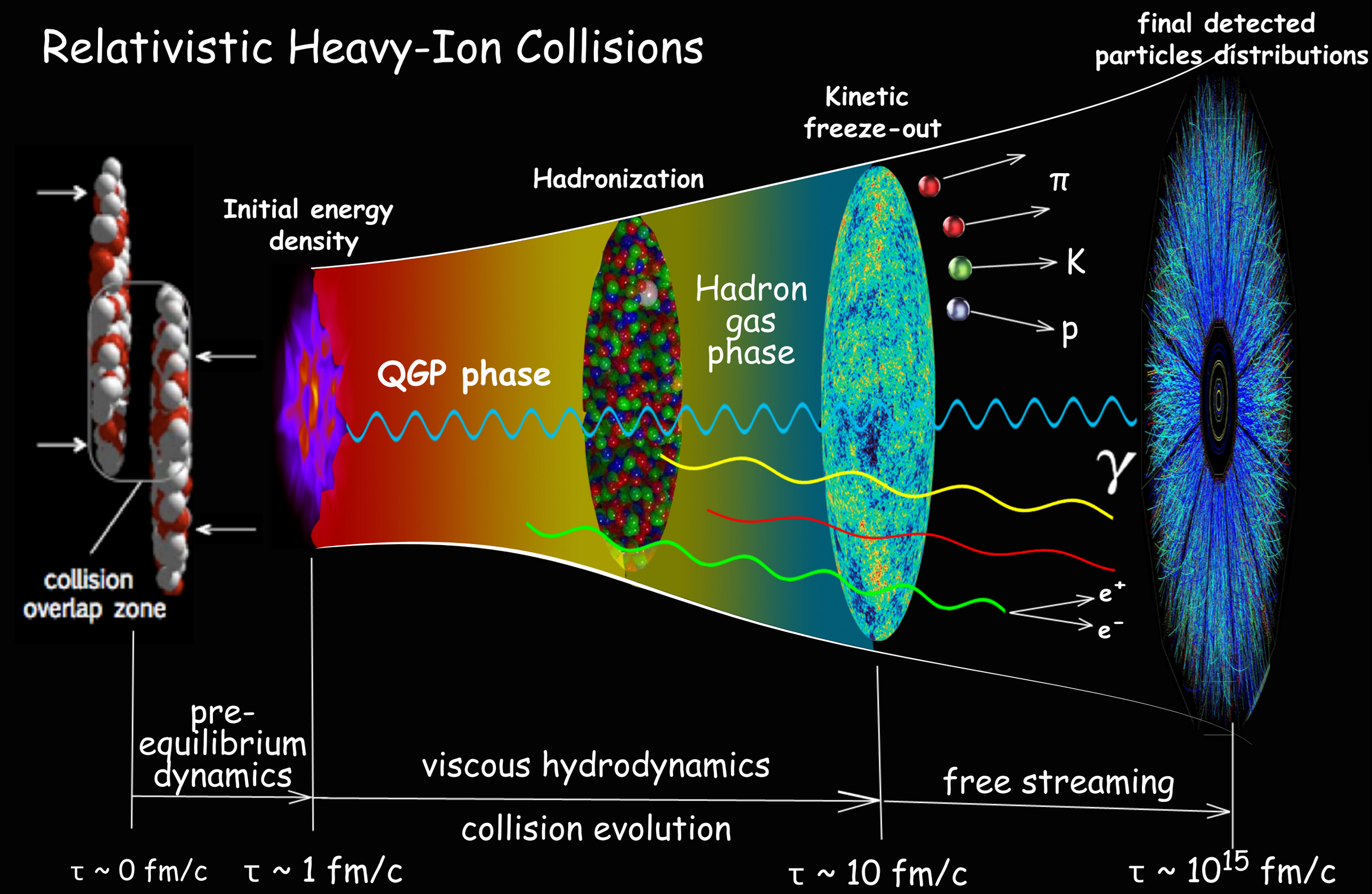
Relativistic Heavy-Ion Collisions
final detected particles distributions
Kinetic freeze-out
Hadronization
Initial energy density
Hadron gas phase
QGP phase
π
K
p
γ
e+
e−
collision overlap zone
pre-equilibrium dynamics
viscous hydrodynamics
free streaming
collision evolution
τ ~ 0 fm/c
τ ~ 1 fm/c
τ ~ 10 fm/c
τ ~ 10^15 fm/c

Hydro evolution

In Collaboration with visualization framework by MADAI collaboration, funded by the NSF under grant# NSF-PHY-09-41373

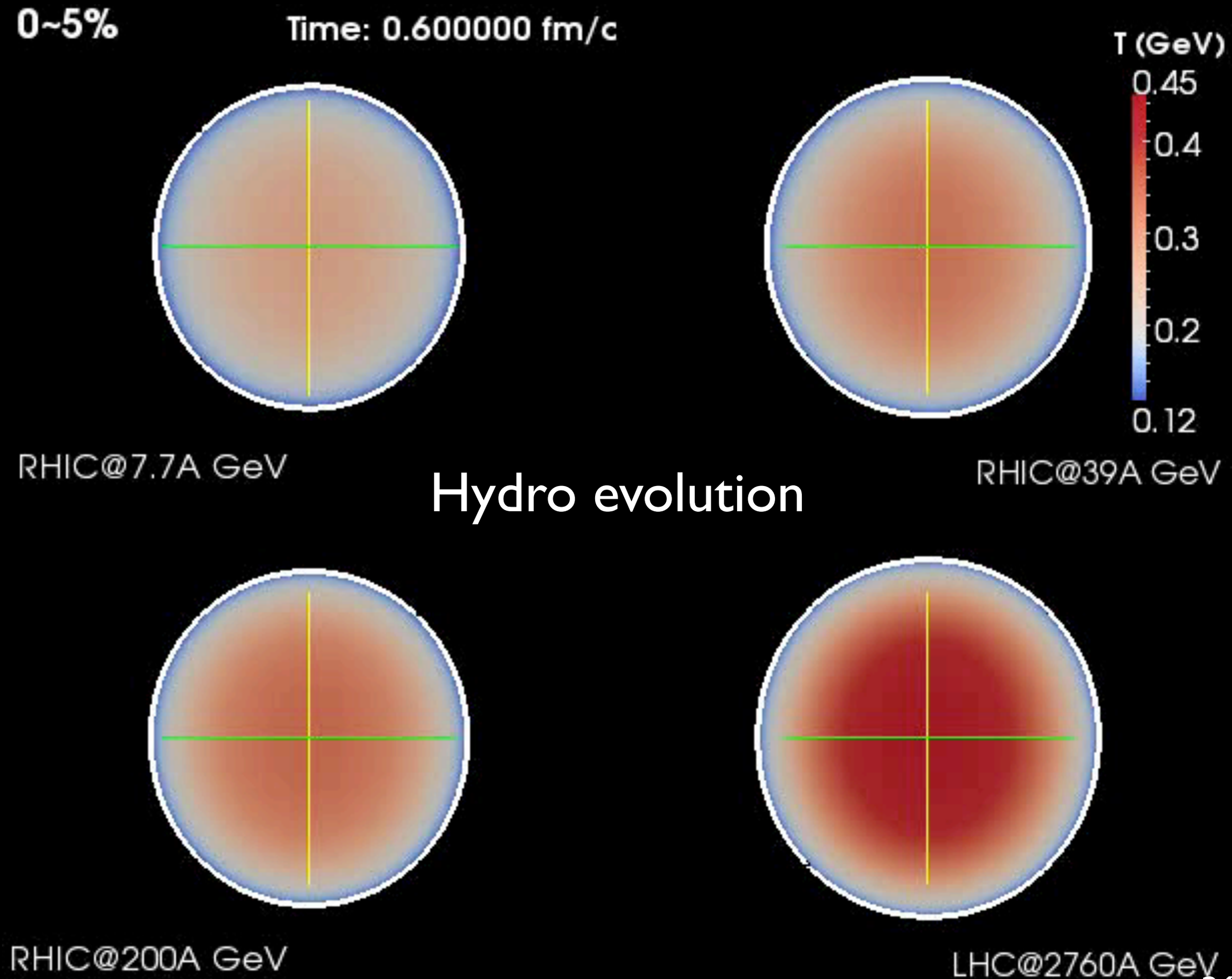

Hydro evolution

In Collaboration with visualization framework by MADAI collaboration, funded by the NSF under grant# NSF-PHY-09-41373

Global Observables

Collision energy (A GeV)	T_0 (MeV)	life time (fm/c)	produced particles per rapidity unit
AuAu@ 7.7	269.2	9.3	212.3
AuAu@ 11.5	287.5	10.0	266.7
AuAu@ 17.7	304.8	10.5	325.3
AuAu@ 19.6	308.7	10.6	339.2
AuAu@ 27	320.1	10.9	382.9
AuAu@ 39	332.2	11.2	432.7
AuAu@ 63	341.1	11.4	472.0
AuAu@ 200	378.6	12.2	661.9
PbPb@ 2760	485.2	14.2	1575.7

80%

50%

600%

$1\text{MeV} \sim 10^{10} K \quad 1\text{fm/c} \sim 3 \times 10^{-24} s$

Centrality dependence of final charged multiplicity

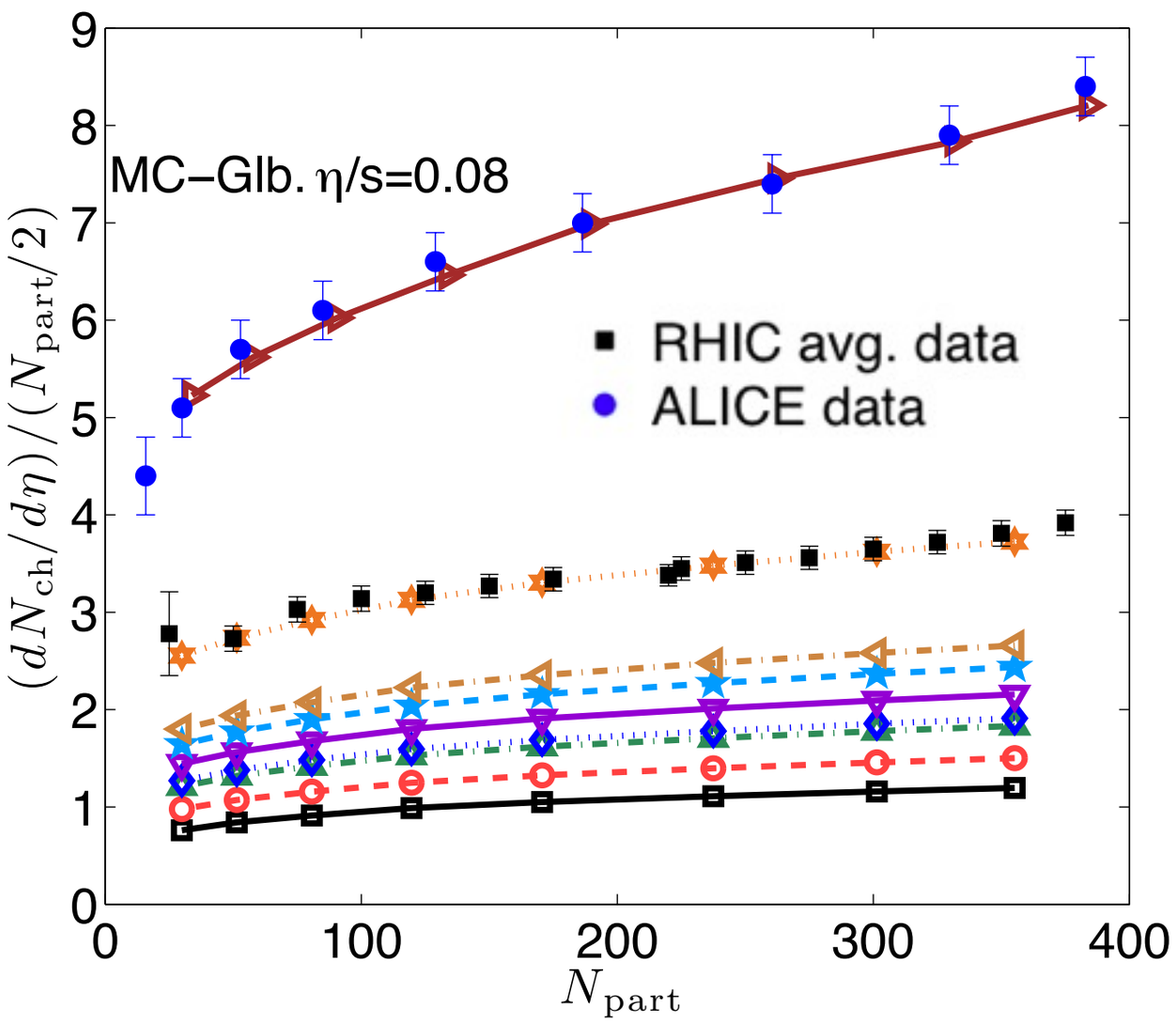

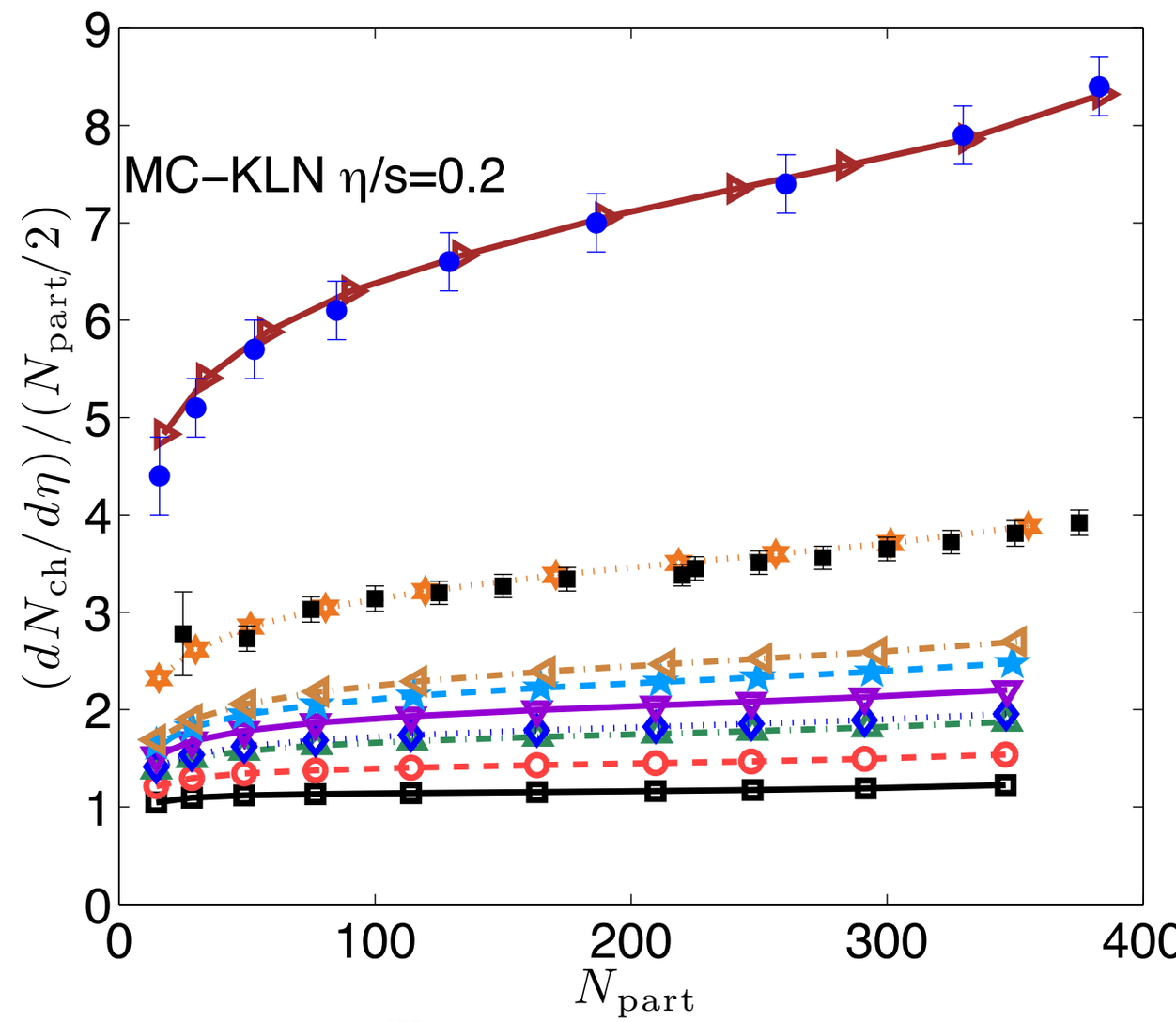

S. Adler *et al.* (PHENIX Collaboration), Phys. Rev. C **71**, 034908 (2005)

K. Aamodt *et al.* (ALICE Collaboration), Phys. Rev. Lett. **106**, 032301 (2011)

- $\sqrt{s} = 7.7$A GeV
- $\sqrt{s} = 11.5$A GeV
- $\sqrt{s} = 17.7$A GeV
- $\sqrt{s} = 19.6$A GeV
- $\sqrt{s} = 27$A GeV
- $\sqrt{s} = 39$A GeV
- $\sqrt{s} = 63$A GeV
- $\sqrt{s} = 200$A GeV
- PbPb $\sqrt{s} = 2760$A GeV

Centrality dependence of final charged multiplicity
Shape comparison

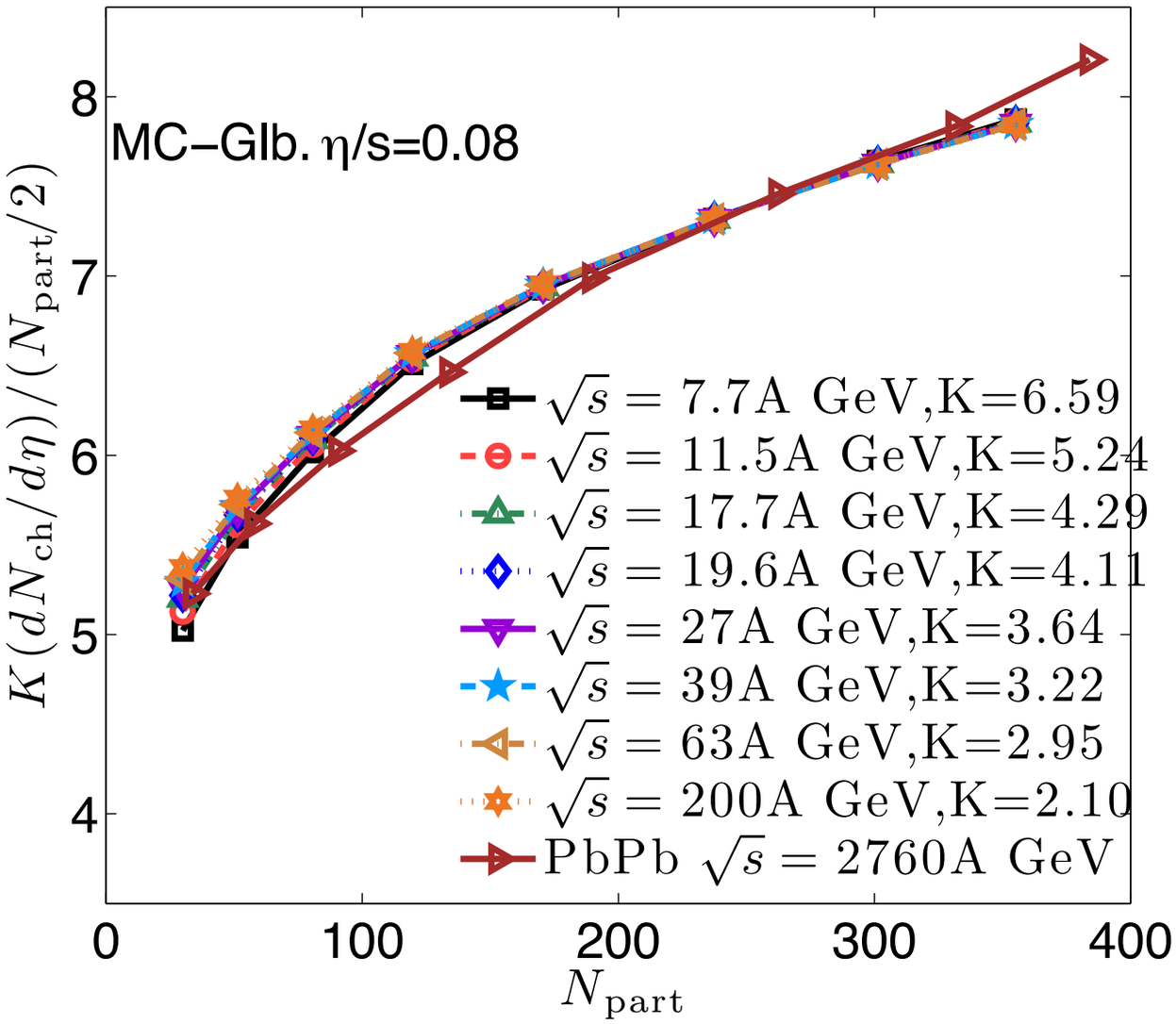

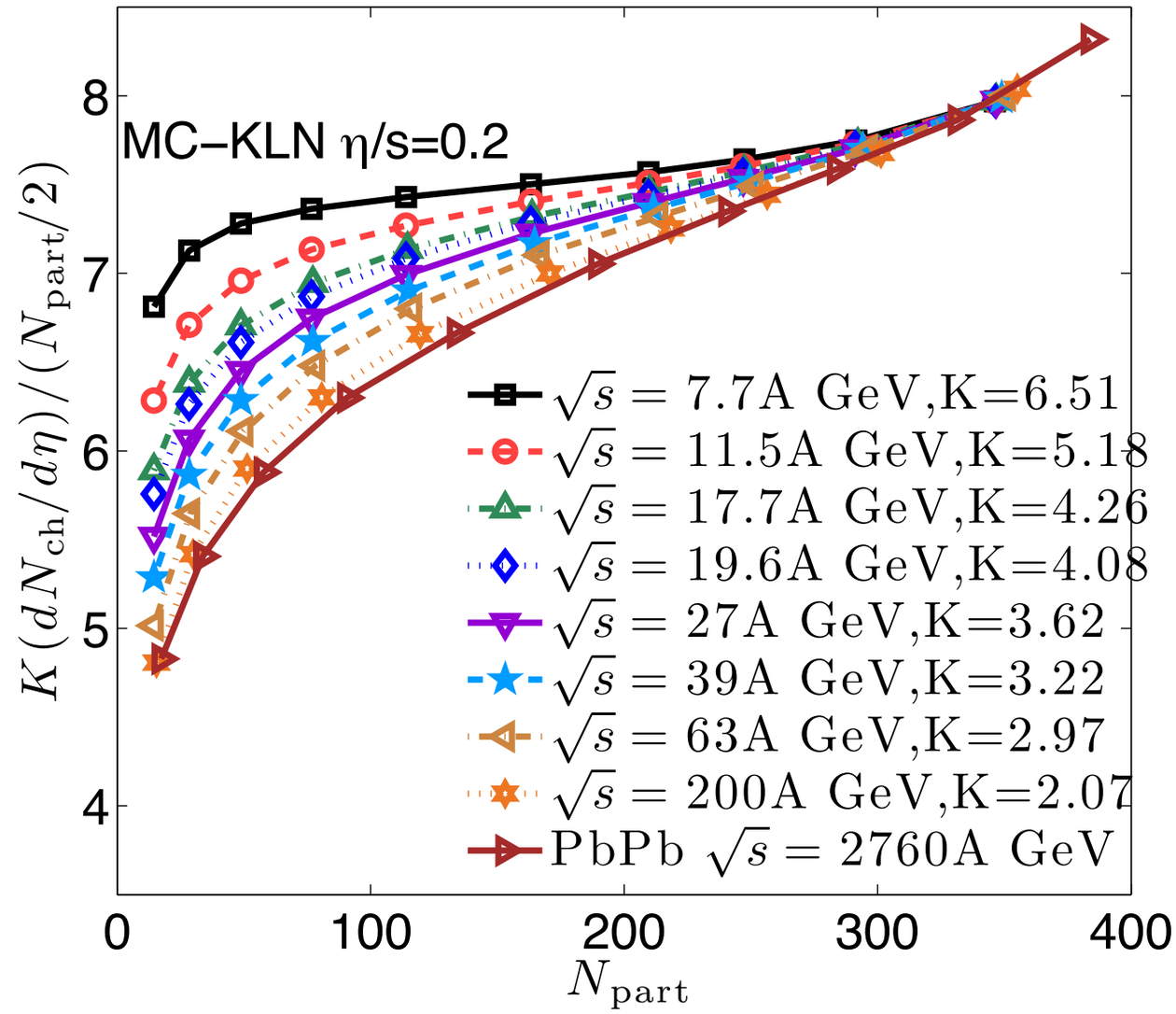

Centrality dependence of final charged multiplicity
Shape comparison

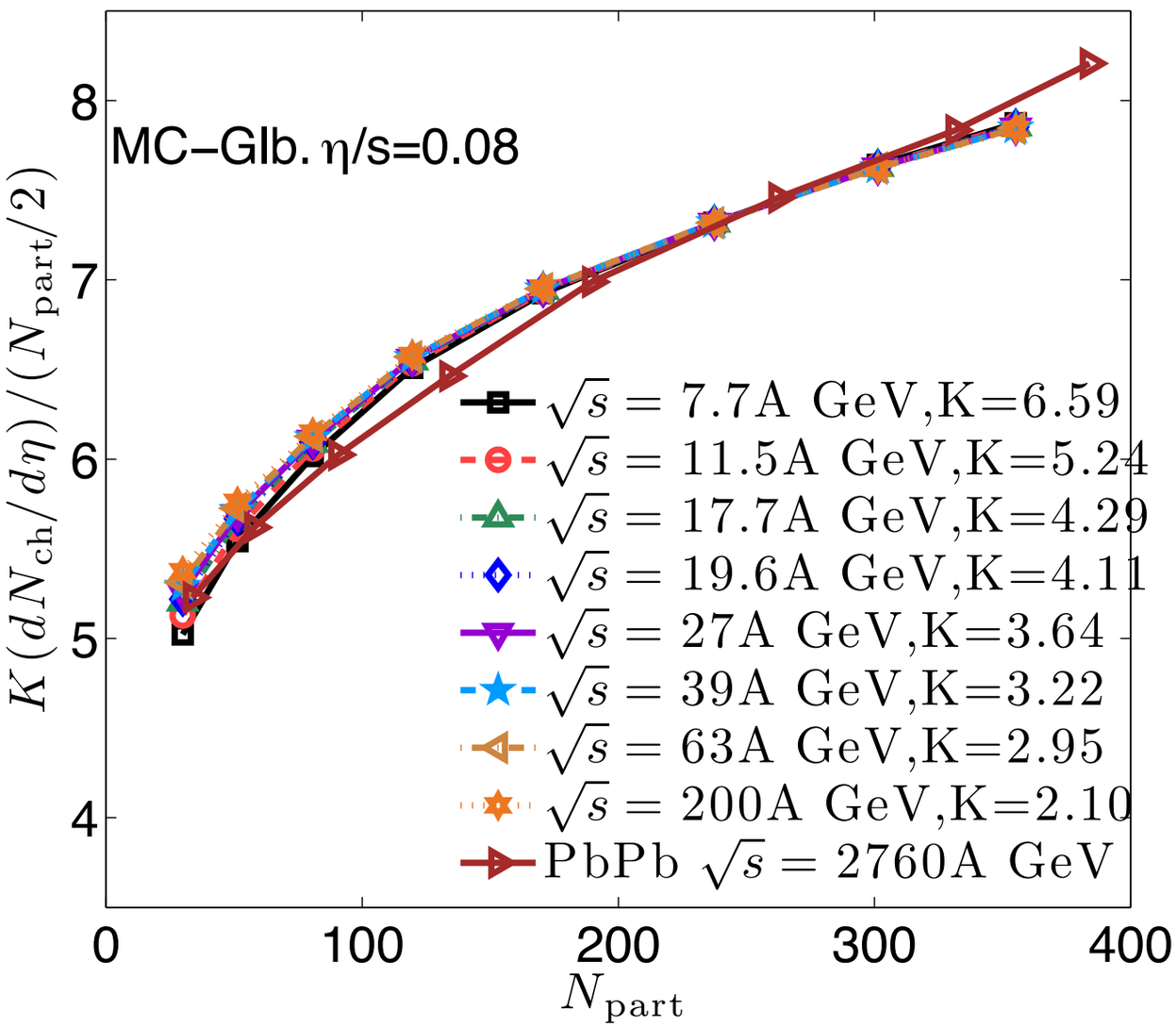

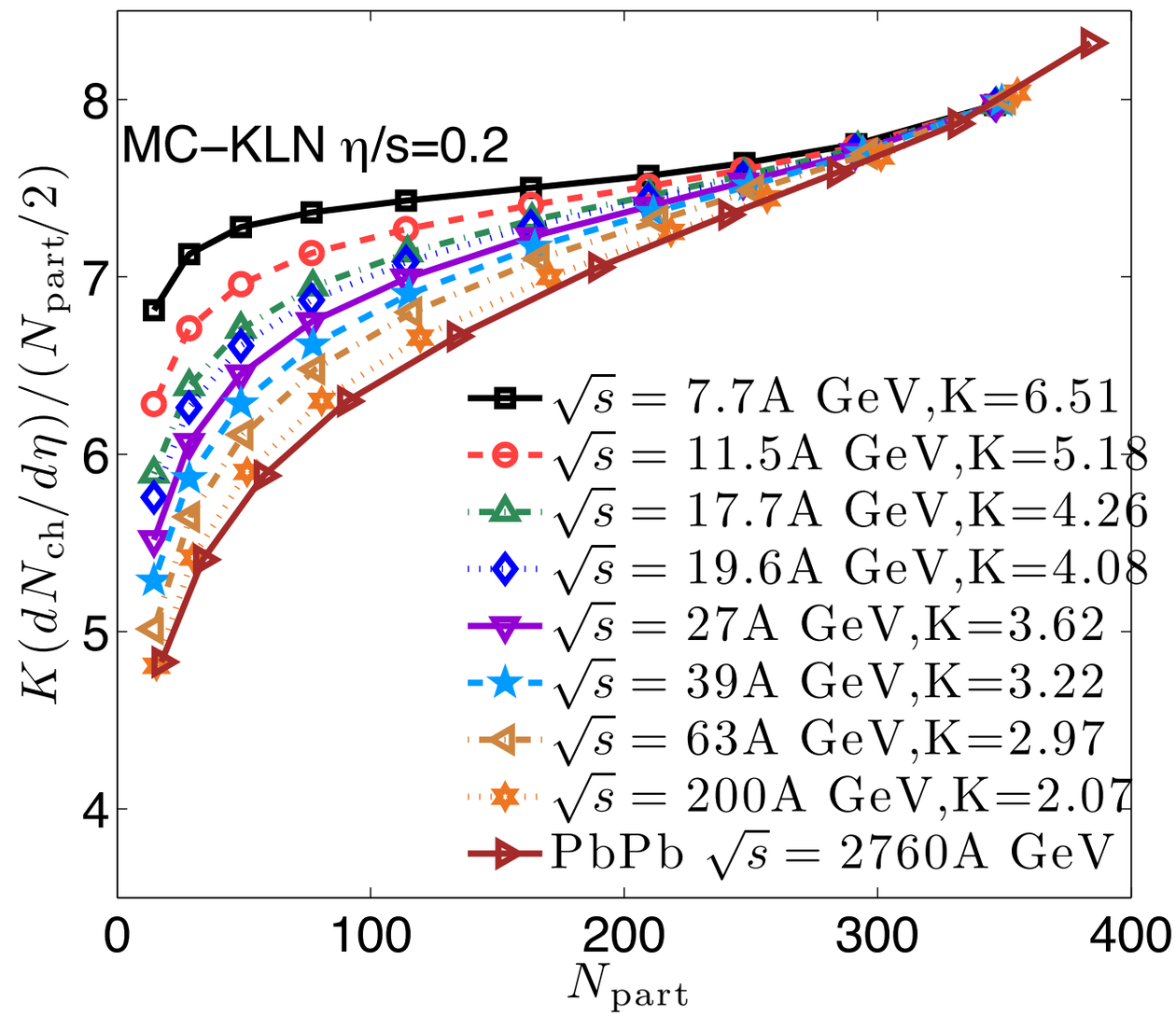

MC-Glb. shows good scaling behavior (fixed hard/soft ratio α)

MC-KLN: the slope of the curves get flatter as we go to the lower collision energy (not a viscous effect!)

radial flow and particle p_T-spectra

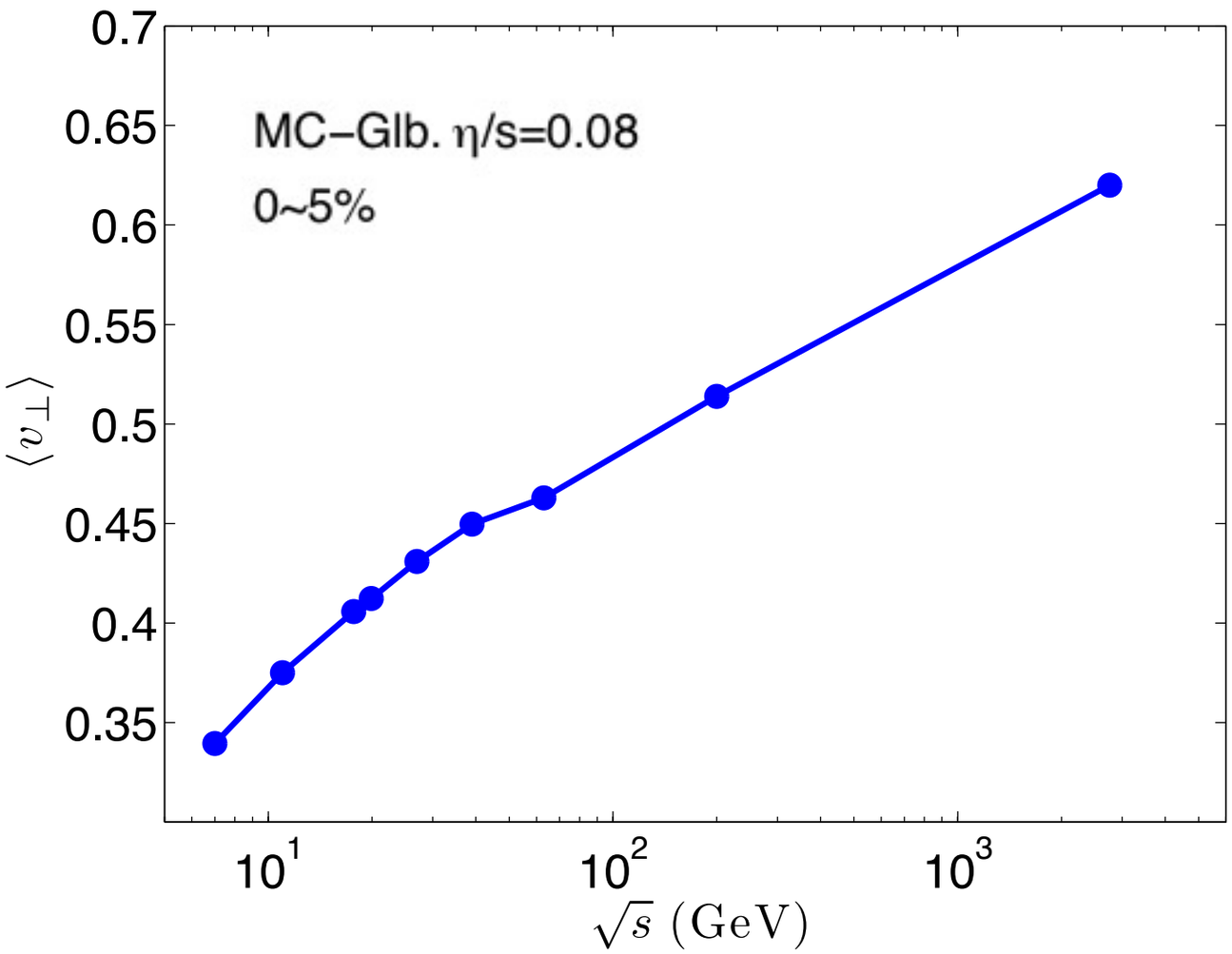

Along with $\sqrt{s}$

average radial flow $\langle v_\perp \rangle$ increases by 80%

radial flow and particle p_T-spectra

$\langle v_\perp \rangle$ increases by 80%

radial flow and particle pT-spectra

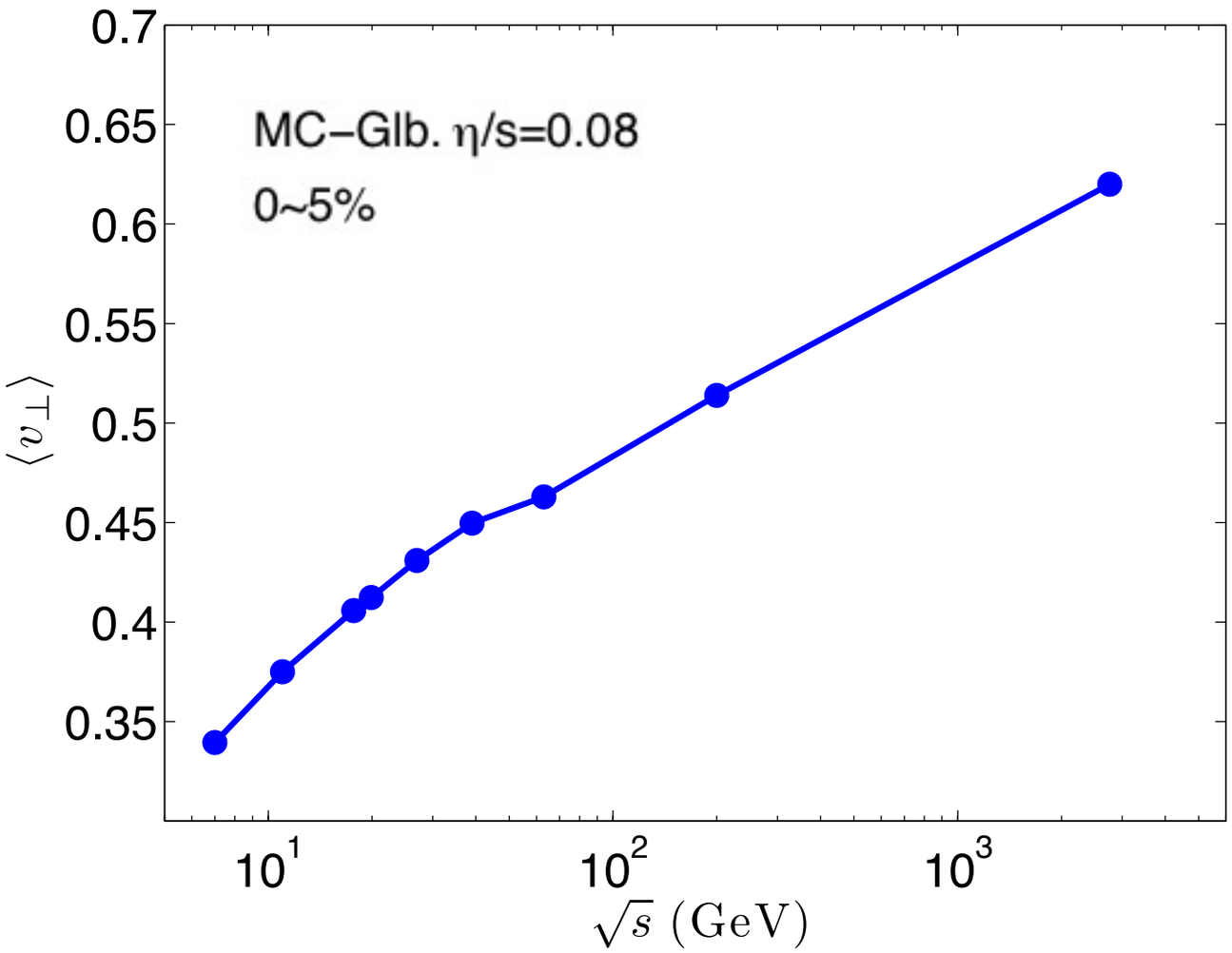

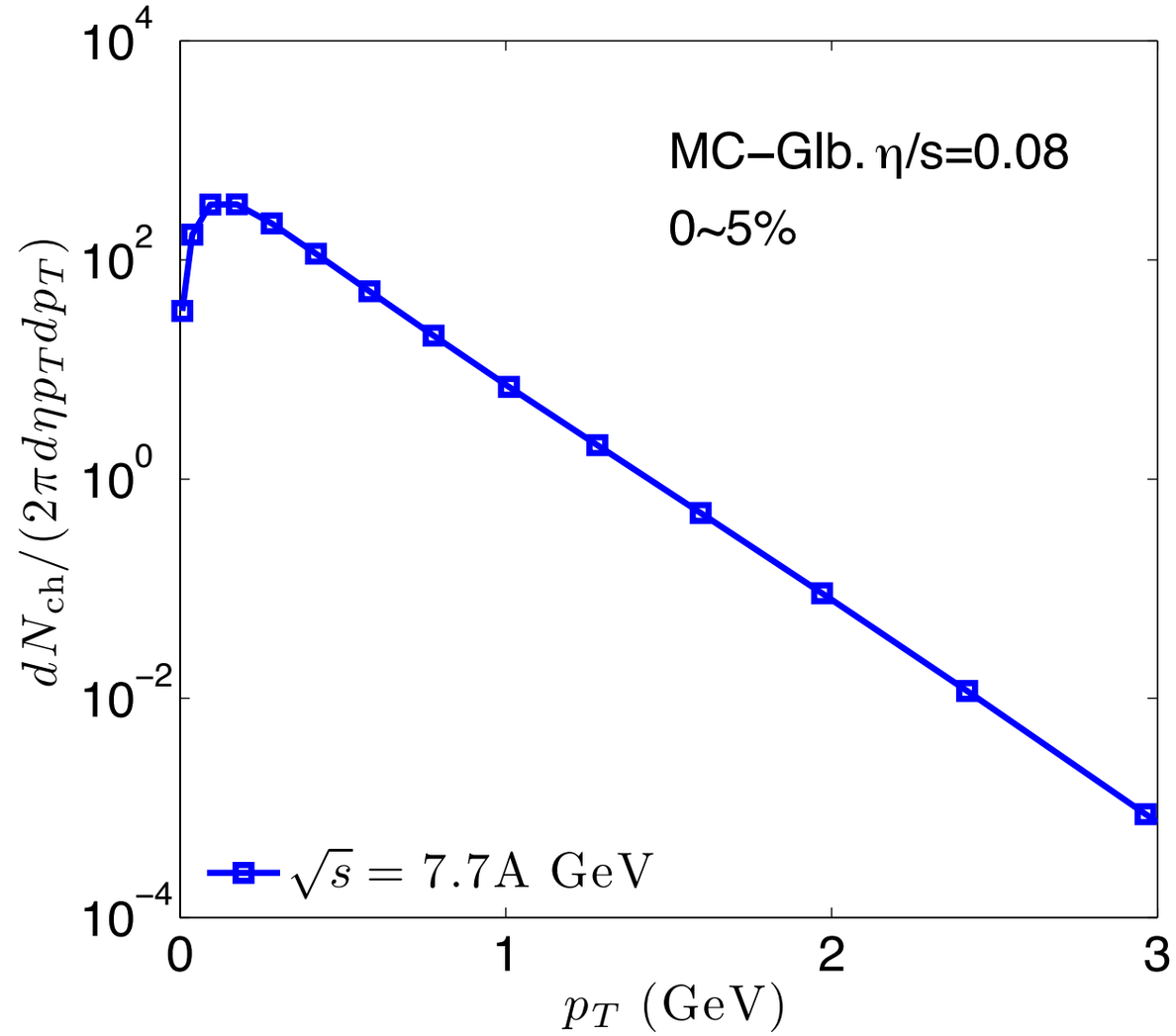

Along with $\sqrt{s}$

average radial flow $\langle v_\perp \rangle$ increases by 80%

the slope of particle pT-spectra gets flatter

radial flow and particle p_T-spectra

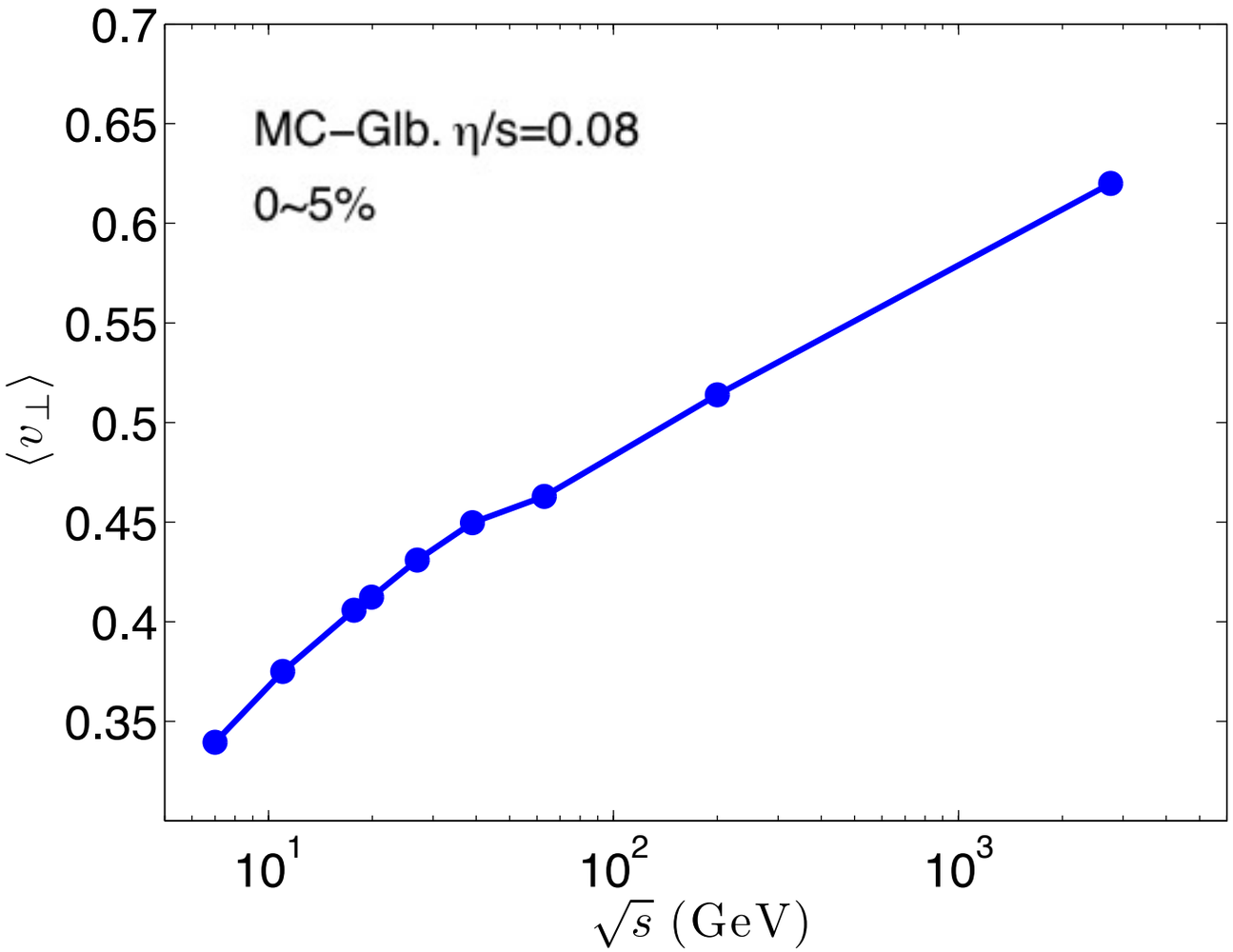

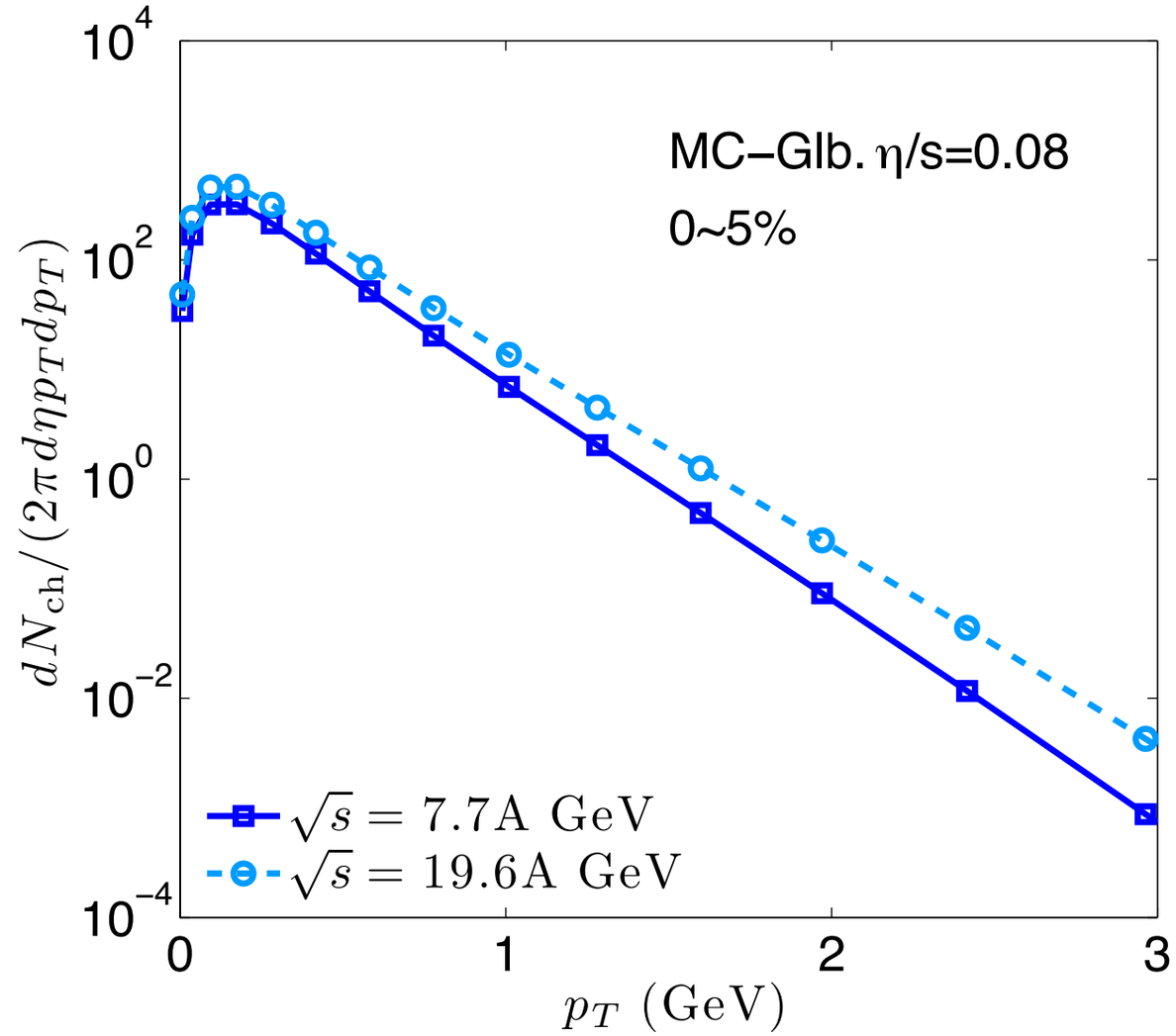

Along with $\sqrt{s}$

average radial flow $\langle v_\perp \rangle$ increases by 80%

the slope of particle p_T-spectra gets flatter

radial flow and particle pT-spectra

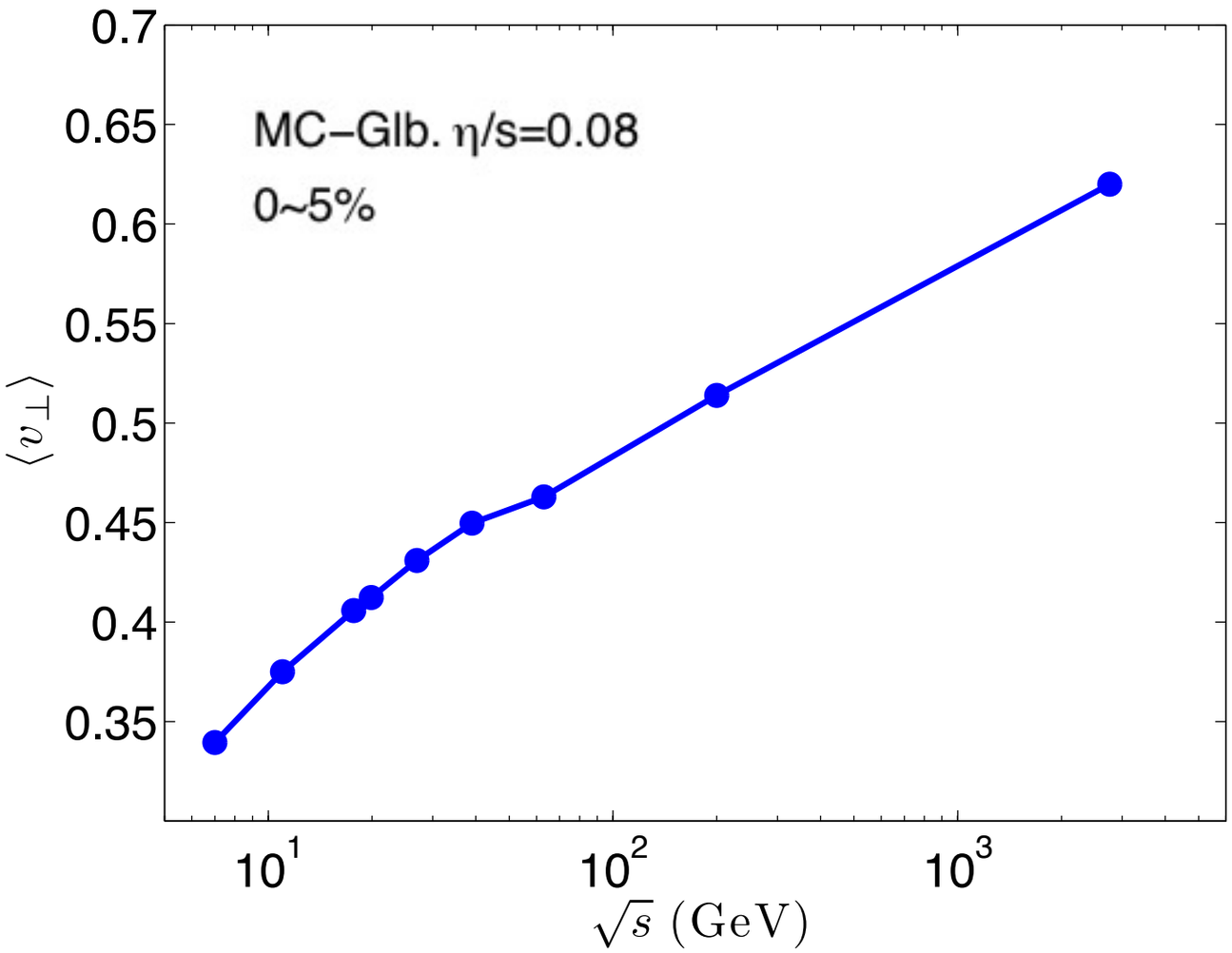

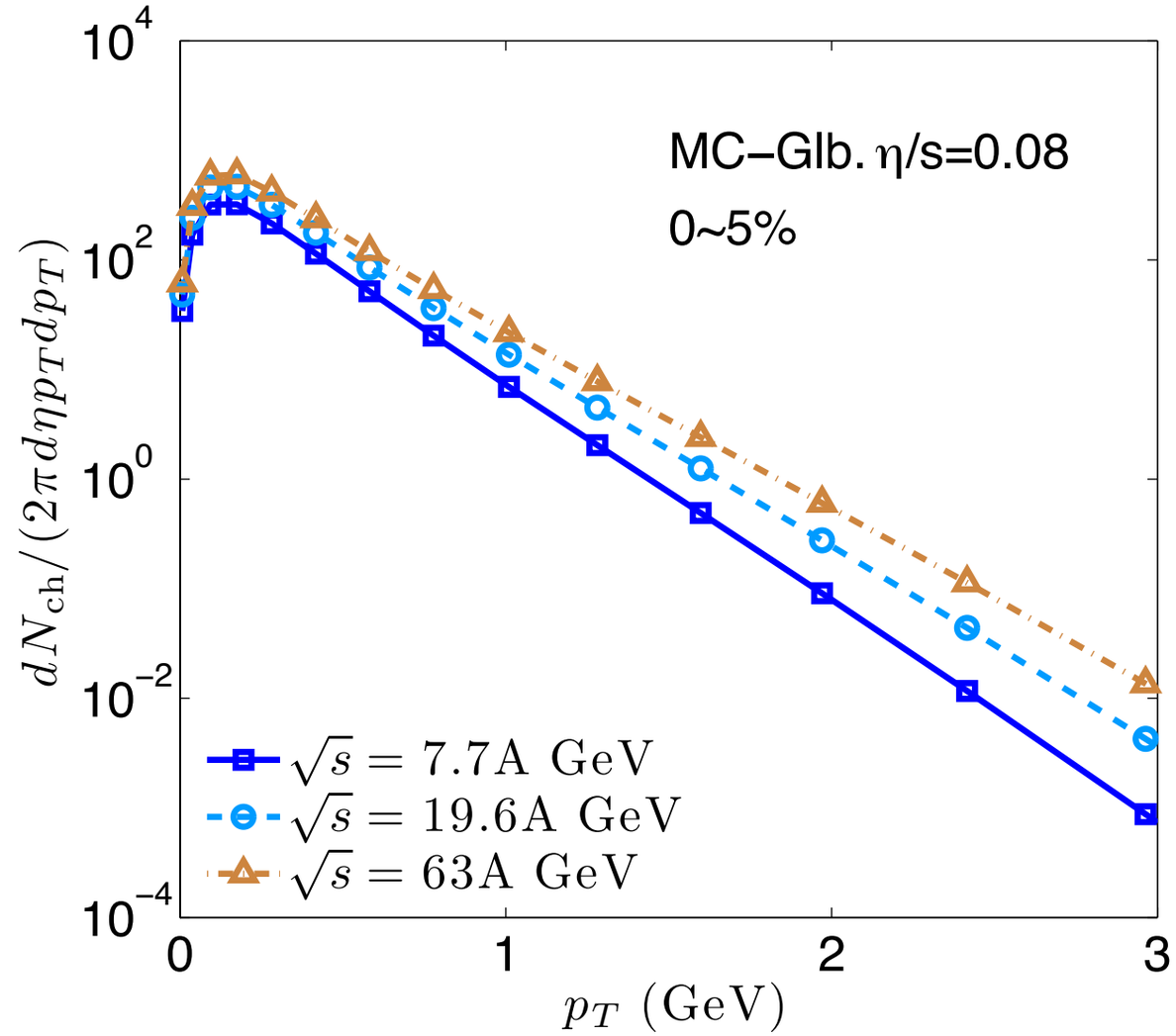

Along with $\sqrt{s}$

average radial flow $\langle v_\perp \rangle$ increases by 80%

the slope of particle pT-spectra gets flatter

radial flow and particle pT-spectra

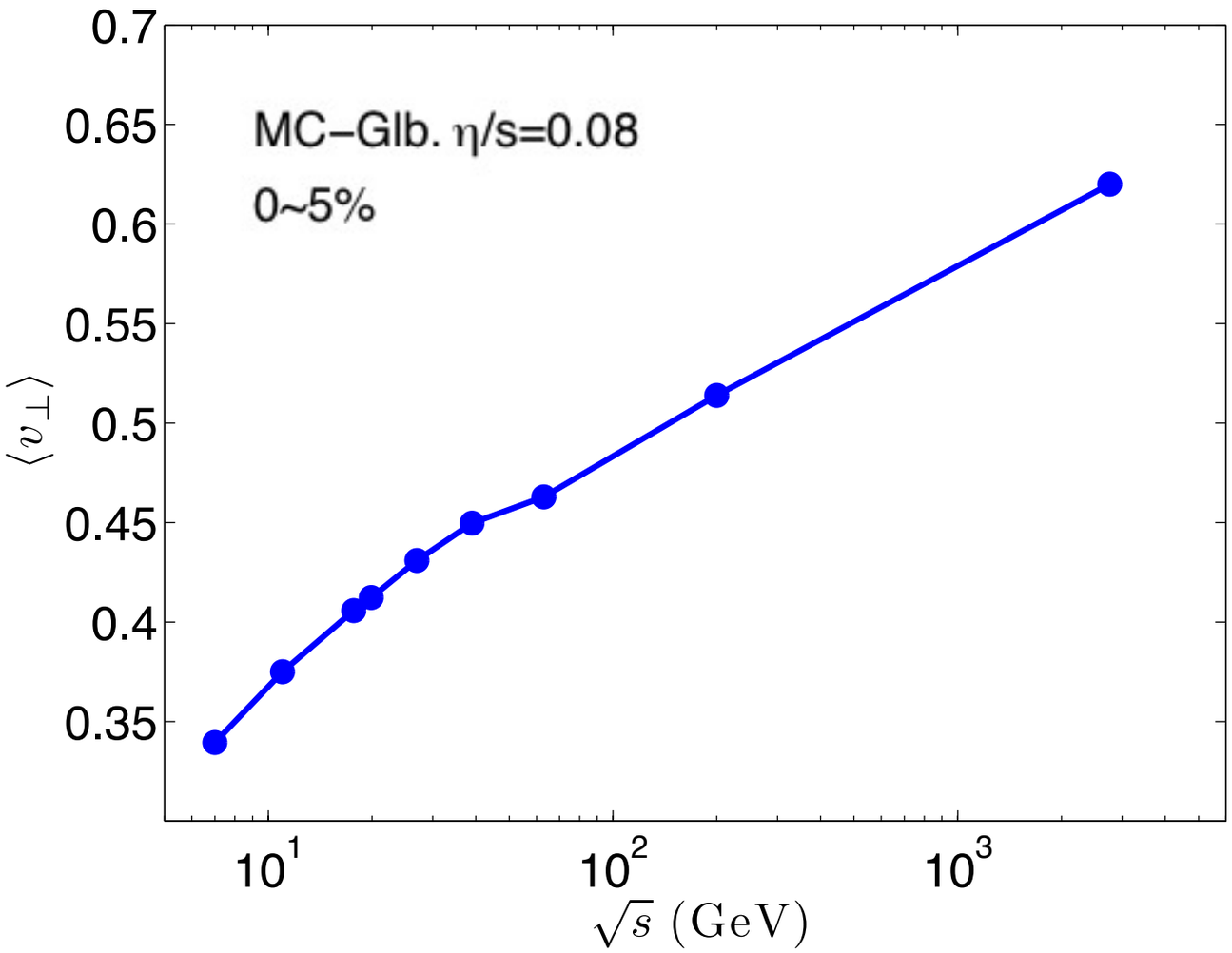

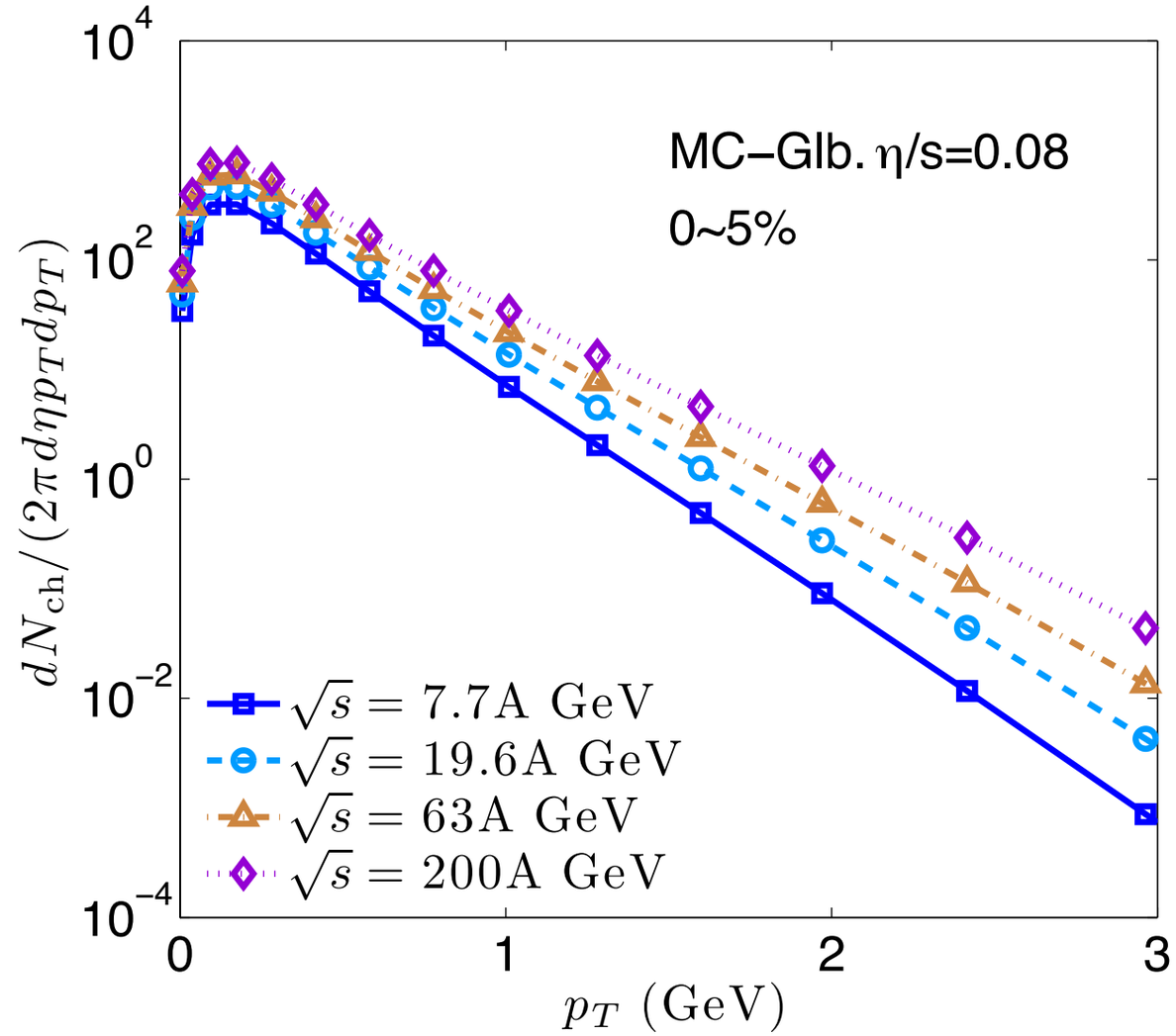

Along with $\sqrt{s}$

average radial flow $\langle v_\perp \rangle$ increases by 80%

the slope of particle pT-spectra gets flatter

radial flow and particle pT-spectra

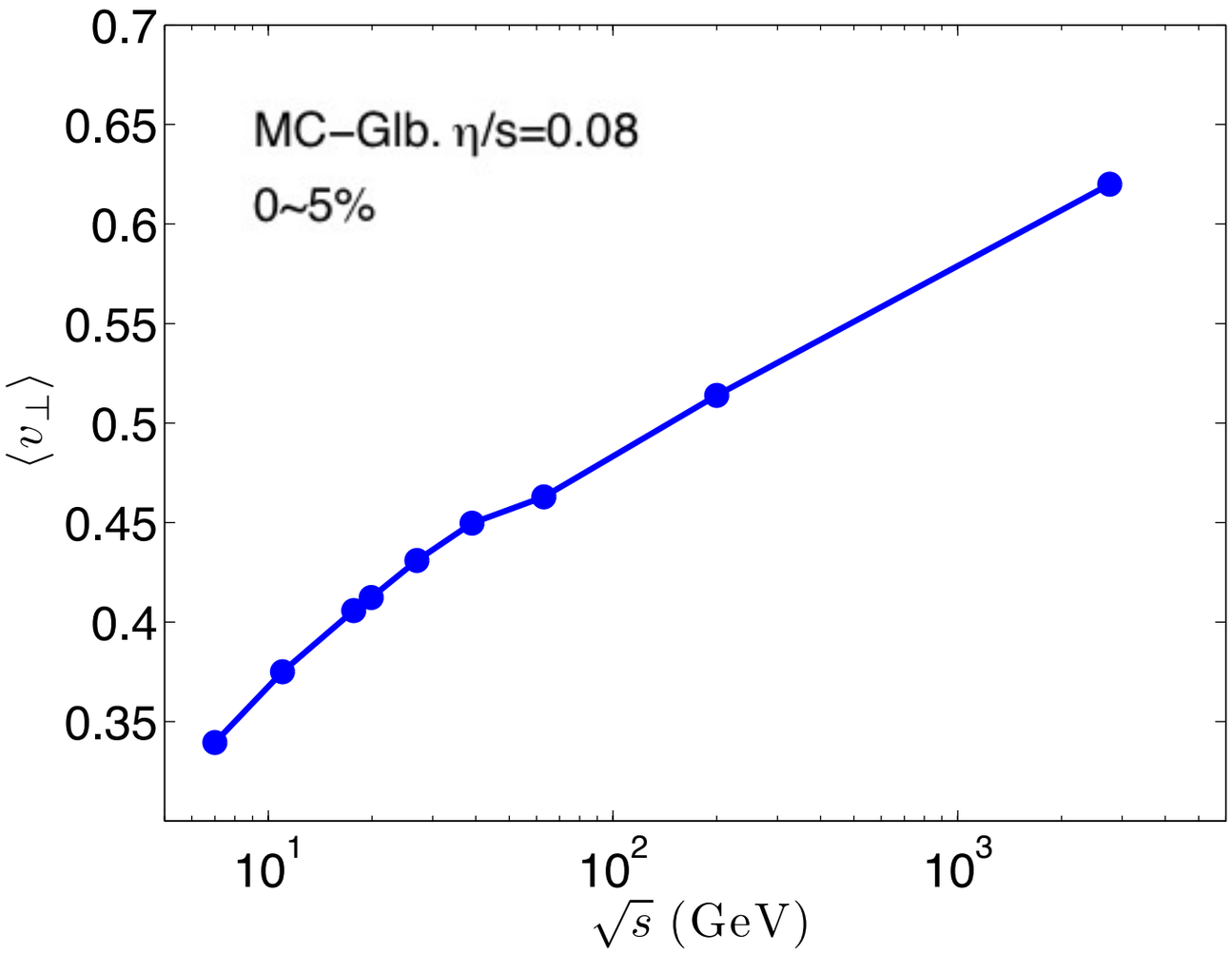

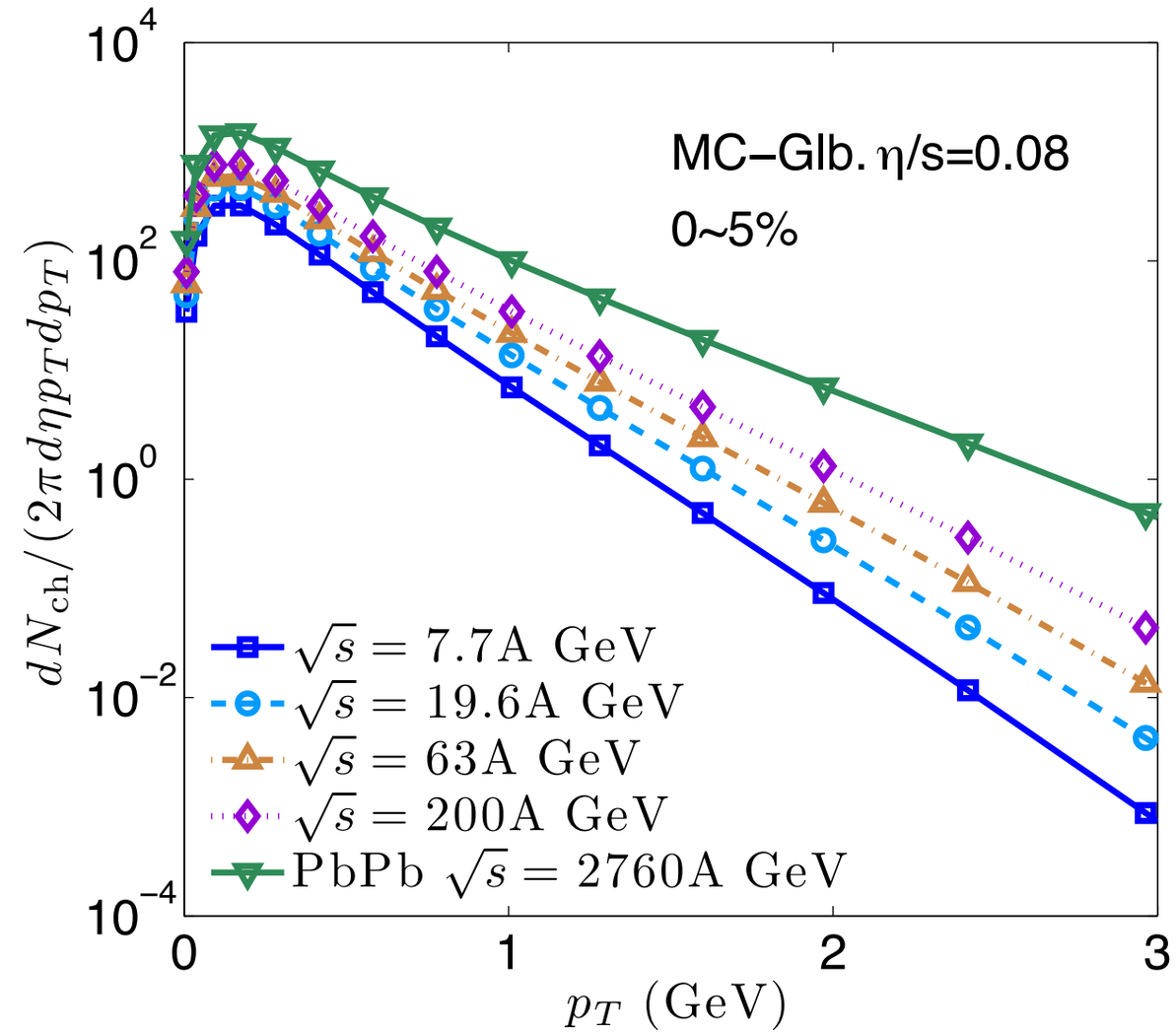

Along with $\sqrt{s}$

average radial flow $\langle v_\perp \rangle$ increases by 80%

the slope of particle pT-spectra gets flatter

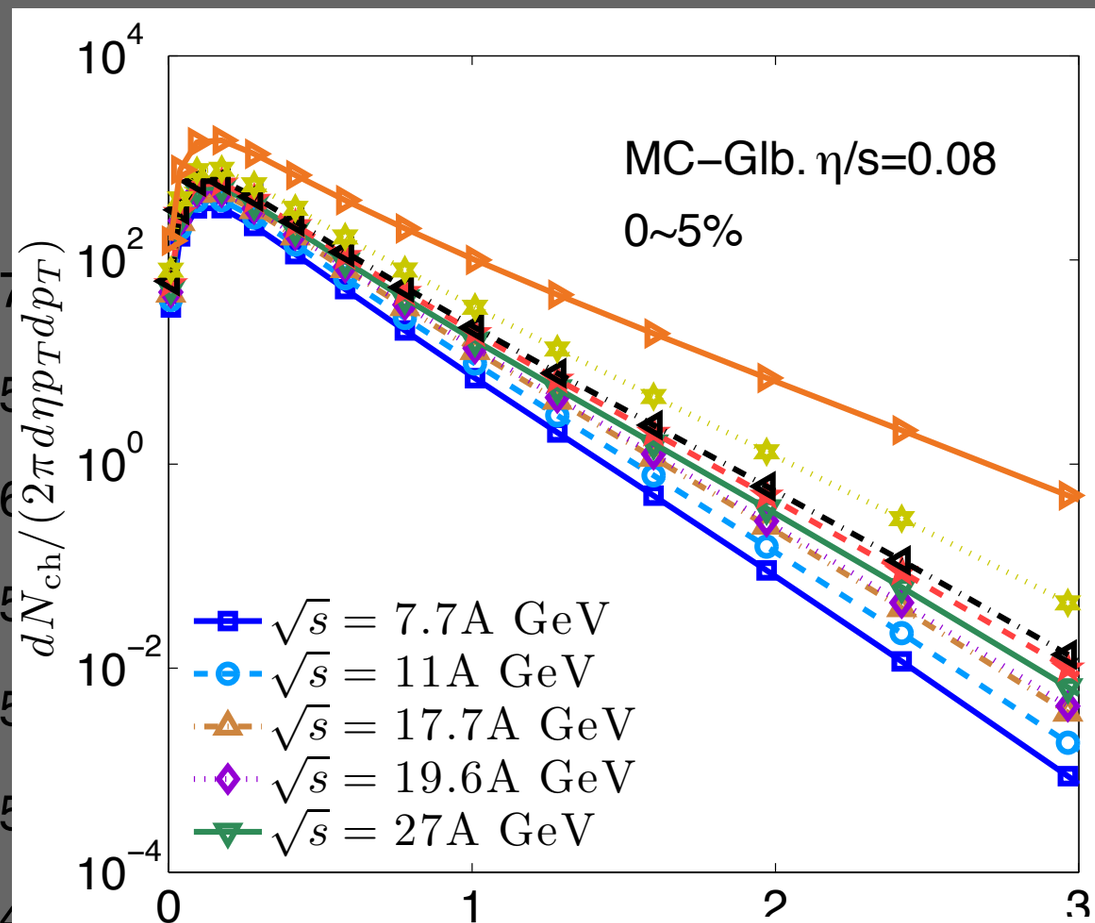

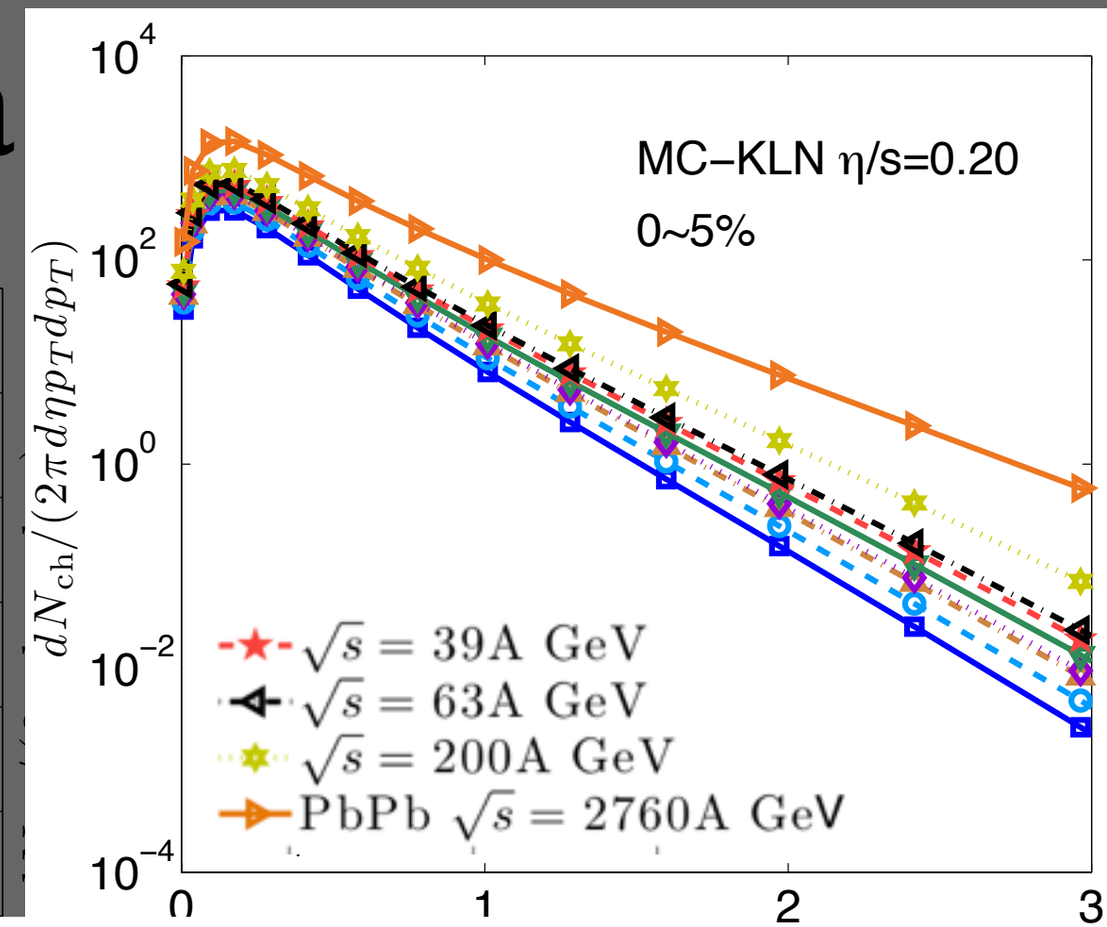

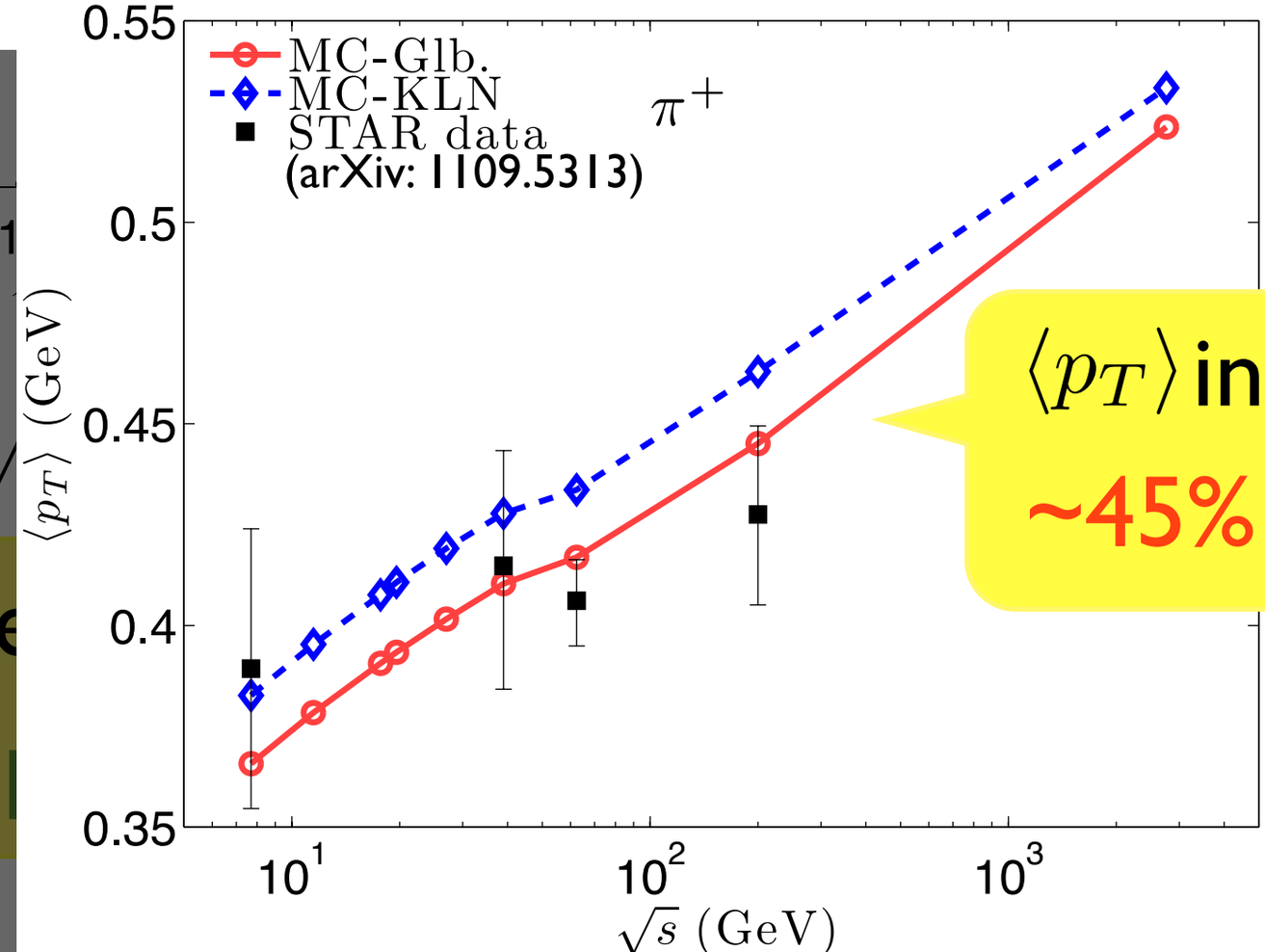

$\langle p_T \rangle$ increases by ~45%

Along with $\sqrt{}$

average

the slop

atter

radial flow and particle p_T-spectra

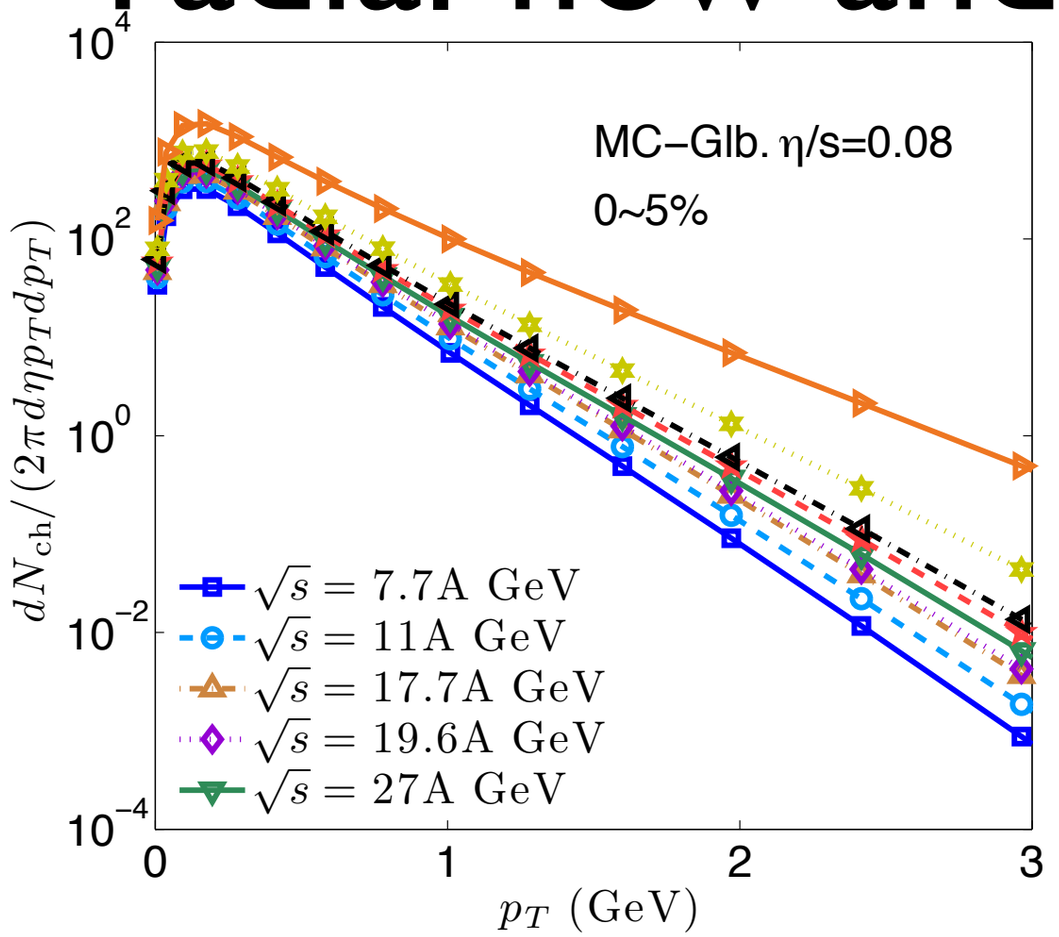

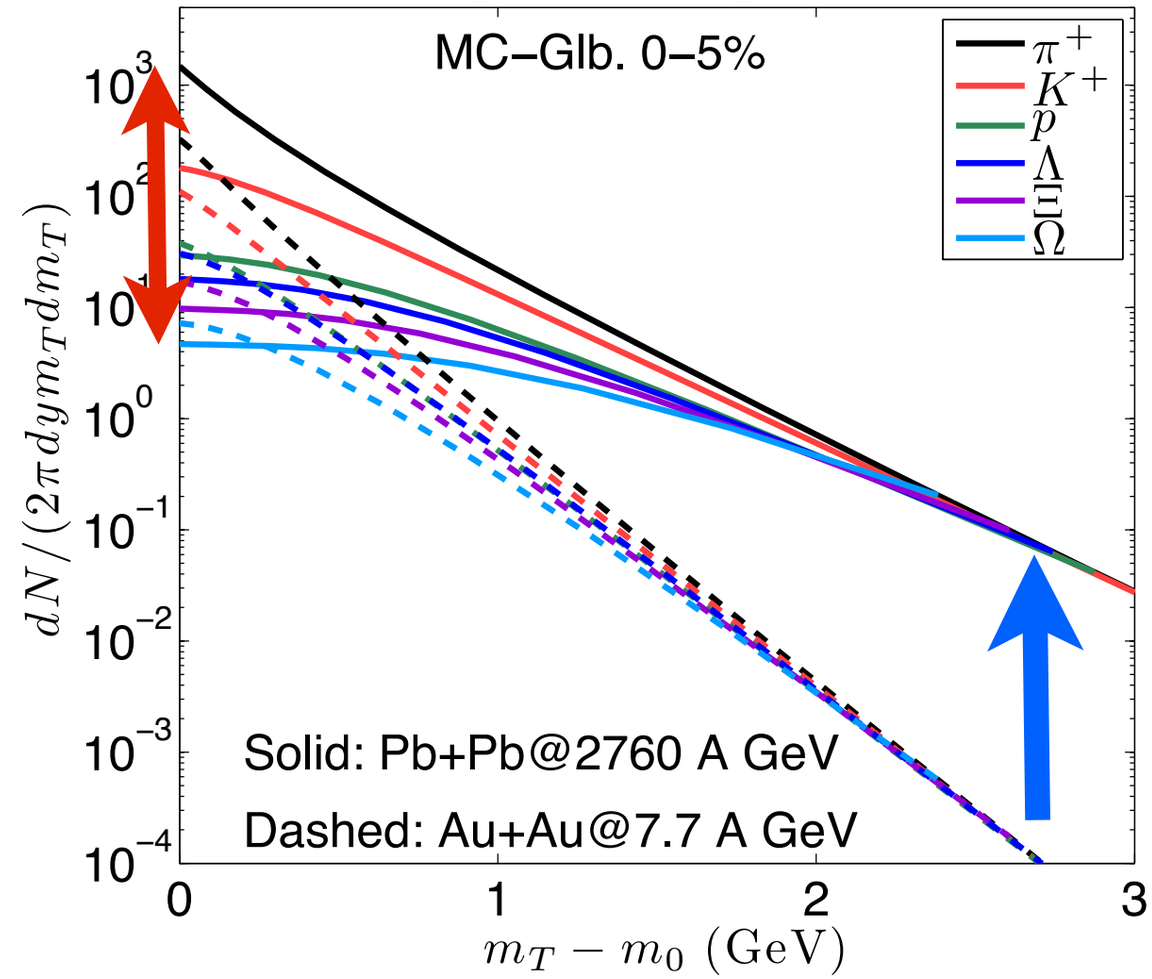

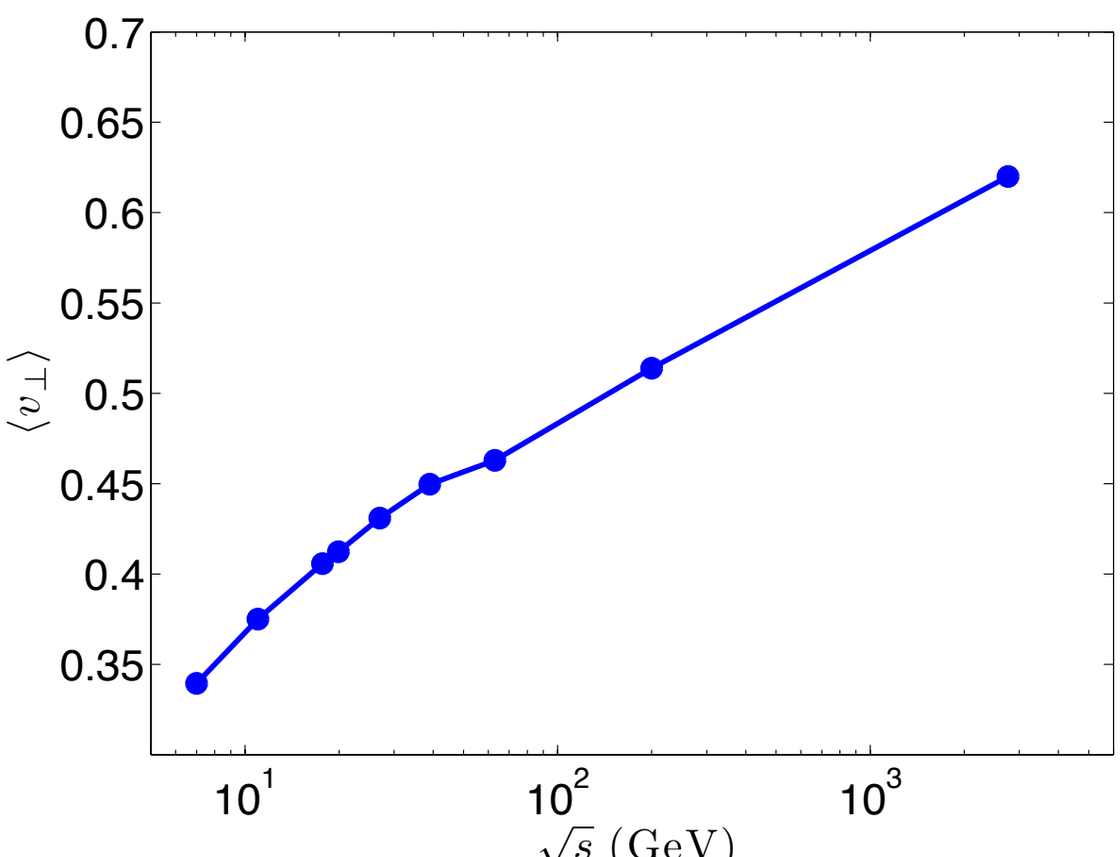

For stronger radial flow:

the slope of the particle spectra get flatter

the splitting between different species of particles get larger

Elliptic flow and v_2

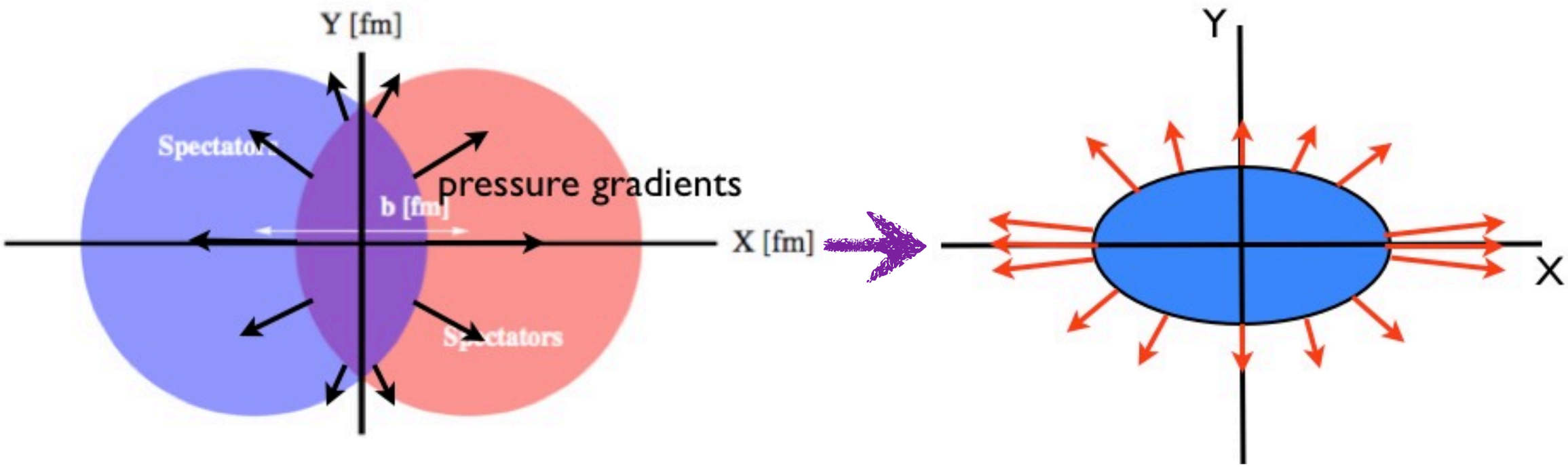

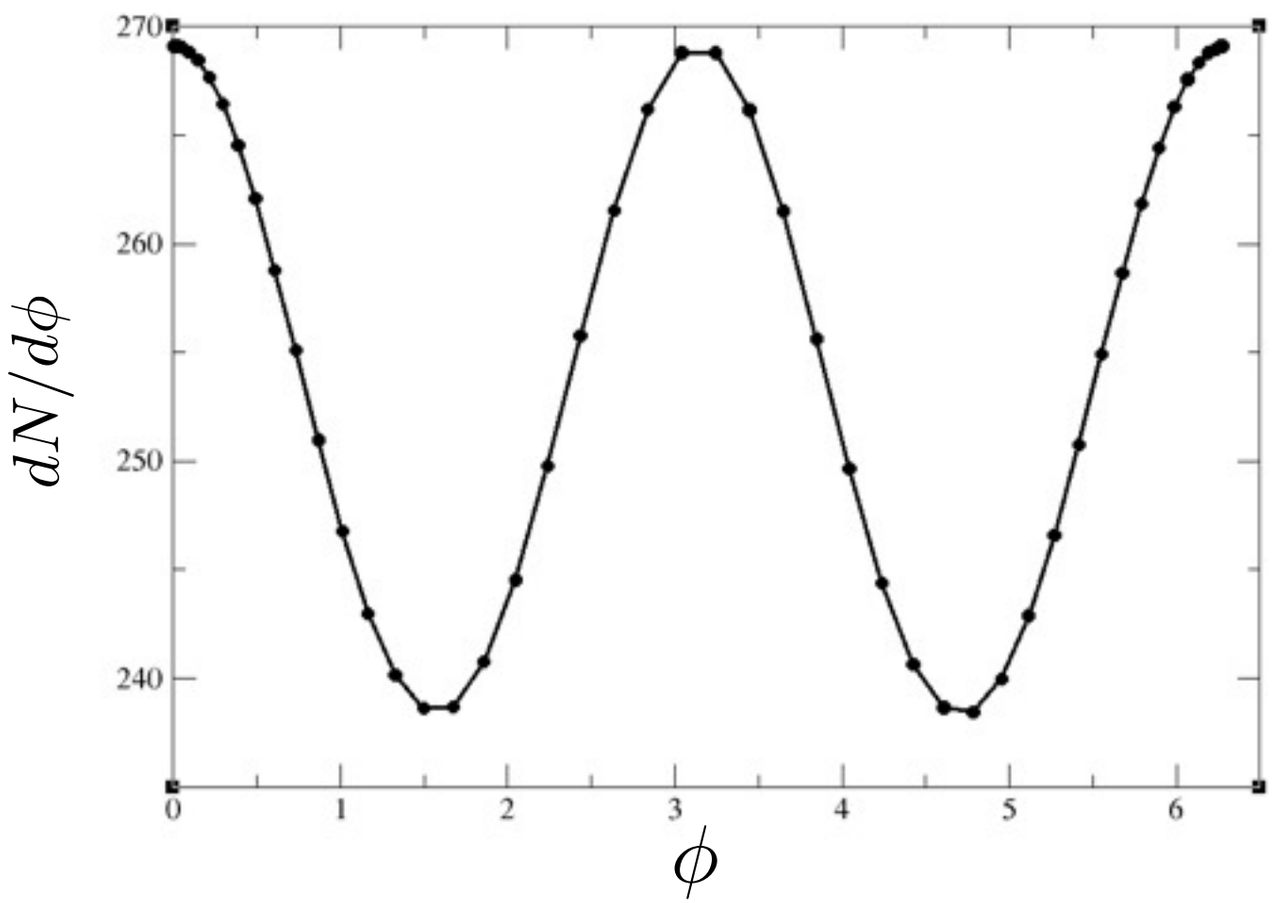

$dN/d\phi$

F.T.

$$A(1 + 2v_2 * \cos(2\phi) + \cdots)$$

In Collaboration with visualization framework by MADAI collaboration, funded by the NSF under grant# NSF-PHY-09-41373

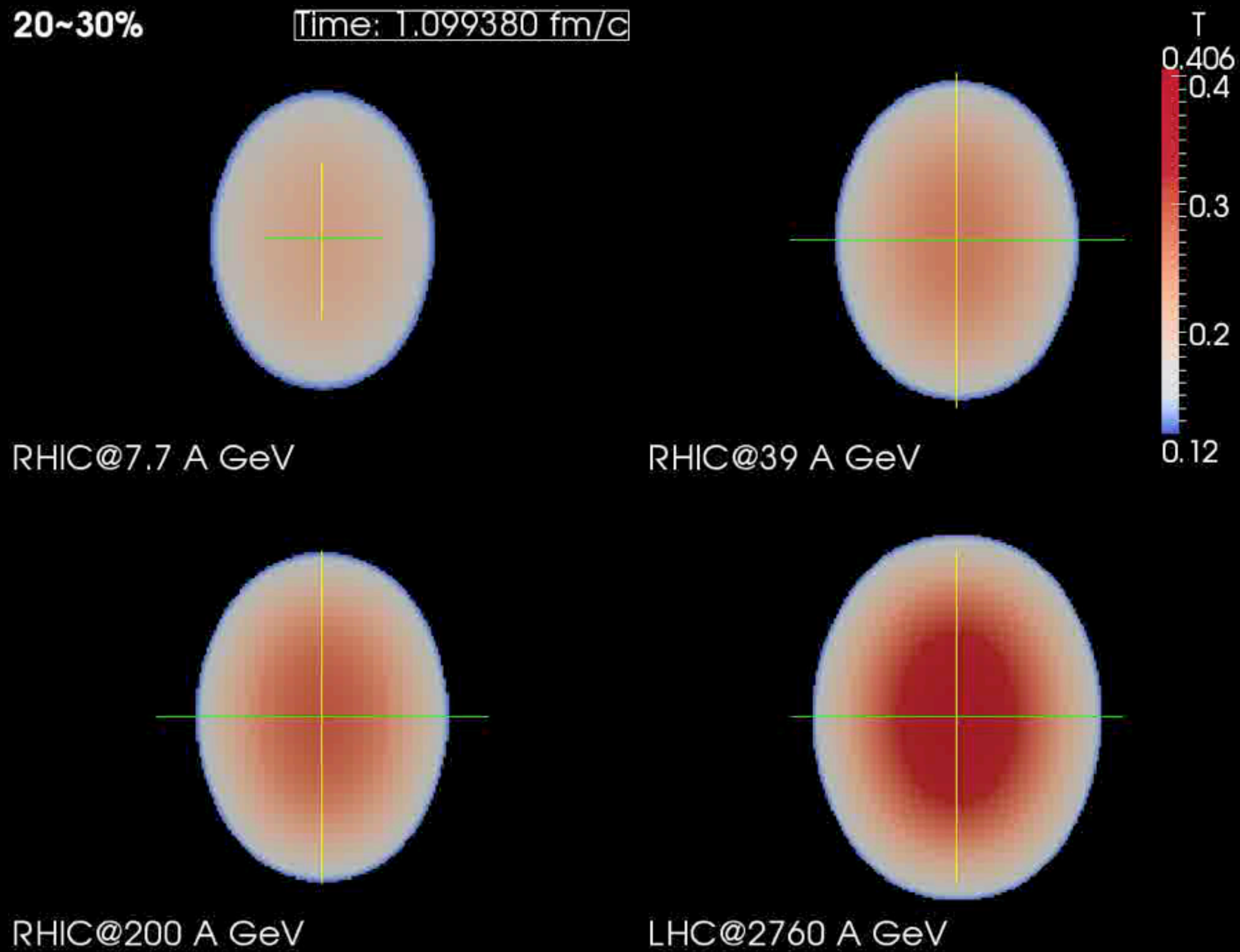

In Collaboration with visualization framework by MADAI collaboration, funded by the NSF under grant# NSF-PHY-09-41373

Elliptic flow

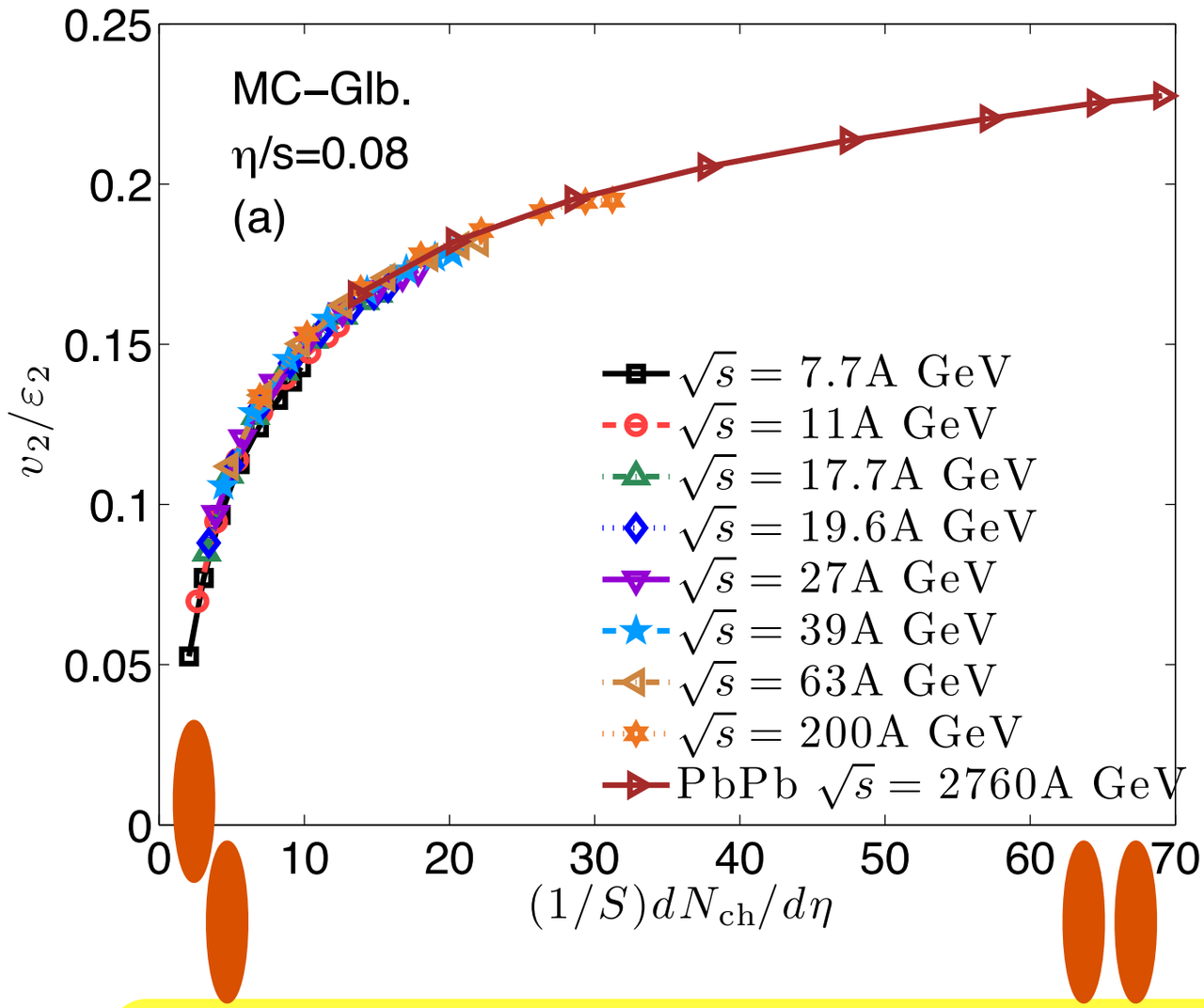

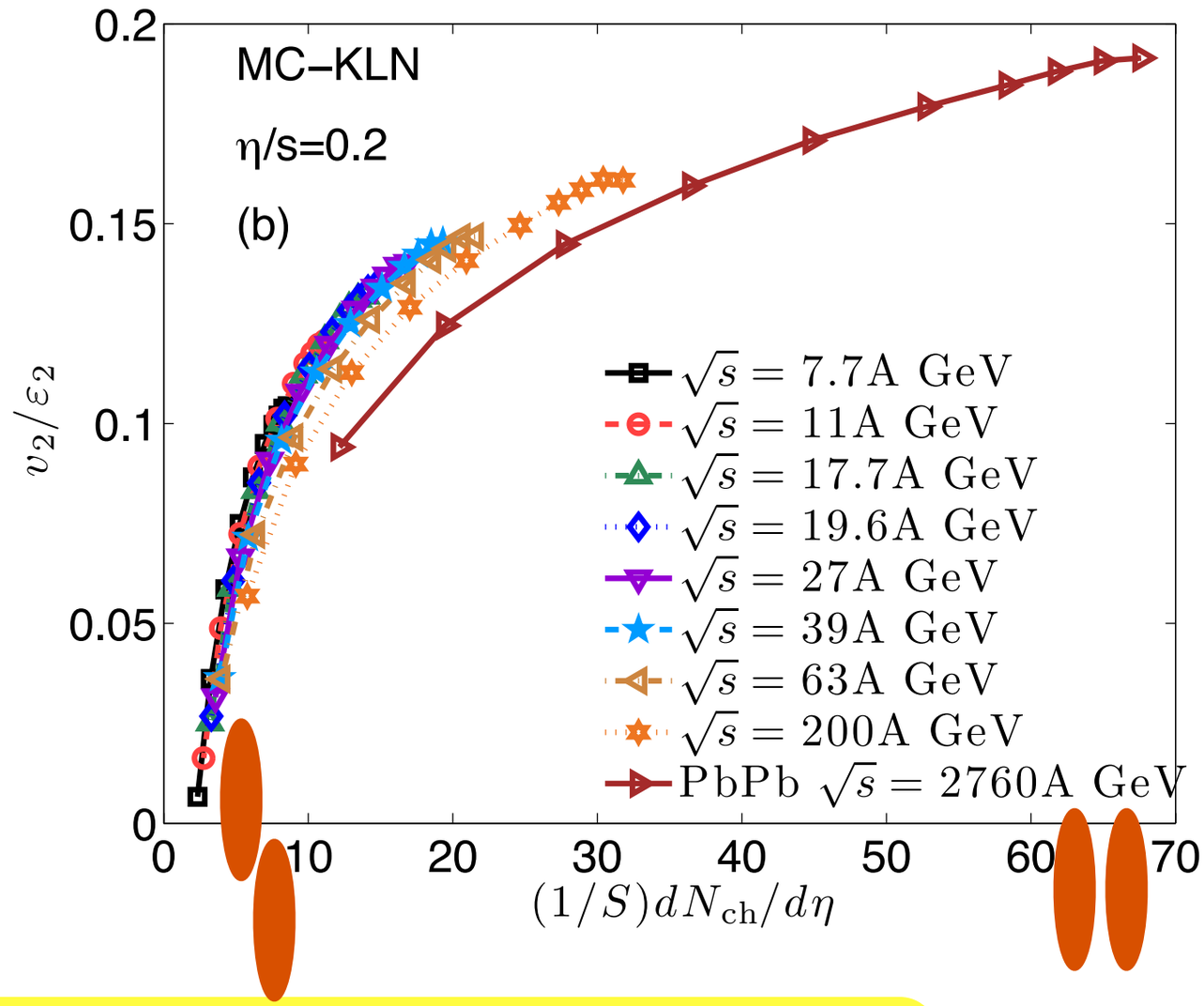

Good $\sqrt{s}$ scaling behavior for MC-Glauber model

Scaling breaks in MC-KLN model due to different centrality dependence of overlapping area

Elliptic flow

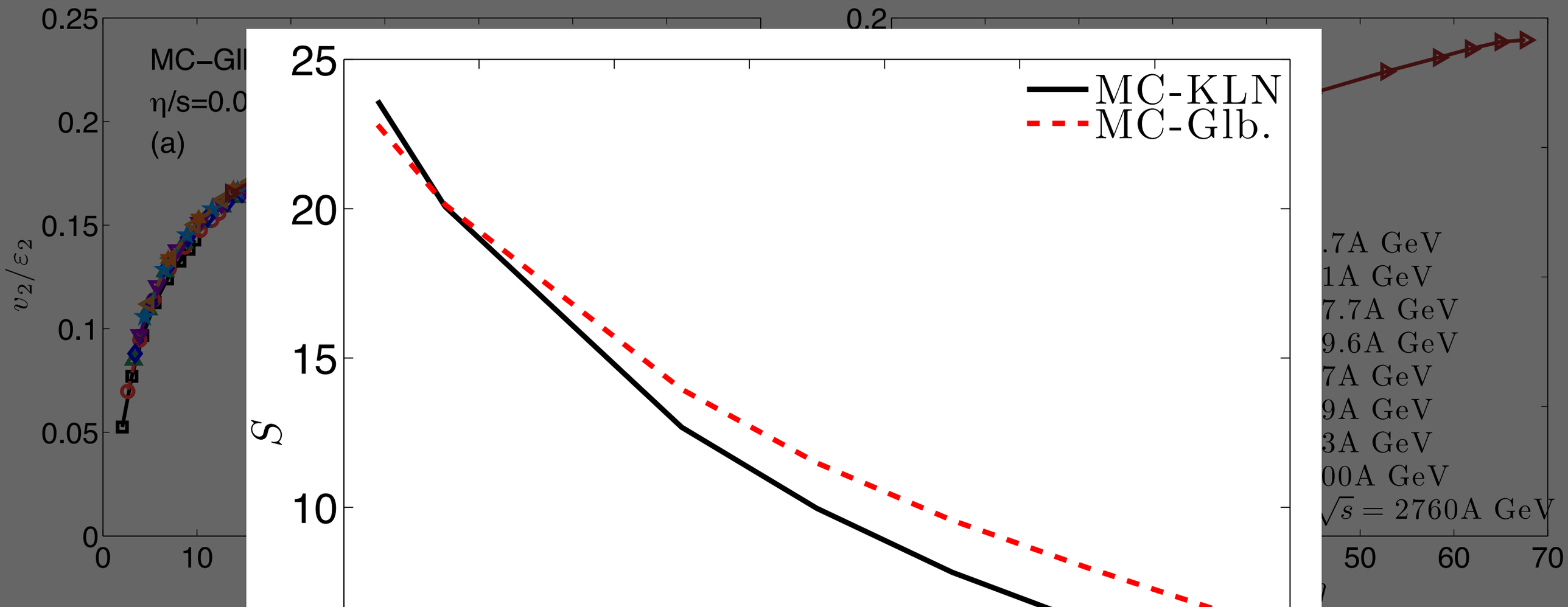

Good

del

Scaling

nt

centrality dependence of overlapping area

Elliptic flow

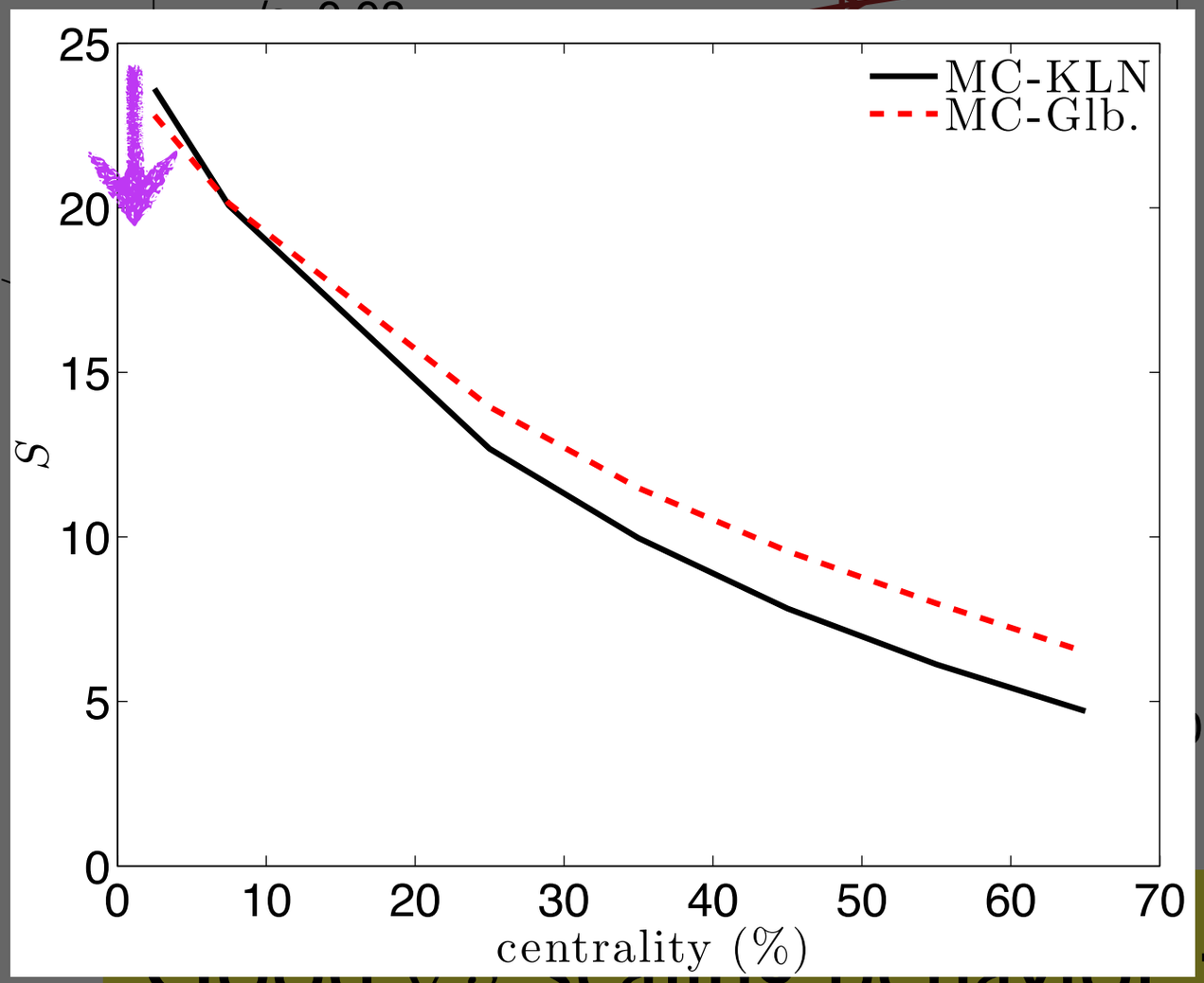

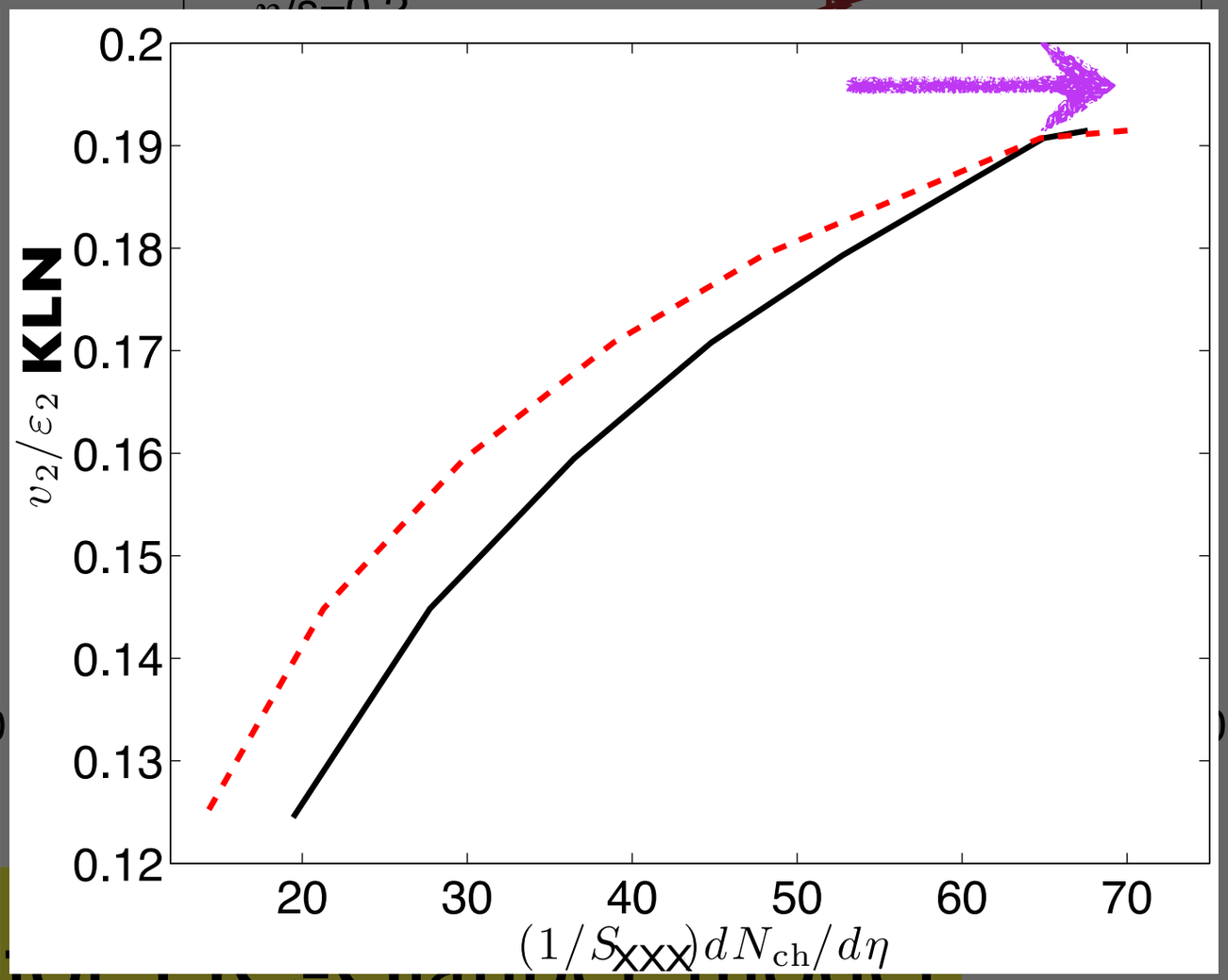

Good $\sqrt{s}$ scaling behavior for MC-Glauber model

Scaling breaks in MC-KLN model due to different centrality dependence of overlapping area

Elliptic flow

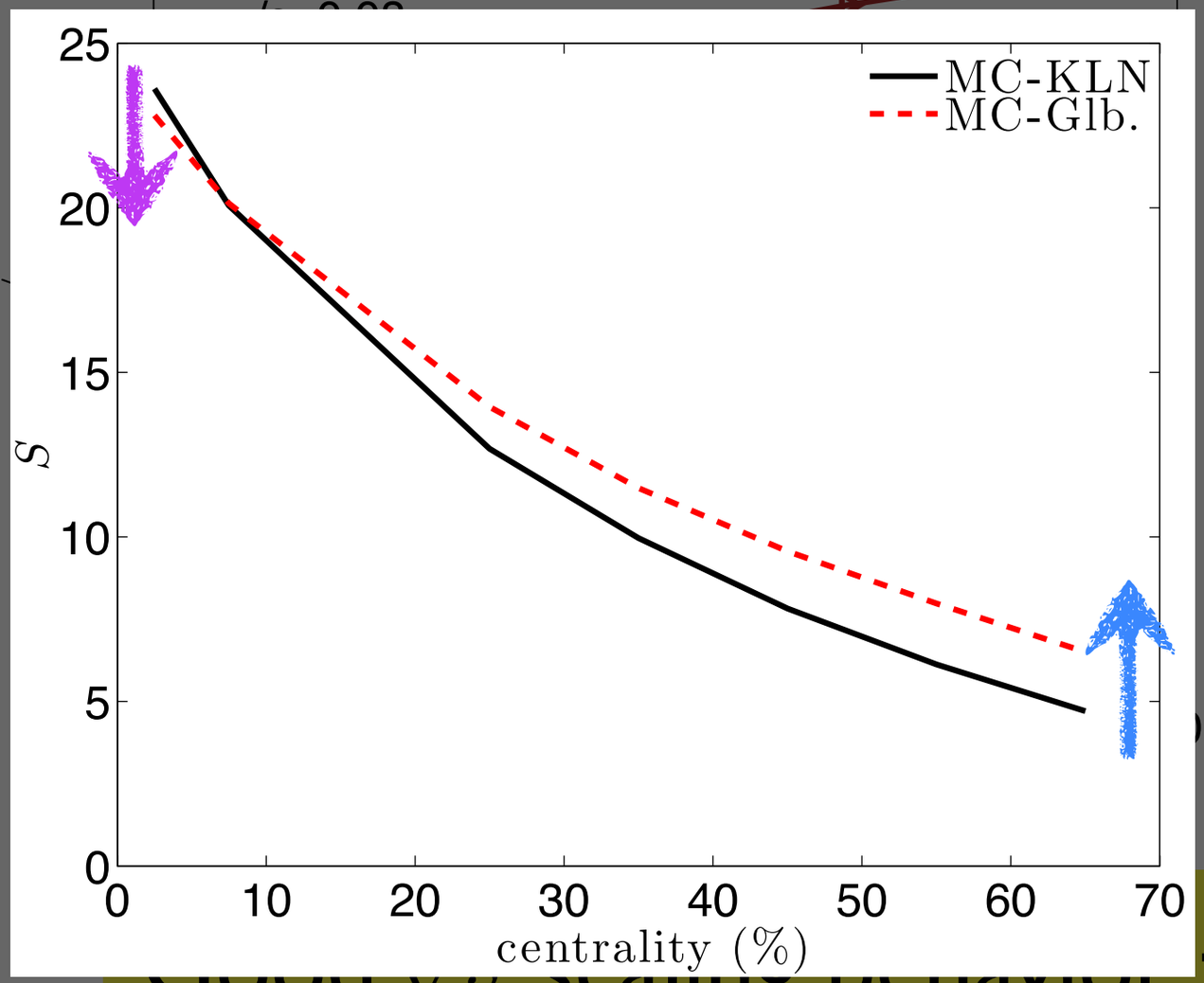

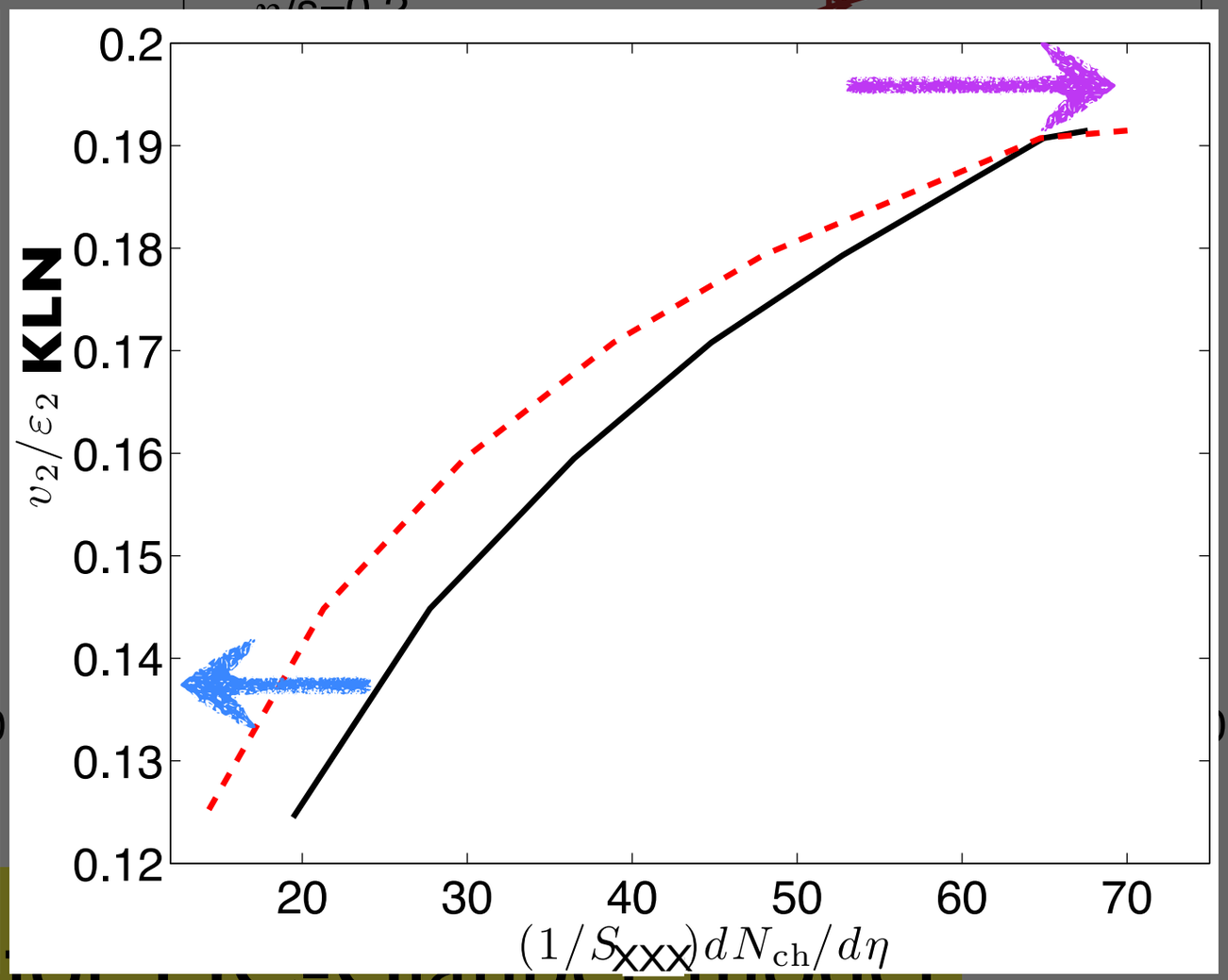

Good v_2 scaling behavior for MC-Glauber model

Scaling breaks in MC-KLN model due to different centrality dependence of overlapping area

otic flow

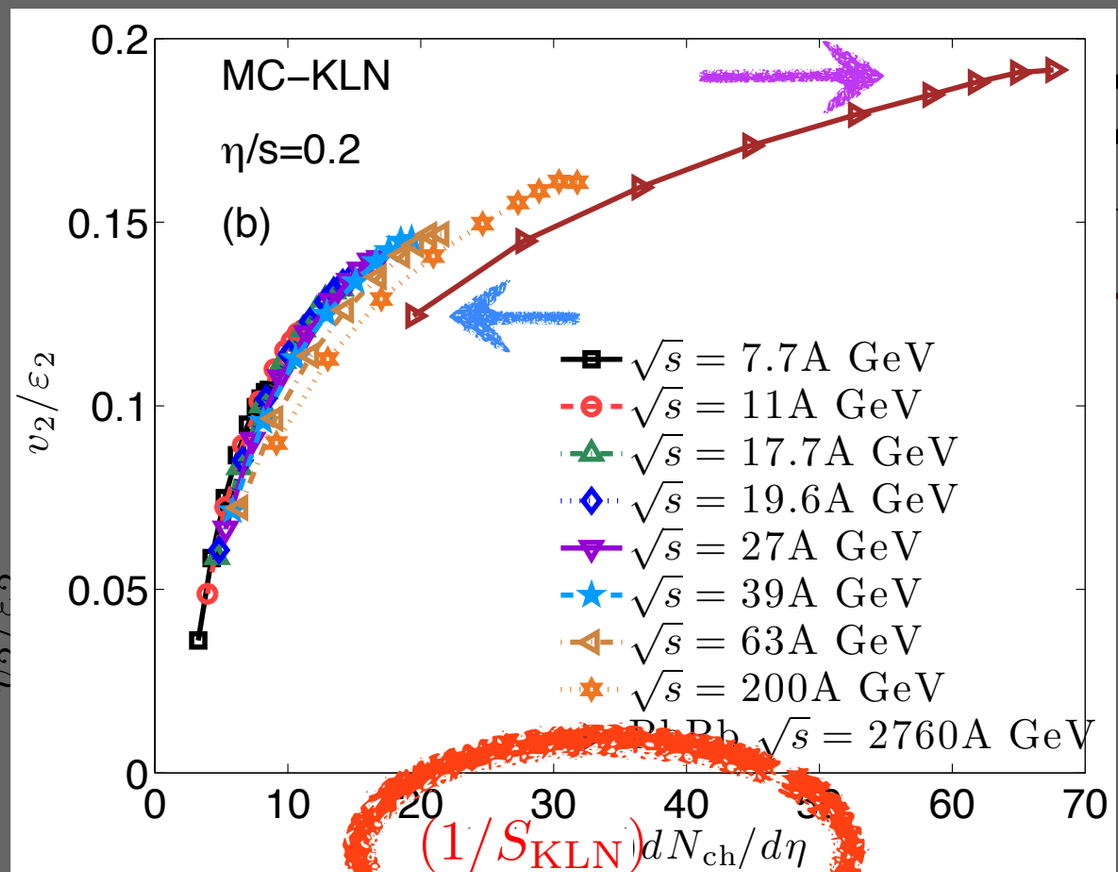

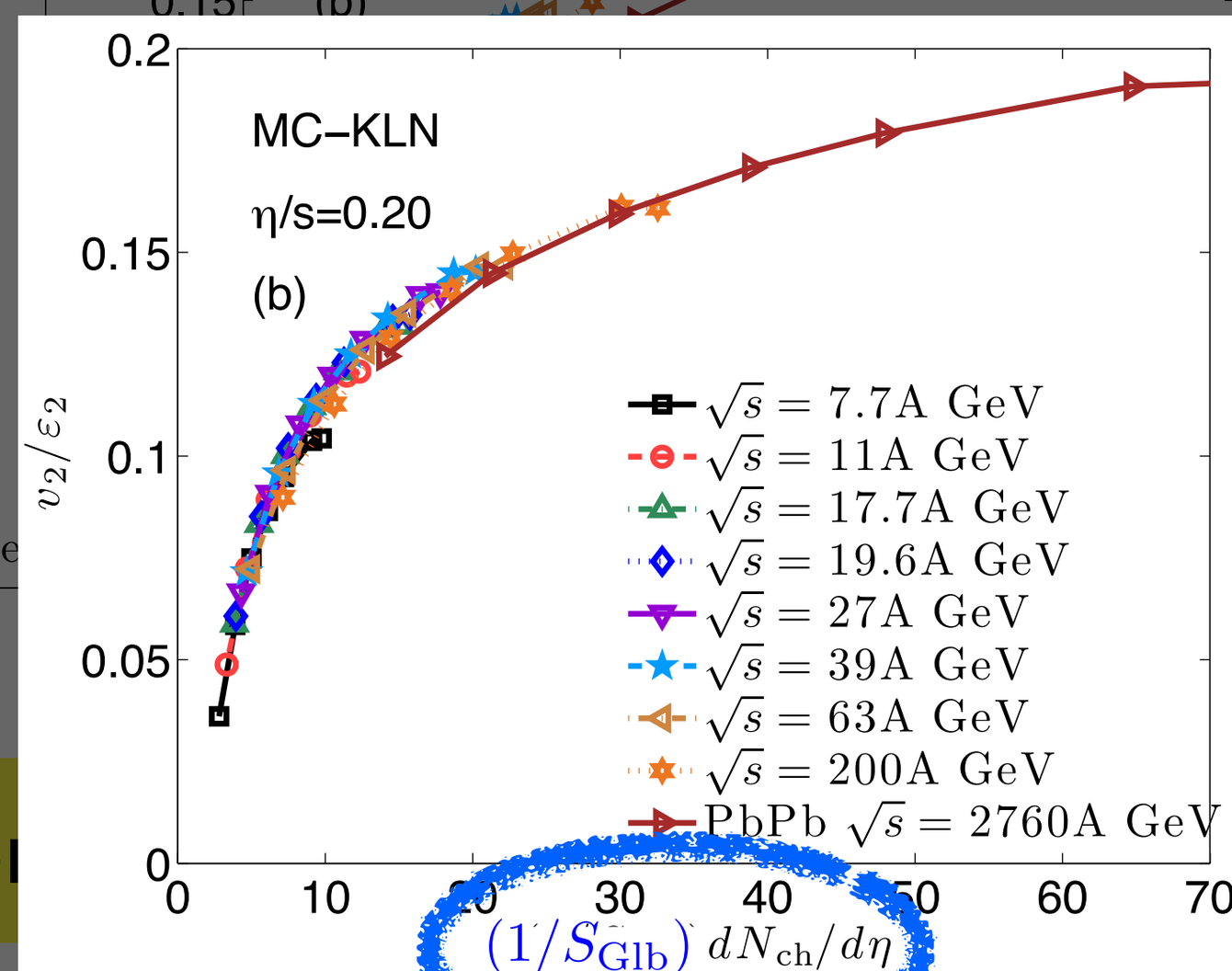

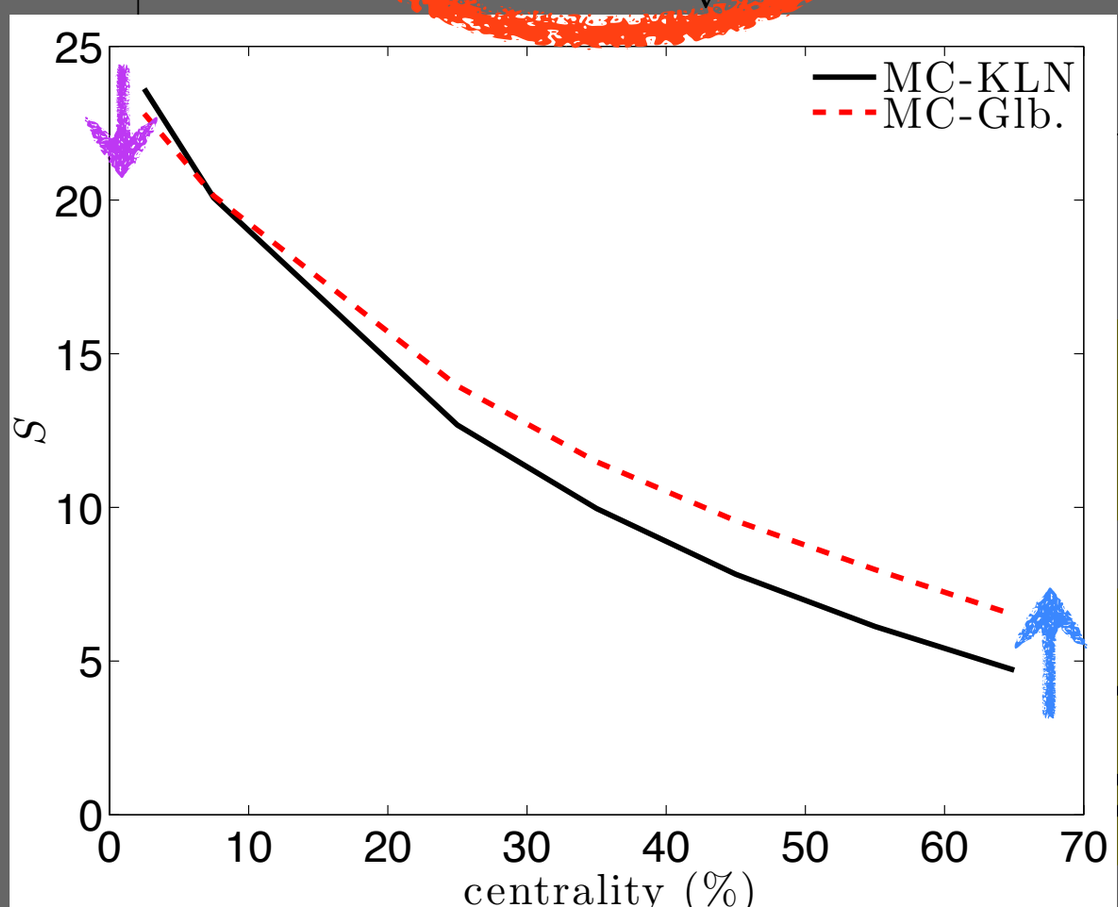

LN model due to different
of overlapping area

Differential $v_2(p_T)$

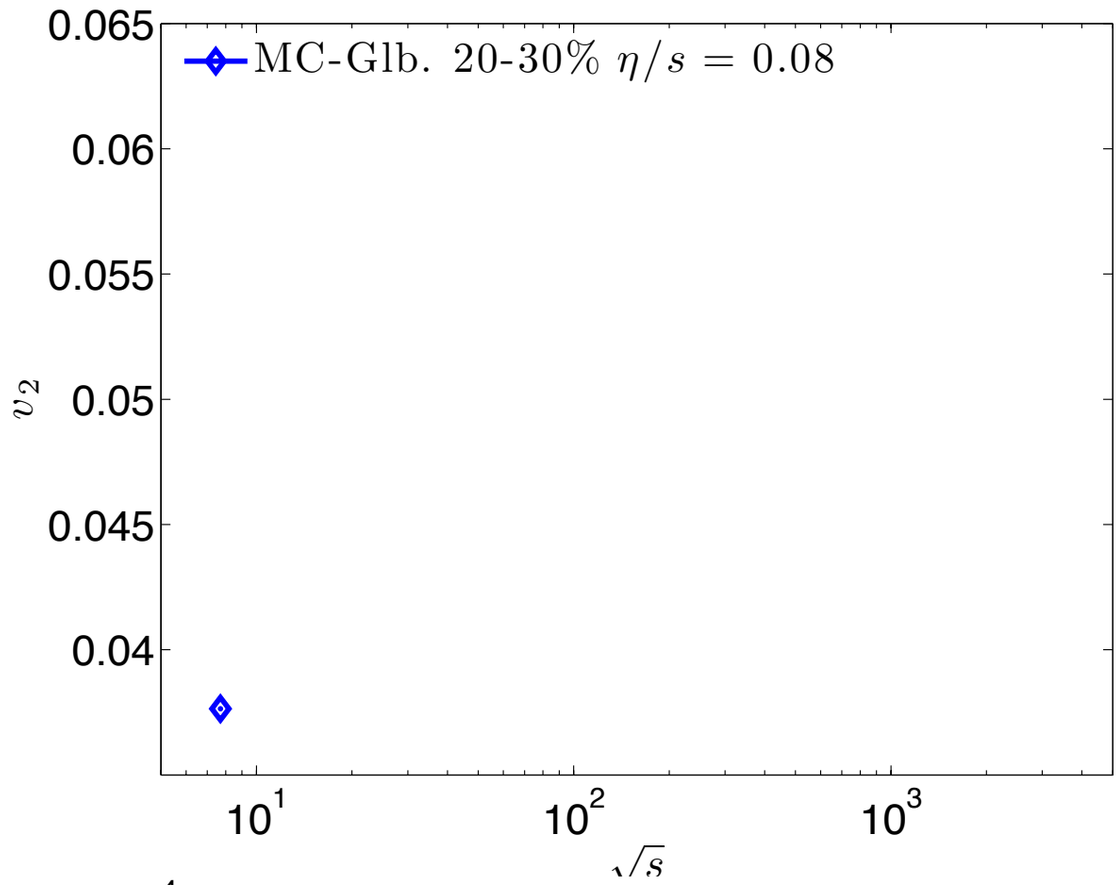

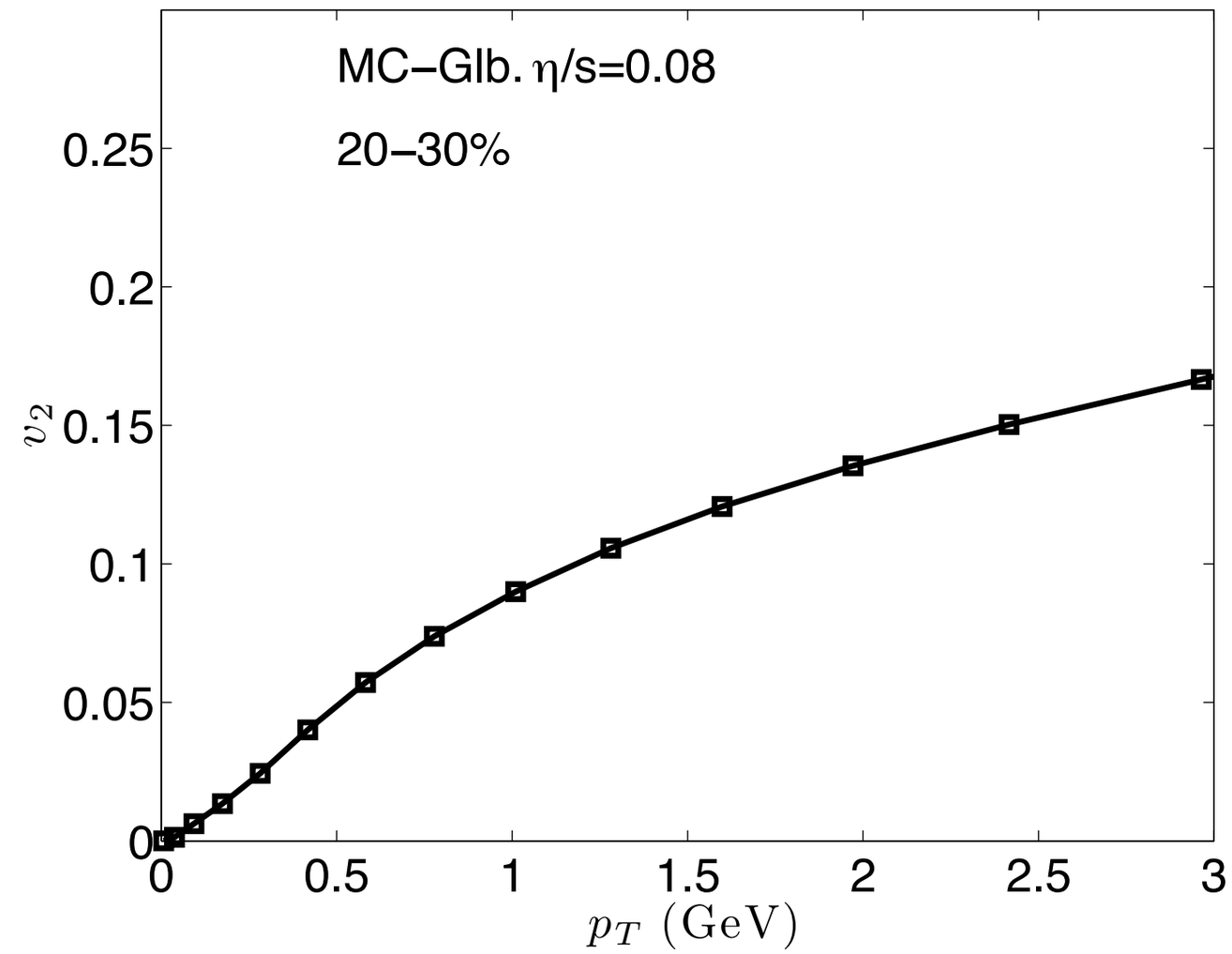

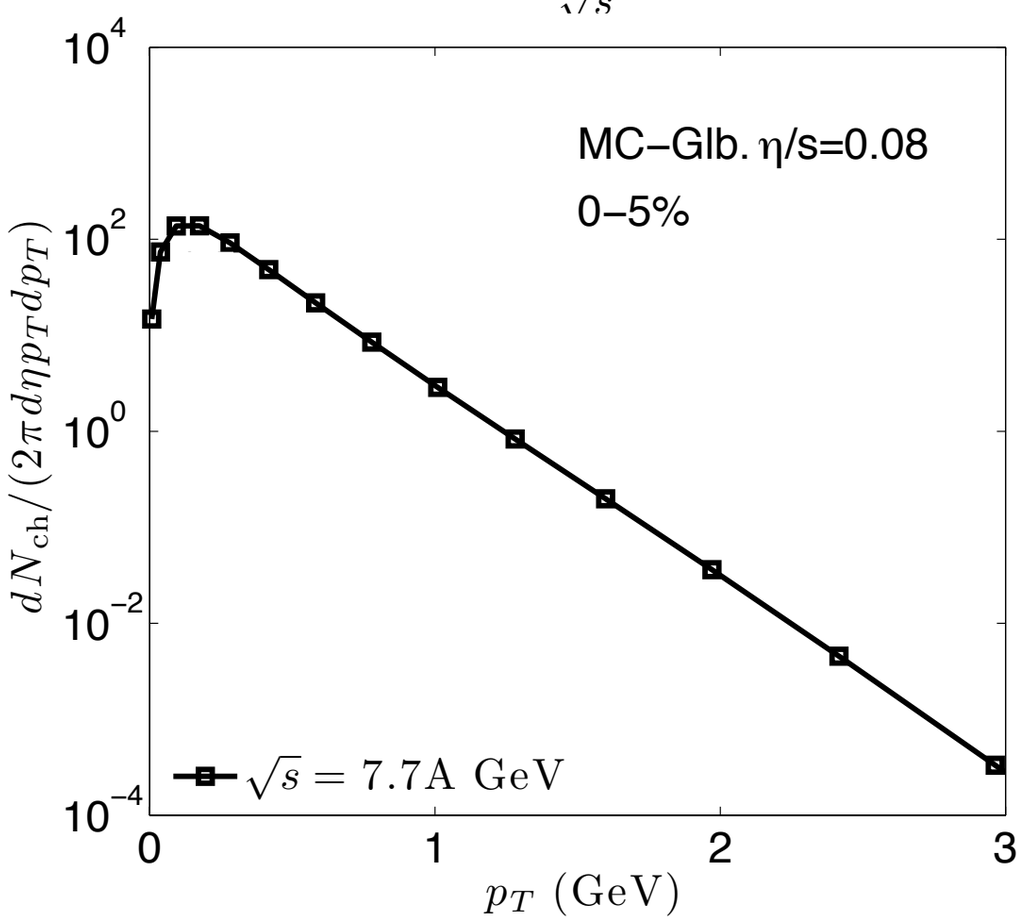

Differential $v_2(p_T)$

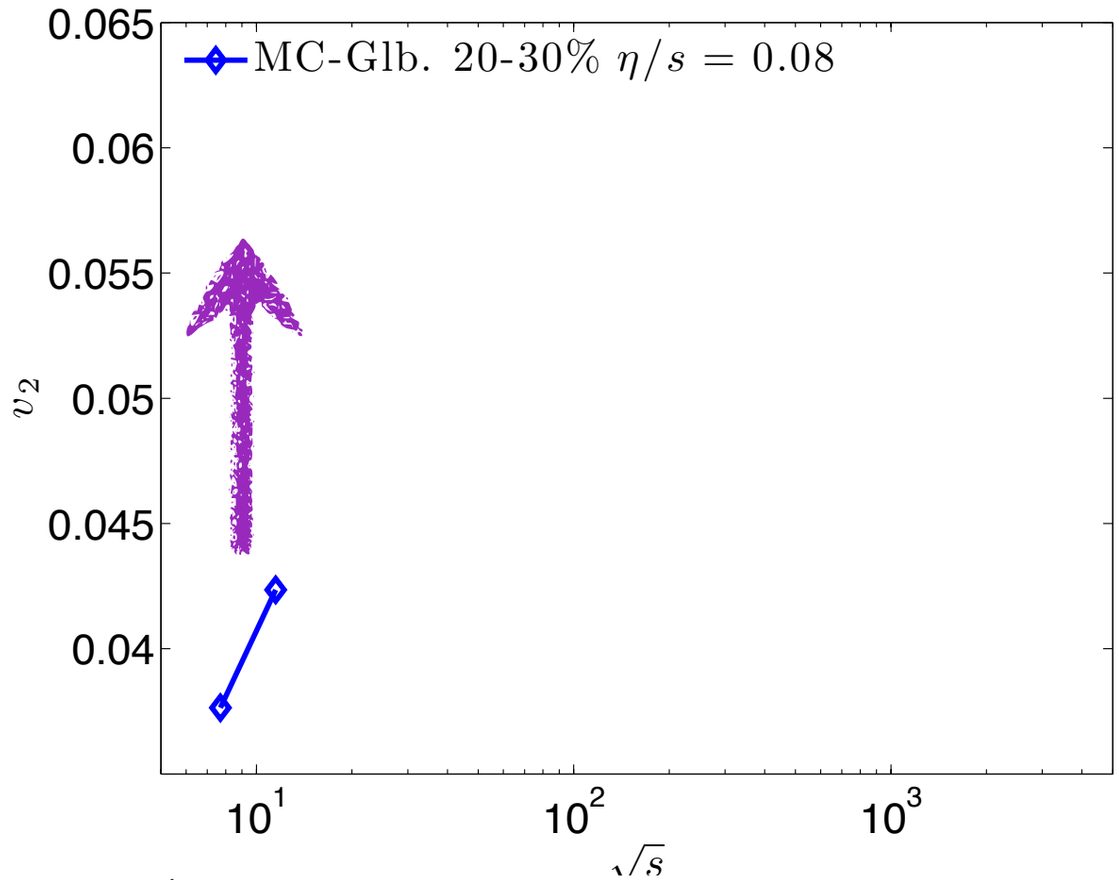

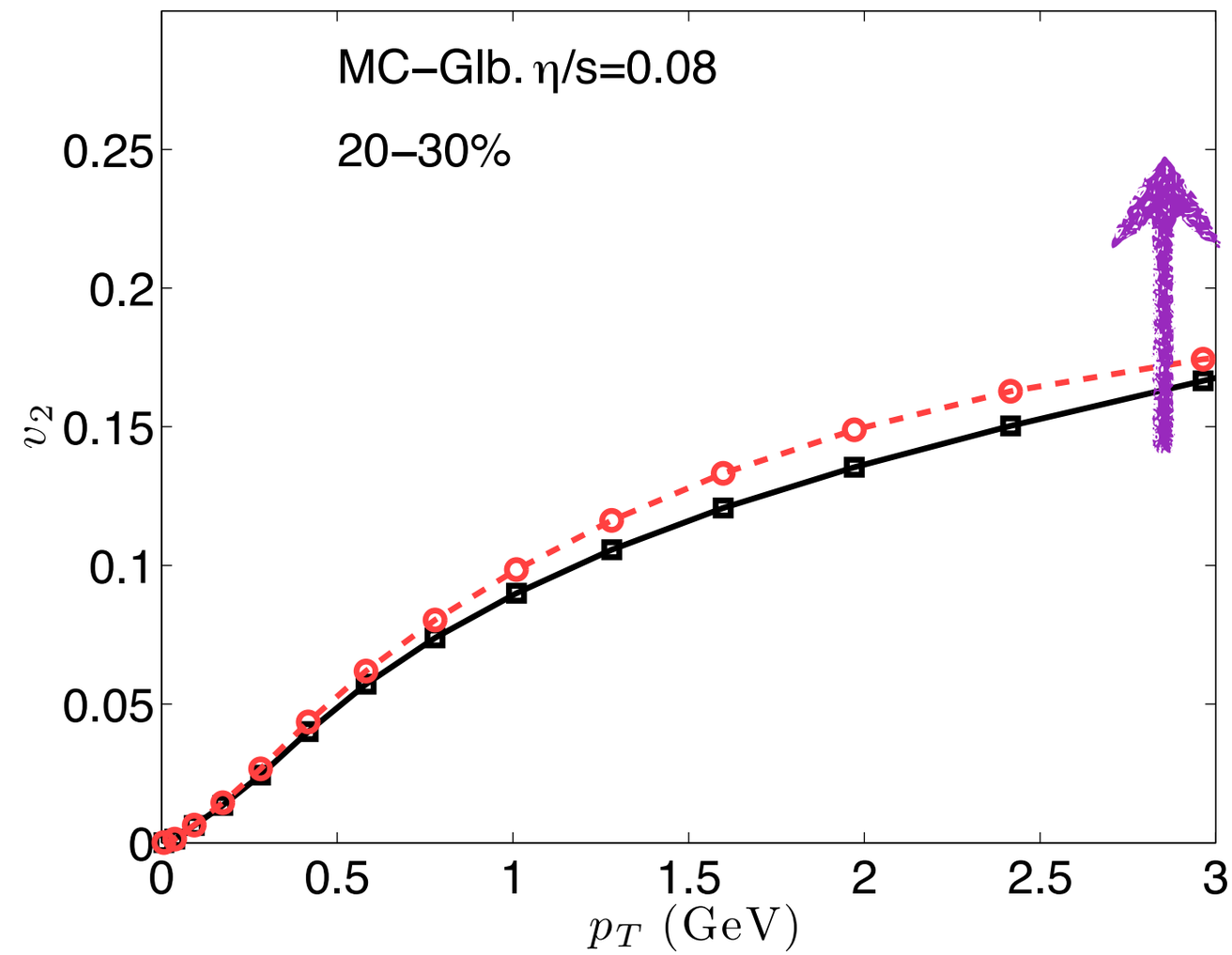

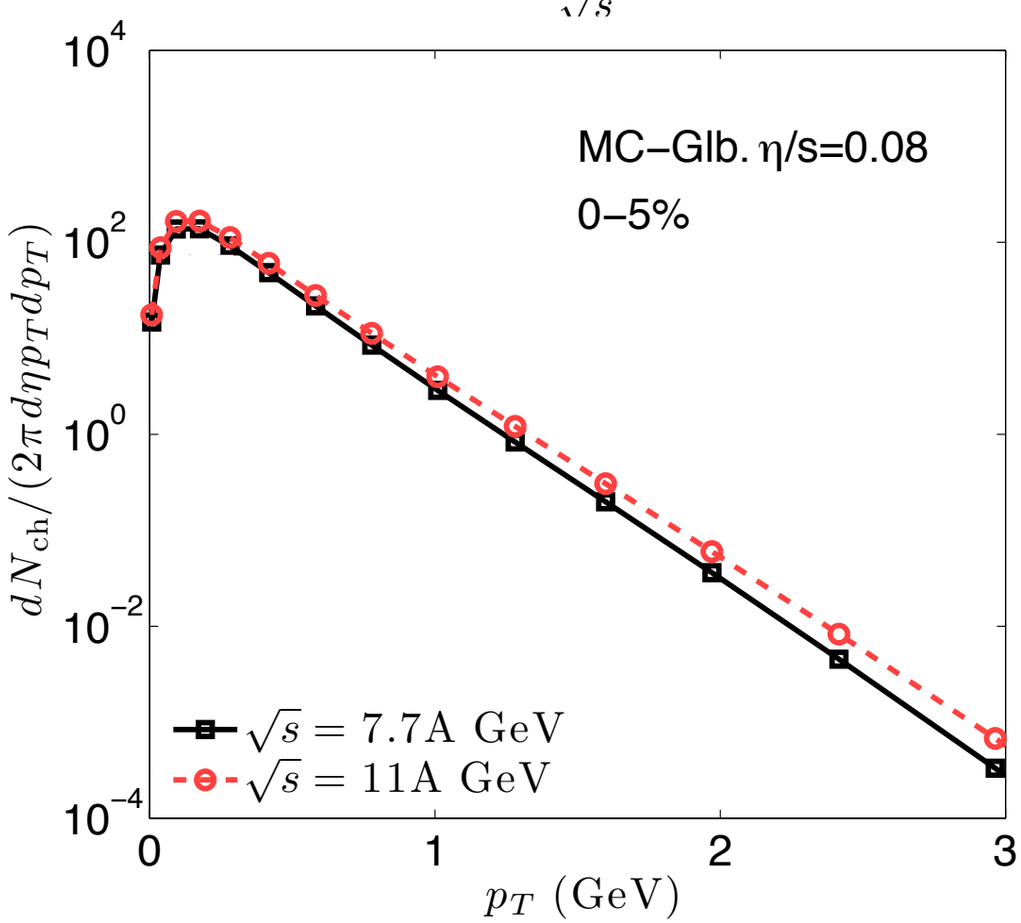

Differential $v_2(p_T)$

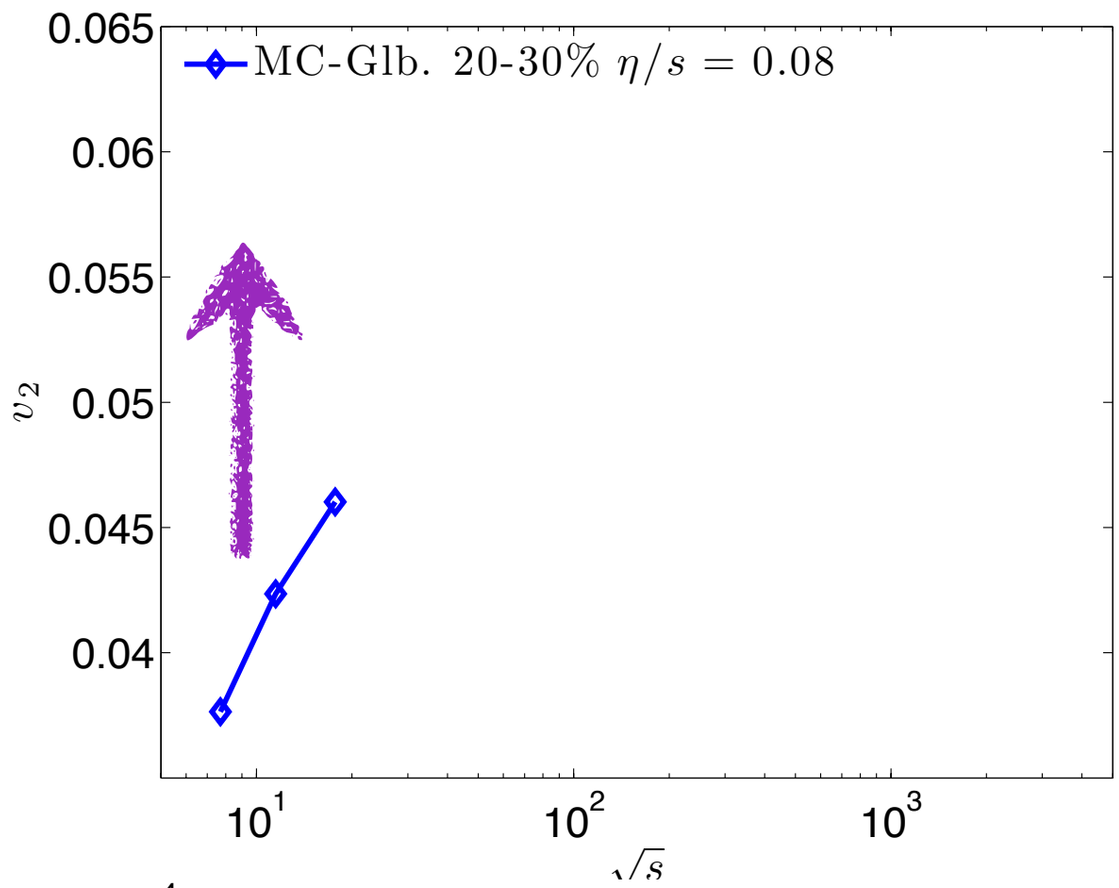

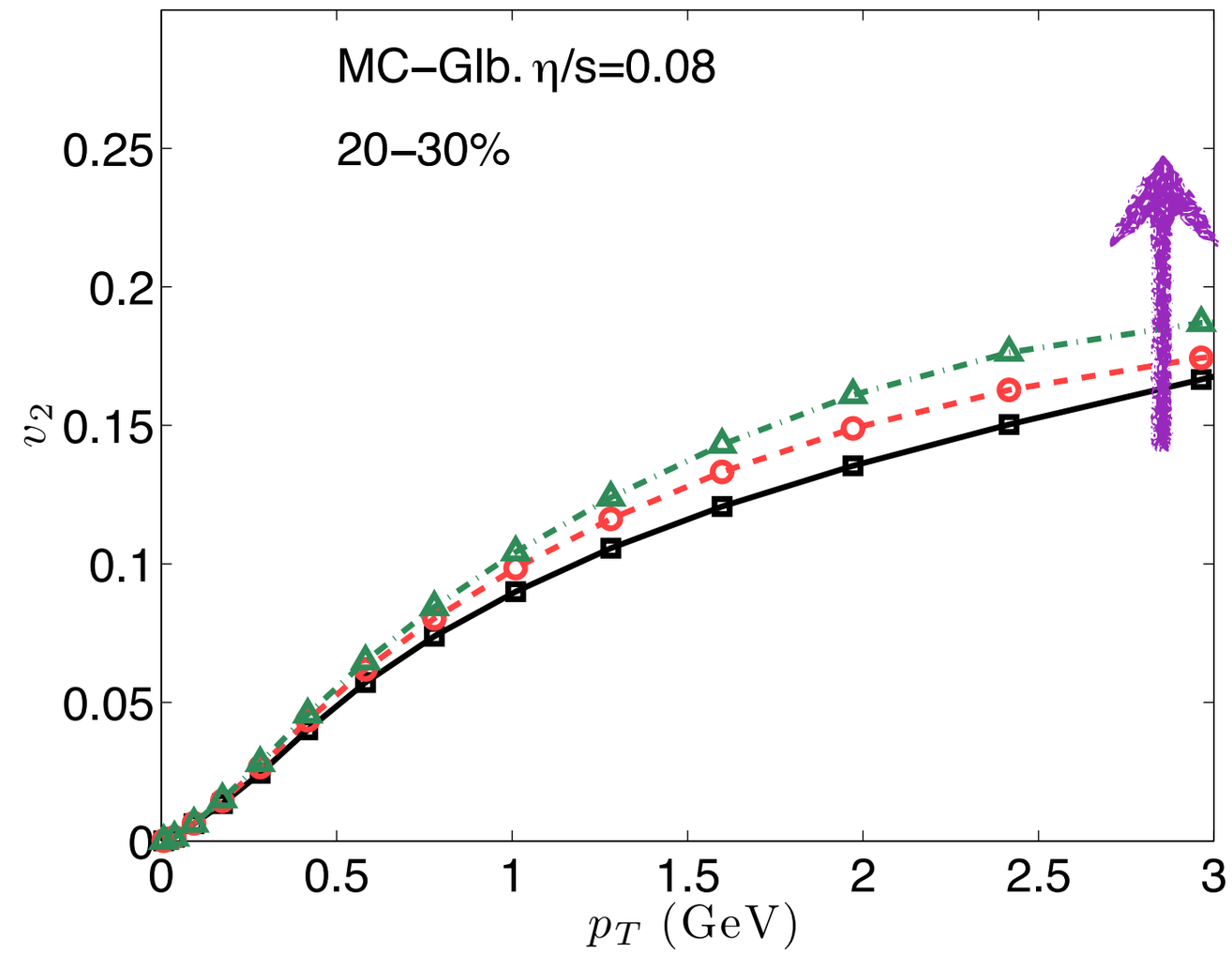

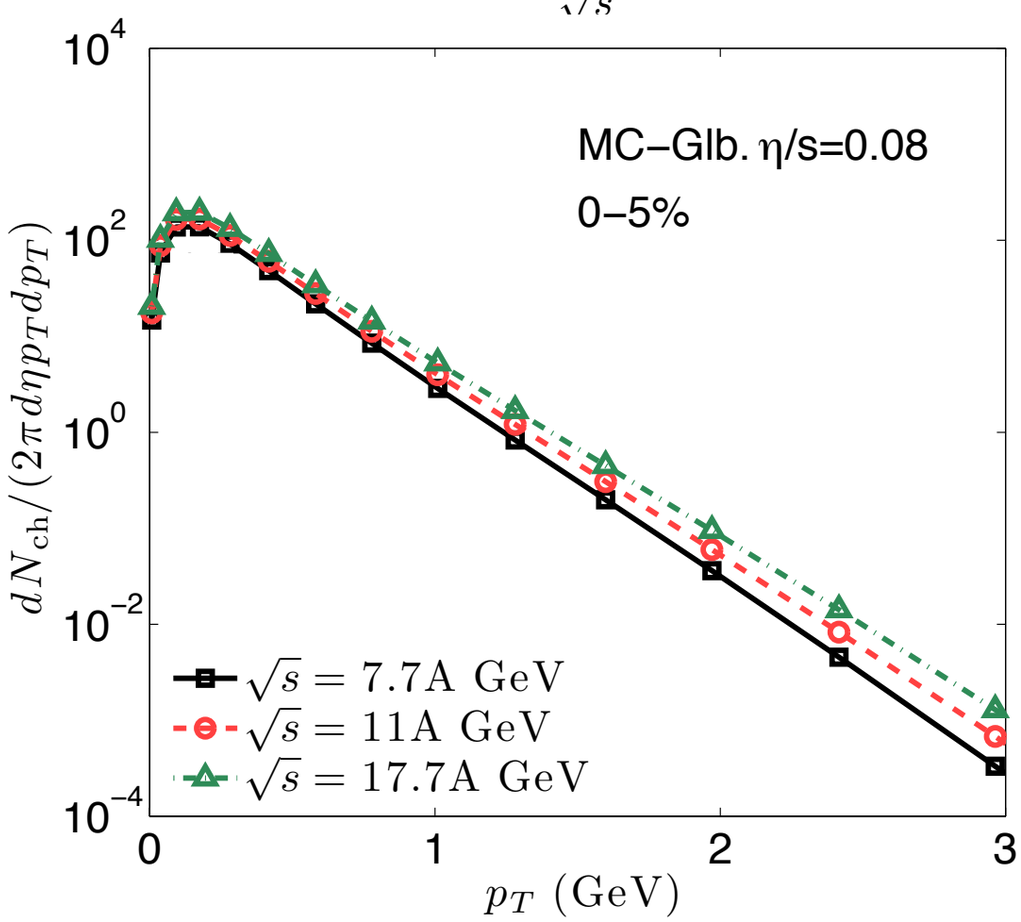

Differential $v_2(p_T)$

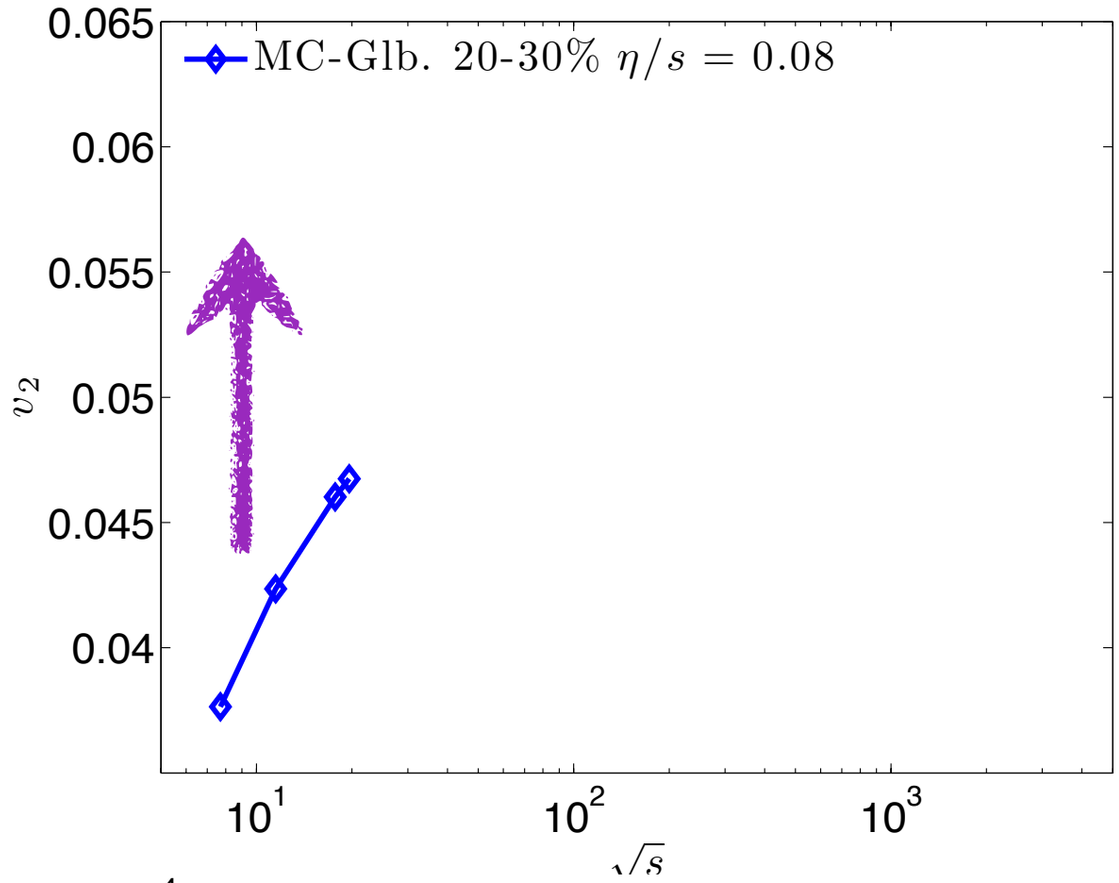

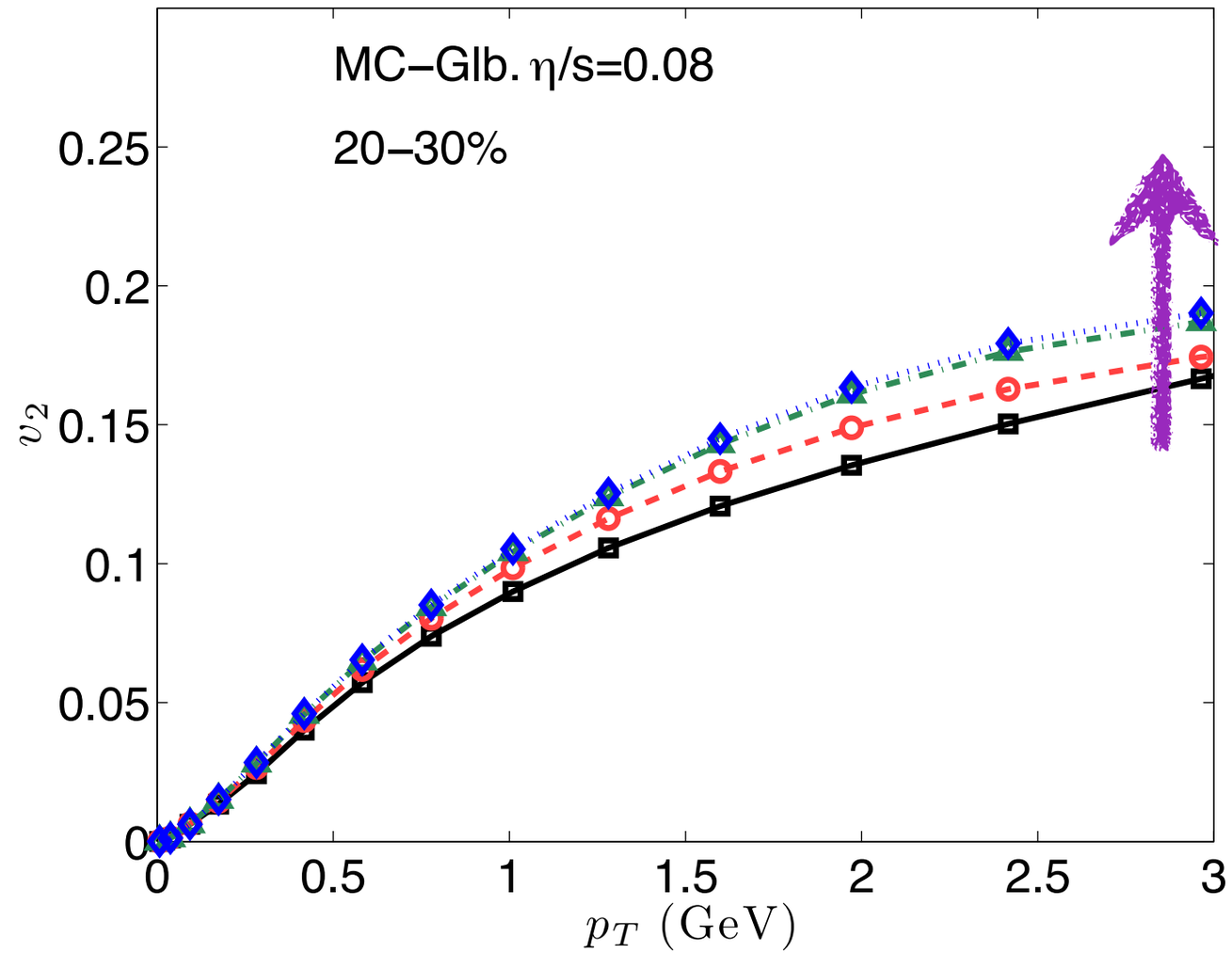

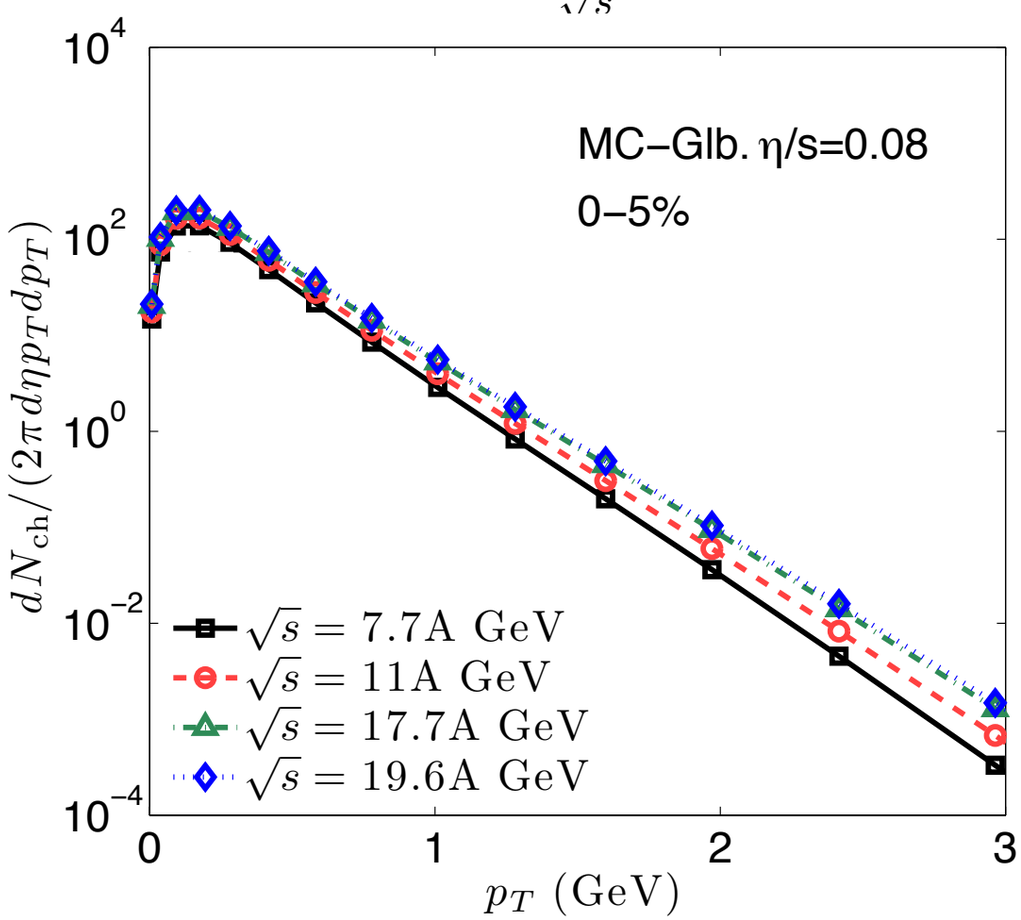

Differential $v_2(p_T)$

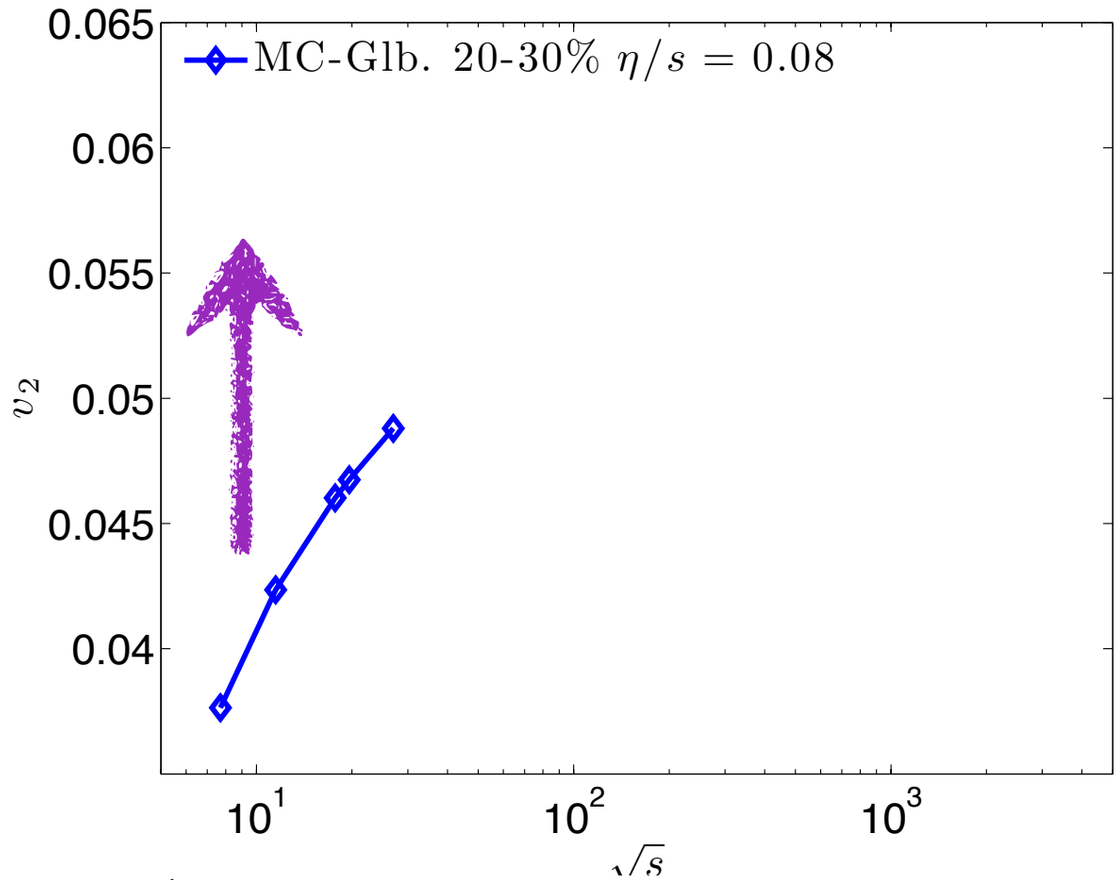

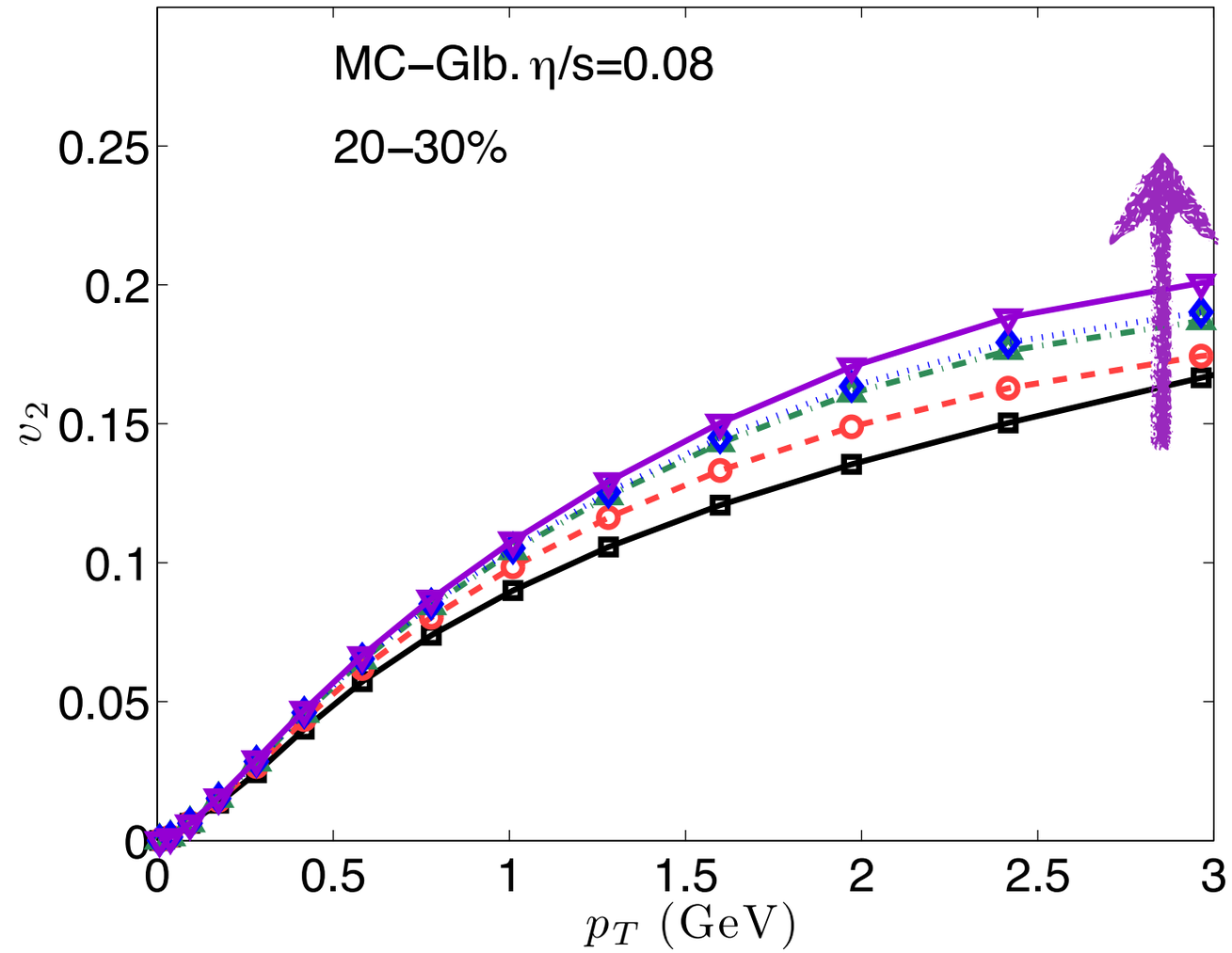

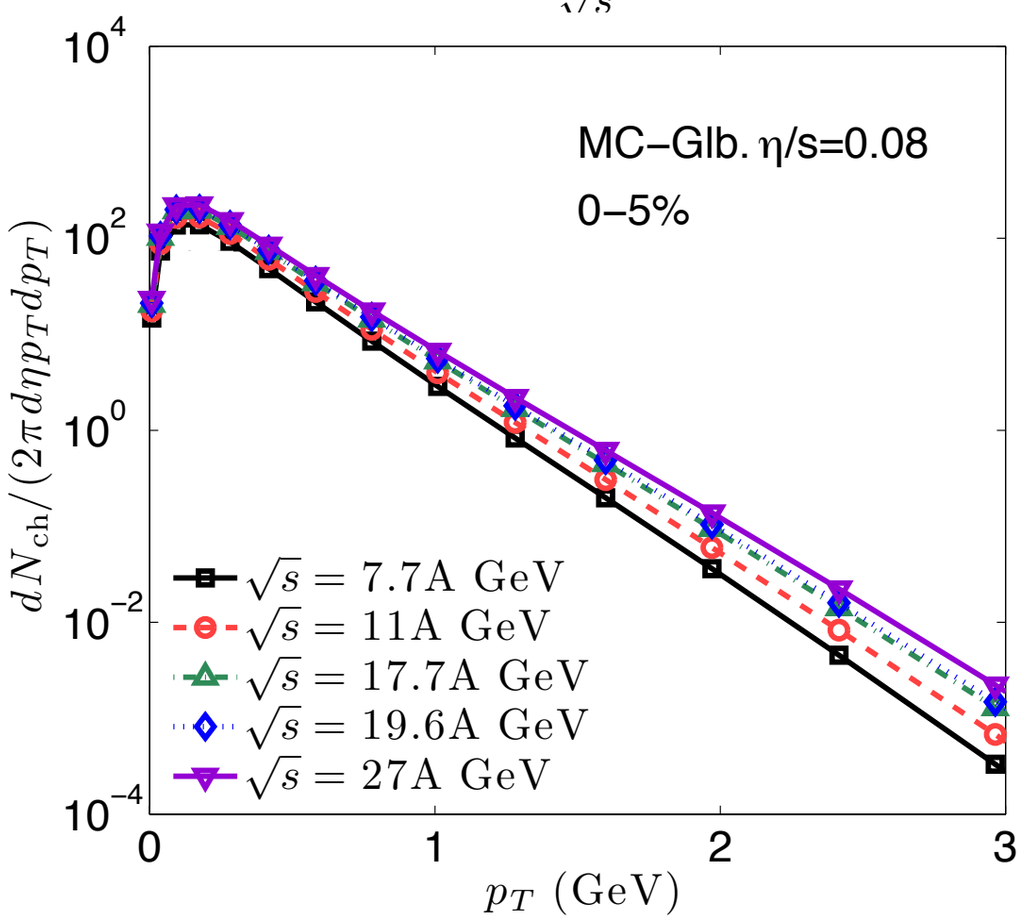

Differential $v_2(p_T)$

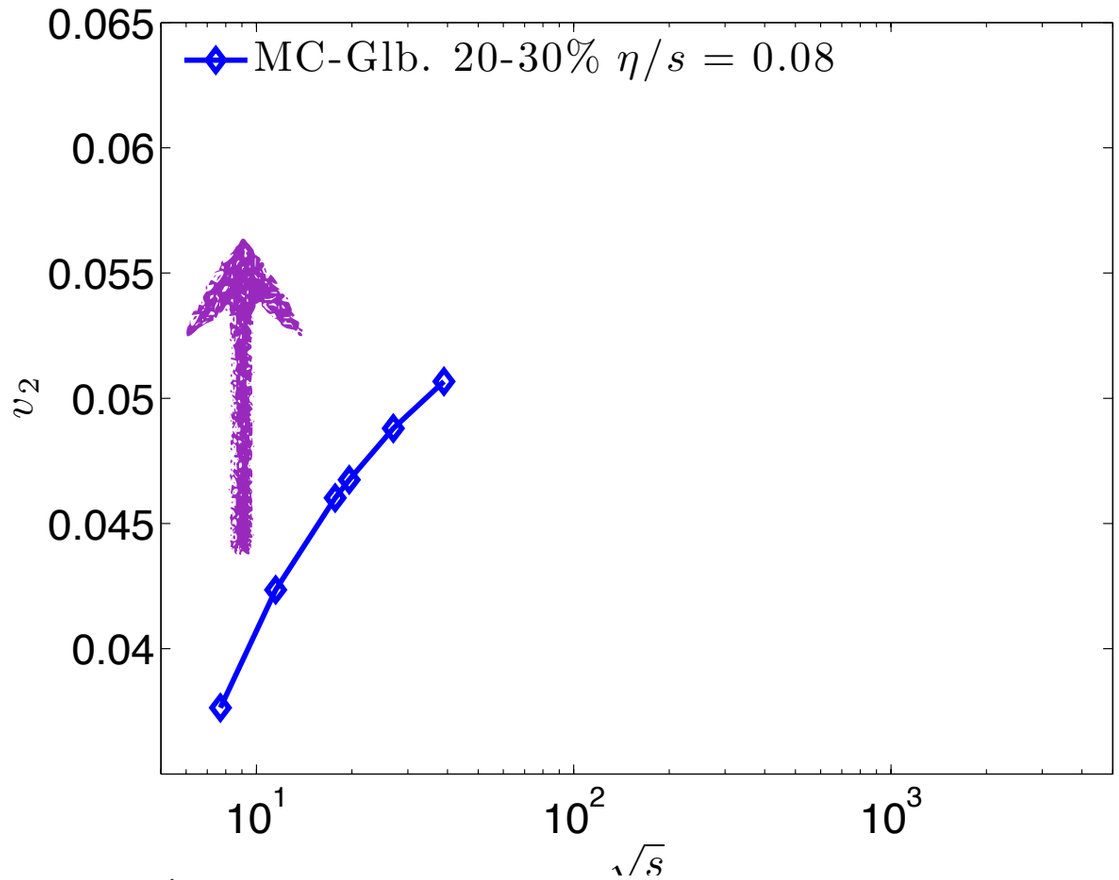

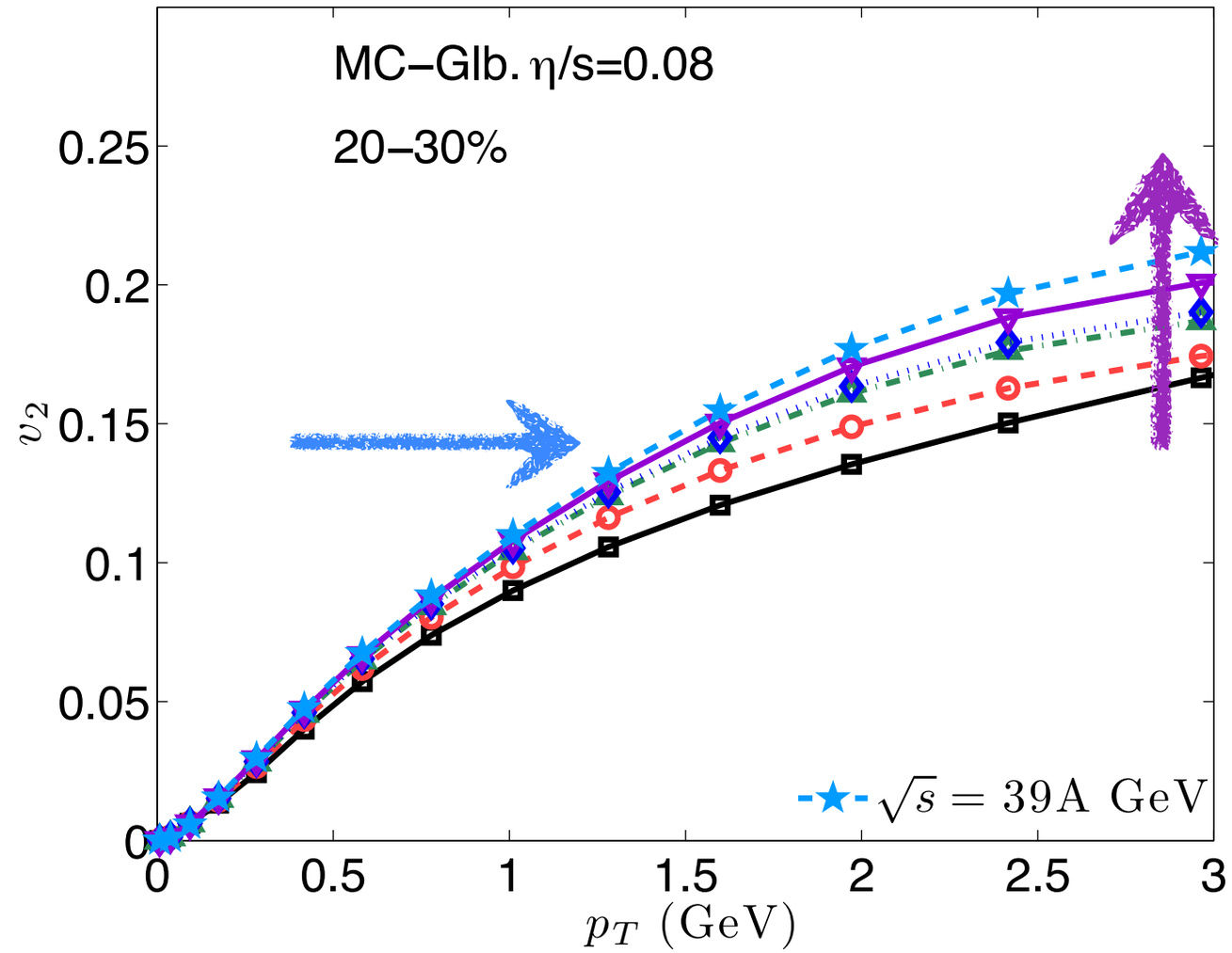

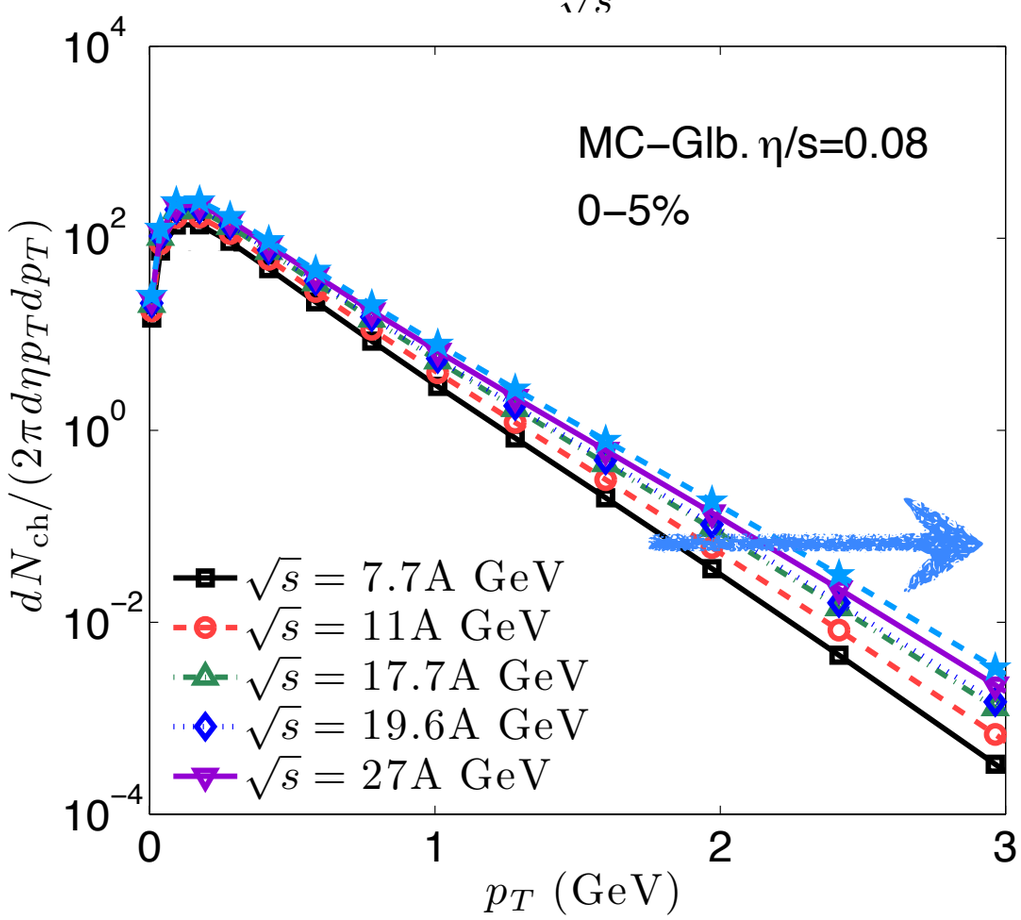

Differential $v_2(p_T)$

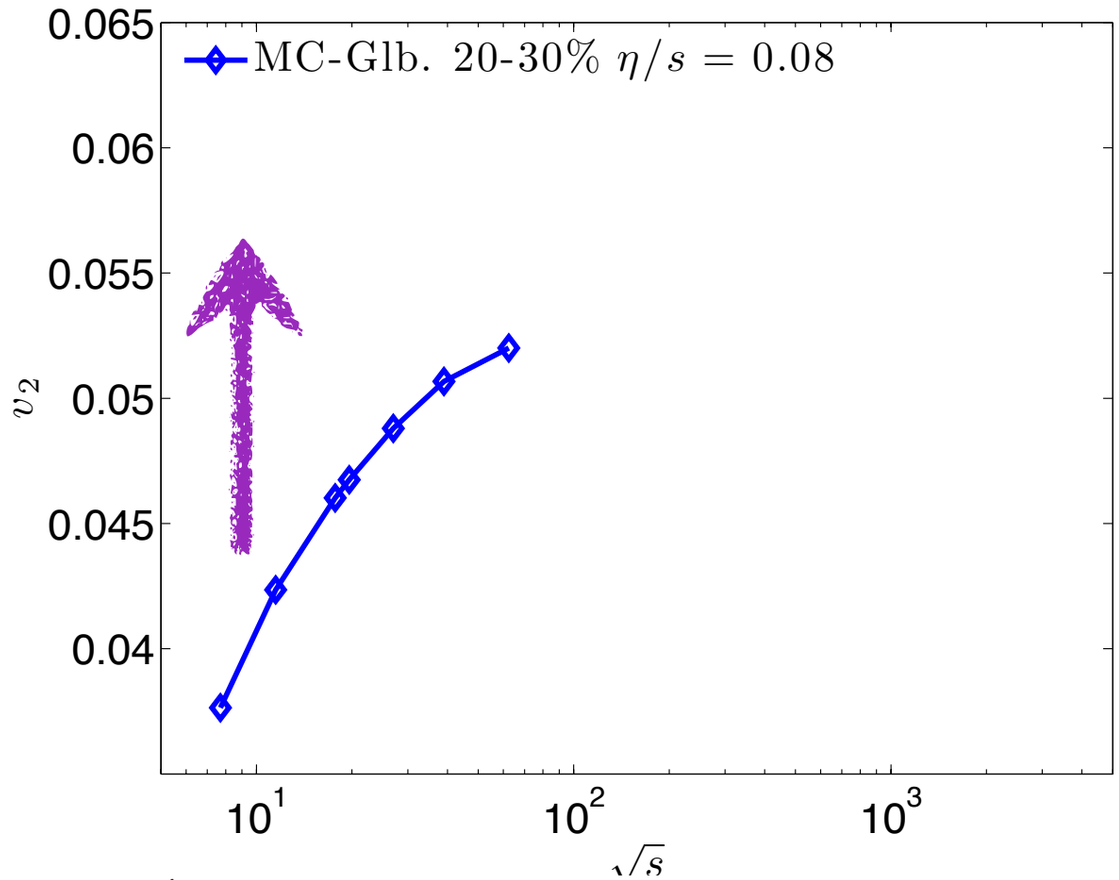

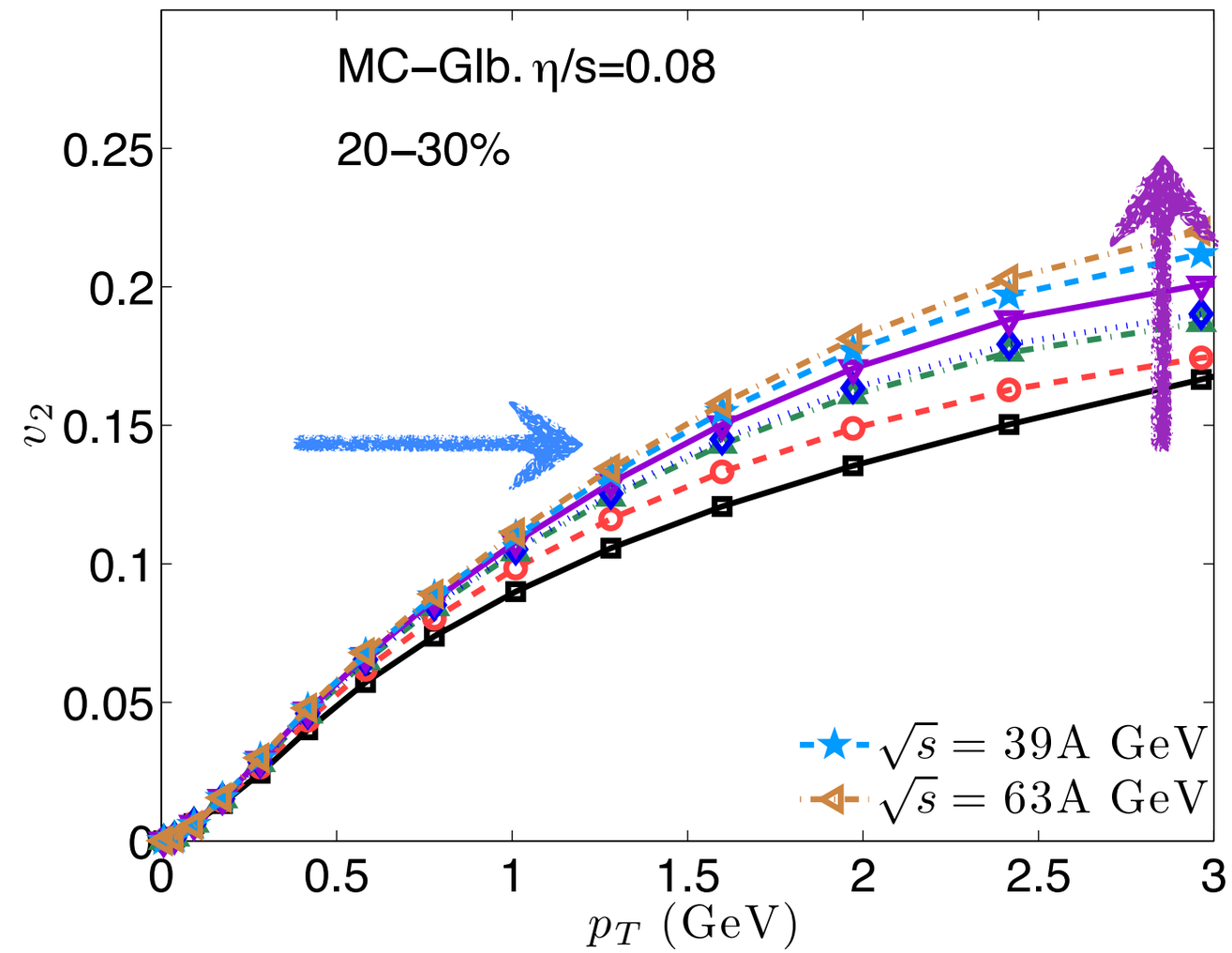

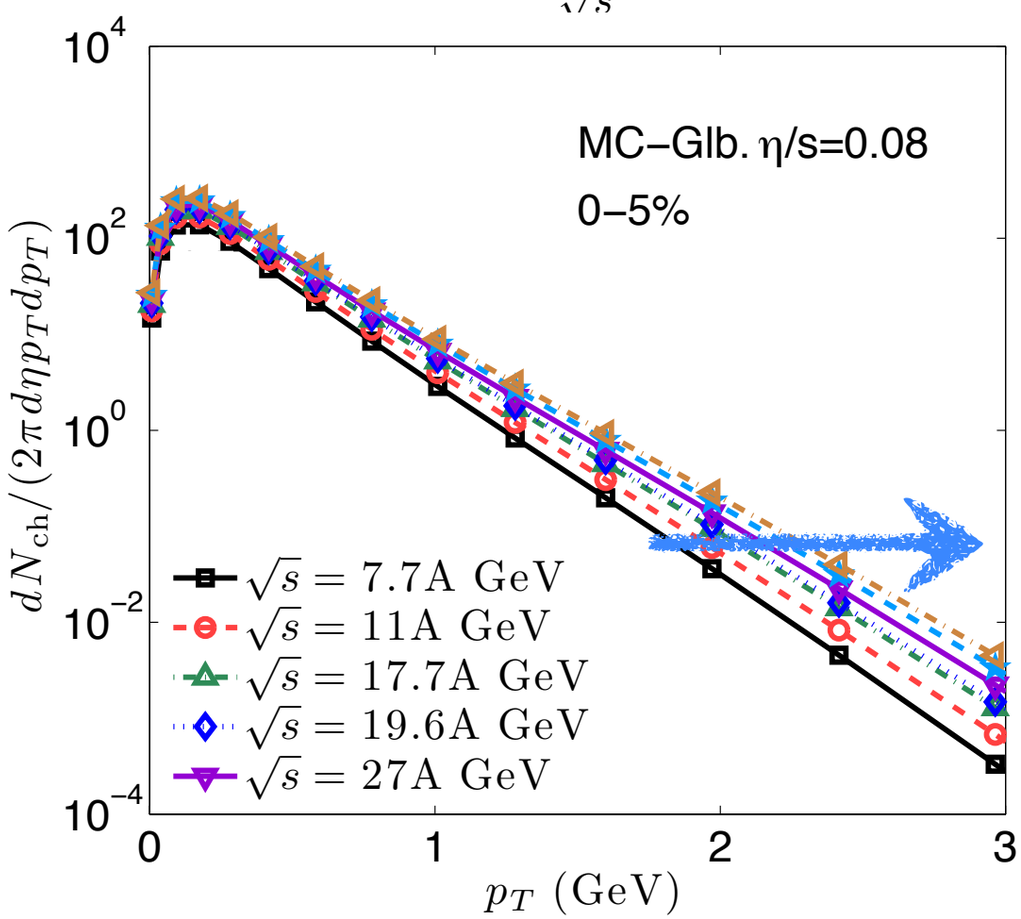

Differential $v_2(p_T)$

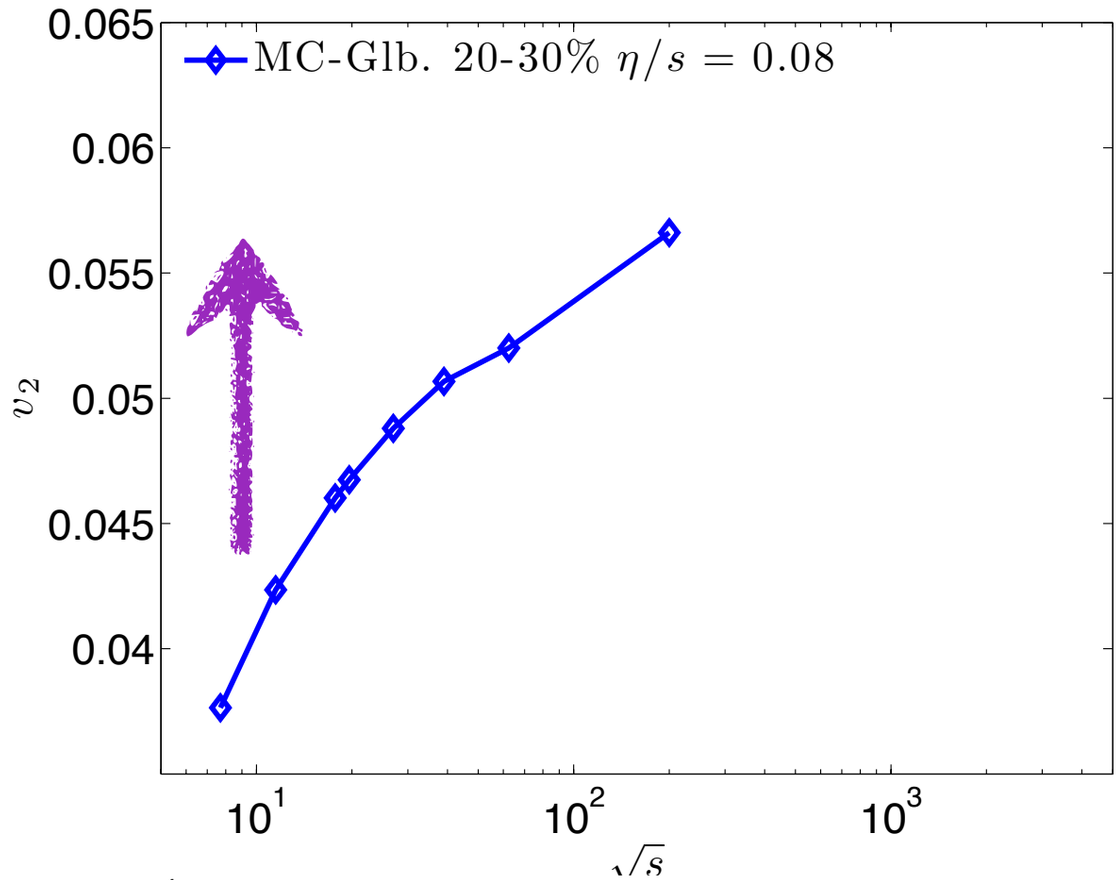

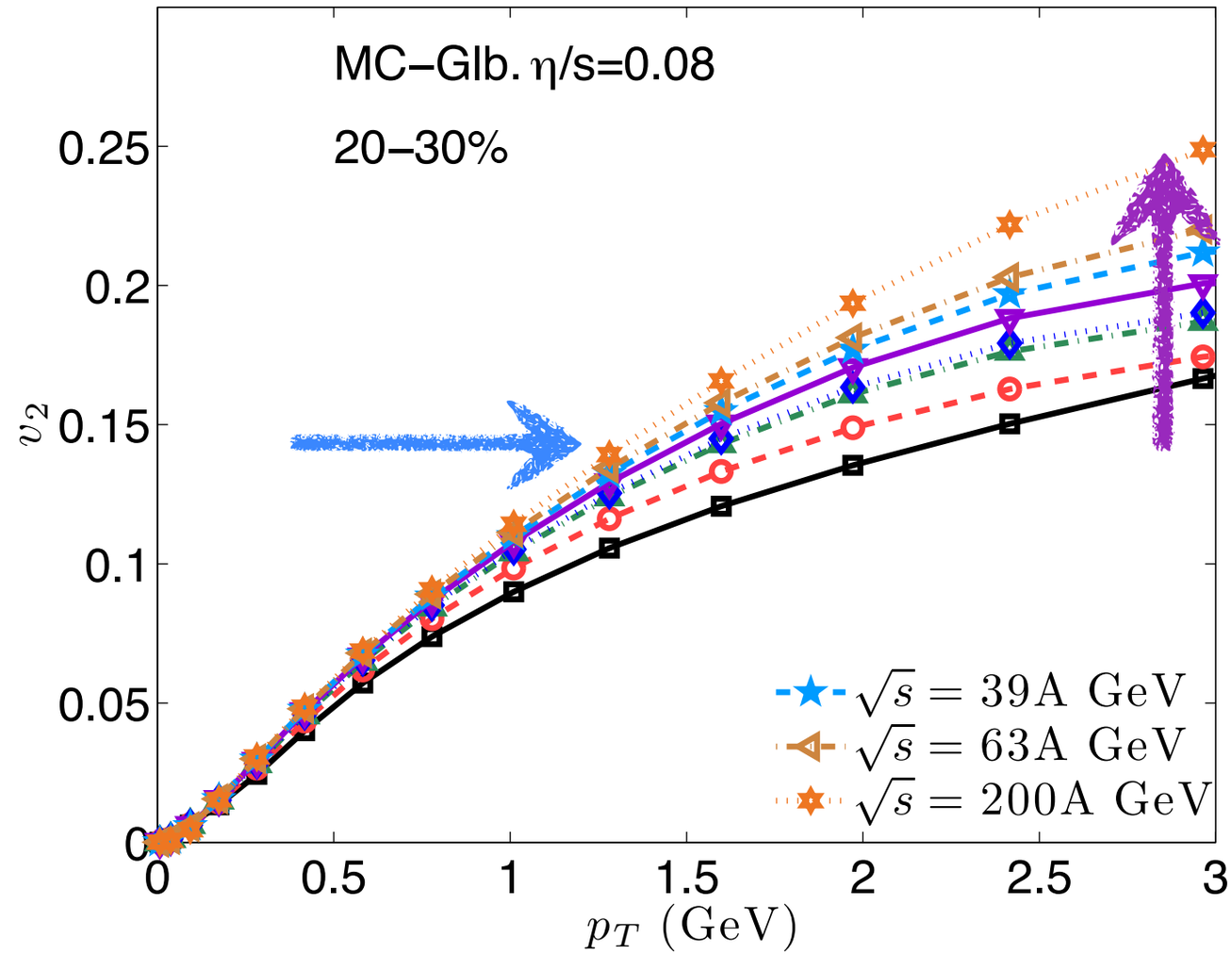

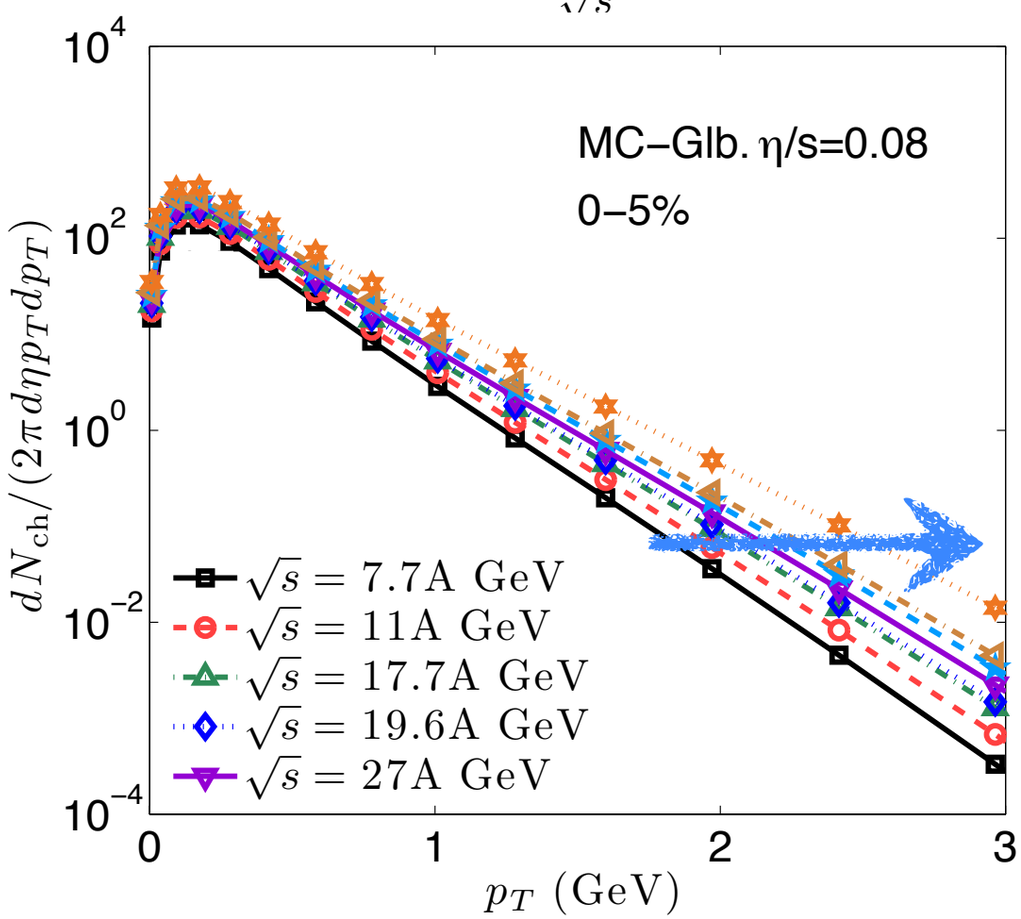

Differential $v_2(p_T)$

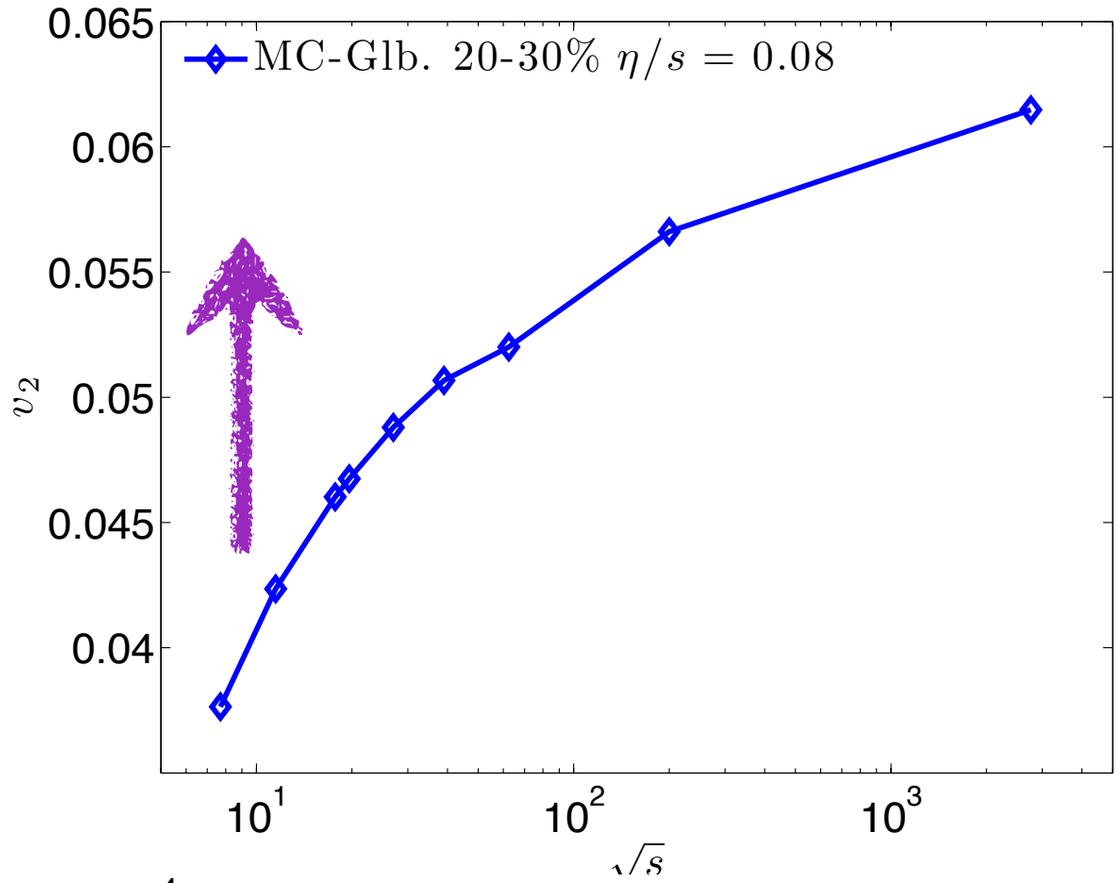

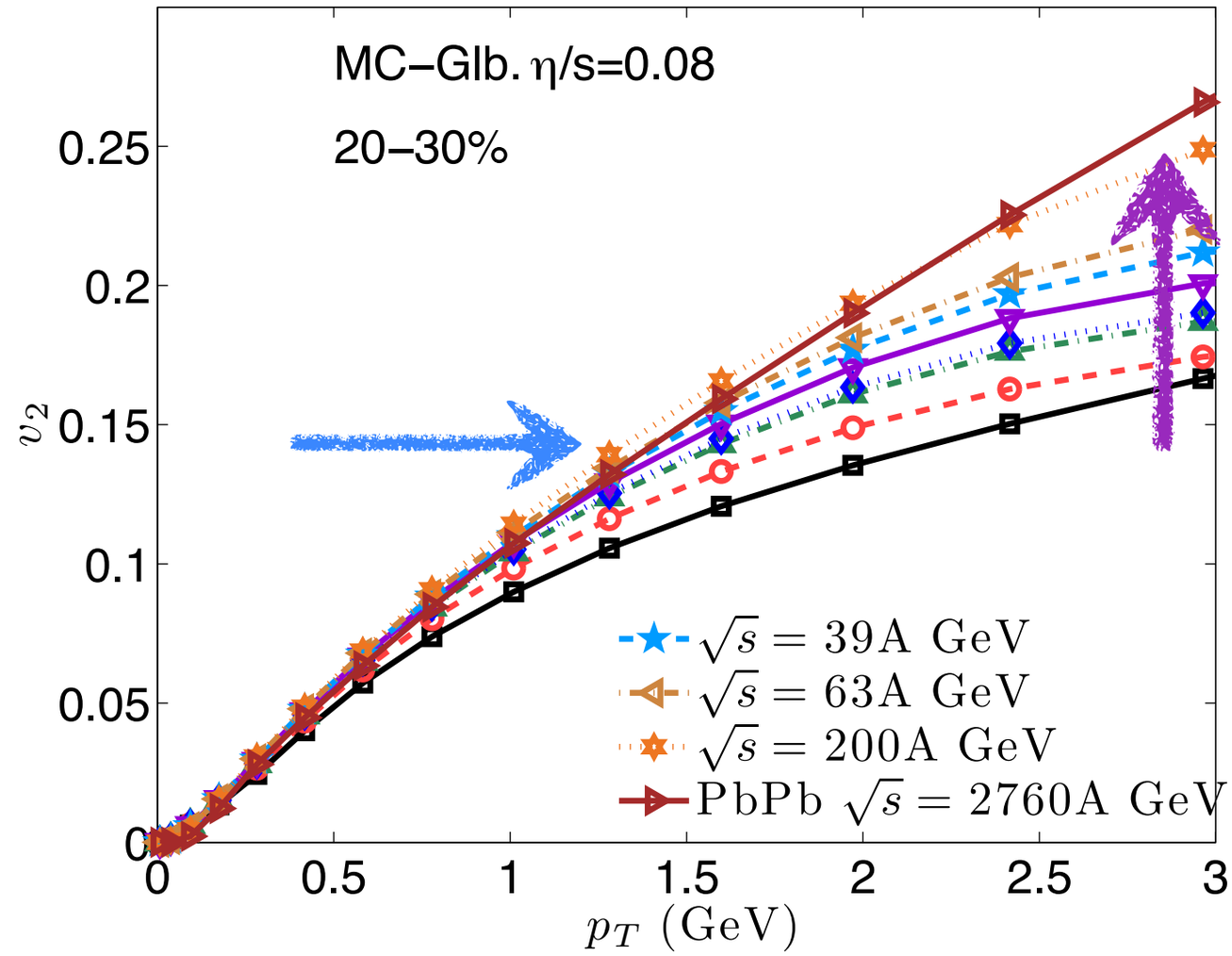

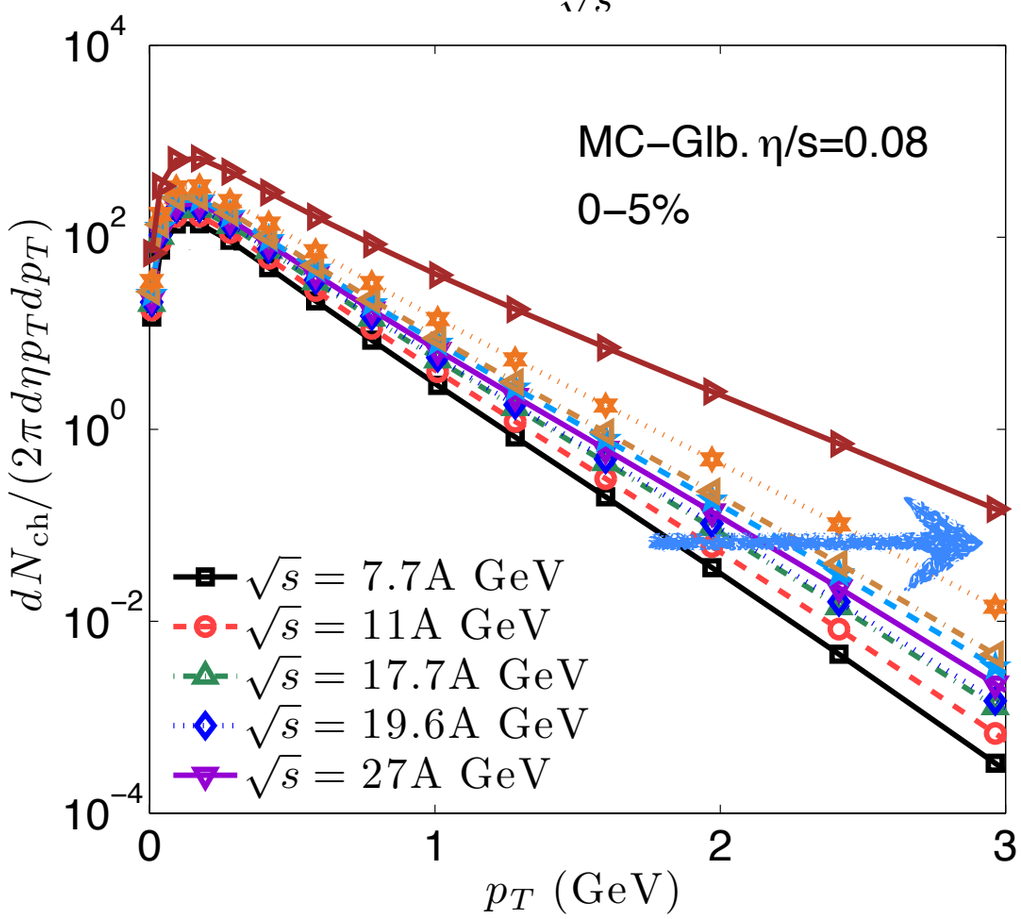

Differential $v_2(p_T)$

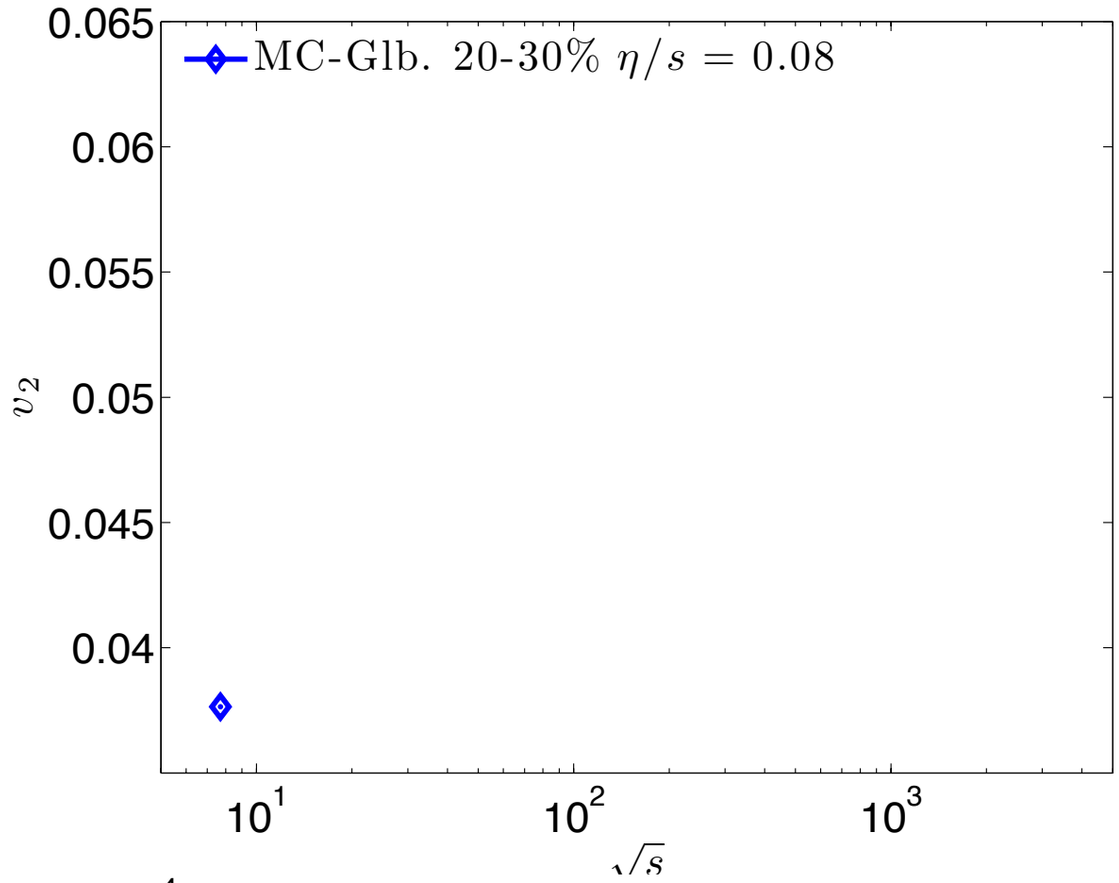

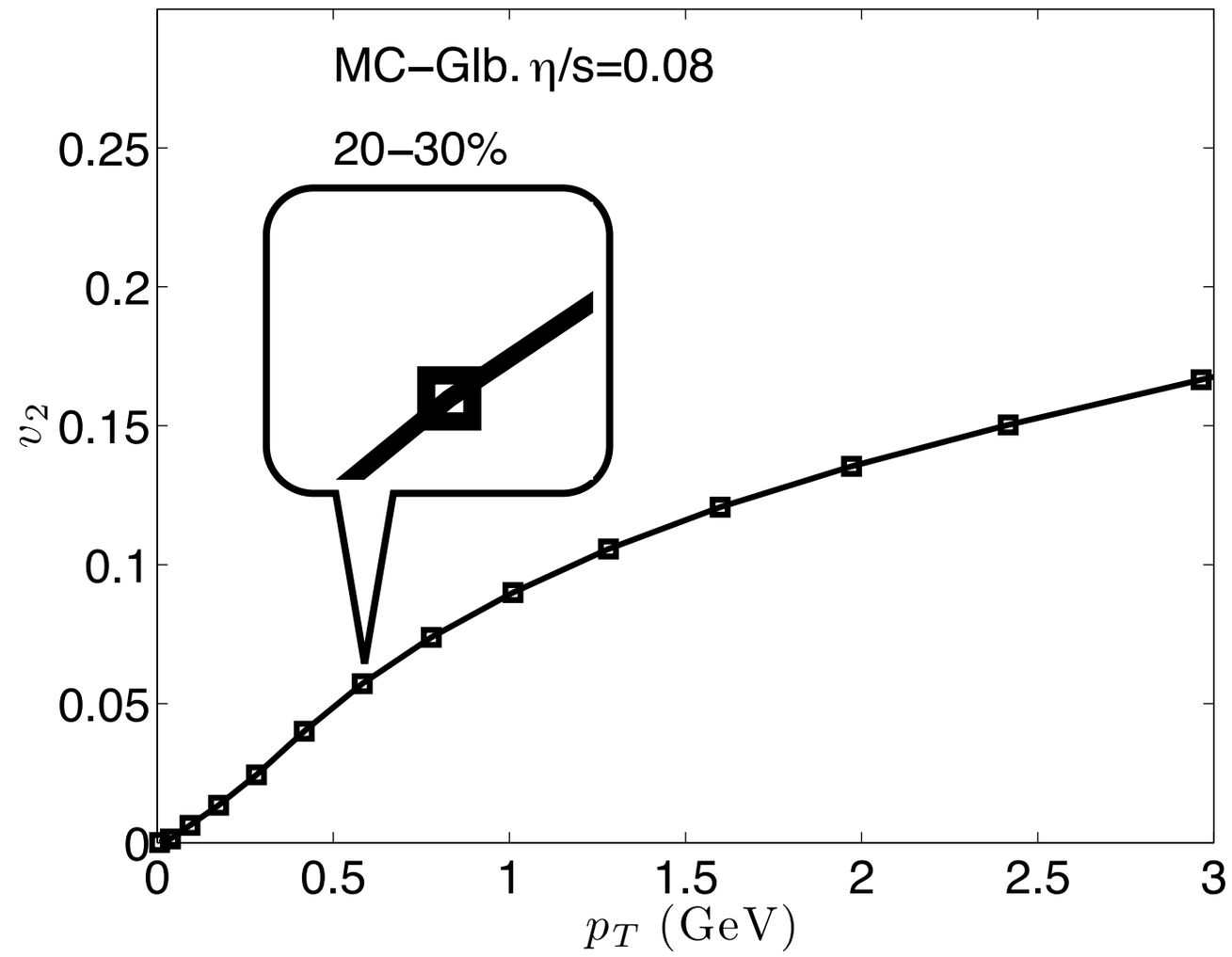

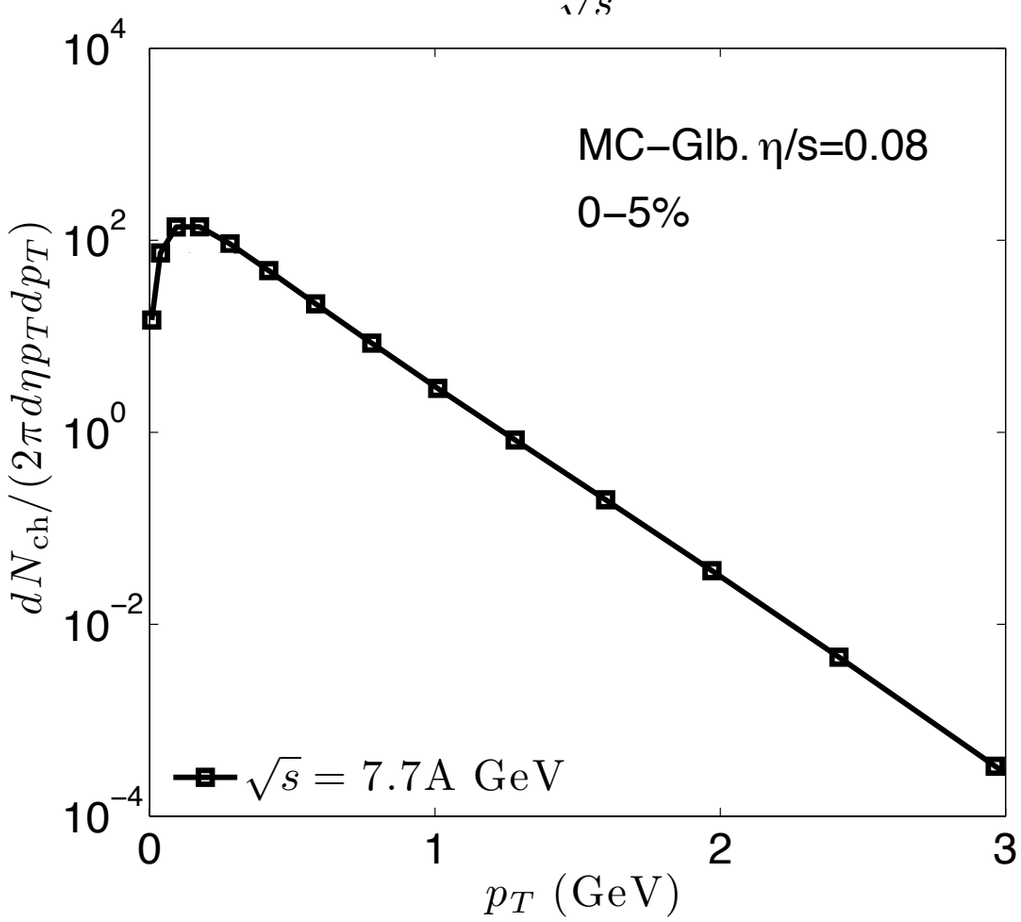

Differential $v_2(p_T)$

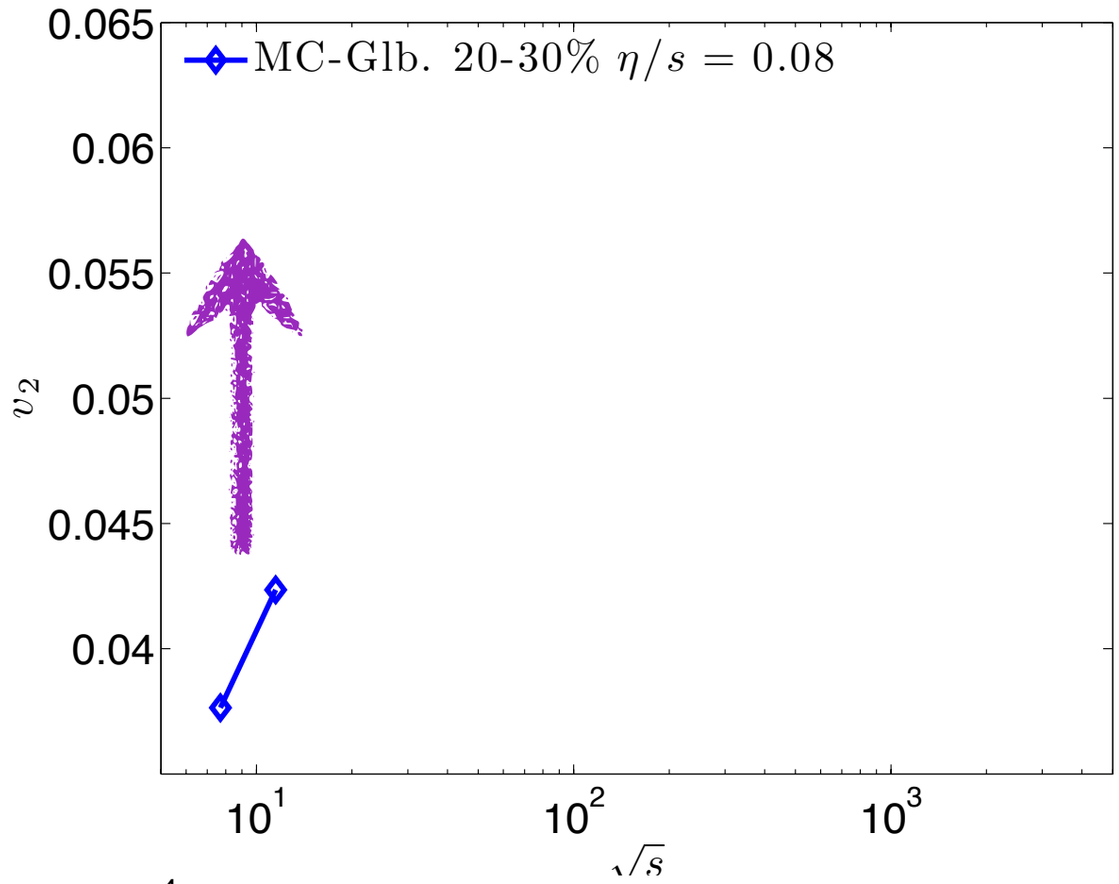

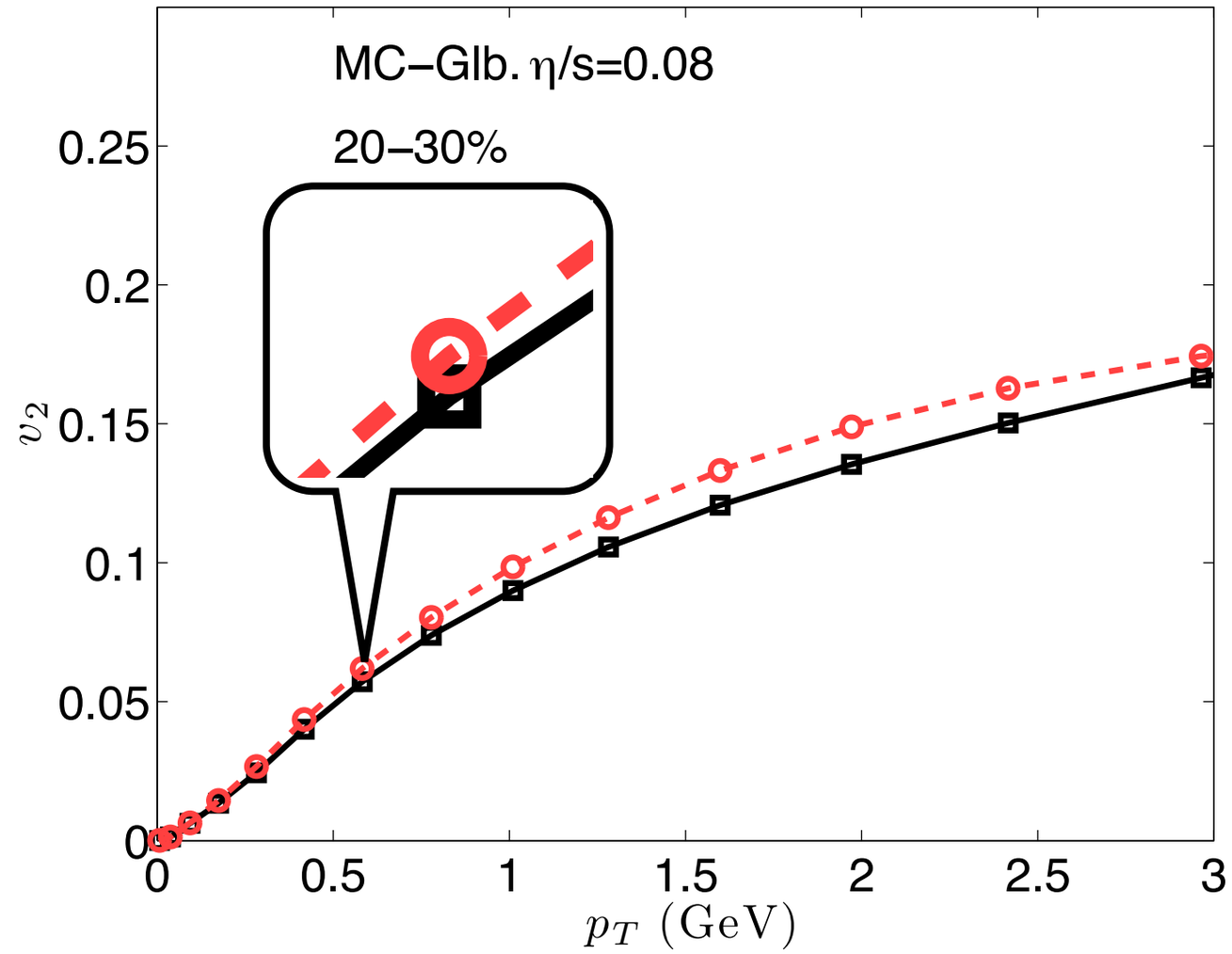

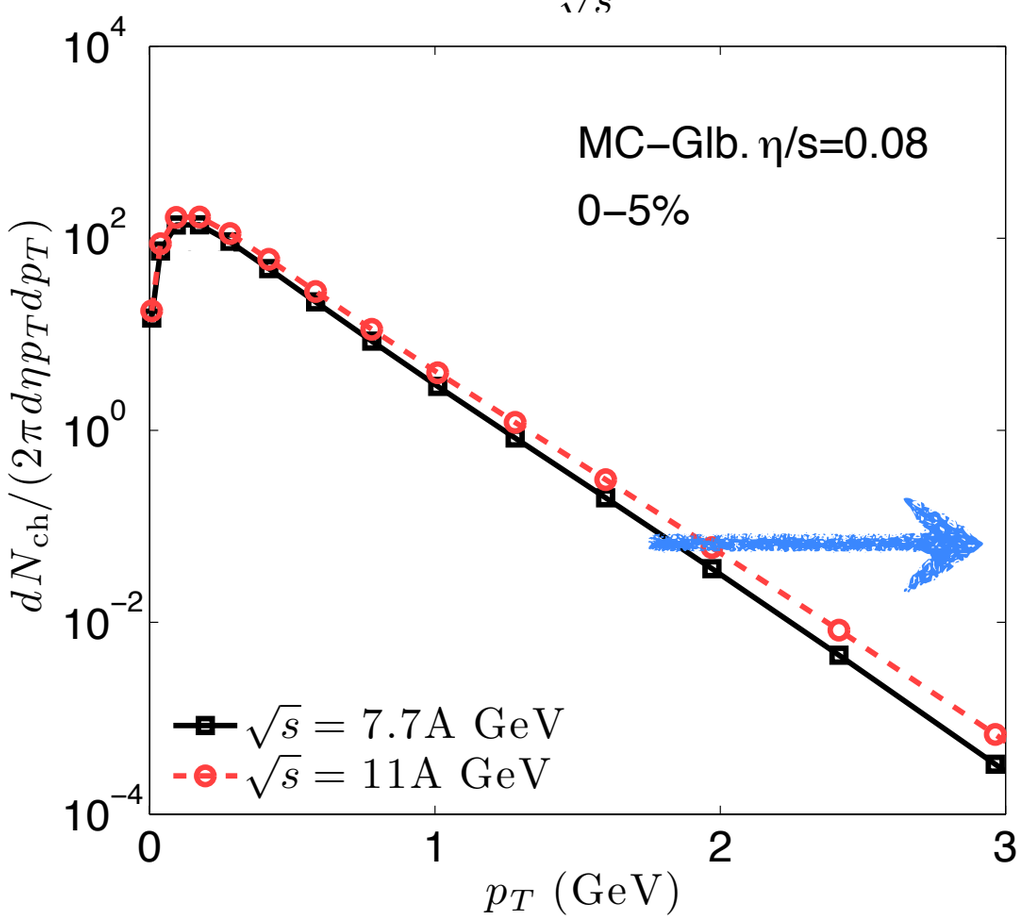

Differential $v_2(p_T)$

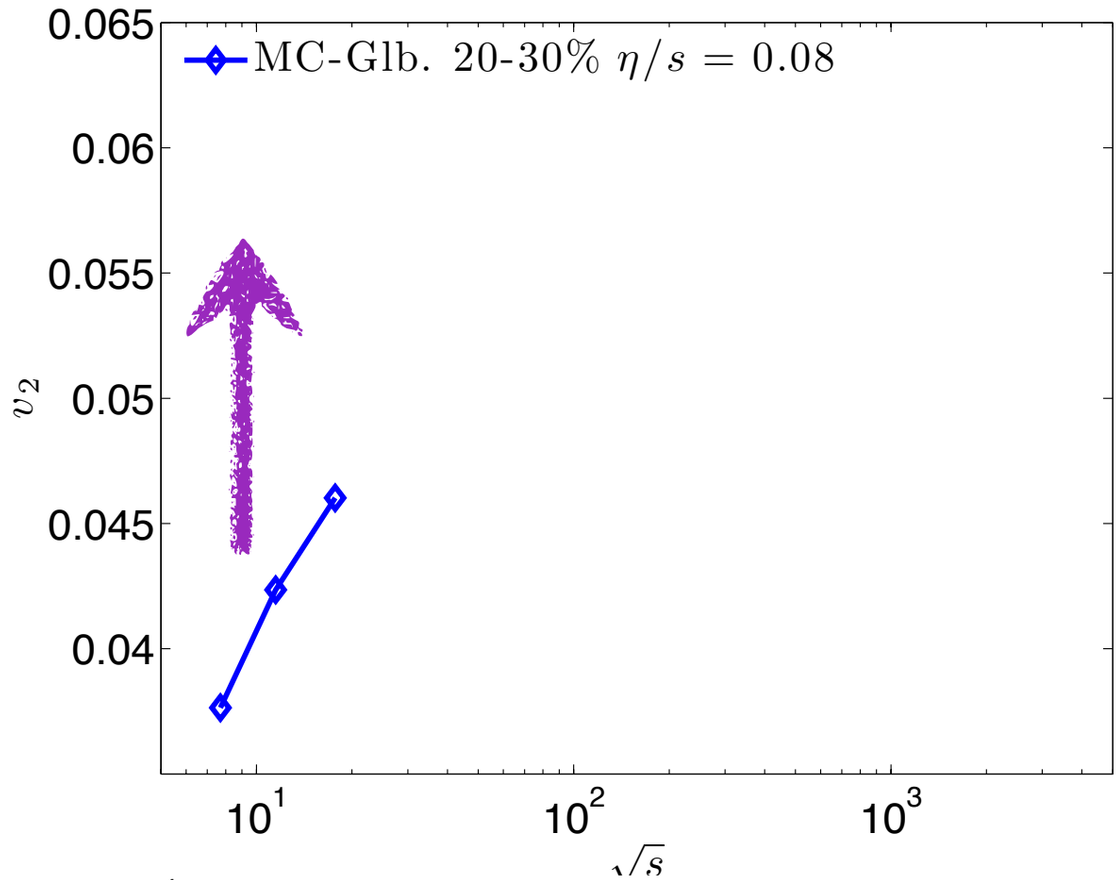

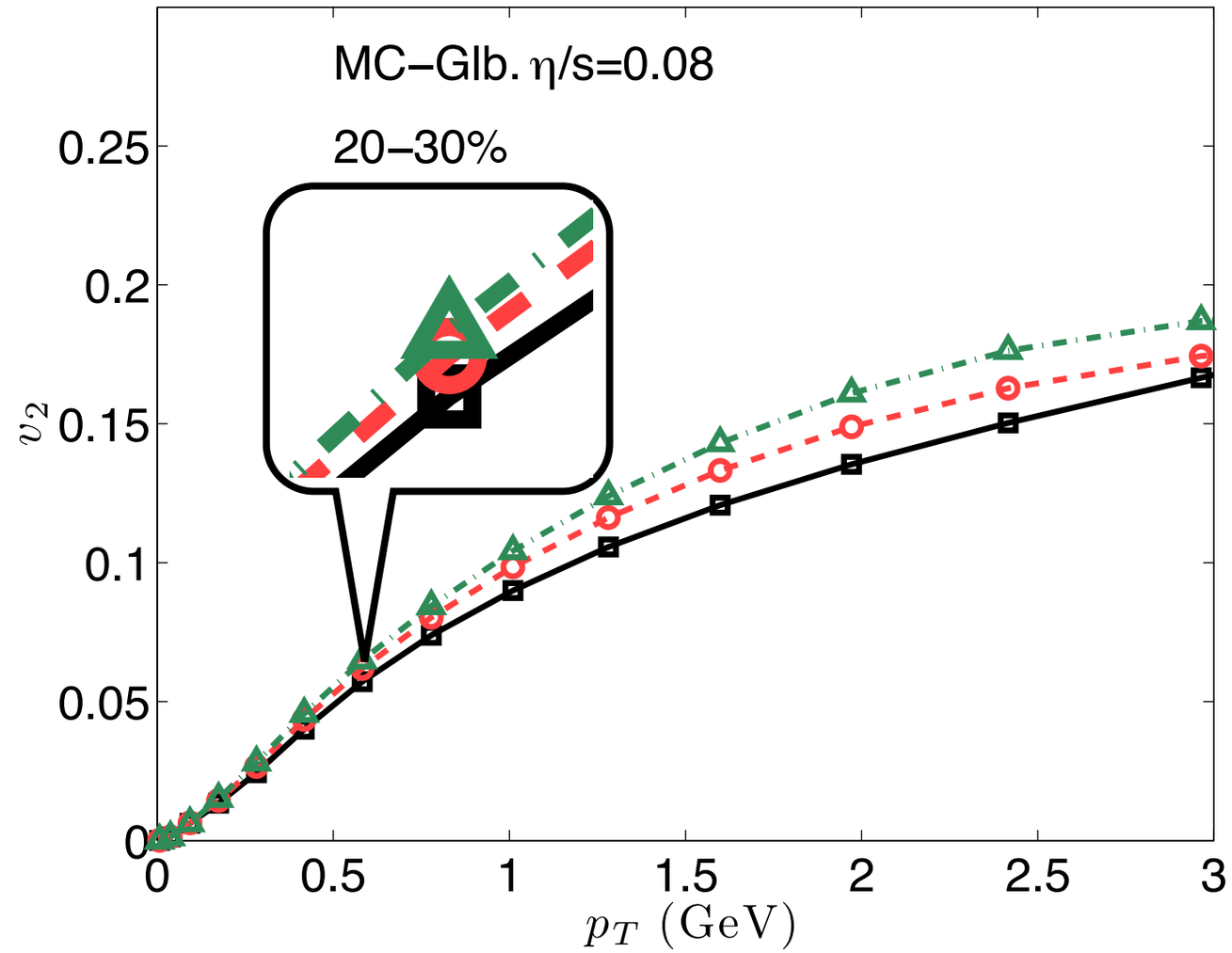

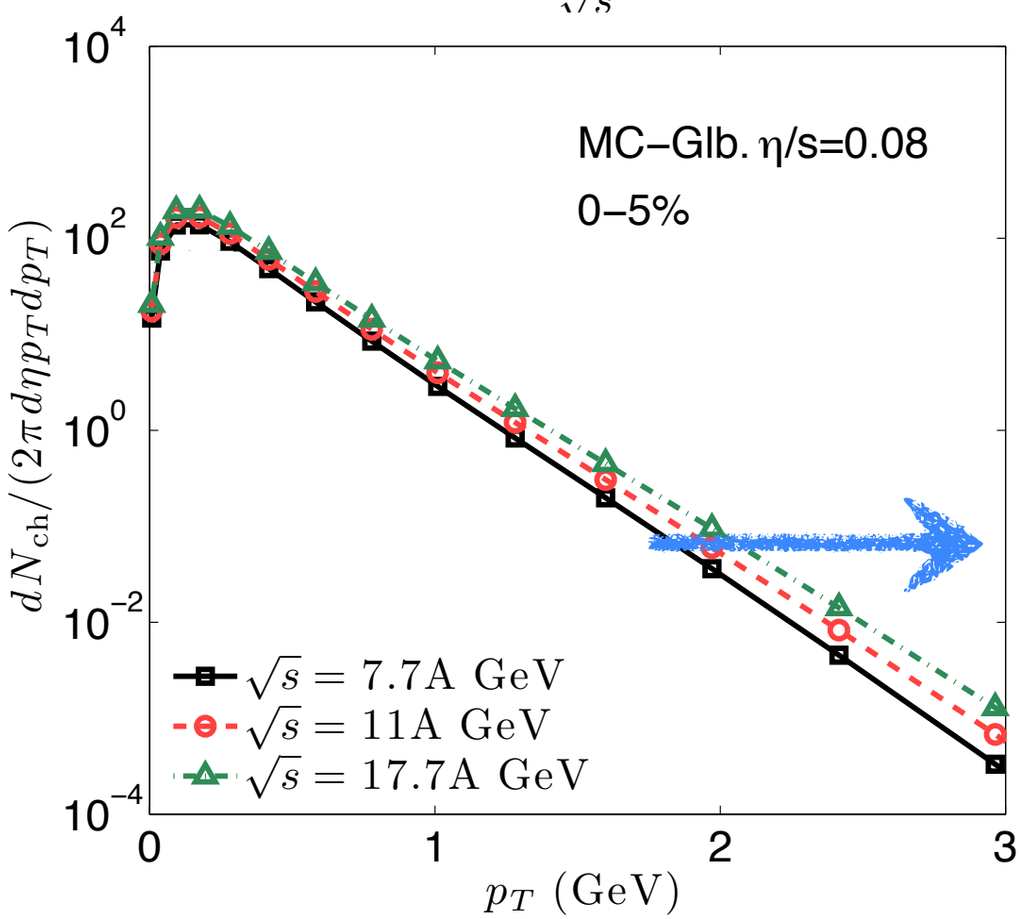

Differential $v_2(p_T)$

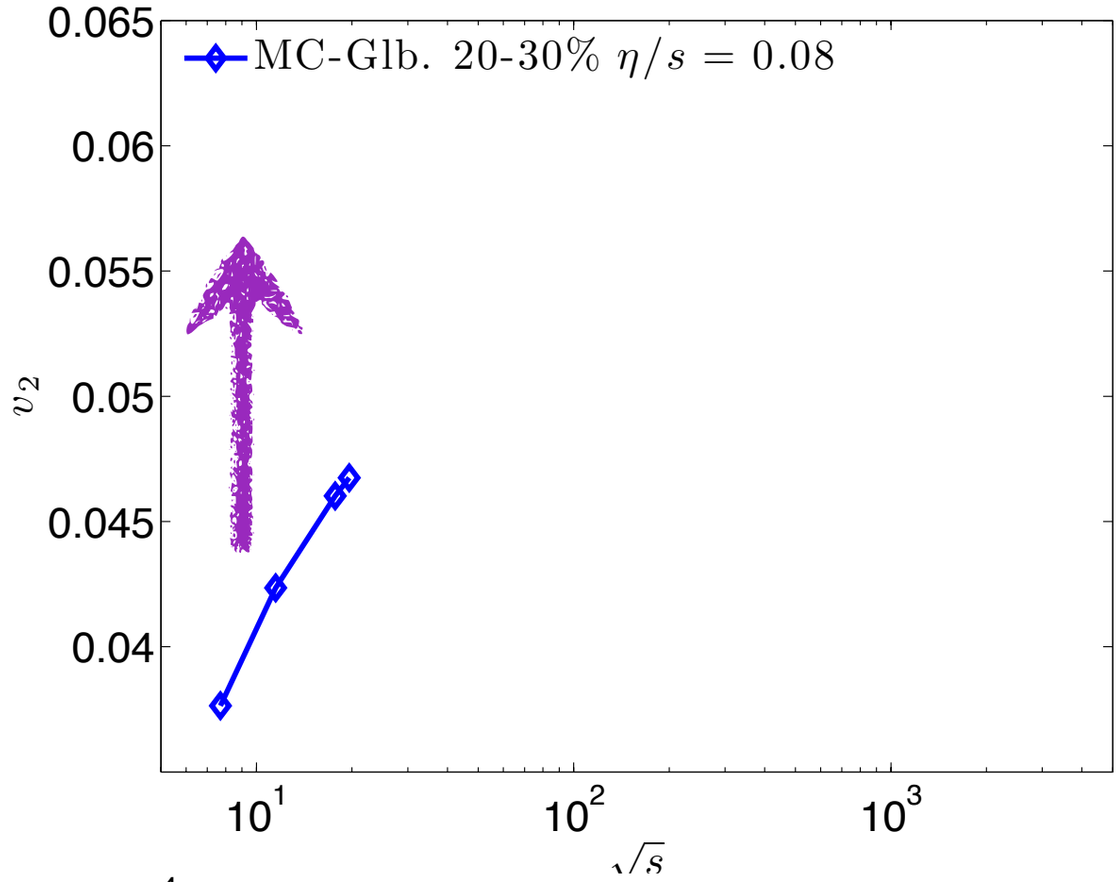

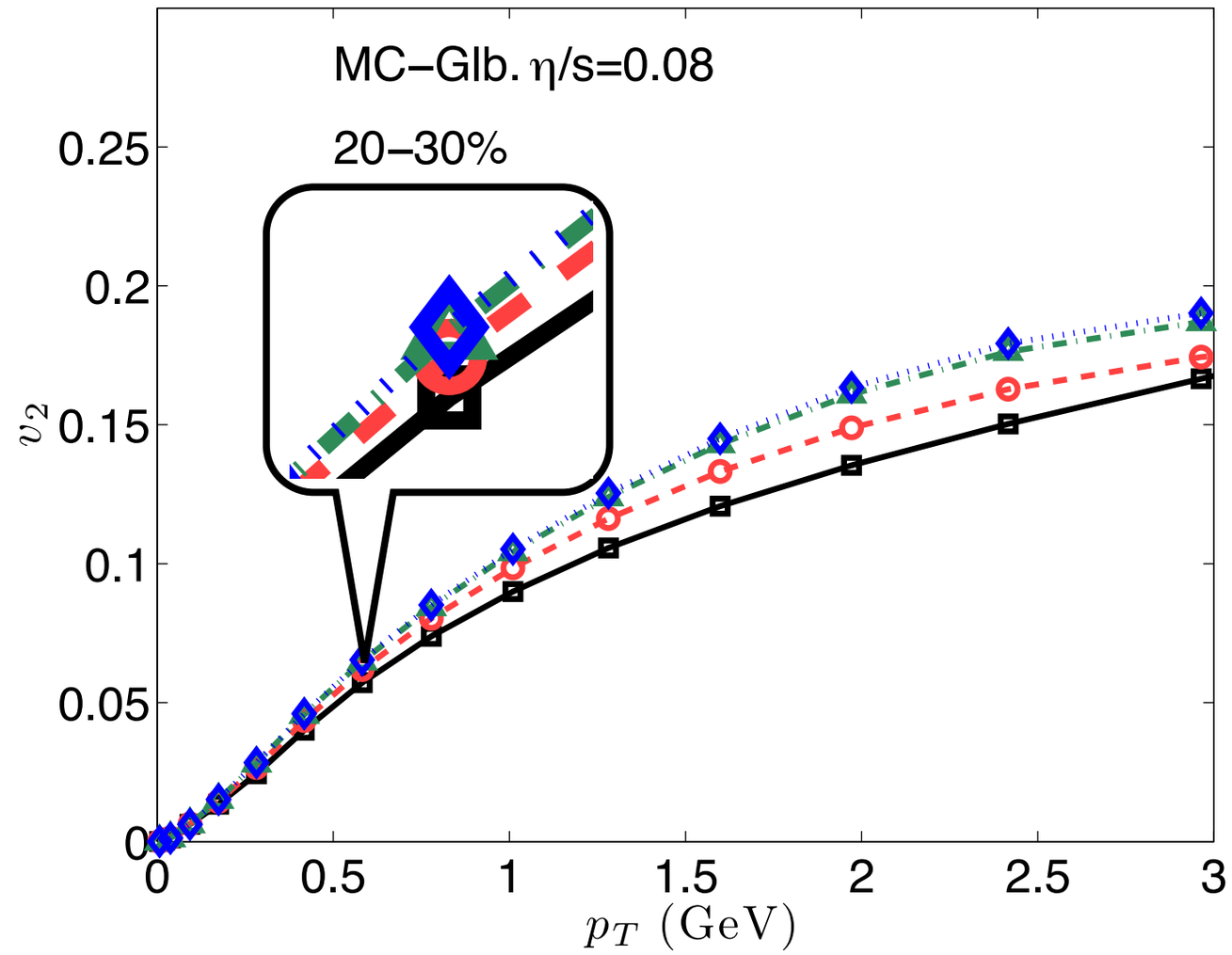

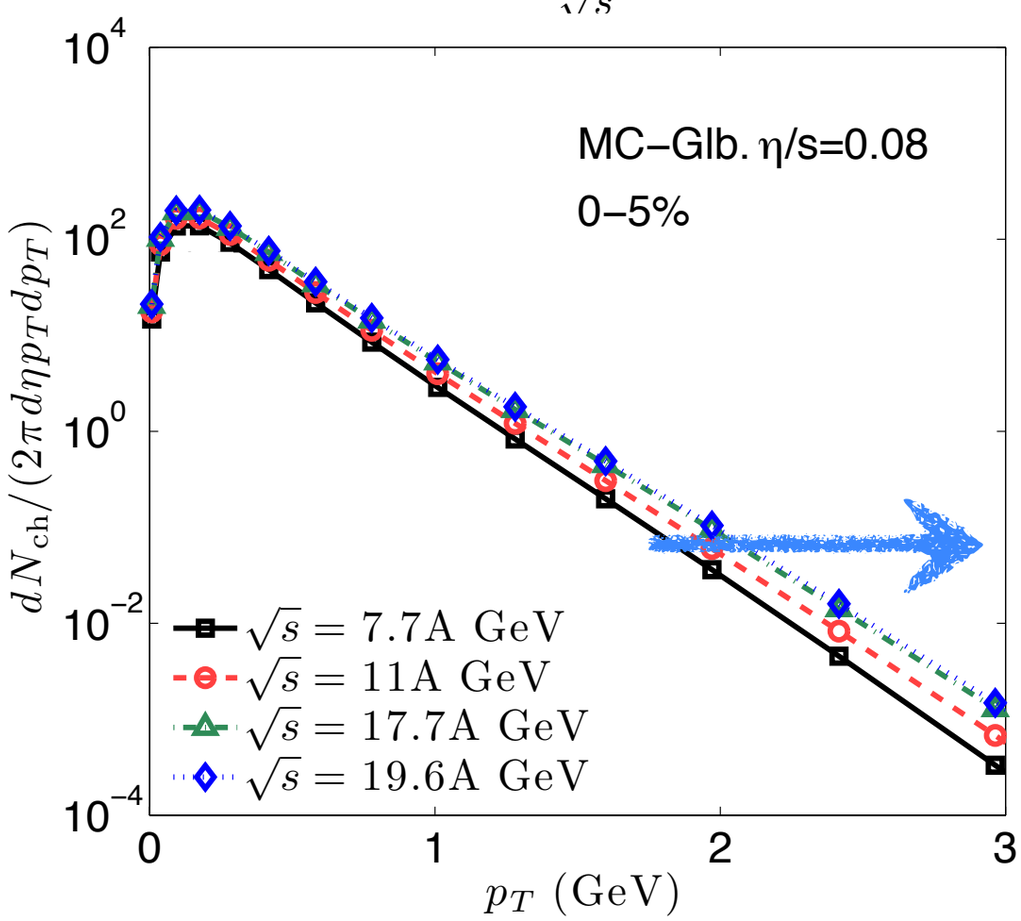

Differential $v_2(p_T)$

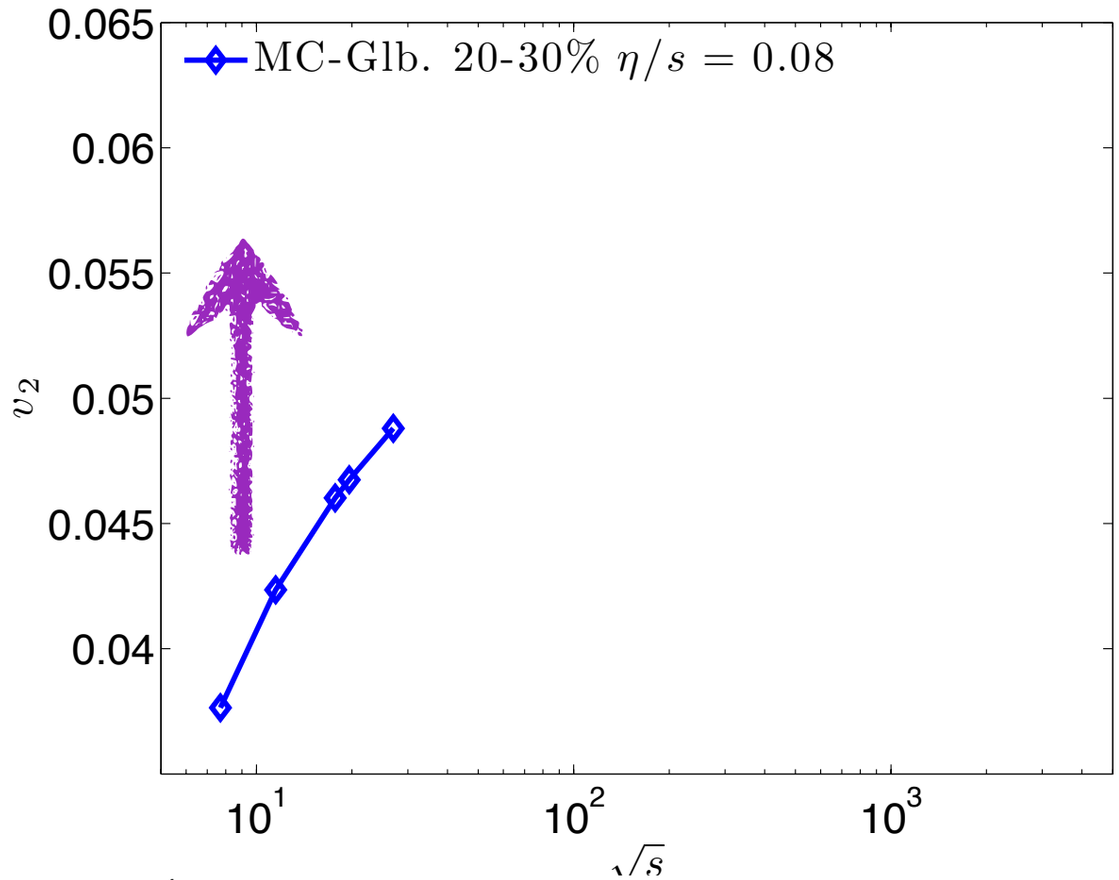

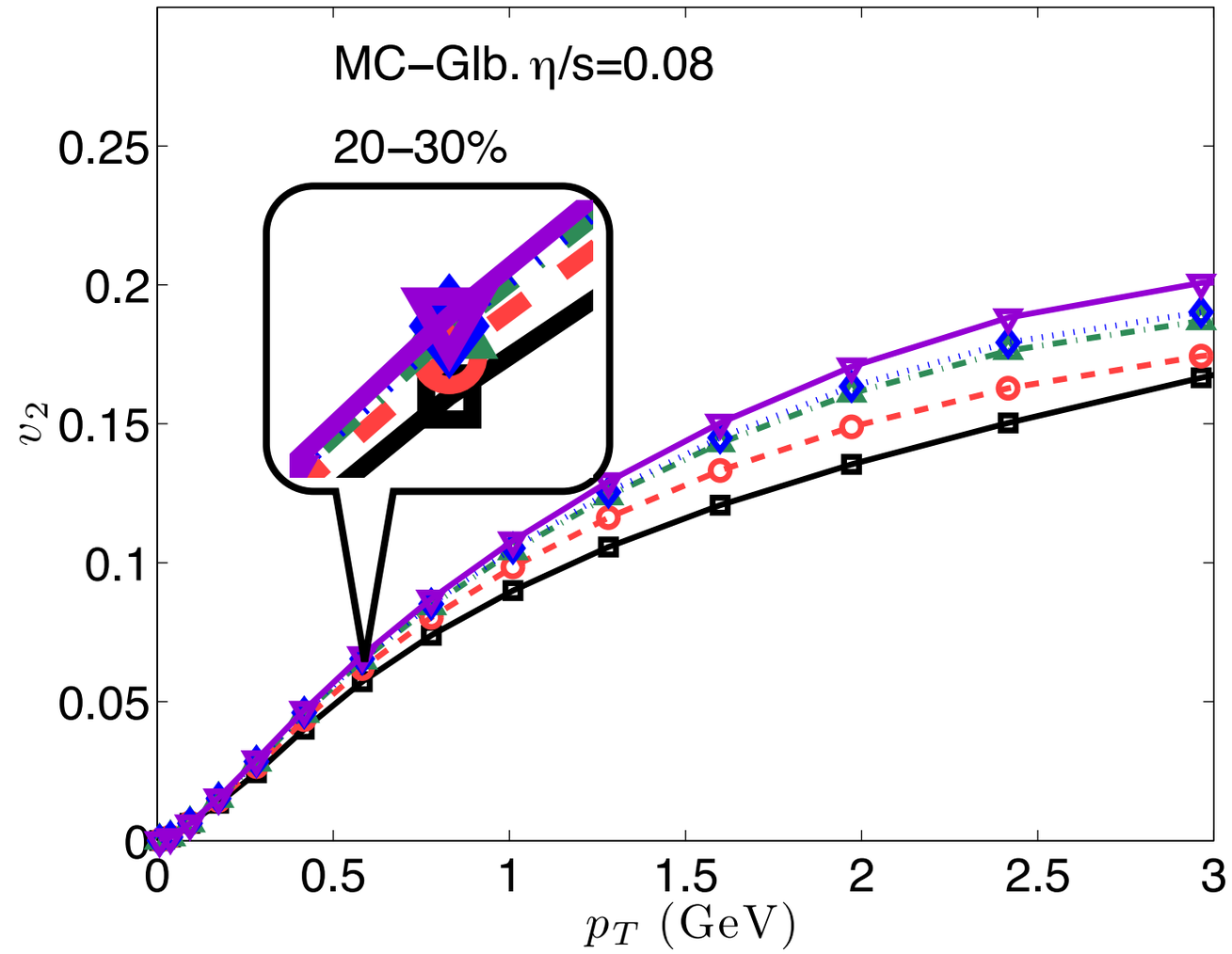

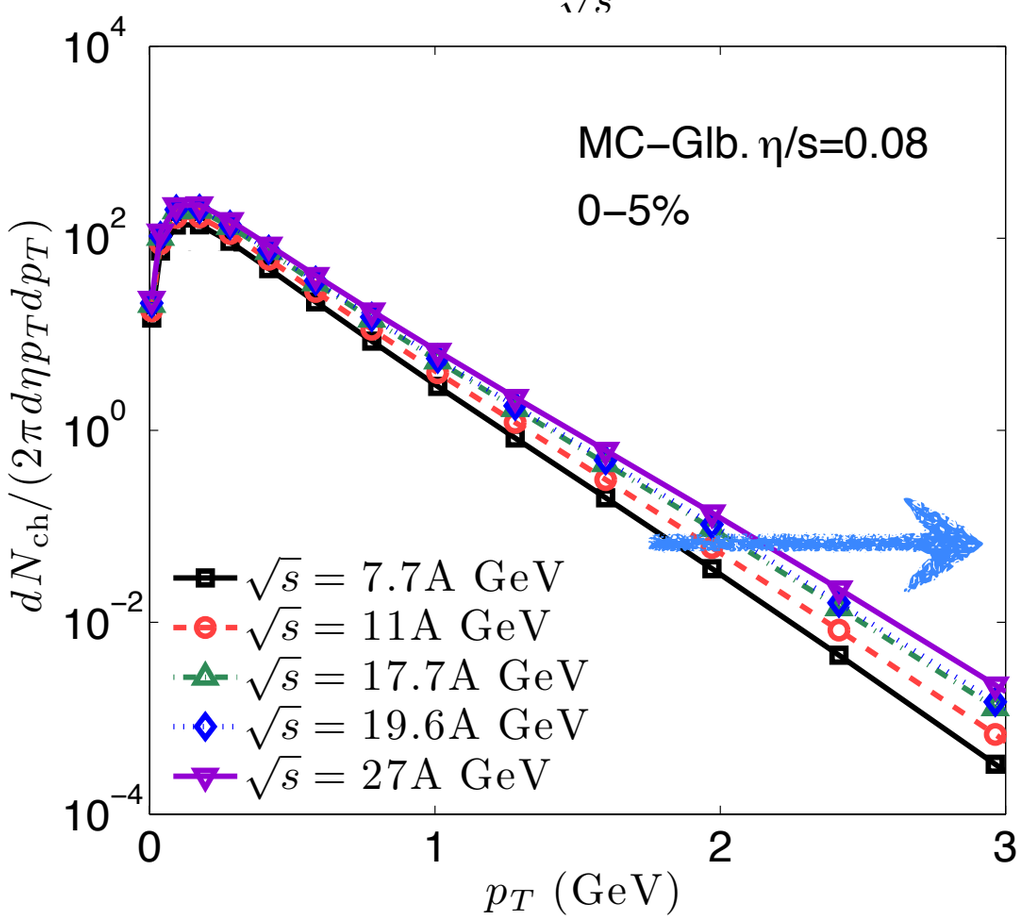

Differential $v_2(p_T)$

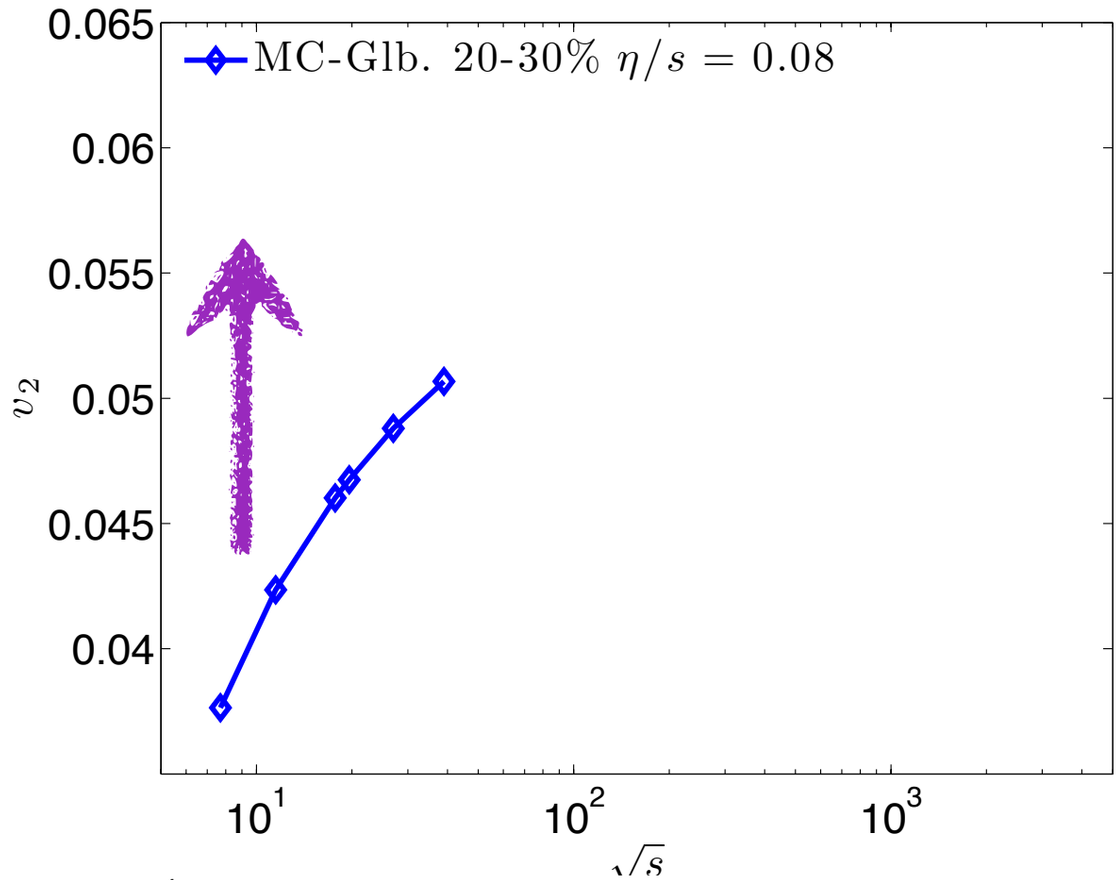

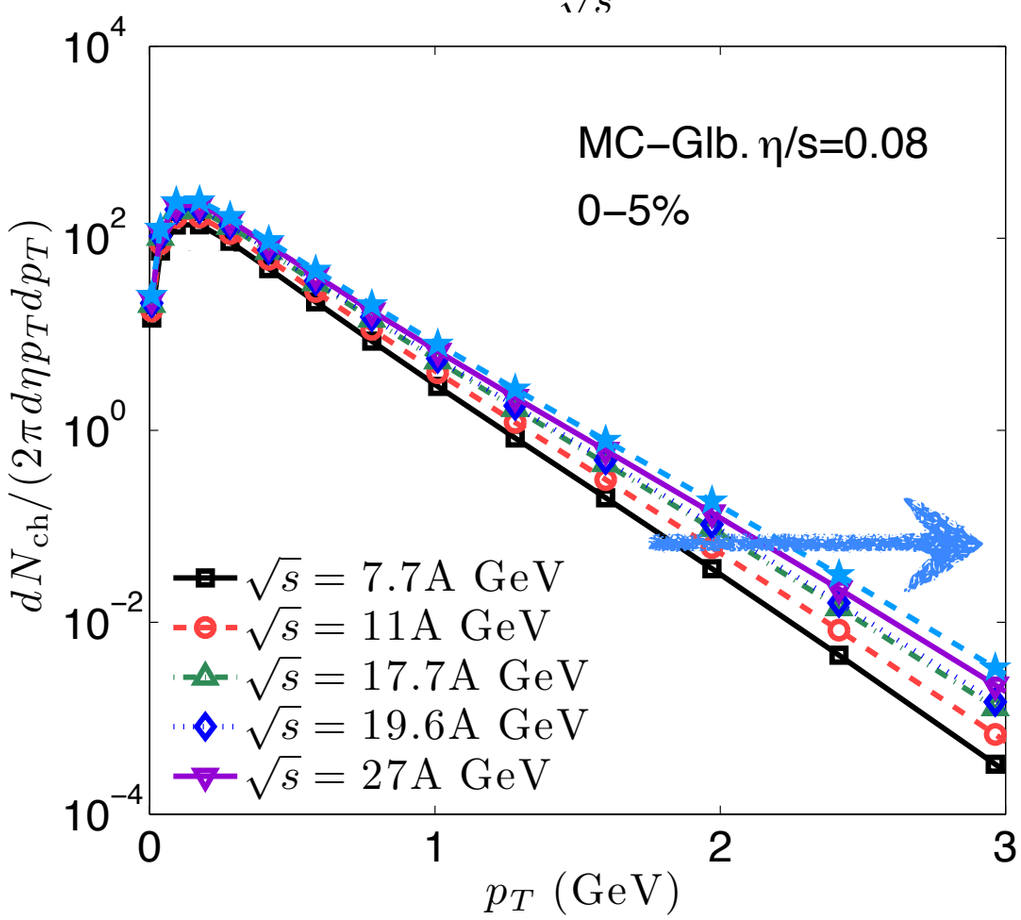

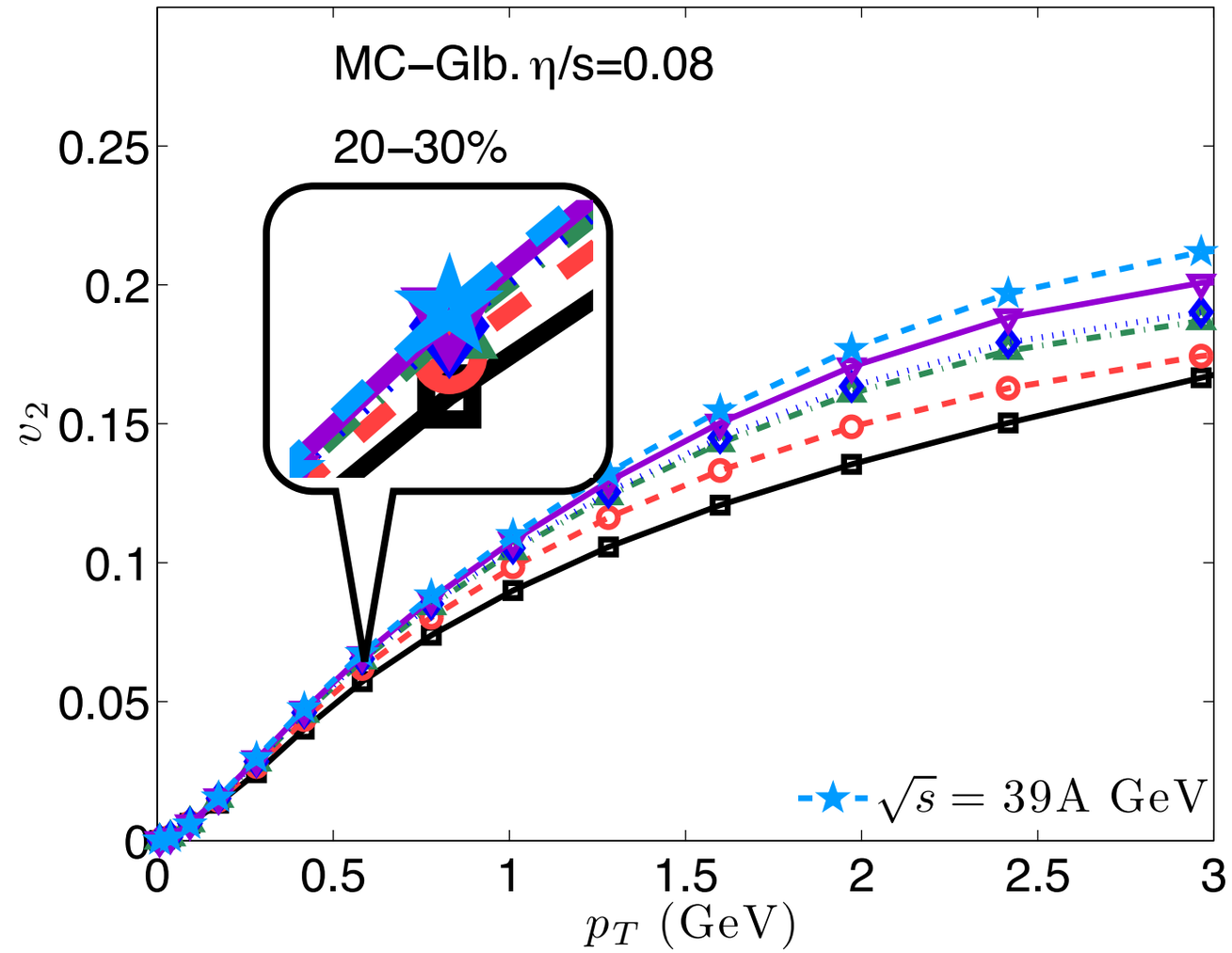

Differential $v_2(p_T)$

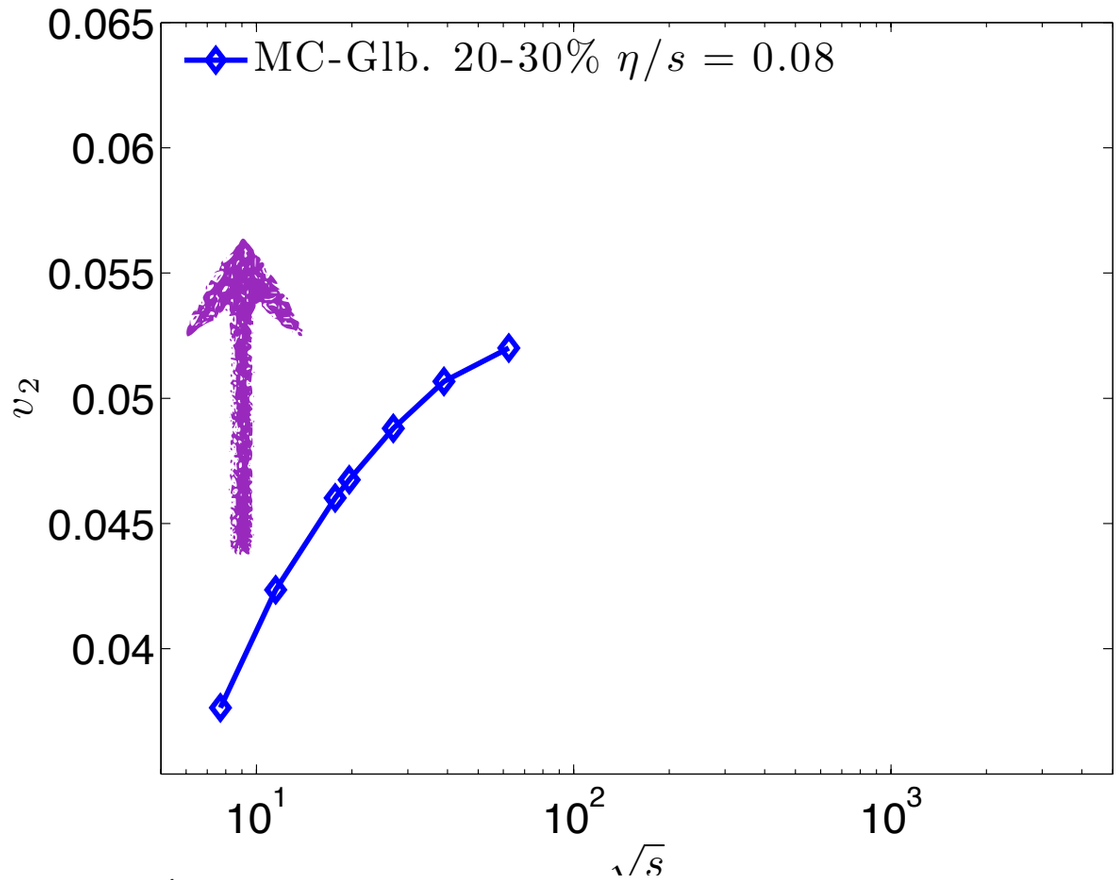

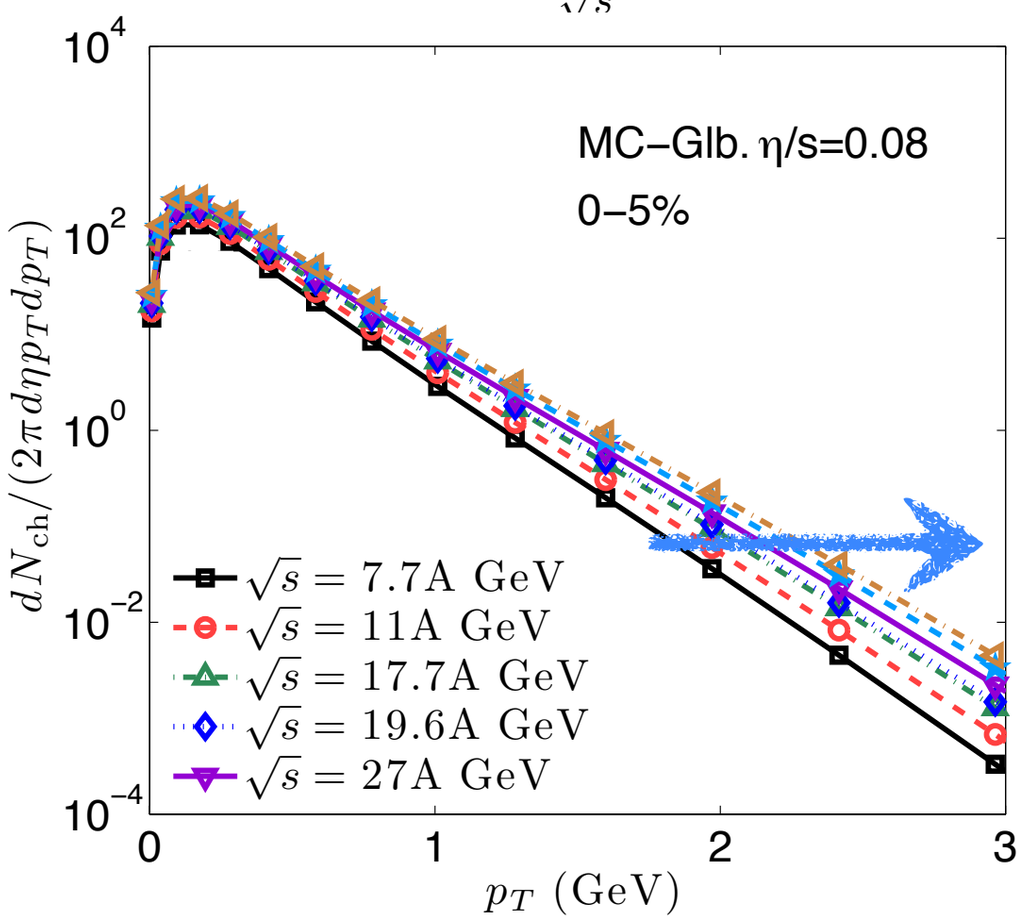

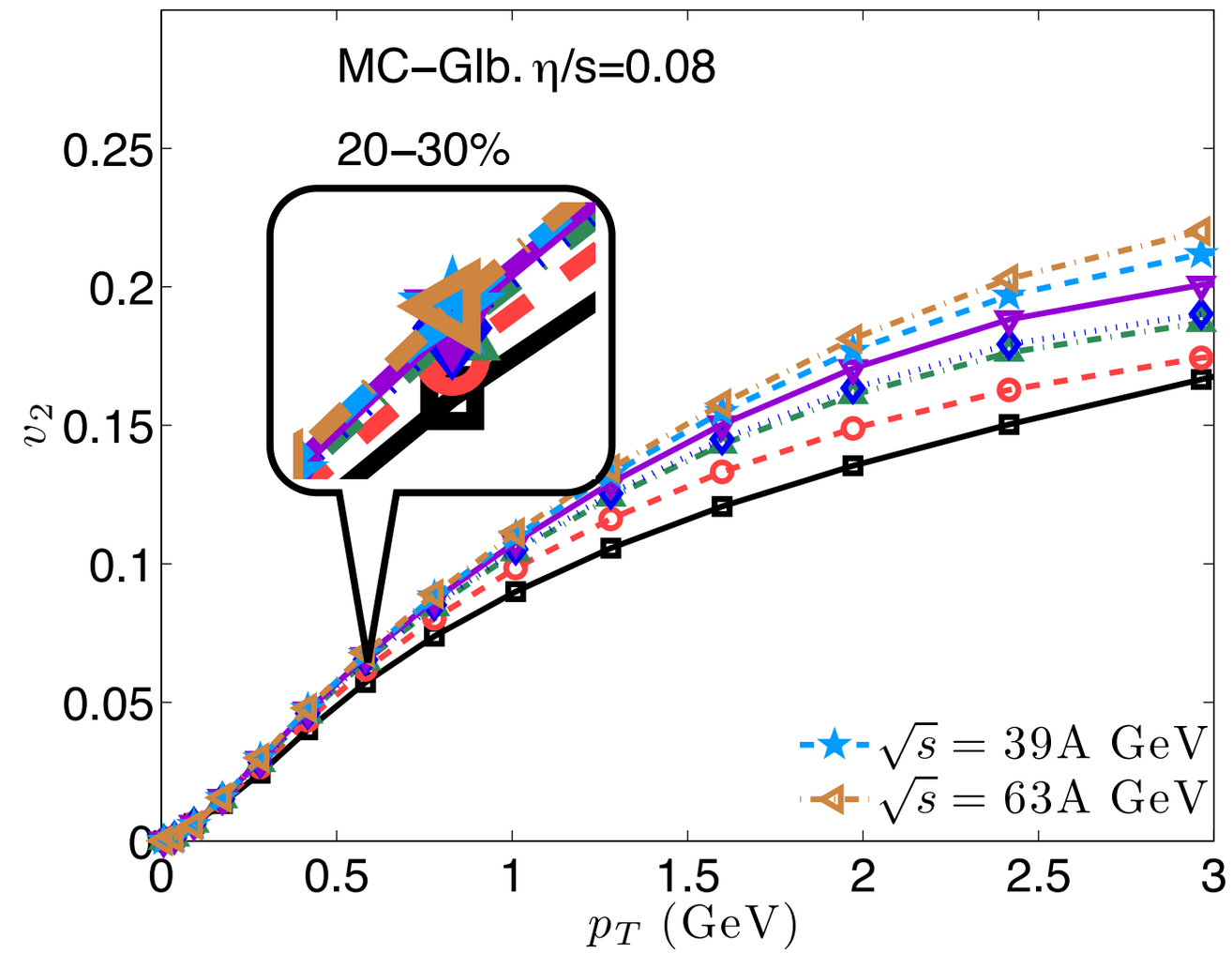

Differential $v_2(p_T)$

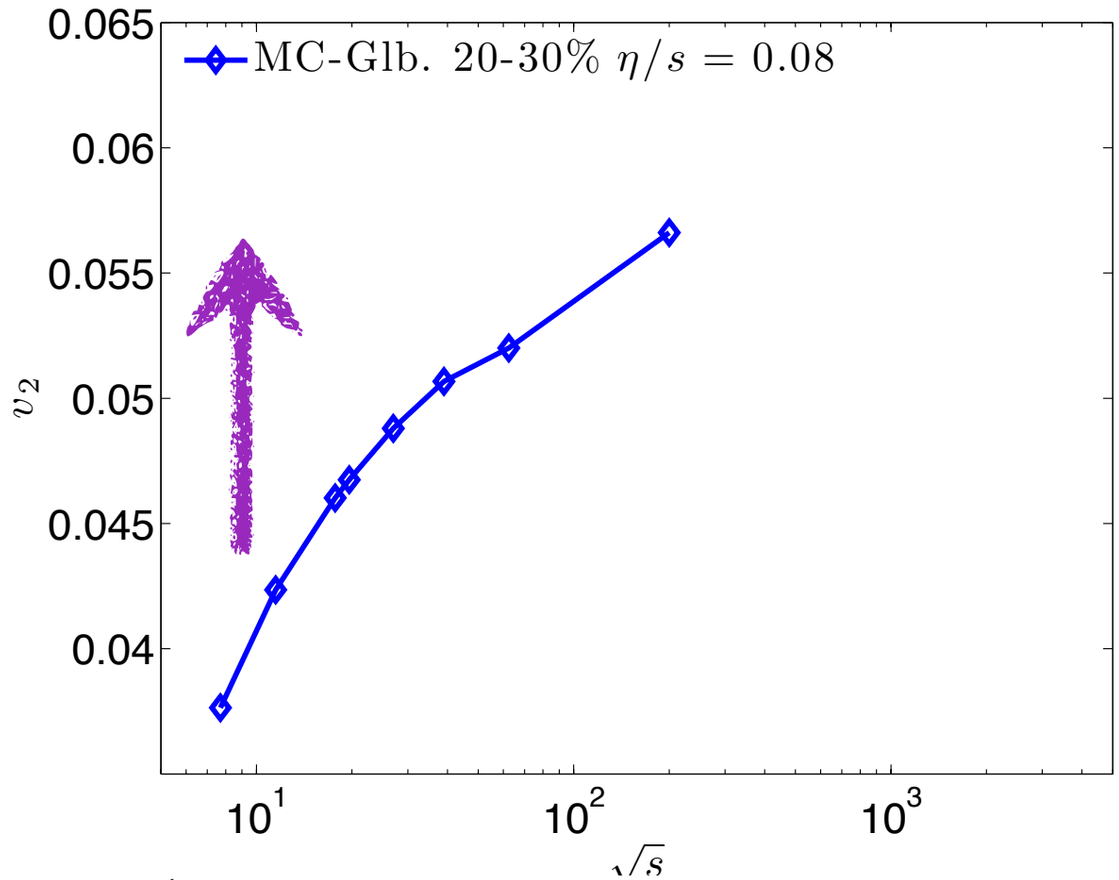

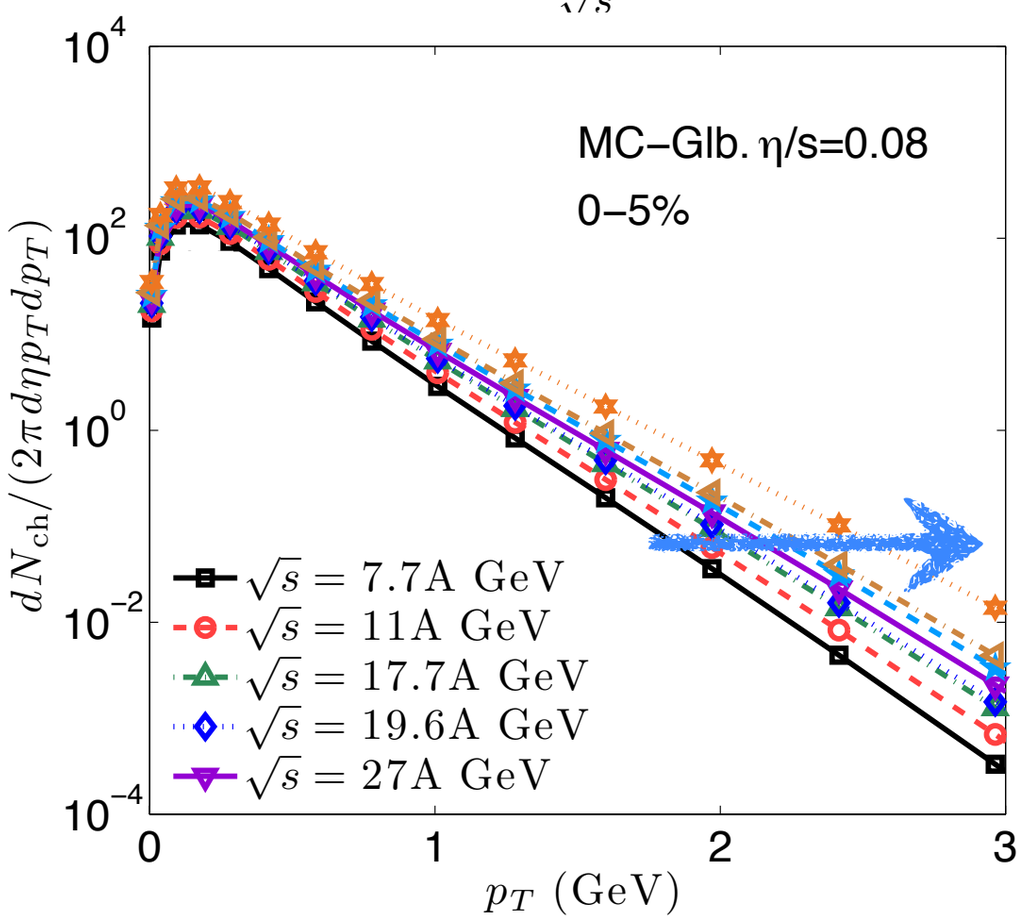

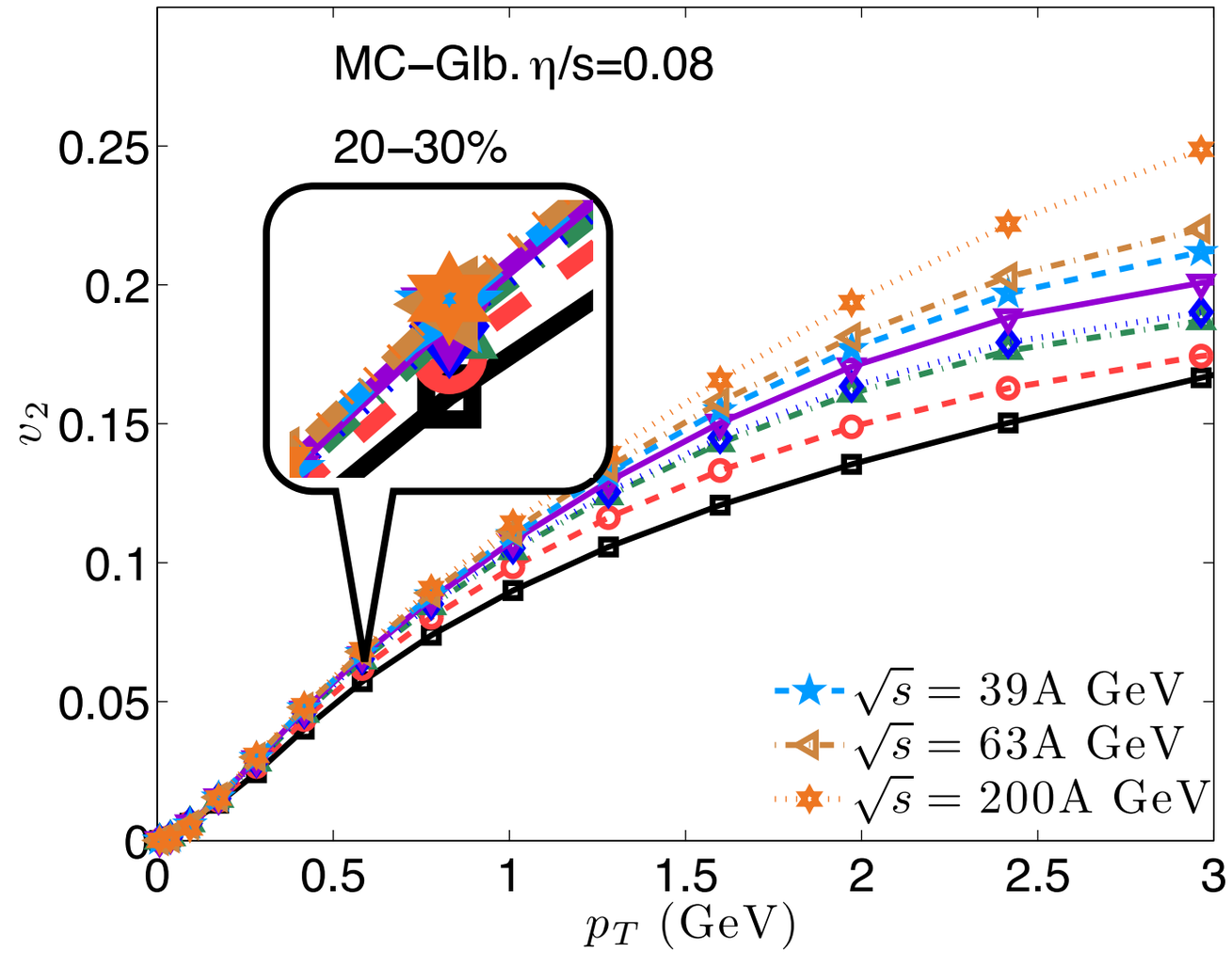

Differential $v_2(p_T)$

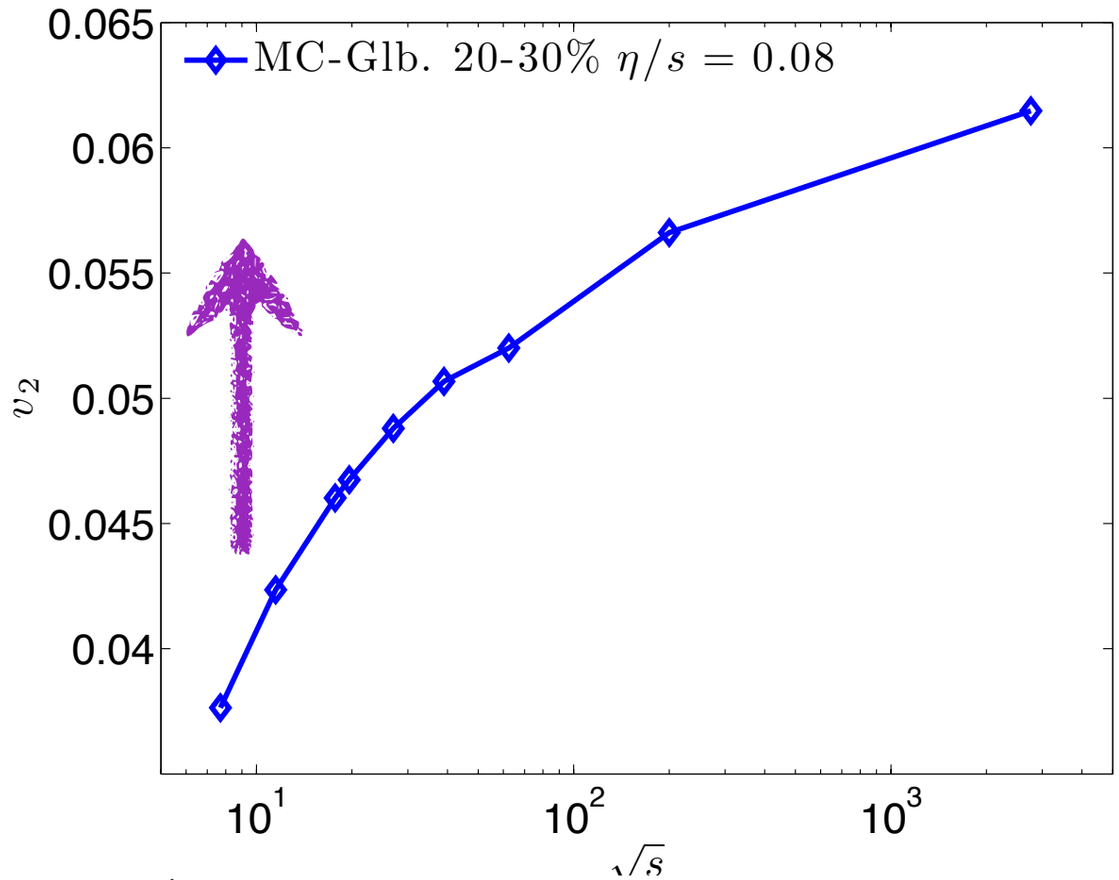

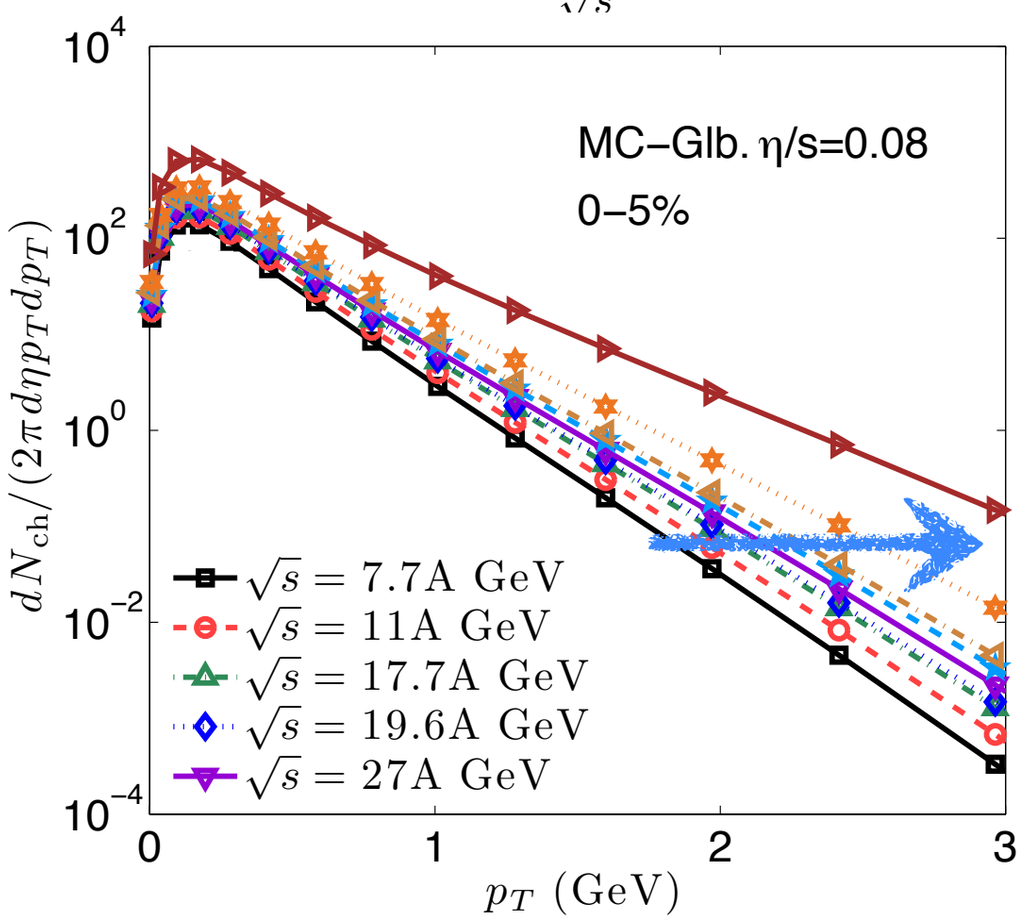

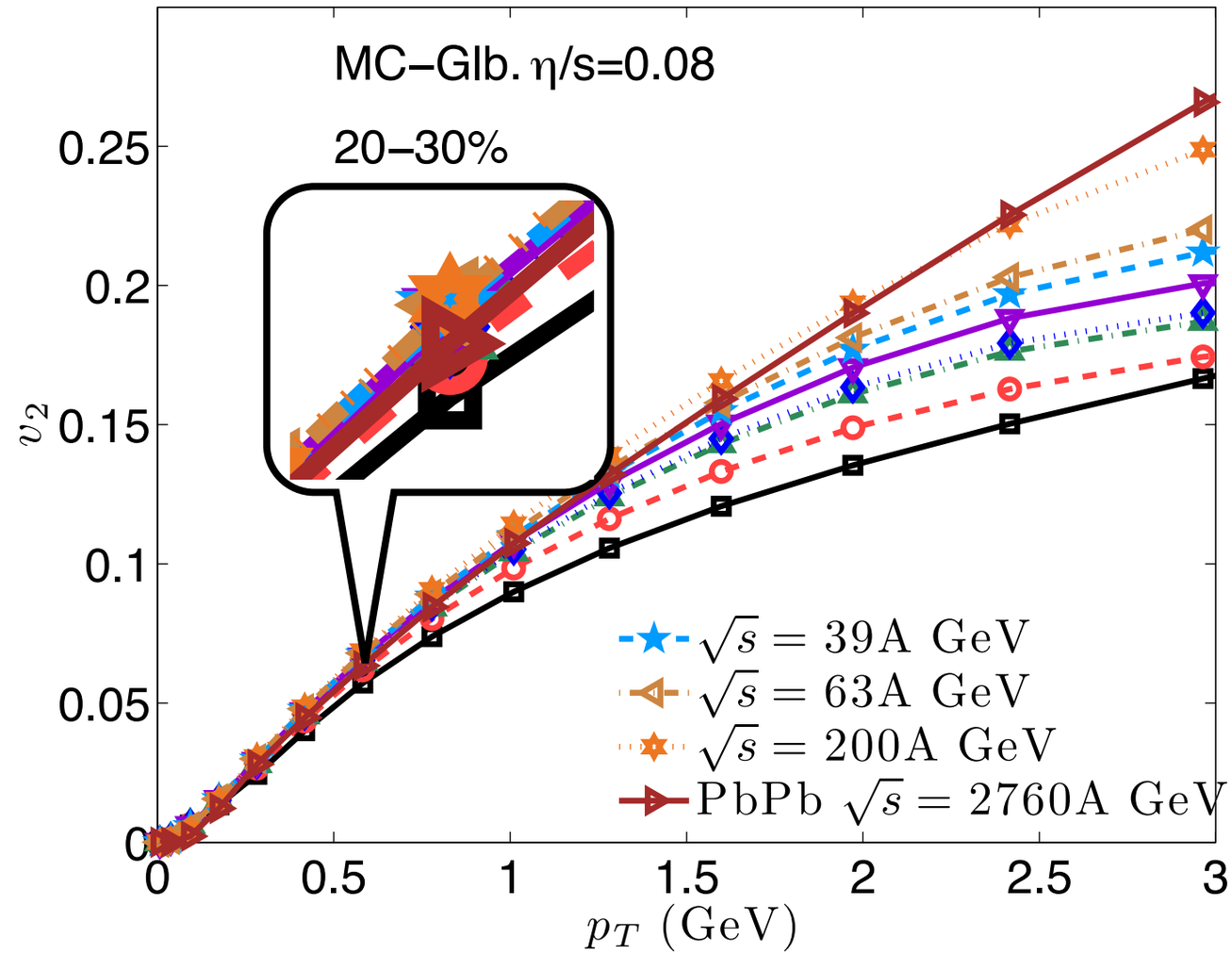

Differential $v_2(p_T)$

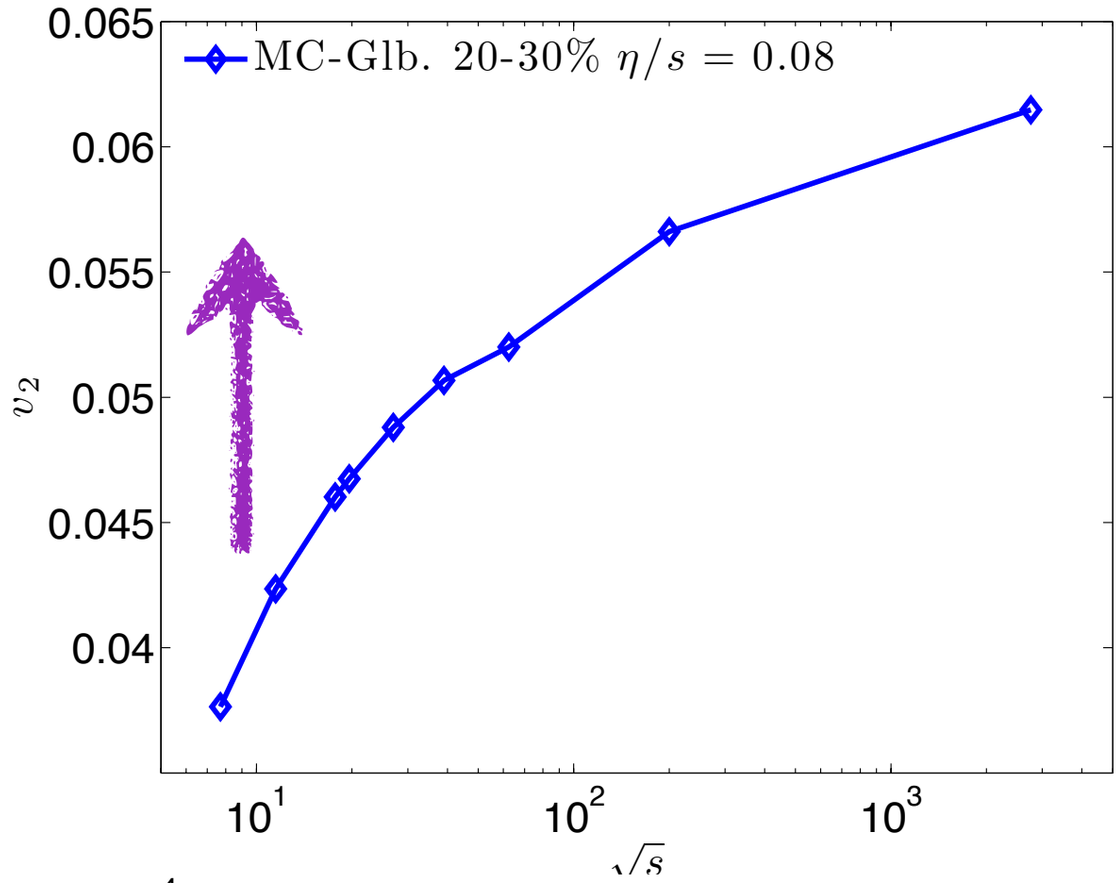

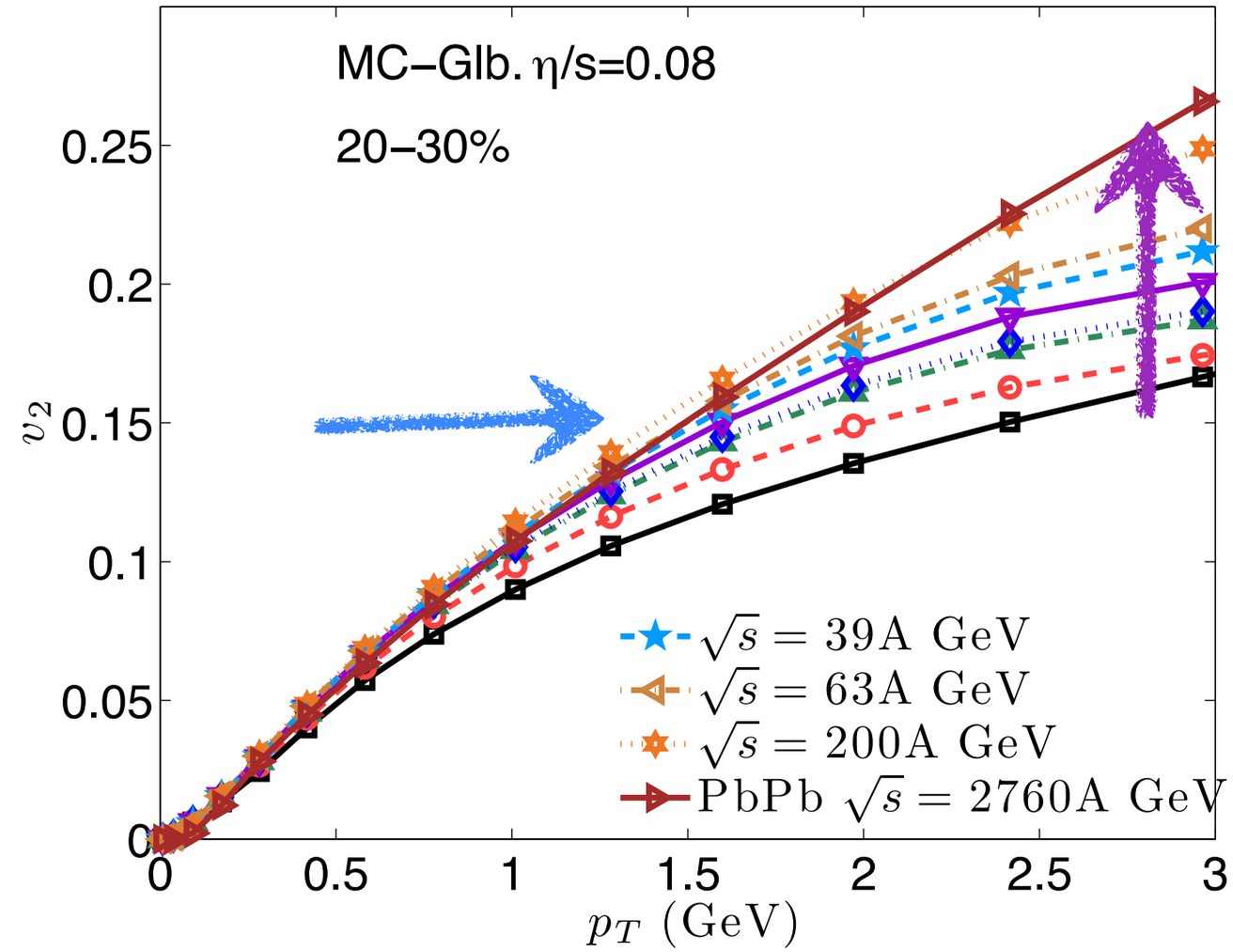

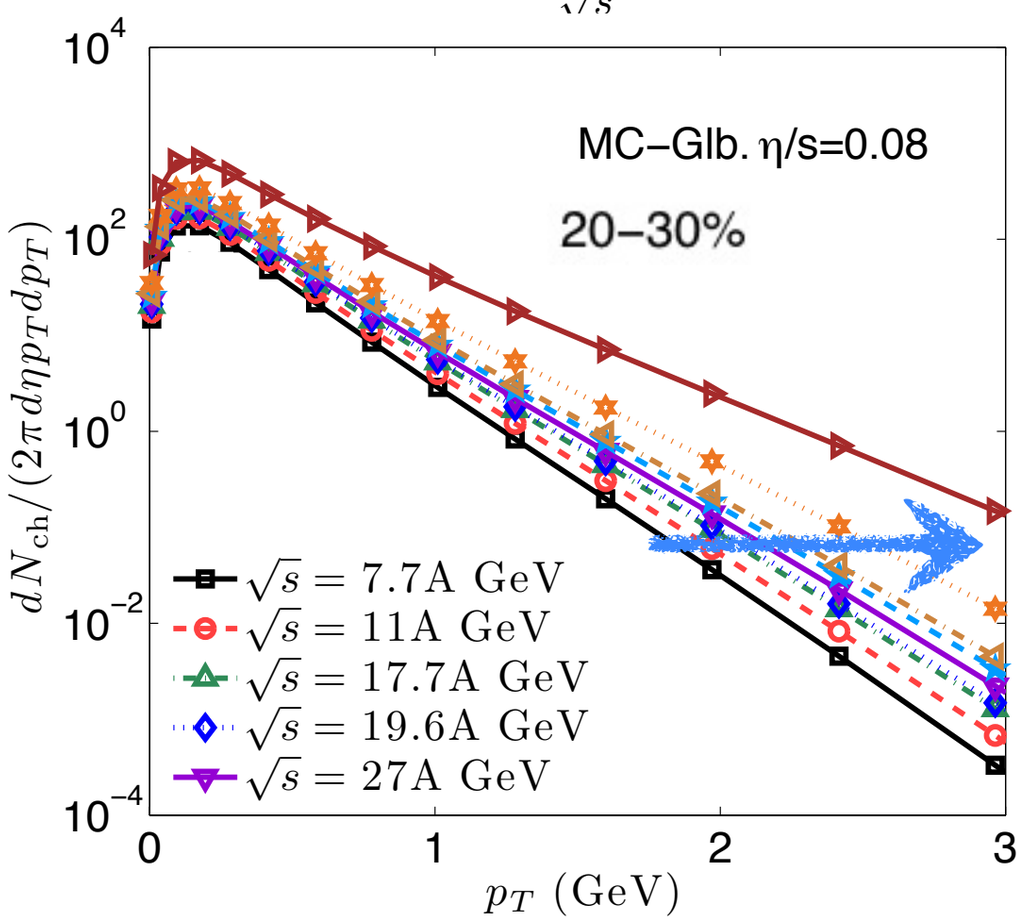

As $\sqrt{s}$ ↗,

the increase of elliptic flow interplays with the stronger radial flow, resulting in a broad maximum for $v_2(p_T, \sqrt{s})$ at fixed p_T as a function of $\sqrt{s}$

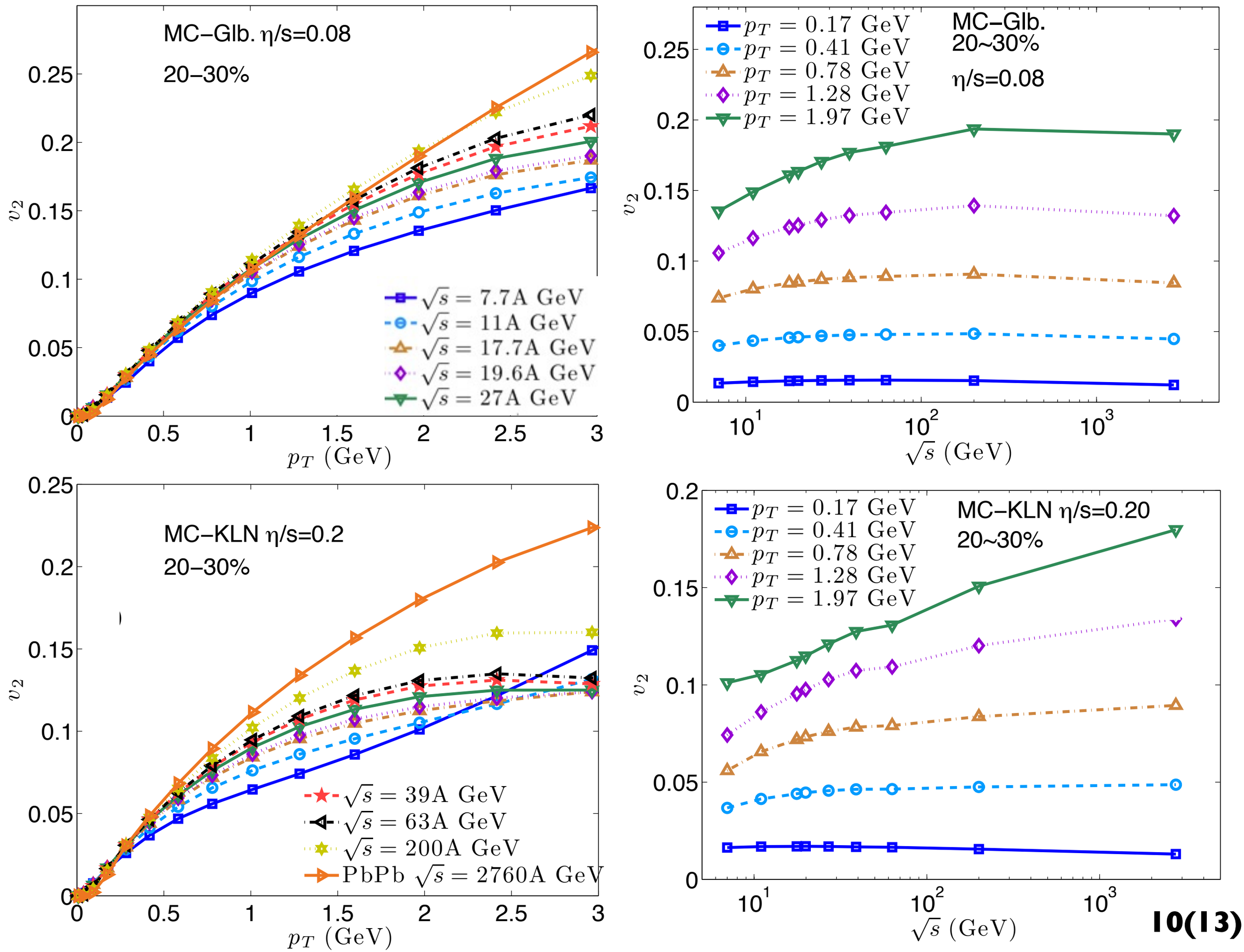
MC–Glb. η/s=0.08
20–30%
$\sqrt{s}$ = 7.7A GeV
$\sqrt{s}$ = 11A GeV
$\sqrt{s}$ = 17.7A GeV
$\sqrt{s}$ = 19.6A GeV
$\sqrt{s}$ = 27A GeV
v_2
p_T (GeV)
p_T = 0.17 GeV
p_T = 0.41 GeV
p_T = 0.78 GeV
p_T = 1.28 GeV
p_T = 1.97 GeV
MC–Glb.
20~30%
η/s=0.08
$\sqrt{s}$ (GeV)
MC–KLN η/s=0.2
20–30%
$\sqrt{s}$ = 39A GeV
$\sqrt{s}$ = 63A GeV
$\sqrt{s}$ = 200A GeV
PbPb $\sqrt{s}$ = 2760A GeV
MC–KLN η/s=0.20
20~30%

Differential $v_2(p_T)$

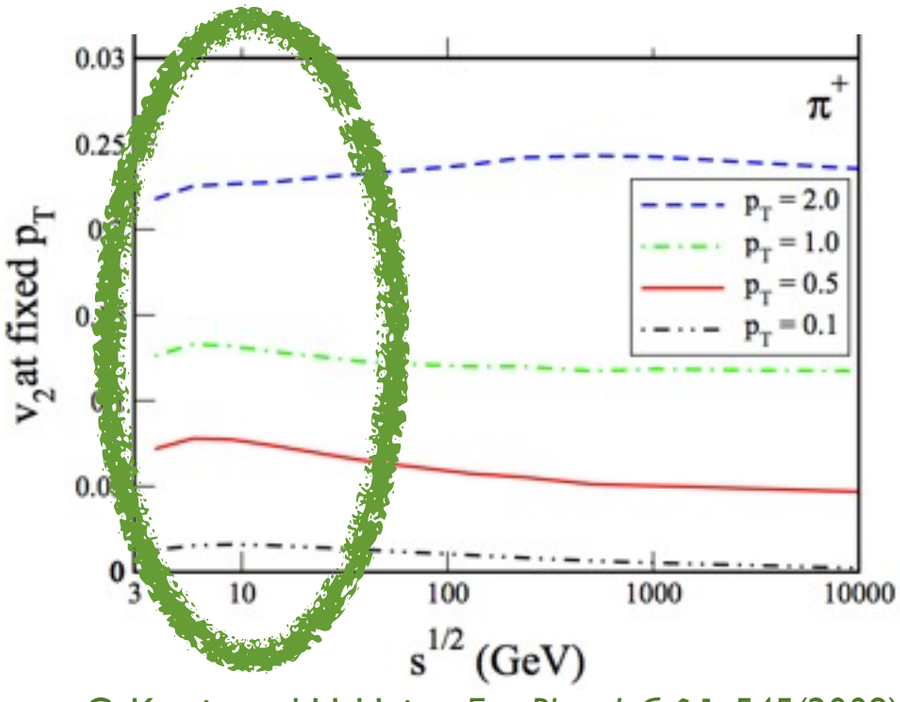

G. Kestin and U. Heinz, *Eur. Phys. J. C* **61**, 545(2009)

$\eta/s = 0$

- Ideal hydro: $v_2(p_T)$ peaks at around $\sqrt{s} \sim 5$ GeV

Differential $v_2(p_T)$

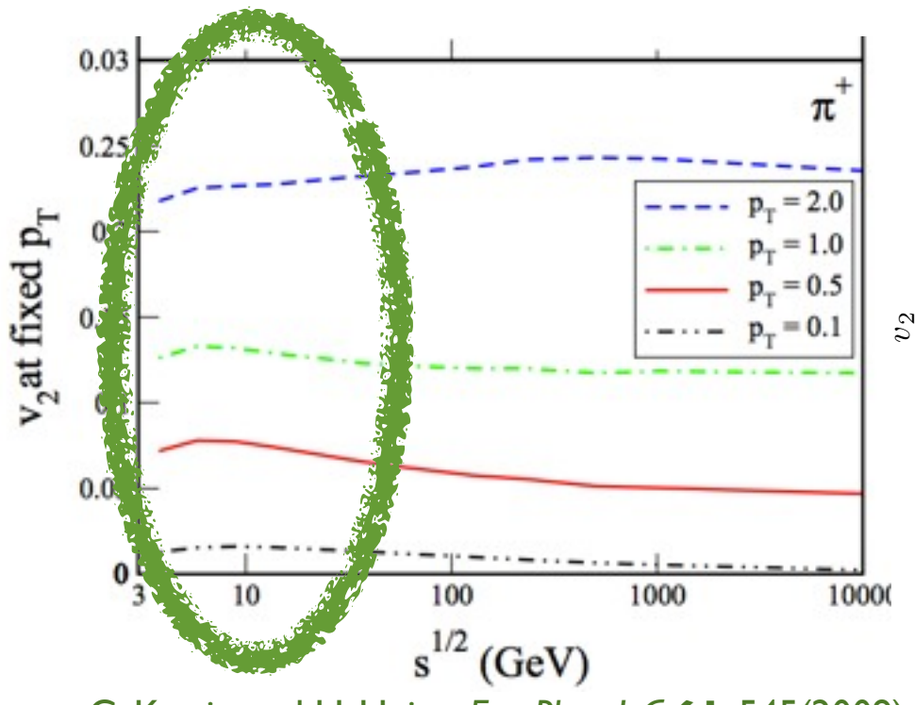

G. Kestin and U. Heinz, *Eur. Phys. J. C* **61**, 545(2009)

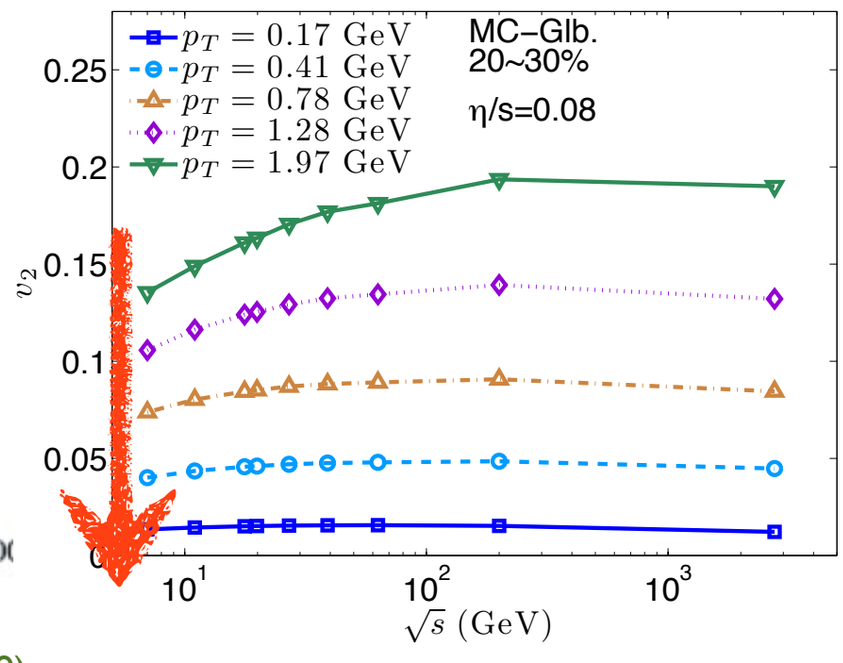

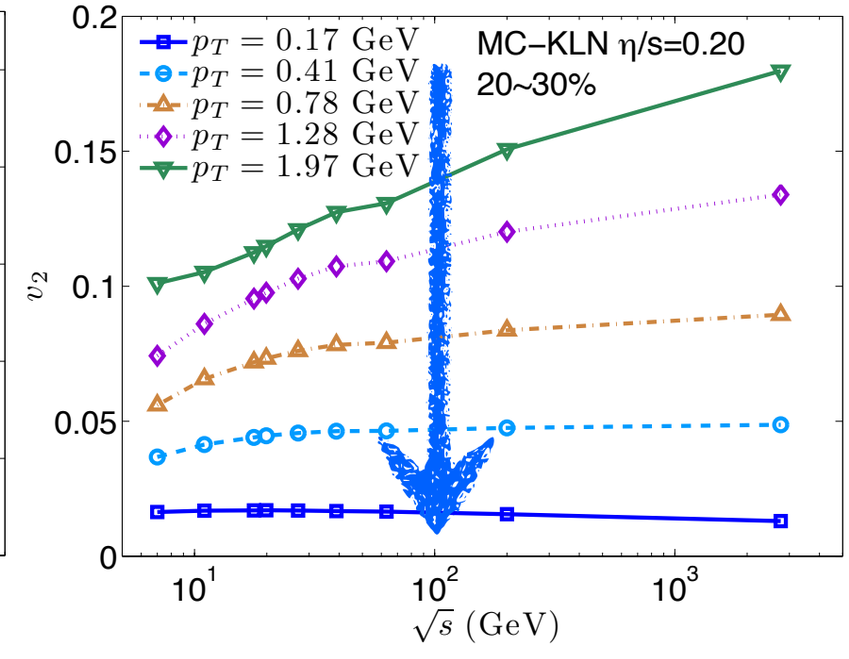

$\eta/s = 0$ $\eta/s = 0.08$ $\eta/s = 0.20$

- Ideal hydro: $v_2(p_T)$ peaks at around $\sqrt{s} \sim 5$ GeV

Differential $v_2(p_T)$

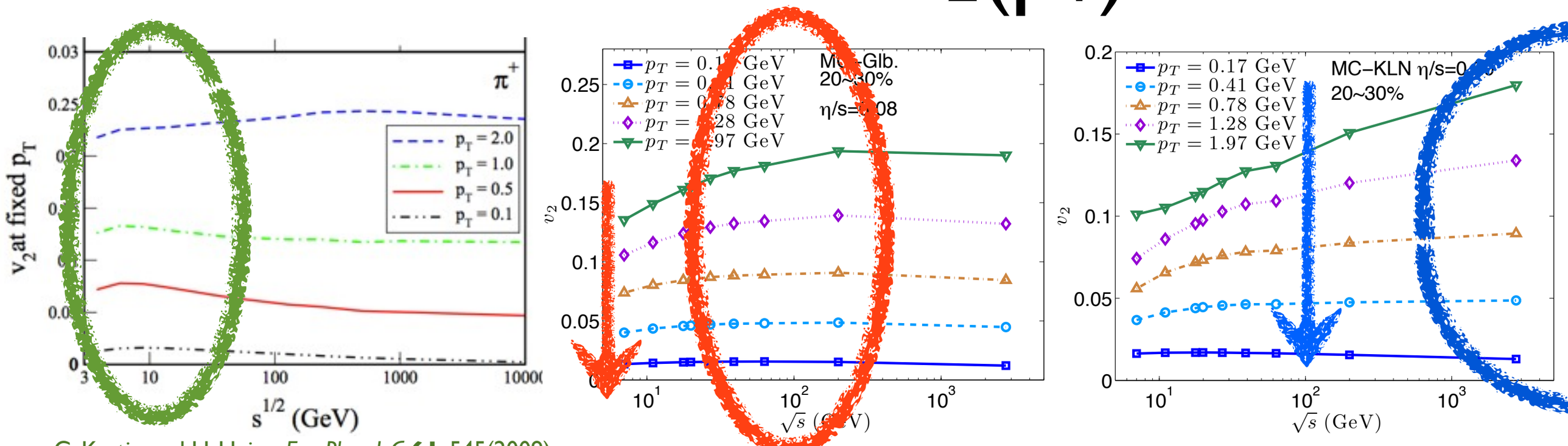

G. Kestin and U. Heinz, *Eur. Phys. J. C* **61**, 545(2009)

$\eta/s = 0$ $\eta/s = 0.08$ $\eta/s = 0.20$

- Ideal hydro: $v_2(p_T)$ peaks at around $\sqrt{s} \sim 5$ GeV
- MC-Glb. : $v_2(p_T)$ reaches broad maximum for $\sqrt{s} \sim 200$ GeV
  $\eta/s = 0.08$
- MC-KLN : $v_2(p_T)$ will peak somewhere at $\sqrt{s} > 2760$ GeV
  $\eta/s = 0.20$

Differential $v_2(p_T)$

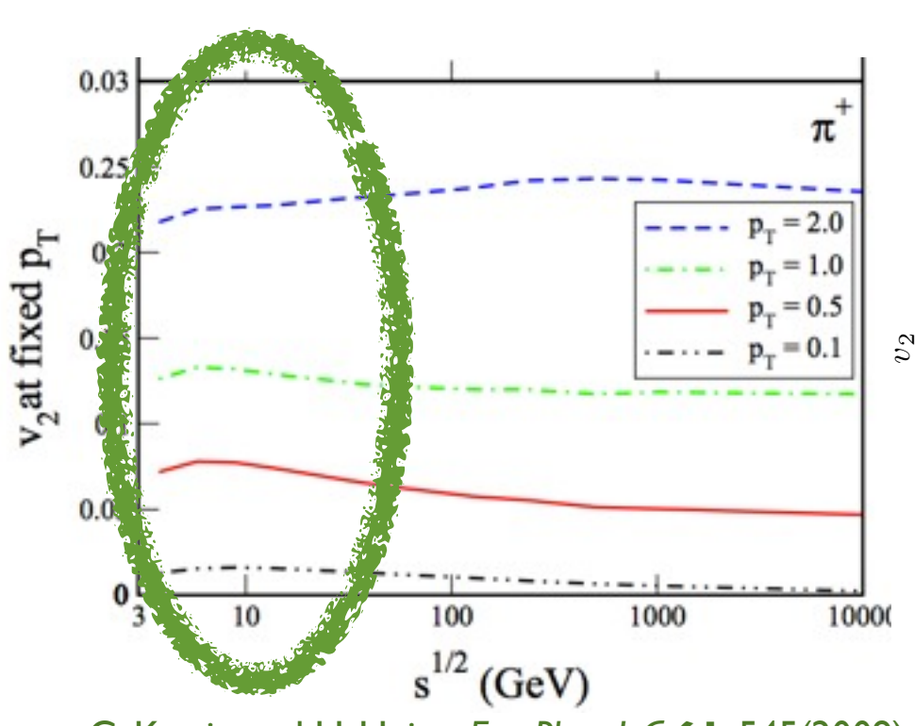

G. Kestin and U. Heinz, *Eur. Phys. J. C* **61**, 545(2009)

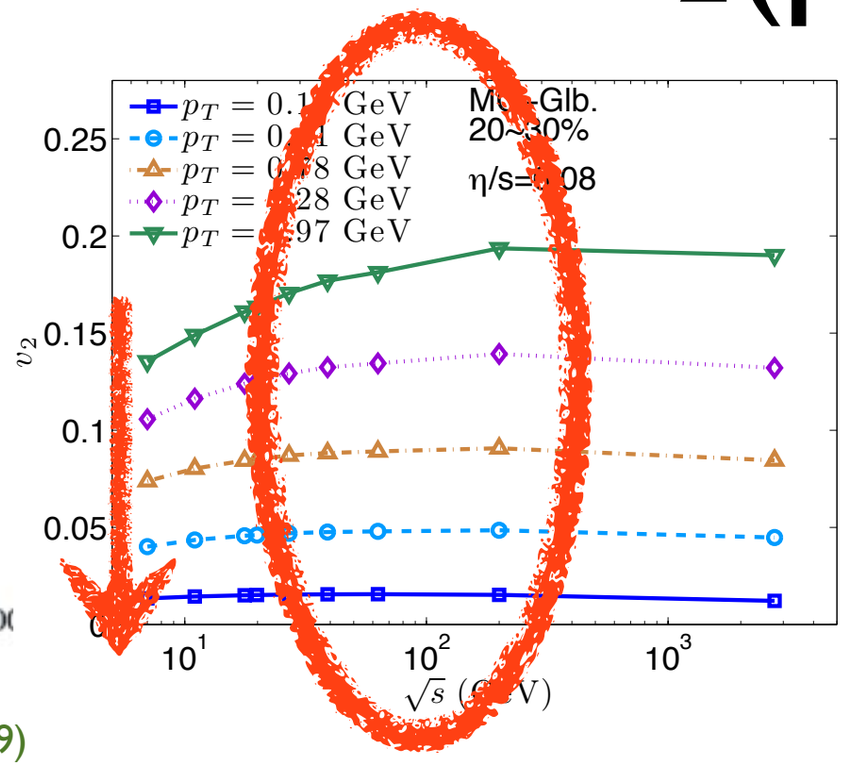

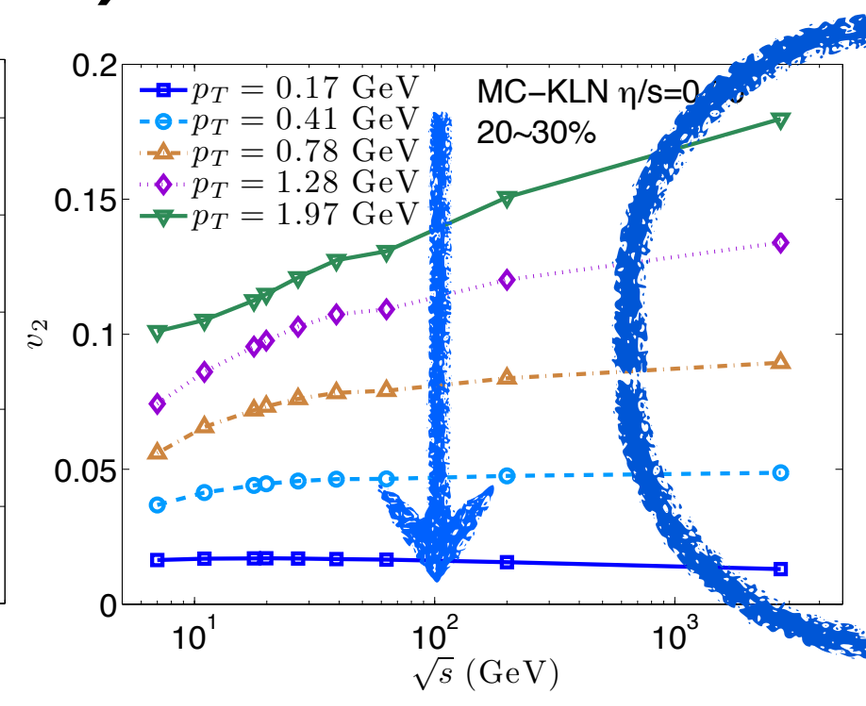

$\eta/s = 0$ $\eta/s = 0.08$ $\eta/s = 0.20$

- Ideal hydro: $v_2(p_T)$ peaks at around $\sqrt{s} \sim 5$ GeV
- MC-Glb. : $v_2(p_T)$ reaches broad maximum for $\sqrt{s} \sim 200$ GeV
  $\eta/s = 0.08$
- MC-KLN : $v_2(p_T)$ will peak somewhere at $\sqrt{s} > 2760$ GeV
  $\eta/s = 0.20$

η/s ⟹ peak in $v_2(p_T, \sqrt{s})$ moves to larger $\sqrt{s}$

Freeze-out shape analysis

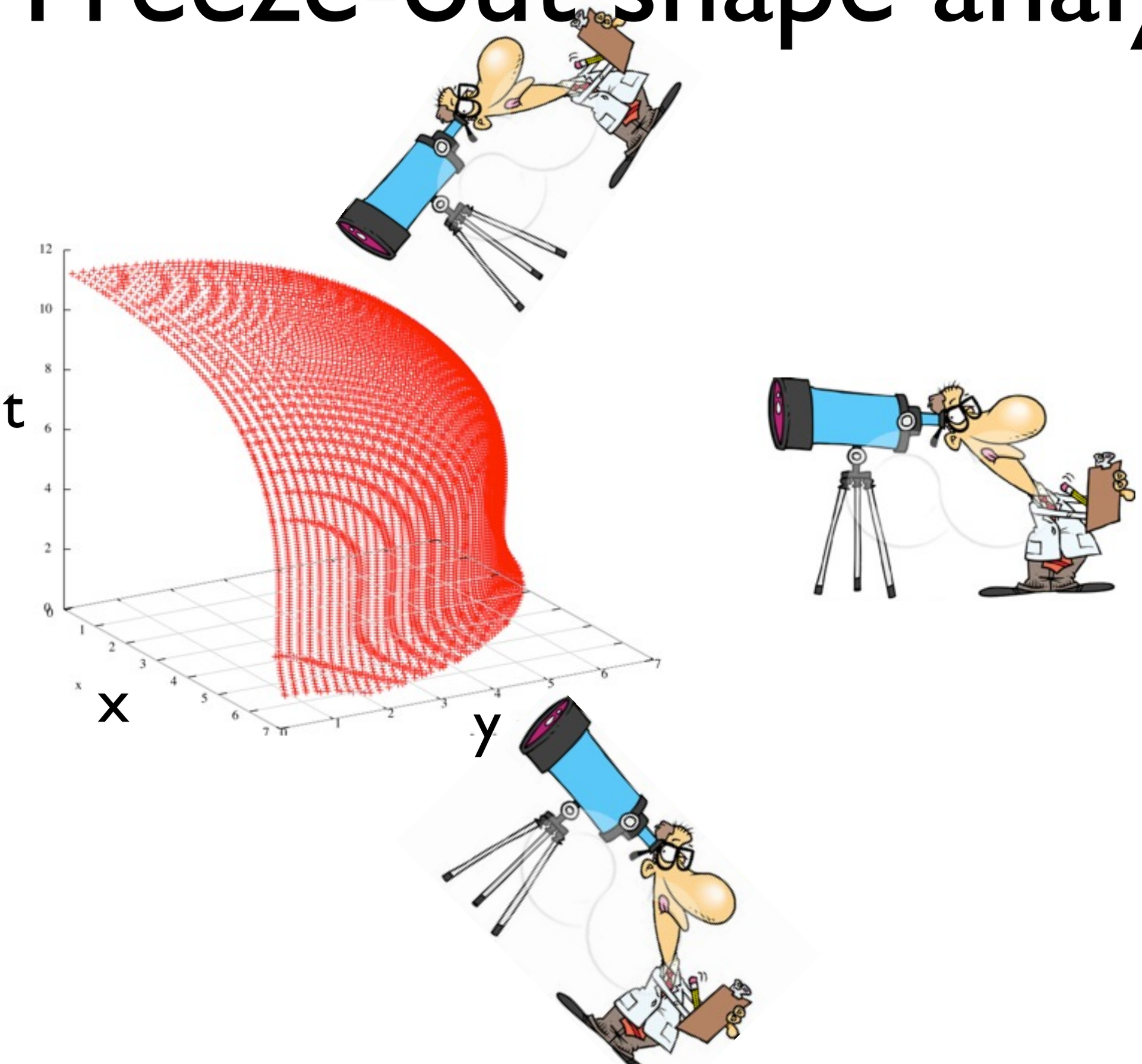

Freeze-out shape analysis

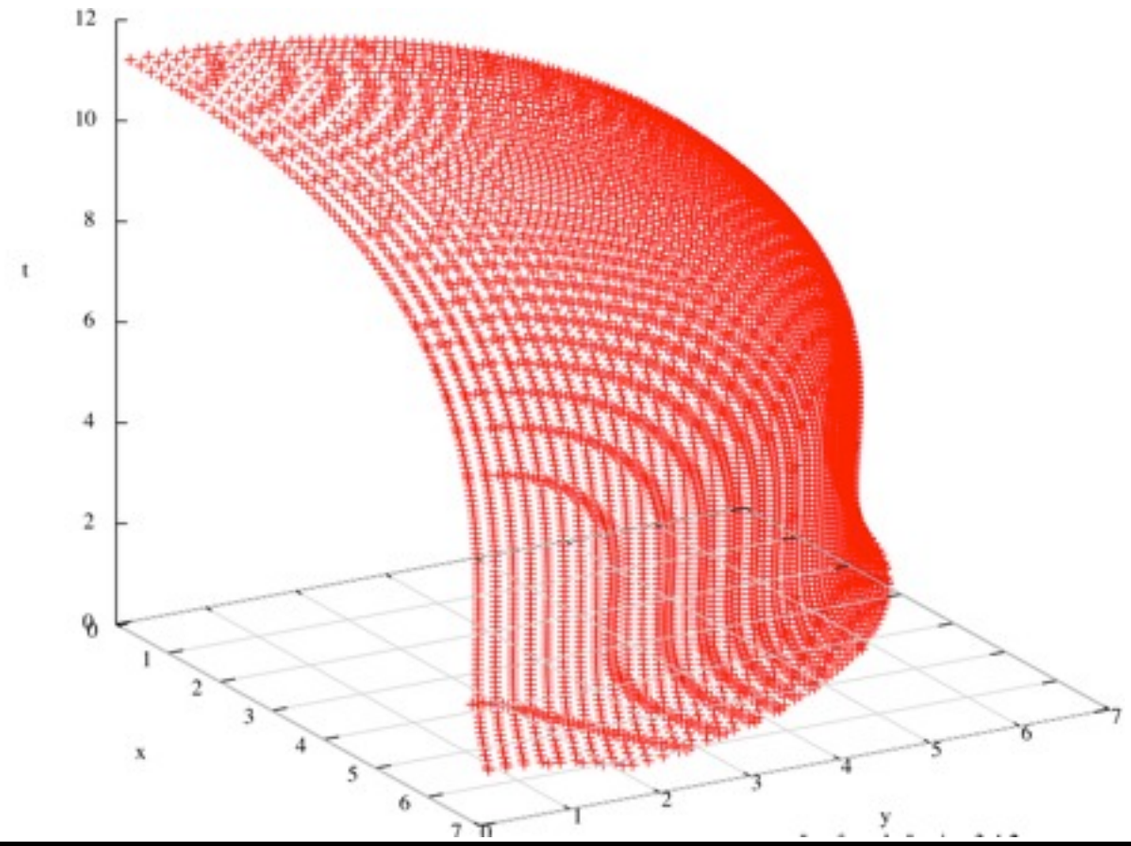

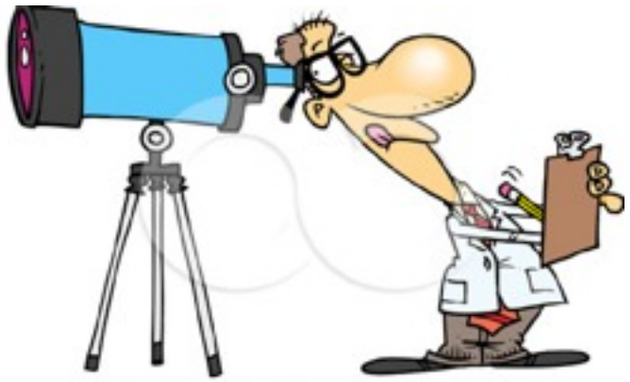

t

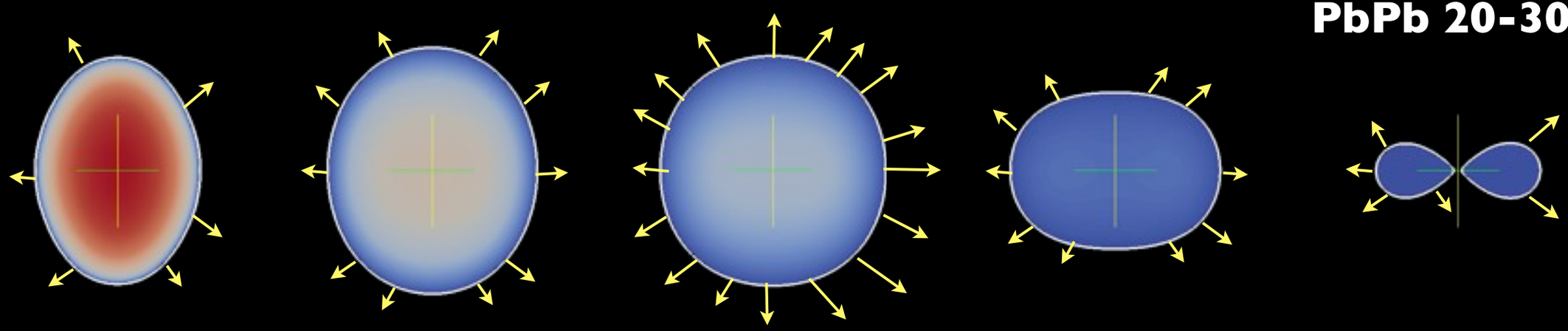

Freeze-out shape analysis

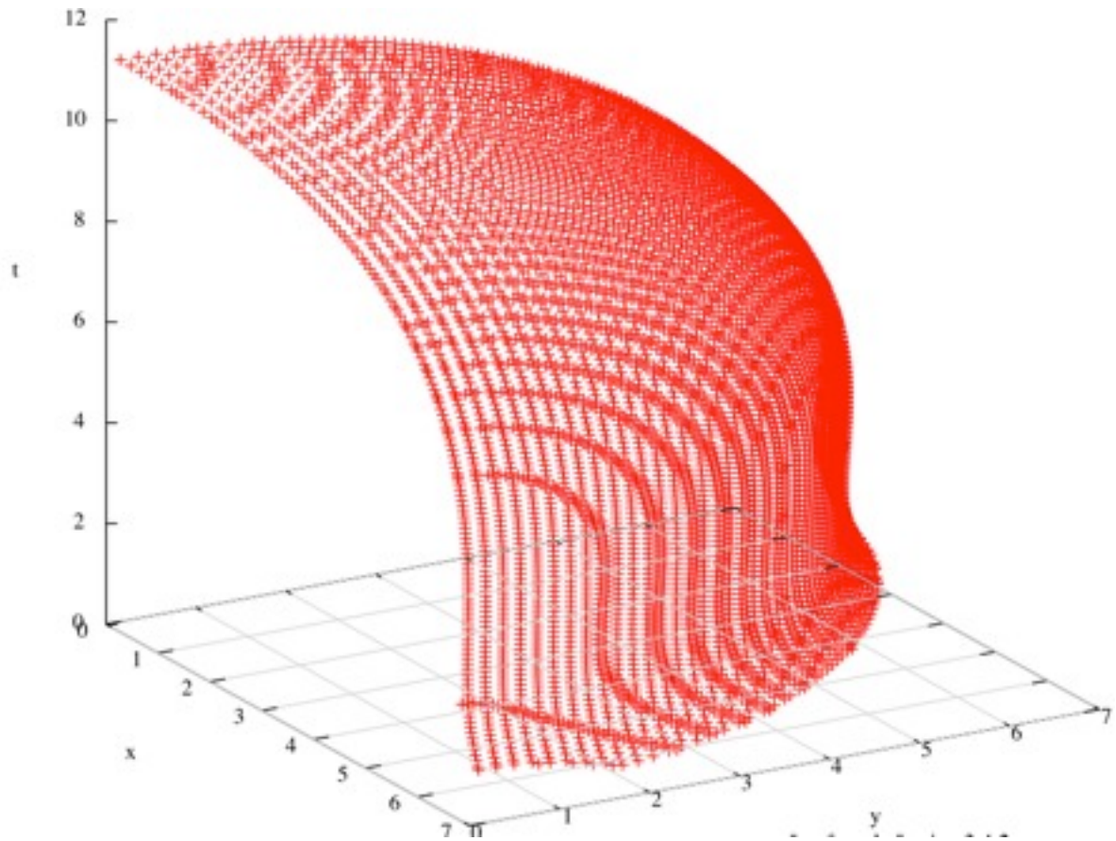

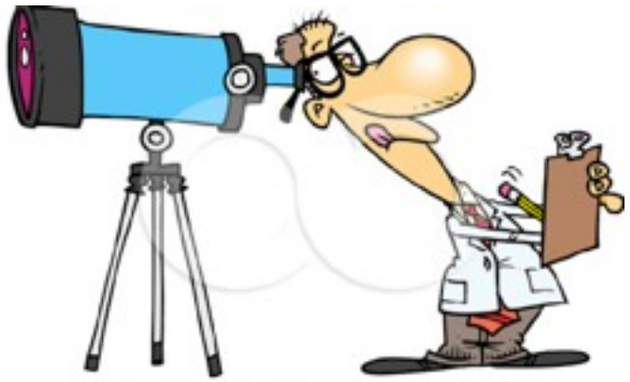

t

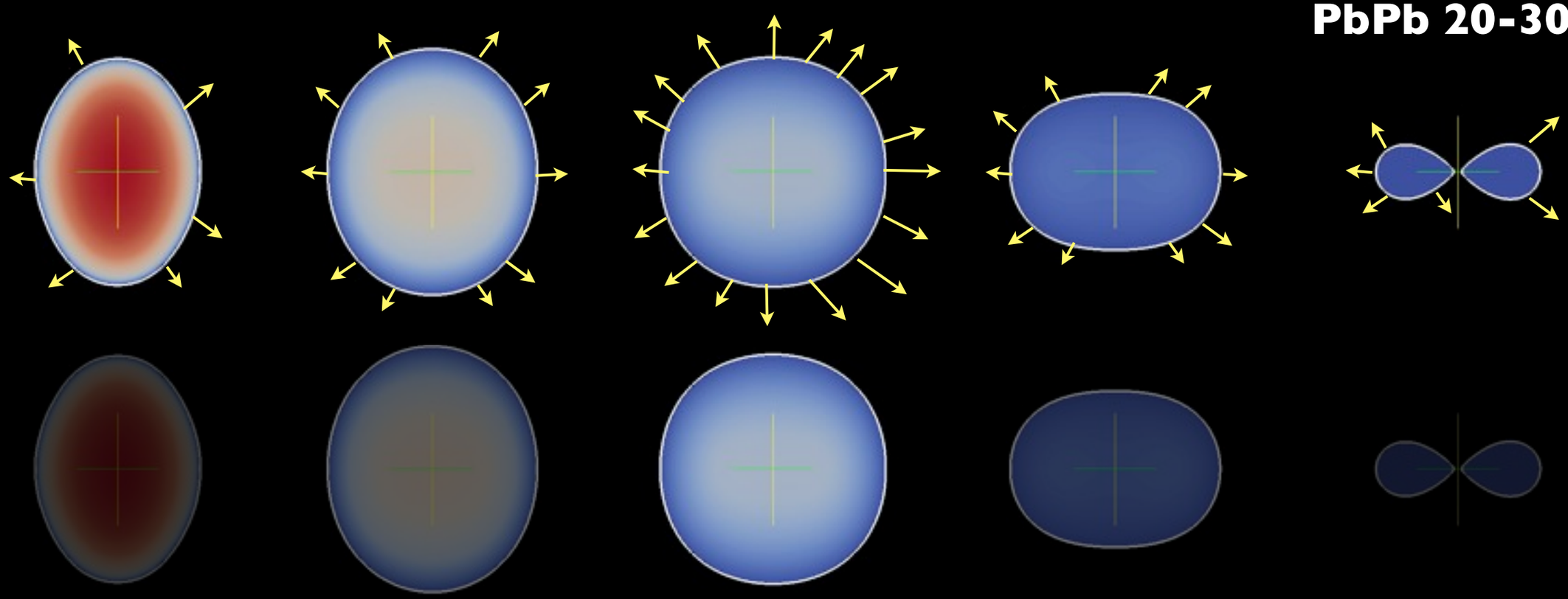

Freeze-out shape analysis

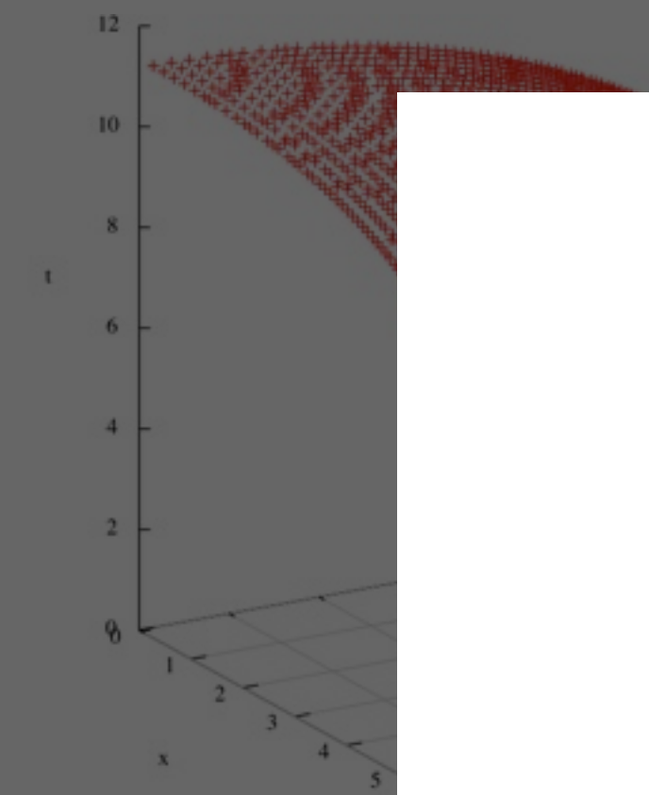

$$\epsilon_x(\Sigma) = \frac{\int_\Sigma u^\mu d^3\sigma_\mu \, (y^2 - x^2)}{\int_\Sigma u^\mu d^3\sigma_\mu \, (y^2 + x^2)},$$

20-30% LHC

Freeze-out shape analysis

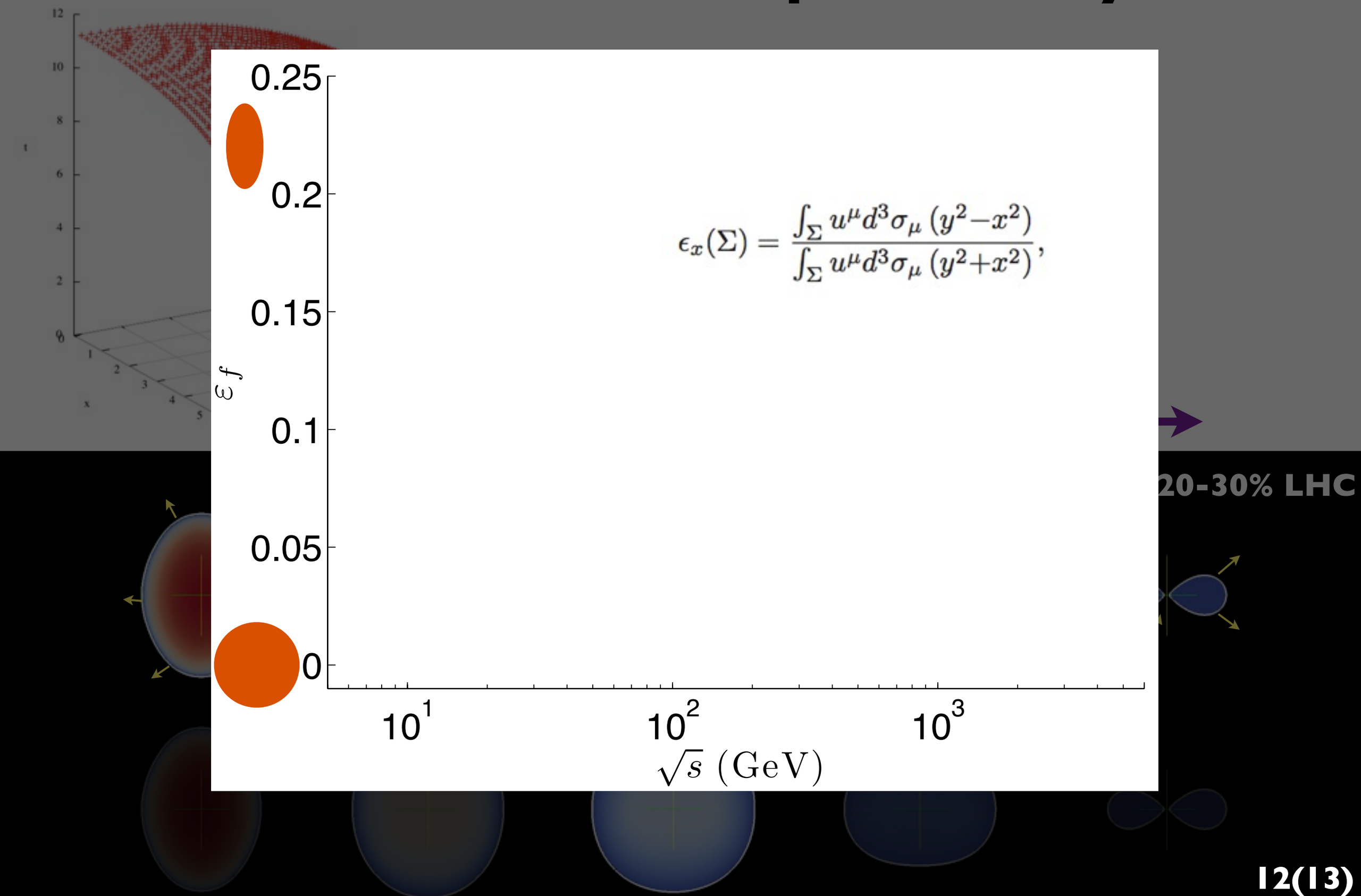

$$\epsilon_x(\Sigma) = \frac{\int_\Sigma u^\mu d^3\sigma_\mu \, (y^2 - x^2)}{\int_\Sigma u^\mu d^3\sigma_\mu \, (y^2 + x^2)},$$

Freeze-out shape analysis

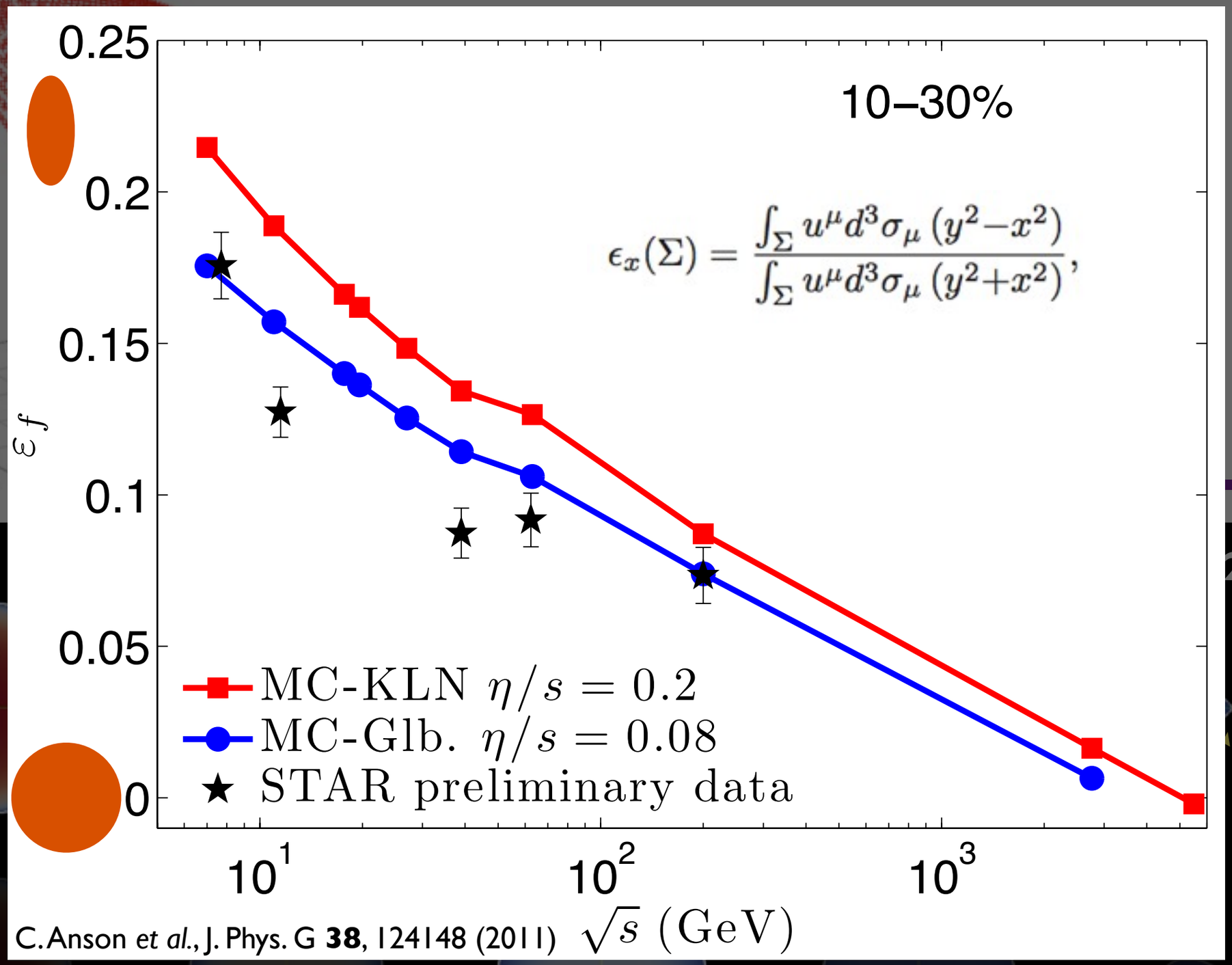

C. Anson *et al.*, J. Phys. G **38**, 124148 (2011)

Freeze-out shape analysis

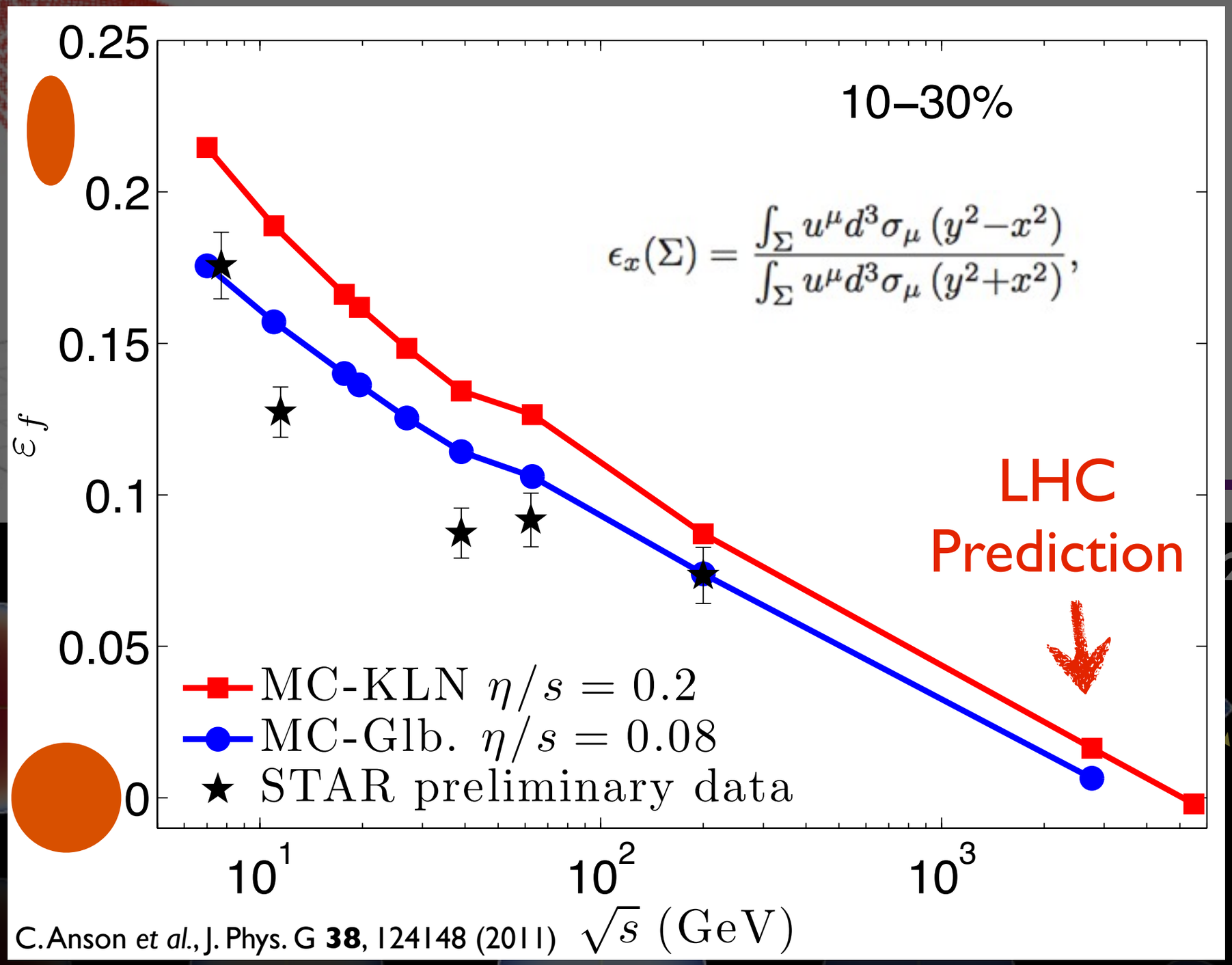

C. Anson *et al.*, J. Phys. G **38**, 124148 (2011)

Summary

Collision energy dependence of soft hadron observables will help us constrain initial conditions as well as evolution dynamics

- MC-Glb. with $\eta/s = 0.08$ shows good $\sqrt{s}$-scaling behavior

$$\frac{dN/d\eta}{N_{\rm part}/2} \text{ vs } N_{\rm part} \qquad v_2/\epsilon_2 \text{ vs } \frac{1}{S}\frac{dN}{d\eta}$$

  MC-KLN model with $\eta/s = 0.20$ does **not**

- Increasing shear viscosity changes the balance between radial and elliptic flow, shifting the peak of $v_2(\sqrt{s}, p_T)$ to larger $\sqrt{s}$

- Novel final shape analysis predicts the spatial eccentricity at freeze-out approaches zero at LHC energy

Back up

Centrality Dependence of the Initial Entropy Densities

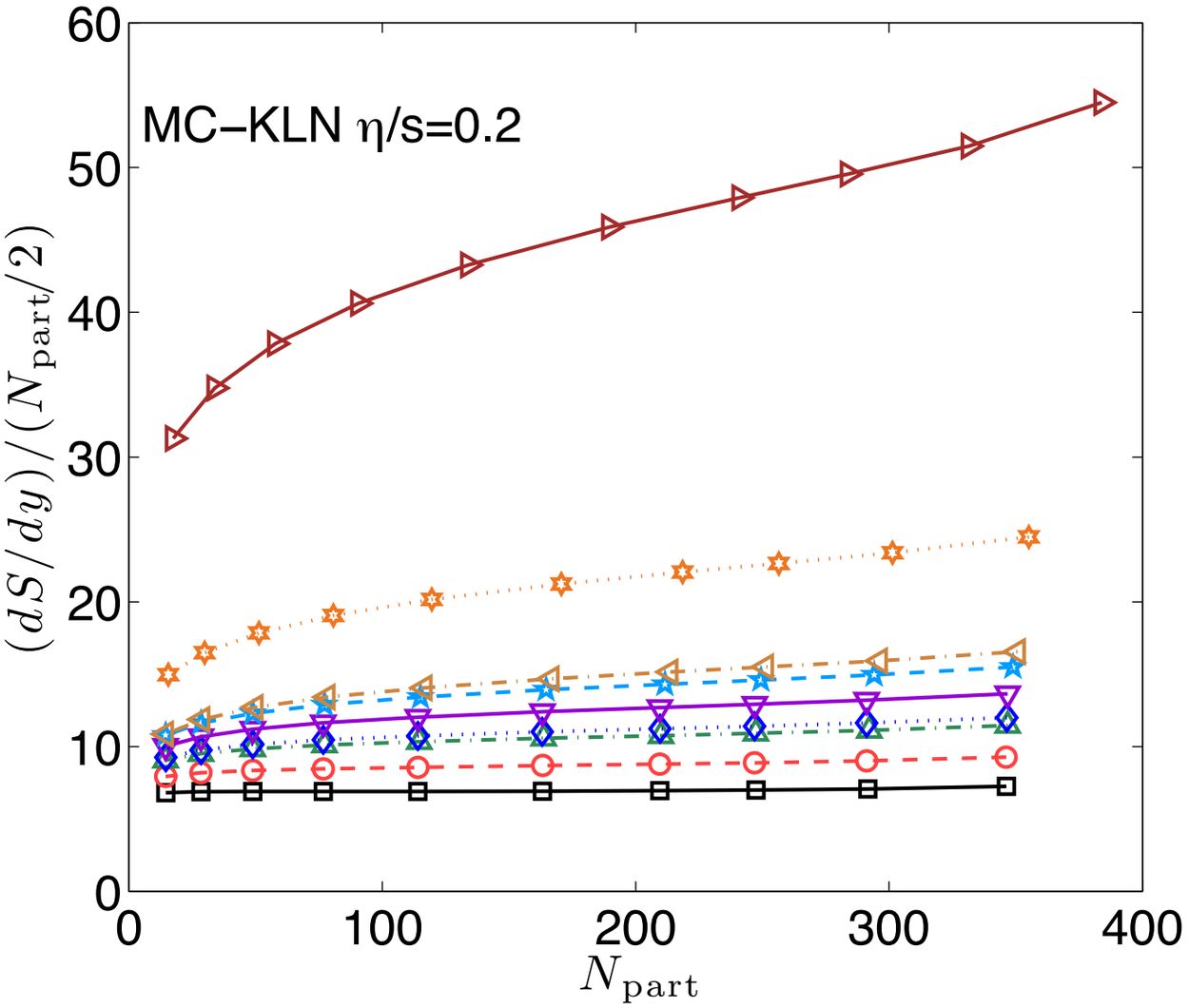

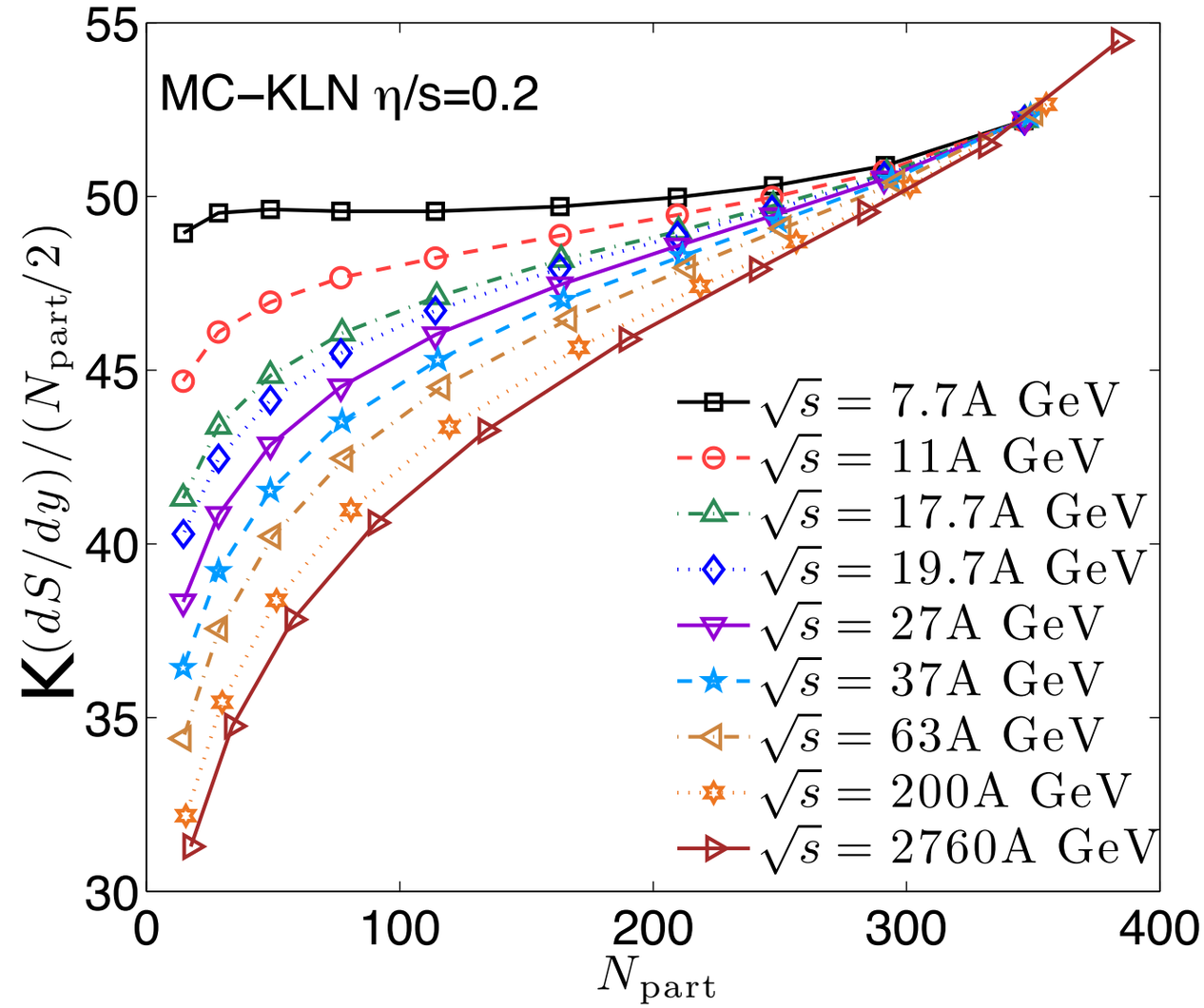

radial flow and particle p_T-spectra

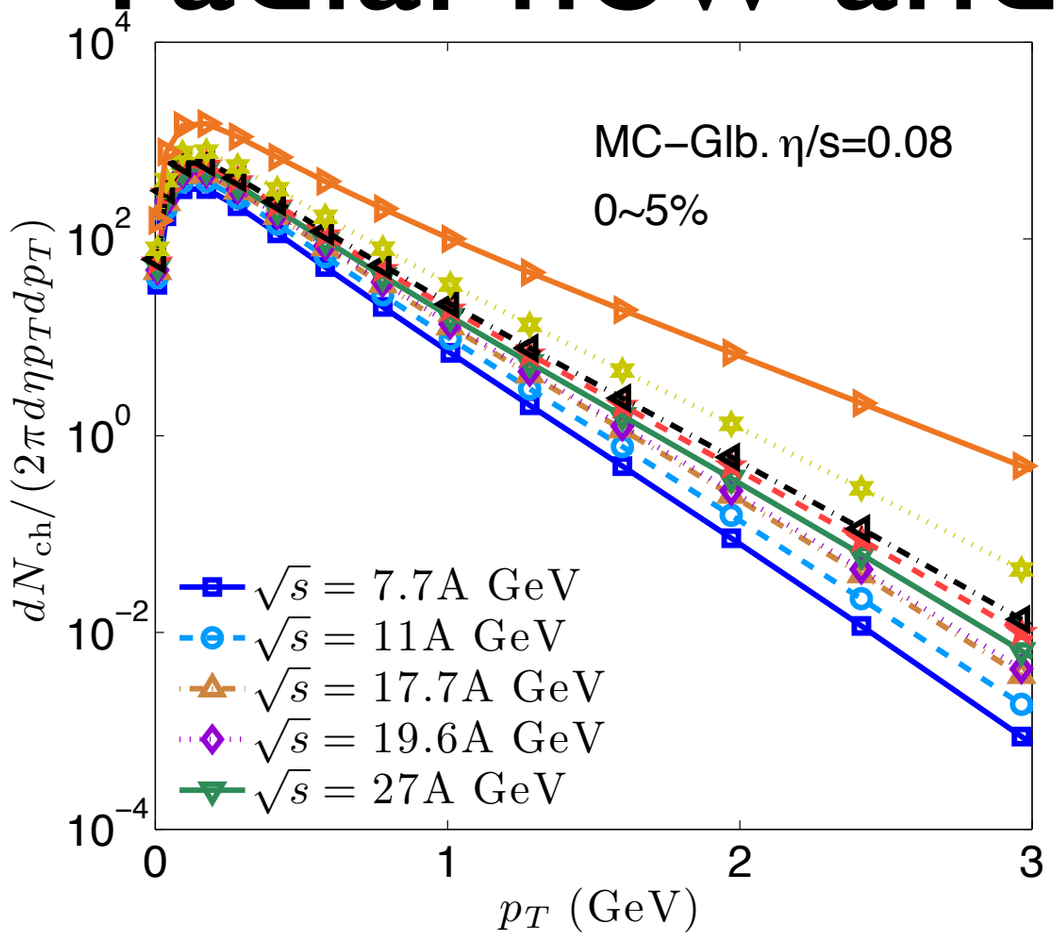

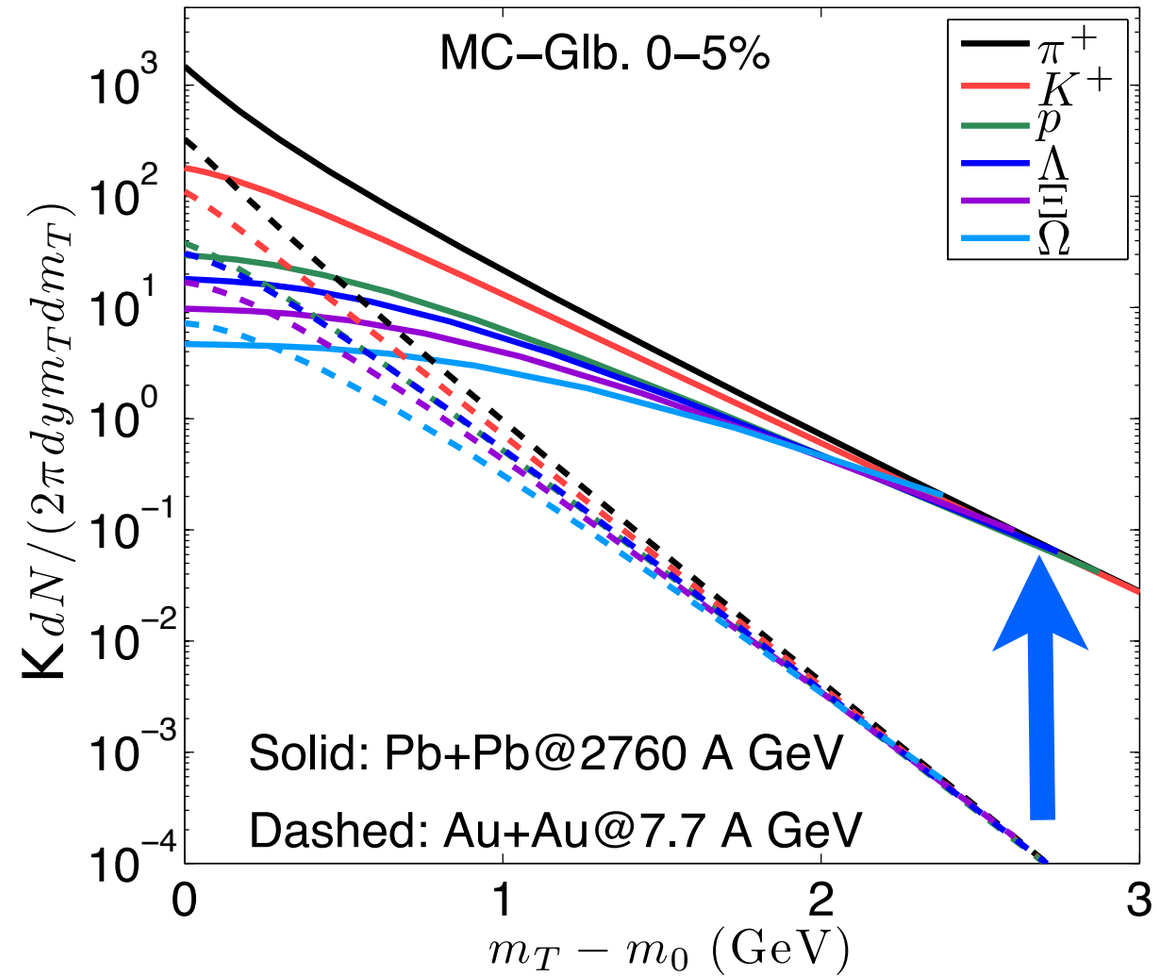

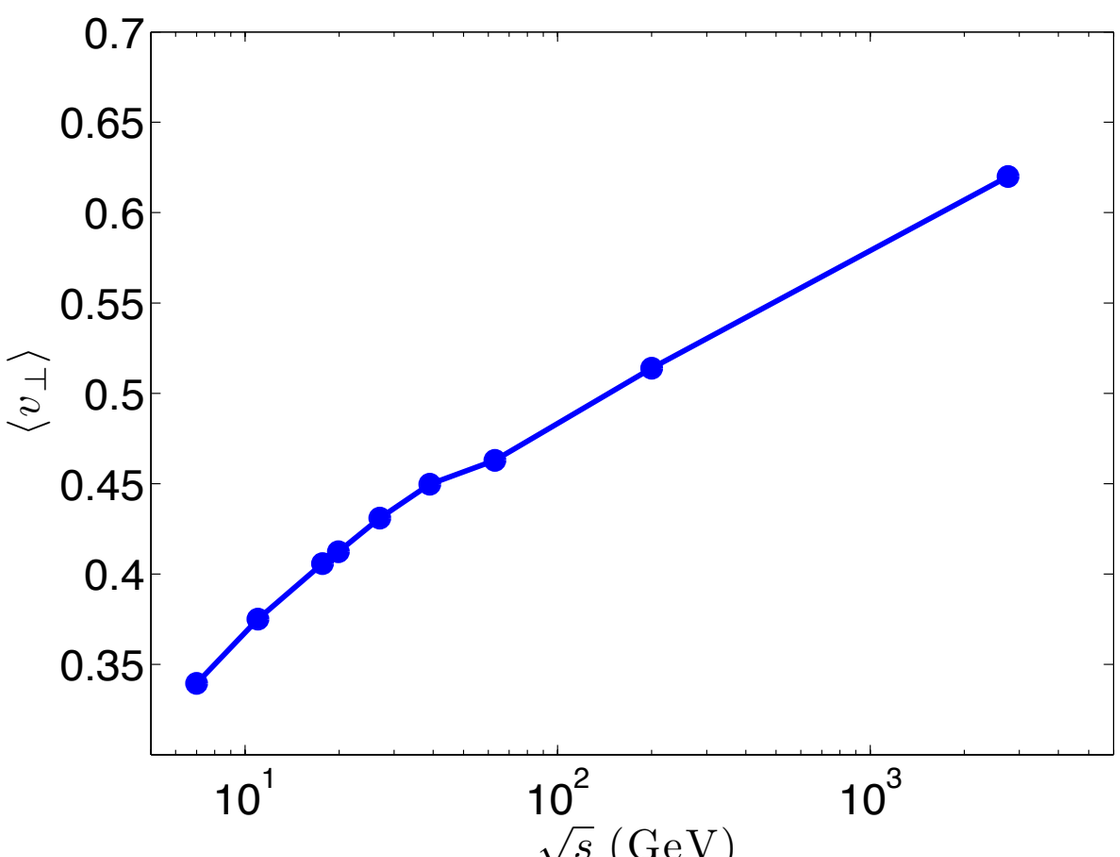

For stronger radial flow:

the slope of the particle spectra get flatter

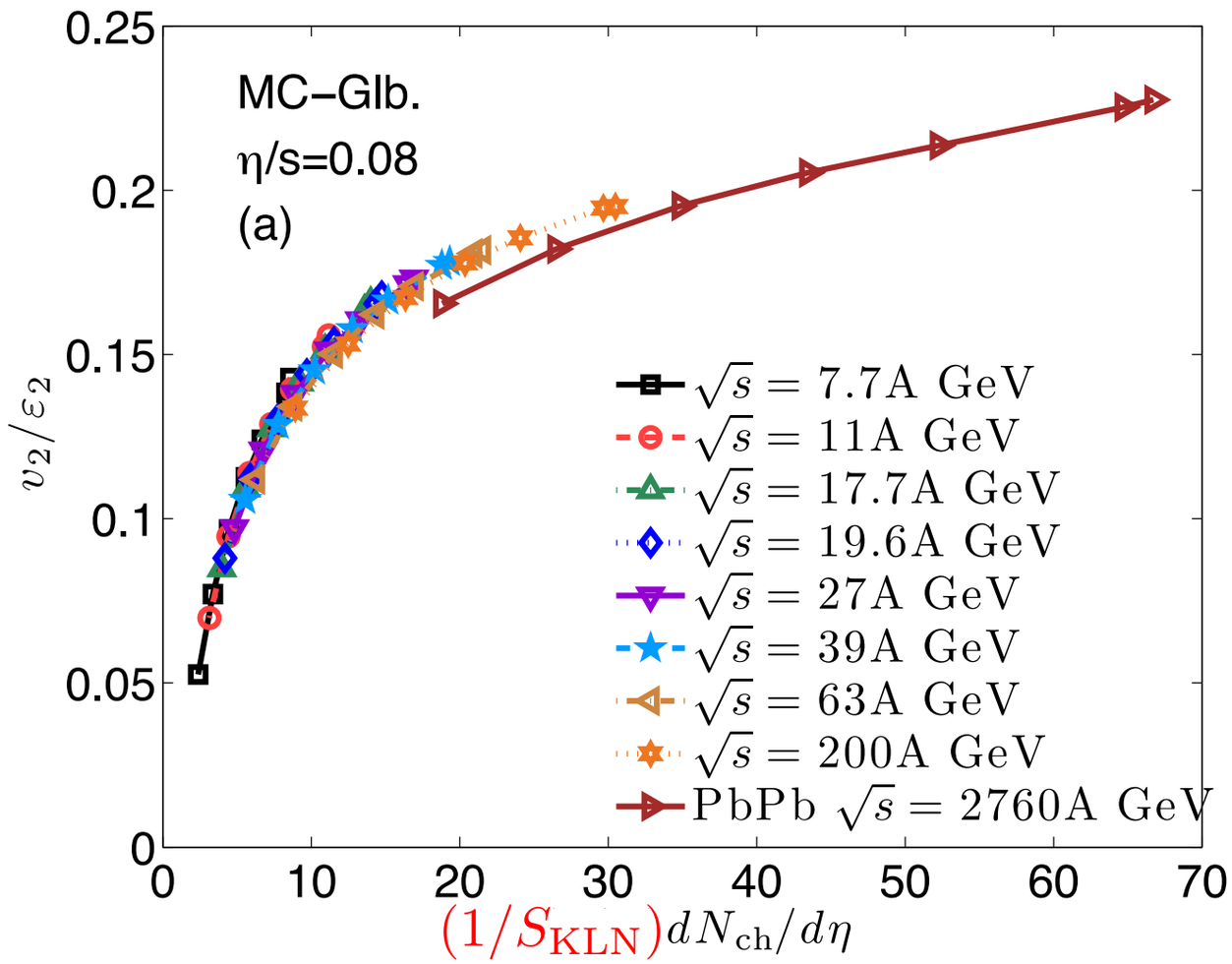
MC−Glb.
η/s=0.08
(a)
$\sqrt{s} = 7.7$A GeV
$\sqrt{s} = 11$A GeV
$\sqrt{s} = 17.7$A GeV
$\sqrt{s} = 19.6$A GeV
$\sqrt{s} = 27$A GeV
$\sqrt{s} = 39$A GeV
$\sqrt{s} = 63$A GeV
$\sqrt{s} = 200$A GeV
PbPb $\sqrt{s} = 2760$A GeV
v_2/ε_2
$(1/S_{\rm KLN})dN_{\rm ch}/d\eta$
0
0.05
0.1
0.15
0.2
0.25
0
10
20
30
40
50
60
70

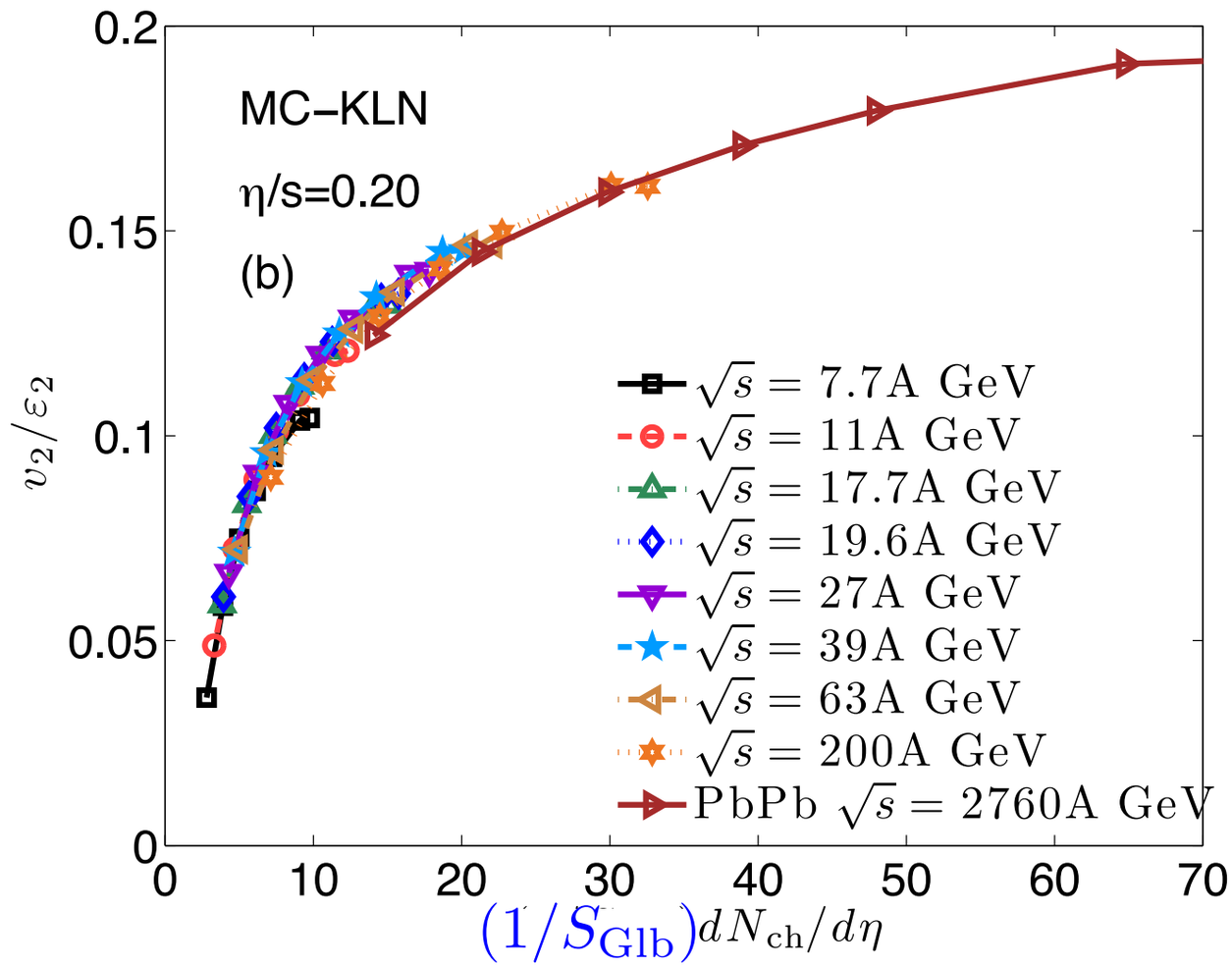
MC−KLN
η/s=0.20
(b)
$\sqrt{s} = 7.7$A GeV
$\sqrt{s} = 11$A GeV
$\sqrt{s} = 17.7$A GeV
$\sqrt{s} = 19.6$A GeV
$\sqrt{s} = 27$A GeV
$\sqrt{s} = 39$A GeV
$\sqrt{s} = 63$A GeV
$\sqrt{s} = 200$A GeV
PbPb $\sqrt{s} = 2760$A GeV
v_2/ε_2
$(1/S_{\rm Glb})dN_{\rm ch}/d\eta$
0
0.05
0.1
0.15
0.2
0
10
20
30
40
50
60
70

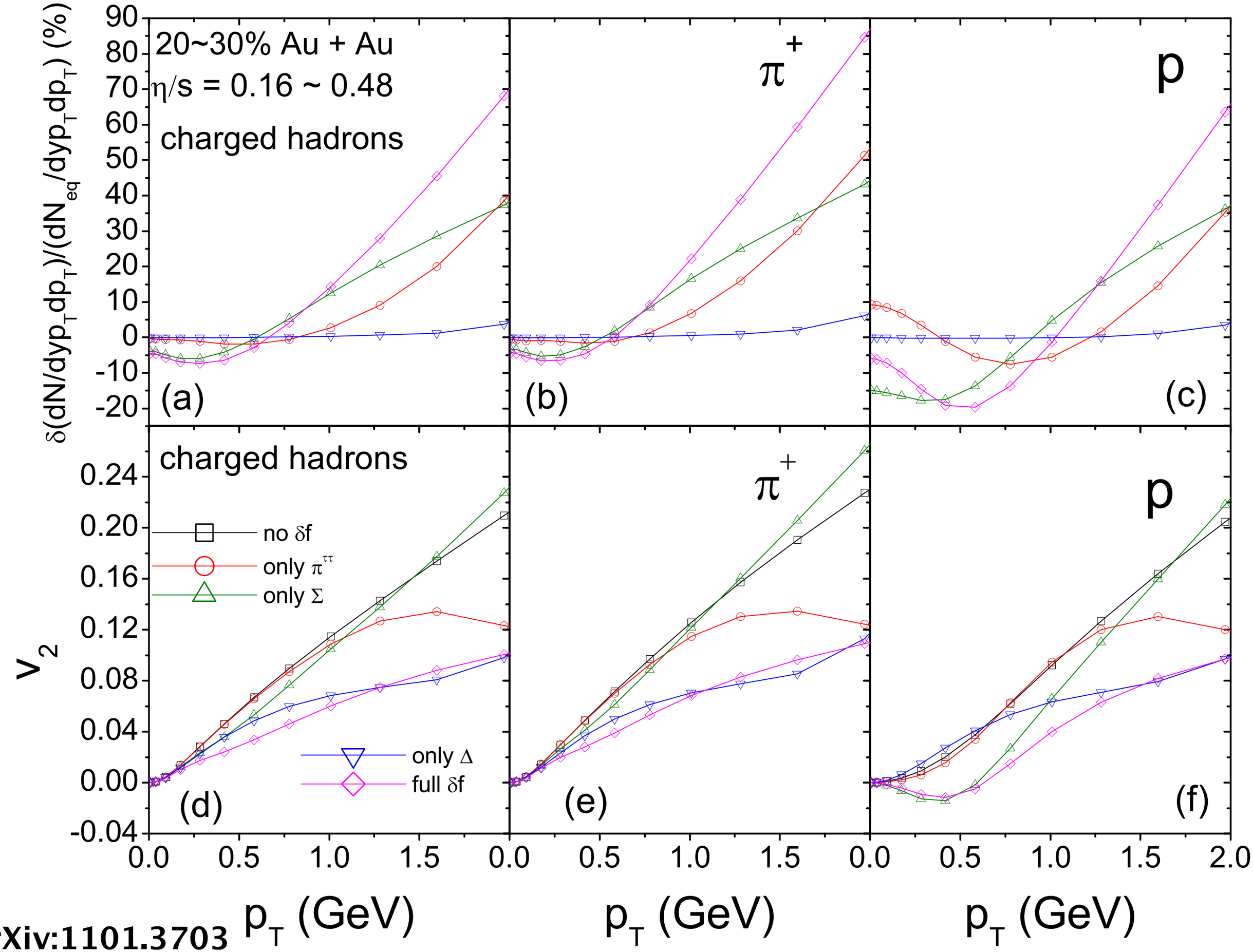

arXiv:1101.3703